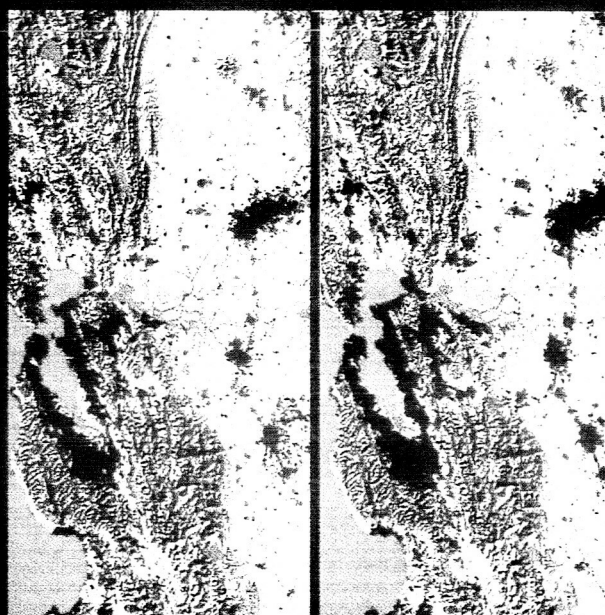
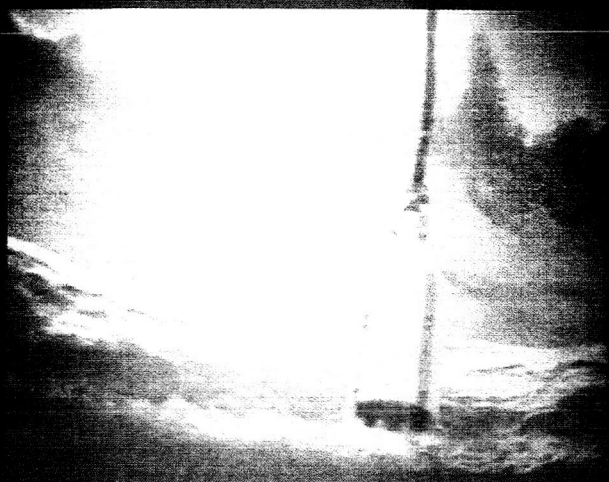
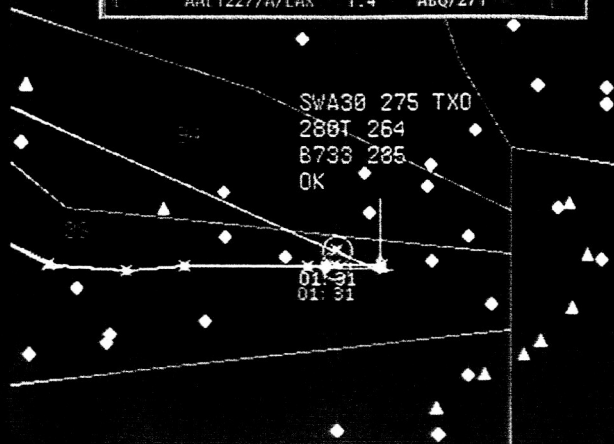


Direct-To Sector 39					
TF	ACID/EQUIP/DEST	Mins	Flx/Hdg	OK/C	-
		Saved			
<input type="checkbox"/>	N797FA/G/SDL	2.9	TXO/279	OK	<input type="checkbox"/>
<input checked="" type="checkbox"/>	SWA30/1/ABQ	1.7	ABQ/270	OK	<input type="checkbox"/>
<input type="checkbox"/>	AA11227/A/LAX	1.4	ABQ/271	OK	<input type="checkbox"/>



RESEARCH & TECHNOLOGY
NASA AMES RESEARCH CENTER

RESEARCH & TECHNOLOGY

NASA AMES RESEARCH CENTER

1399



NATIONAL AERONAUTICS AND SPACE ADMINISTRATION
AMES RESEARCH CENTER • MOFFETT FIELD, CALIFORNIA

NASA/TM-2000-209618

Notice

The use of trade names and manufacturers in this document does not constitute an official endorsement of such products or manufacturers, either expressed or implied, by the National Aeronautics and Space Administration.

Available from:

NASA Center for AeroSpace Information
7121 Standard Drive
Hanover, MD 21076-1320
(301) 621-0390

National Technical Information Service
5285 Port Royal Road
Springfield, VA 22161
(703) 487-4650

Foreword

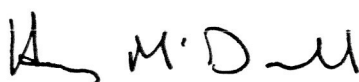
This report highlights the research accomplished during fiscal year 1999 by Ames Research Center scientists and engineers. The work is divided into accomplishments that support four of NASA's Strategic Enterprises: Aero-Space Technology, Space Science, Earth Science, and Human Exploration and Development of Space (HEDS). The key purpose of this report is to communicate information to our stakeholders about the scope and diversity of Ames' mission and the nature of Ames' research and technology activities.

Ames Research Center is making significant contributions to the Aero-Space Technology Enterprise mission by developing and commercializing high-payoff aeronautics and space transportation technologies. Ames has the Agency's lead role for basic research in Aviation Operations Systems, Information Systems Technology, and Rotorcraft. Ames is also the Lead Center for focused programs in Aviation System Capacity and High-Performance Computing and Communications. The Center's key core competencies include human factors, air traffic management, information systems, rotorcraft, vertical/short takeoff and landing technology, and thermal protection systems technology.

Ames is recognized as a world leader in Astrobiology, the study of life in the Universe and of the chemical and physical forces and adaptations that influence life's origin, evolution, and destiny. Key areas of research include the study of the abundance and distribution of biogenic compounds conducive to the origin of life, the study of extrasolar matter such as interstellar gas and dust, and the study of planet-forming regions around other stars. Ames supports the Office of Earth Science by conducting research in biogeochemical cycling, ecosystem dynamics, and the chemical and transport processes that determine atmospheric composition, dynamics, and climate. This supports the astrobiology effort, because the physical processes that determine the behavior of Earth's atmosphere are operative on extrasolar planets as well. Support for the HEDS Enterprise includes conducting research in space, supporting ground-based facilities, and managing spaceflight projects. Ames has been instrumental in determining how varying gravity levels affect living systems. Work continues on developing life-support capabilities for long-duration travel and habitation on other planets, as well as equipment to operate safely and effectively in microgravity.

Ames has also been designated the Agency's Center of Excellence for Information Technology. The three cornerstones of Information Technology research at Ames are automated reasoning human-centered computing, and high performance computing and networking. The mission critical capabilities enabled by NASA's three cornerstones of Information Technology span all of NASA's strategic enterprises.

For further information on Ames' research and technology projects, please contact the person designated as the point of contact at the end of each article. For further information about the report itself, contact Dr. Stephanie Langhoff, Chief Scientist, Mail Stop 230-3, NASA Ames Research Center, Moffett Field, CA 94035. An electronic version of this report is available on the Ames home page.



Henry McDonald
Director
Ames Research Center

Aero-Space Technology Enterprise

Overview	1
GLOBAL CIVIL AVIATION	
Direct-To Controller Tool	4
<i>Heinz Erzberger, Dave McNally</i>	
Active Final Approach Spacing Tool Development	5
<i>John E. Robinson, Cheryl Quinn, Douglas Isaacson</i>	
Distributed Air/Ground Traffic Management	6
<i>Karl Bilimoria, Steve Green</i>	
Information Management for Airline Operations	8
<i>Roxana Wales, John O'Neill</i>	
Taxiway Navigation and Situation Awareness Operational Integration	9
<i>Becky Hooey, David C. Foyle, Anthony Andre</i>	
Hybrid Systems	10
<i>George Meyer</i>	
Inflight Activity Breaks Reduce Sleepiness in Pilots	11
<i>David Neri, Melissa Mallis</i>	
Communication Strategies for Correcting Errors	12
<i>J. Orasanu, U. Fischer, C. Van Aken, L. McDonnell</i>	
Rotor Design Options for Whirl Flutter	14
<i>C. W. Acree, R. J. Peyran, Wayne Johnson</i>	
Efficient Computational Fluid Dynamics for Rotorcraft Analysis	15
<i>Frank Caradonna</i>	
Analysis of Advanced Rotorcraft Configurations	16
<i>Wayne Johnson</i>	
Prediction of Rotorcraft Pitch-Link Loads	18
<i>Sesi Kottapalli</i>	
Model Hingeless Rotor Dynamics Program	19
<i>Thomas H. Maier</i>	
Active Control of Stall on Helicopter Rotors	20
<i>Khanh Q. Nguyen</i>	
Large-Rotor Research Program	21
<i>Thomas R. Norman, Patrick M. Shinoda, Stephen A. Jacklin</i>	

A Study of Dynamic Stall Using Two-Dimensional Oscillating Wing Experimental Data	22
<i>Myung Rhee</i>	
Rotor Blade Analysis Using the Mixed Finite-Element Method	24
<i>Gene Ruzicka, Dewey H. Hodges</i>	
Three-Component Velocity Measurements in the Wake of a Rotor in Hover	25
<i>Alan J. Wadcock, Gloria K. Yamauchi, James T. Heineck</i>	
Evaluation of Aeronautical Design Standard-33 Using a UH-60A Black Hawk	26
<i>Christopher L. Blanken, David R. Arterburn, Luigi S. Cicolani</i>	
Vision Model Applications to Display Optimization	27
<i>James Larimer, Jennifer Gille</i>	
Human Factors Field Evaluation of Cockpit Display of Traffic Information (CDTI)	29
<i>Rose Ashford, Vernol Battiste</i>	
Rotorcraft Uninhabited Aerial Vehicle (RUAV) System Identification, Modeling, and Flight Control System Development	30
<i>Mark B. Tischler, Luigi S. Cicolani, Jason D. Colbourne, Chad R. Frost</i>	
Piloted Simulation Investigation of Helicopter Flight Envelope Tactile Cueing	32
<i>Matthew S. Whalley</i>	
Tilt-Rotor Noise Reduction	33
<i>Mark D. Betzina, Cahit Kitaplioglu, Khanh Q. Nguyen</i>	
A Numerical and Experimental Study of Wind Turbine Unsteady Aerodynamics	35
<i>Earl Duque, Robert Kufeld</i>	
Analysis of On-Blade Control	36
<i>Mark V. Fulton</i>	
Full-Span Tilt-Rotor Aeroacoustic Model	37
<i>Megan S. McCluer, Jeffrey L. Johnson</i>	
Active Control of Tilt-Rotor Aeroacoustics	38
<i>Khanh Q. Nguyen, Doug L. Lillie</i>	
Tilt-Rotor Noise Reduction Study	39
<i>Thomas R. Norman</i>	
Isolated Tilt-Rotor Aeroacoustics	40
<i>Gloria Yamauchi, Larry Young, Earl Booth</i>	
Single-Point and Multi-Point Aerodynamic Shape Optimization of a High Speed Civil Transport	41
<i>Susan Cliff</i>	
Resound Microphone Wind Noise Reduction	43
<i>Clifton Horne, Paul T. Soderman</i>	
Stealth Technology Reduces Airframe Noise	44
<i>Paul T. Soderman</i>	

REVOLUTIONARY TECHNOLOGY

Improved Rotorcraft Airfoil Designs Using Genetic Algorithms	45
<i>David W. Fanjoy, William A. Crossley, Anastasios Lyrantzis, Sesi Kottapalli</i>	
Overset Structured Grids for Unsteady Aerodynamics	46
<i>Robert L. Meakin</i>	
Planar Doppler Velocimetry: Three-Component Velocity Measurements in a Full-Scale Rotor Flow Field	48
<i>Michael S. Reinath, Robert L. McKenzie</i>	
Photonic Switching Using Light Bullets	50
<i>Peter M. Goorjian</i>	
A Computational Model of Situational Awareness	51
<i>Robert J. Shively</i>	
A Computational Tool for Rotor Design	53
<i>Roger Strawn</i>	
Java PathFinder: A Tool for Verifying and Validating Software	54
<i>Guillaume Brat, Klaus Havelund, Seungjoon Park, Willem Visser</i>	
An Electromagnetic Actuator for Helicopter Rotor Active Control	55
<i>Brent Wellman, Robert A. Ormiston</i>	
MATRIX_x Automated Testing Tool	56
<i>Ann Patterson-Hine, Joel Henry</i>	
Nanoelectronics Modeling	56
<i>M. P. Anantram, Liu Yang, T. R. Govindan, Jie Han, Alexei Svizhenko</i>	
Plasticity and Kinky Chemistry of Carbon Nanotubes	58
<i>Deepak Srivastava, Fedor Dzegilenko</i>	
Characterization of Carbon Nanotubes under Deformation	60
<i>Richard L. Jaffe, Liu Yang, Jie Han, M. P. Anantram</i>	
Computational Quantum Optoelectronics for Information Technology	61
<i>C. Z. Ning, S. C. Cheung, P. M. Goorjian, J. Li, A. Liu</i>	
A Liquifier for Mars Surface Applications	62
<i>Louis J. Salerno, Ben Helvensteijn, Peter Kittel</i>	
Integration of Pressure-Sensitive Paint Data to Obtain Loads	63
<i>James Bell</i>	
Wind Tunnel Testing with Fast Time-Response PSP	64
<i>Edward Schairer, James Bell</i>	
Distributed Remote Management of Aerospace Data	65
<i>Joan D. Walton, David J. Korsmeyer</i>	
Release of Distributed Collaborative Virtual Wind Tunnel	67
<i>Steve Bryson, Bryan Green, David Whitney, Sandy Johan, Leslie Keely, Michael Gerald-Yamasaki, Creon Levit</i>	

Wake Flow in Adverse Pressure Gradient	68
<i>Dave Driver</i>	
V-22 Osprey Shipboard Interactional Aerodynamics Investigation	69
<i>Kurt Long, Greg Zilliac</i>	
Distortion and Elevated Growth of Instabilities by Vortices Induced by Free-Stream Nonuniformity	71
<i>Johnathan H. Watmuff</i>	
The Effects of Thin Paint Coatings on the Aerodynamics of Semi-Span Wings	72
<i>Edward Schairer, Rabi Mehta, Mike Olsen</i>	
Three Degree-of-Freedom Architecture for Hand-Controllers and Robots	74
<i>Bernard D. Adelstein, Peter Ho</i>	
Performance of the COSMOS Multi-Level Parallelism Molecular Dynamics Code on the 512 CPU Origin System	75
<i>James R. Taft</i>	
Space Technology and CFD Applied to the Development of the DeBakey Heart Assist Device	76
<i>Cetin Kiris, Dochan Kwak</i>	
 ACCESS TO SPACE	
Application of Rotary-Wing Technologies to Planetary Science Missions	78
<i>Larry A. Young</i>	
Ballistic Range Tests Verify Stability of a Loaf-Shaped Entry Vehicle	79
<i>Peter Gage, Gary Allen, Chul Park, Jeff Brown, Paul Wercinski, Tim Tam</i>	
Aerothermal Analysis of X-33 Elevon Control Surface Deflection	80
<i>Dean Kontinos, Dinesh Prabhu</i>	
CFD Analysis of Arc-Jet and Flight Environments for the B-2 Flight Experiment	81
<i>Mark Loomis, Grant Palmer</i>	
Web-Based Analyses for Vehicle Engineering	82
<i>Michael Wright, Peter Gage, Dinesh Prabhu, Periklis Papadopoulos, Joe Olejniczak, Dave Olynick</i>	
Aerodynamic Shape Optimization of the X-37 Configuration for Improved Stability and Performance	84
<i>Susan Cliff</i>	

Space Science Enterprise

Overview	87
----------------	----

EXO BIOLOGY

Tracer-Gas Production and Consumption in Microbial Mats	90
<i>Brad M. Bebout</i>	

Synthesis of Organic Molecules in the Fracture Zone of Meteorite Impacts on Europa	90
<i>Jerome G. Borucki, Bishun N. Khare</i>	

Impacts and Meteorite Organic Compounds	92
<i>George Cooper, Friedrich Horz, Alanna O'leary, Sherwood Chang</i>	

Biogeochemistry of Early Earth Photosynthetic Ecosystems: Production of Hydrogen and Carbon Monoxide	92
<i>Tori M. Hoehler, Brad M. Bebout, David J. DesMarais</i>	

Evolutionary Relationships of Stromatolite-Building Cyanobacteria	94
<i>Linda Jahnke, Kenneth Cullings, Detlev Vogler, Harold P. Klein</i>	

Astrobiology Leonid Meteor Shower Mission	95
<i>Peter Jenniskens, Steven J. Butow, Mark Fonda</i>	

Exploring Evolution Without a Genome	97
<i>Michael H. New, Andrew Pohorille</i>	

Reduced Nitrogen for an Acidic Early Ocean	98
<i>David P. Summers</i>	

Search for the Upper Temperature Limit of Multicellular Organisms Not Seen by Traditional Environmental Researchers (MONSTERS)	100
<i>Jonathan Trent</i>	

Prebiotic Peptide Synthesis	102
<i>Arthur L. Weber</i>	

ASTROPHYSICS

The Nearby Stars (NStars) Project	103
<i>Dana E. Backman</i>	

Observations of Extrasolar Planets	103
<i>Tim Castellano</i>	

Composition of Dust Along the Line of Sight Toward the Galactic Center	104
<i>Jean Chiar, Alexander Tielens, Douglas Whittet</i>	

Organic Matter in the Outer Solar System	106
<i>Dale P. Cruikshank, Ted L. Roush, Yvonne J. Pendleton, Cristina Dalle Ore, Tobias C. Owen, Thomas R. Geballe, Catherine de Bergh, Bishun N. Khare</i>	

AIRES—The SOFIA Facility Spectrometer	106
<i>Edwin Erickson, Michael Haas, Sean Colgan</i>	
Conceptual Study of NGST Science Instruments	108
<i>Thomas Greene, Kimberly Ennico</i>	
The SOFIA Telescope Assembly Alignment Simulator	109
<i>Michael R. Haas, David S. Black, Jeffrey C. Blair, Paul A. Cardinale, Nghia N. Mai, Michael S. Mak, John A. Marmie, Michael J. McIntyre, David D. Squires, Eric Stokely, Ka-cheung Tsui, Bryant C. Yount</i>	
The Center for Star Formation Studies	110
<i>D. Hollenbach, K. R. Bell, P. Cassen, G. Laughlin</i>	
CCD Photometry Tests for Planet Detection	111
<i>David G. Koch, William J. Borucki, Jon Jenkins, Larry D. Webster, Fred Witteborn</i>	
Minimizing Infrared Stray Light on SOFIA	112
<i>Allan W. Meyer, Sheldon M. Smith, Chris T. Koerber</i>	
Identification of Nitriles in the Interstellar Medium	113
<i>Yvonne J. Pendleton</i>	
Identification of Hydrocarbons in the Diffuse Interstellar Medium	114
<i>Yvonne J. Pendleton, Louis J. Allamandola</i>	
The SOFIA Water-Vapor Monitor	115
<i>Thomas L. Roellig, Robert Cooper, Anna Glukhaya, Michael Rennick, Brian Shiroyama</i>	
The Interstellar Production of Biologically Important Organics	116
<i>Scott A. Sandford, Max P. Bernstein, Jason Dworkin, Louis J. Allamandola</i>	
 PLANETARY SCIENCE	
Illumination of Young Stellar Disks	118
<i>K. Robbins Bell</i>	
Detection of an Extrasolar Planet	119
<i>William J. Borucki, Douglas Caldwell, David G. Koch, Larry D. Webster, Jon M. Jenkins, Zoran Ninkov, Robert Showen</i>	
Planetary Rings	120
<i>J. N. Cuzzi, J. Lissauer, I. Mosqueira, M. Showalter</i>	
Primary Accretion in the Protoplanetary Nebula	122
<i>J. N. Cuzzi, R. C. Hogan, S. J. Desch, J. M. Paque, A. R. Dobrovolskis</i>	
The Calculation of Molecular Opacities	124
<i>Richard Freedman</i>	
Mars Atmosphere and Climate	124
<i>Jeffrey L. Hollingsworth, Robert M. Haberle, James Schaeffer</i>	

Stability and Chaos in Planetary Systems	127
<i>Gregory Laughlin</i>	
Stability of the Upsilon Andromedae Planetary System	128
<i>Jack J. Lissauer, Eugenio Rivera</i>	
Hydrodynamic Simulations of Asteroid Impacts on Venus	128
<i>Kevin Zahnle, Donald G. Korycansky</i>	

SPACE TECHNOLOGY

Onboard Autonomy and Contingent Planning for Rovers	129
<i>J. L. Bresina, R. Washington, D. E. Smith, K. Golden</i>	
Automated Hardware Design via Evolutionary Search	131
<i>Jason D. Lohn, Silvano P. Colombano</i>	
AutoBayes—Automatic Synthesis of Statistical Data Analysis Programs from Bayesian Networks	133
<i>Bernd Fischer, Tom Pressburger, Johann Schumann</i>	
Propellant Preservation for Mars Missions	134
<i>Peter Kittel</i>	
Verification and Validation of Autonomous Systems	135
<i>Charles Pecheur</i>	
Knowledge Management for Distributed Scientific Project Teams	136
<i>Richard Keller</i>	

Human Exploration and Development of Space Enterprise

Overview	139
-----------------------	------------

ASTRONAUT HEALTH

The Effect of Unloading on the Metatarsal Bone of the Rat	141
<i>Sara B. Arnaud, R. E. Grindeland</i>	
Inducing Presyncope in Men: A Comparison of Two Stimuli	142
<i>Patricia S. Cowings, William B. Toscano, Bruce Taylor</i>	

FUNDAMENTAL SCIENCE

Synaptogenesis in Microgravity (NIH.B1)	143
<i>Deborah Reiss-Bubenheim, Paul Savage</i>	
Visual Motion Integration and Segmentation	145
<i>Lee Stone, Brent Beutter, Jean Lorenceau, Guillaume Masson, Daniel Mestre</i>	

Computational Models of Human Eye-Movement Behavior	146
<i>Lee Stone, Brent Beutter, Miguel Eckstein, Jean Lorenceau</i>	

IMPROVING SPACE TRAVEL

pH Biotelemetry Transmitter	148
<i>John W. Hines, Michael G. Skidmore</i>	
Physiologic Signal Conditioner for Crew Hazards and Error Management	149
<i>John W. Hines, Charlie Friedericks, Robert Ricks</i>	
BIONA-C Inflight Technology Demonstration	150
<i>John W. Hines</i>	
Solid-State Compressors for Mars ISRU	150
<i>John Finn, Lila Mulloth, Bruce Borchers</i>	
Dynamic Modeling of Life Support Systems	151
<i>Cory Finn and Harry Jones</i>	
Activated Carbon from Inedible Biomass	152
<i>John Fisher, Suresh Pisharody</i>	
Mobile Exploration System	154
<i>Richard Alena</i>	
Development of the Vapor Phase Catalytic Ammonia Removal Process	155
<i>Michael Flynn, Bruce Borchers</i>	
Human-Centered Computing Studies on the NASA Haughton-Mars Project	156
<i>William J. Clancey, Maarten Sierhuis, Pascal Lee</i>	
Brahms: Human-Centered Modeling and Simulation	158
<i>Maarten Sierhuis, William J. Clancey, Ron van Hoof</i>	
Human-Centered Computing at Mission Control	160
<i>John O'Neill, Roxana Wales</i>	

TECHNOLOGY TRANSFER

NASA Technology Helps Patients on Earth and Addresses Fundamental Questions on Human Autonomic Function	161
<i>Patricia S. Cowings, William B. Toscano, Hani Rashed</i>	
Perceptual Impact of Predictive Compensation for Time Delays in Virtual Environments	162
<i>Bernard D. Adelstein, Stephen R. Ellis, Jae Y. Jung</i>	
Center for Health Applications of Aerospace Related Technologies (CHAART)	163
<i>Byron Wood, Louisa Beck, Brad Lobitz, Matt Bobo, Cindy Schmidt, Jian Zheng</i>	

ASTROBIOLOGY IMPLEMENTATION

Geothermal Springs Camera and Sensor Probe	164
<i>Jonathan Trent, John W. Hines, Charlie Friedericks, Richard Daily</i>	

Earth Science Enterprise

Overview	167
-----------------------	------------

ECOSYSTEM SCIENCE AND TECHNOLOGY

A Design Model for the Digital Array Scanned Interferometer	169
<i>Stephen E. Dunagan, Philip D. Hammer</i>	
Fires, Floods, and Deforestation—Disaster Management Using Remote Sensing Technology	170
<i>James A. Brass, Vincent Ambrosia, Robert Higgins</i>	
Modeling Leaf and Canopy Reflectance	171
<i>Lee Johnson, Christine Hlavka</i>	
New Approaches to Using Remotely Sensed Data for Mapping Biophysical Variables	172
<i>Jennifer Dungan, Joseph Coughlan</i>	
Satellite Estimates of Terrestrial Biomass and the Effects of Deforestation on the Global Carbon Cycle	172
<i>Christopher Potter, Steven Klooster, Vanessa Brooks Genovese, Alicia Torregrosa, Matthew Bobo</i>	
Urban Dynamics—Analyzing Land Use Change in Urban Environments	174
<i>William Acevedo, Lora R. Richards, Janis T. Buchanan, Whitney R. Wegener</i>	

ATMOSPHERIC CHEMISTRY AND DYNAMICS

Calculation of Global Warming Potentials	176
<i>Timothy J. Lee</i>	
Environmental Research Aircraft and Sensor Technology—New Technologies for Earth Science	177
<i>Stephen S. Wegener, James Brass</i>	
Estimation of Aerosol Direct Radiative Effects from Satellite and In Situ Measurements	178
<i>Robert W. Bergstrom, Philip B. Russell, Beat Schmid, Jens Redemann, Dawn McIntosh</i>	
Quantifying the Intercontinental and Global Reach and Effects of Pollution	180
<i>Robert B. Chatfield, Zitan Guo</i>	
SAGE III Ozone Loss and Validation Experiment	182
<i>Michael Craig, Stephen Hipskind, Wendy Dolci</i>	

Stratospheric Tracer-Field Measurements with a New Lightweight Instrument: The Argus Spectrometer	182
<i>Max Loewenstein, Hansjürg Jost, B. Jeffries Greenblatt</i>	
TRMM/Large-Scale Biosphere Atmosphere Experiment in Amazonia (LBA)	183
<i>Steve Hipskind, Michael Craig, Tom Kalaskey</i>	
 ATMOSPHERIC PHYSICS	
Corrections and Additions for the HITRAN Water Vapor Spectroscopic Database	185
<i>Lawrence P. Giver, Charles Chackerian, Jr., David W. Schwenke</i>	
How Effectively Can Freeze-Drying by Optically Thin, Laminar Cirrus Dehydrate Air Rising Slowly Across the Tropical Tropopause	185
<i>Eric Jensen, Andrew Ackerman, Leonhard Pfister</i>	
Lofting of Soot Particles into the Middle Atmosphere by Gravito-Photophoresis	186
<i>Rudolf F. Pueschel, Guy V. Ferry, Anthony W. Strawa</i>	
Physical and Chemical Properties of Aerosols and Cloud Particles.....	187
<i>Anthony W. Strawa, Rudolf F. Pueschel, Katja Drdla, Guy V. Ferry, Max Loewenstein, Paul Bui</i>	
Quantifying Denitrification and Its Effect on Ozone Recovery	188
<i>Azadeh Tabazadeh</i>	
Reduction of Trade-Cumulus Cloud Cover Due to Solar Heating by Dark Haze	189
<i>Andrew Ackerman</i>	
Uncertainty and Validity of Aerosol Radiative Forcing Determinations	191
<i>Peter Pilewskie, Warren Gore, Larry Pezzolo</i>	

Aero-Space Technology Enterprise



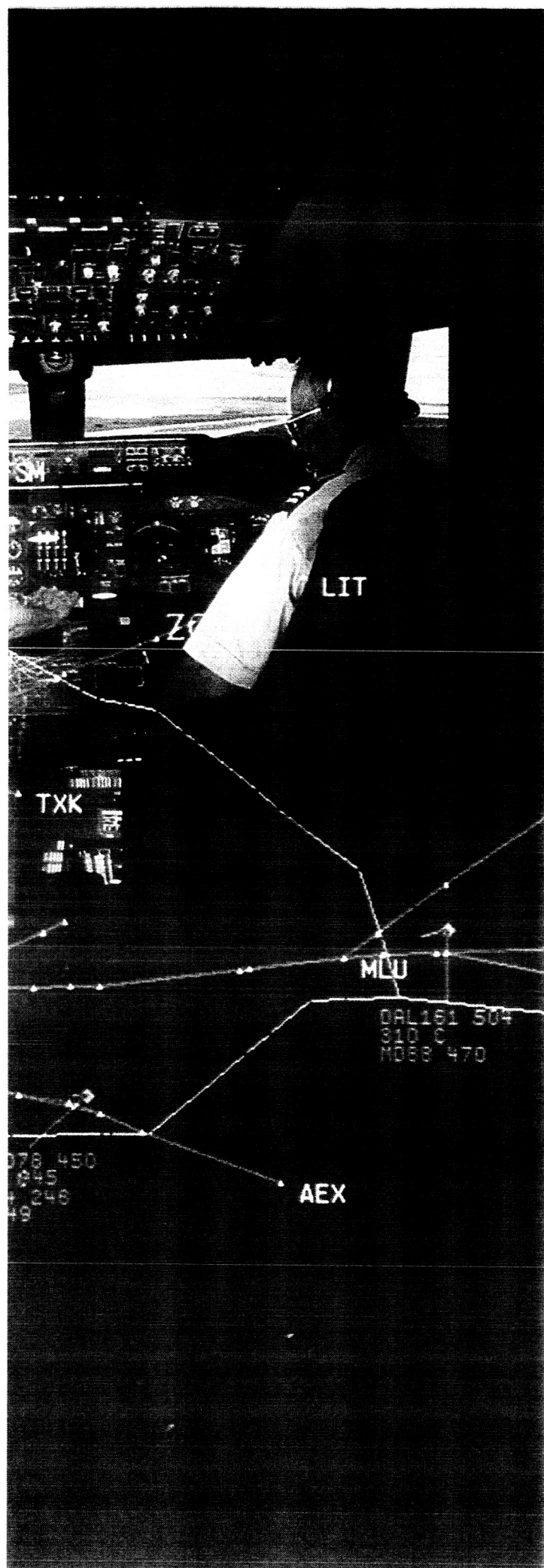
Overview

NASA's mission for the Office of Aero-Space Technology (OAT) Enterprise is to pioneer the identification, development, application, and commercialization of high-payoff aeronautics and space transportation technologies. The Enterprise's research and technology programs promote economic growth and contribute to national security through advances that will lead to a safe and efficient national aviation system, affordable and reliable space transportation, and improved information management systems.

The Agency manages principally through Enterprises. The OAT Enterprise manages through a carefully defined set of technology areas that are aligned with designated Center Missions. Lead Centers have the responsibility to manage the implementation and execution phases of technology programs. To achieve this mission, NASA has designated Ames Research Center as the Center of Excellence for Information Technology and has delegated to Ames the lead role for basic research in Aviation Operations Systems, Information Systems Technology, and Rotorcraft. In addition, Ames is the NASA Lead Center for focused programs in Aviation System Capacity and High-Performance Computing and Communications. Ames also leads the Enterprise in the core competency areas of human factors research, air-traffic management, information systems technologies, rotorcraft, vertical/short takeoff and landing technology, and thermal protection systems technology.

The Slender Hypersonic Aerothermodynamic Research Probe—Lifting #1 (SHARP-L1) is an example of a revolutionary lifting-body concept designed to maximize hypersonic aerodynamic performance. The reusable ultrahigh-temperature ceramic composite (UHTC) material on the sharp leading edge will allow this newly shaped vehicle to withstand the nearly 5000 °F temperatures of reentry

NASA Technology at work in the Nation's Air Traffic Management System.



into the atmosphere and to provide dramatically improved spacecraft flight performance and safety.

The plans and goals of the OAT Enterprise directly support the national policy in both aeronautics and space that is documented in "Goals for a National Partnership in Aeronautics Research and Technology" and the "National Space Transportation Policy." The Aero-Space Technology Enterprise has three major technology goals. The first, Global Civil Aviation, enables the Nation's leadership in global civil aviation through safer, cleaner, quieter, and more affordable air travel. The second, Revolutionary Technology Leaps, revolutionizes air travel and the way in which aircraft are designed, built, and operated. And the third, Access to Space, enables the full commercial potential of space research and exploration. The following paragraphs highlight Ames Research Center's accomplishments in FY99 toward achieving the goals of the Enterprise.

Global Civil Aviation

Air transportation has become an essential component of the economic progress of the United States. Efficient aviation operations assist in domestic industrial progress and help U.S. businesses to compete in the increasingly global marketplace. Aviation products are also a major contributor to a positive U.S. industrial balance of trade. Projections linked to world economic growth suggest that the demand for air travel will triple over the next 20 years. To preserve the Nation's economic health and the welfare of the traveling public, NASA must provide technology advances for safer, cleaner, quieter, and more affordable air travel. Ames has unsurpassed expertise in key areas that are requisite for addressing these challenges. These include human-centered air-traffic management automation tools, innovative rotorcraft and short takeoff vehicles, integrated design-automation tools, and technologies for managing and communicating information on every level. Ames maintains key national facilities that are crucial for performing the basic and applied research needed to support the U.S. aerospace industry. These efforts are all part of Ames' contribution to the objectives of safety, capacity, and affordability.

Airlines and businesses lose billions of dollars annually as a result of delays and lost productivity owing to weather and traffic congestion in the current

airspace system. Under the Aviation System Capacity program, Ames has developed air-traffic management decision-support tools such as the Active Final Approach Spacing Tool (aFAST) component of the Center/TRACON Automation System (CTAS). The success of the CTAS system has led to widespread Federal Aviation Administration (FAA) acceptance of the system including plans to field CTAS at numerous major airports across the country. Ames also leads in the development of innovative vehicles, such as the Civil Tilt Rotor transport, that lay the foundation for changes in airport operations to help decrease aviation congestion.

While increasing aviation system capacity and affordability, Ames is improving safety with innovative research into new aircraft crew station designs and display systems, and human-centered air-traffic controller station design. In addition, advanced neural network control systems promise the ability to autonomously reconfigure a vehicle so that it can survive the failure of virtually any of its systems.

A major challenge in deploying rotorcraft vehicles to alleviate air-traffic congestion is noise abatement. Ames projects are providing revolutionary technological advances in aeroacoustics including Higher Harmonic Control (HHC) for blade-vortex interaction noise reduction, phased microphone array technology, and development of a Tilt Rotor Aeroacoustic Model (TRAM).

Revolutionary Technology Leaps

NASA's charter is to explore high-risk-technology areas that can revolutionize air travel and create new markets for U.S. industry. The technology challenges for NASA include eliminating the barriers to affordable and environmentally friendly high-speed travel, expanding general aviation, and accelerating the application of technological advances to increase design confidence and decrease design cycle time.

Next-generation design tools will revolutionize the aviation industry, and their effect will benefit all three OAT Enterprise goals, contributing to every technology objective. Ames' aerospace and information technology research programs are developing aerospace-vehicle design tools that integrate the design system with performance analysis and high-accuracy computational and wind tunnel performance testing. These Ames-developed systems have demonstrated order-of-magnitude

improvements in the time required to develop and validate a successful design. The Control Designer's Unified Interface (CONDUIT) technology, developed at Ames to greatly reduce the time required to design control systems, is now in widespread use in both government and industry. Additional research at Ames in information technology will elevate the power of computing tools to artificial domain experts through application of fuzzy logic, neural networks, and other new artificial intelligence methods. New tools will integrate multidisciplinary product teams, linking design, operations, and training databases in order to dramatically cut design cycle times and improve operational efficiency. Ames' accomplishments include the application of neural networks and genetic algorithms to real-time reconfiguration of integrated flight controls to alleviate system failures, to aerodynamic optimization design and analysis tools, and to the Environmental Research Aircraft and Sensor Technology (ERAST) flight program.

Access to Space

Low-cost space access is key to realizing the commercial potential of space and to greatly expanding space research and exploration. By integrating aviation technologies and flight operations principles with commercial launch vehicles, a tenfold reduction in the cost of placing payloads in low-Earth orbit is anticipated within the next decade. High reliability and rapid turnaround are the necessary first steps in delivering payloads on time with smaller ground crews. NASA has initiated research on a broad range of technology advancements that have the potential to reduce costs well beyond the initial reusable launch vehicle goals. Involved are new technologies and the integration of aeronautical principles such as

air-breathing propulsion and advanced structures. This will enable a cost-to-orbit that can be measured in hundreds, not thousands, of dollars per pound. Additional innovative work in the thermal protection of interplanetary spacecraft and in autonomous vehicle systems promises to decrease the mass of interplanetary spacecraft while dramatically improving their reliability and performance.

Ames is developing new thermal protection systems that will enable radical improvements in vehicle entry performance. If forced to de-orbit in an emergency, current spacecraft, such as the space shuttle, have very limited cross-range capability; consequently, the crew has very few available landing sites. Dramatic improvements in thermal protection technology, such as the SHARP (Slender Hypervelocity Aerothermodynamic Research Probe), will allow radically different aerodynamic shapes that will lead to dramatic improvements in cross-range capability. Advanced sensor technology and intelligent vehicle health management research will provide order-of-magnitude decreases in the cost and time required to inspect and refurbish reusable launch vehicles. These Ames technologies are at the heart of system-wide improvements in the launch-to-low-Earth-orbit space transportation market.

Since their inception, aviation and space transportation have been exciting and challenging areas of scientific and engineering endeavor. The basic aerospace paradigm is shifting from large hardware developments to information-based design and data system management. As NASA's Center of Excellence for Information Technology, Ames Research Center's contribution will continue to grow throughout the new century.

Direct-To Controller Tool

Heinz Erzberger, Dave McNally

Instead of being able to fly the most efficient route to a destination, aircraft operators in today's air traffic control system are usually constrained to follow established airways that are often composed of inefficient route segments. Current air traffic control user-interface inefficiencies inhibit controllers from issuing user-preferred routes, even under light traffic conditions. The objective was to develop and validate a controller tool that identifies and facilitates time-saving direct routes in en route (or "Center") airspace. The Direct-To Controller Tool identifies aircraft that can save at least 1 minute flying time by

flying direct to a downstream fix along their route of flight. A list ordered by time-savings is displayed on the controller's monitor showing the call sign, time savings, Direct-To fix, wind-corrected magnetic heading to the fix, and conflict status for eligible aircraft. A point-and-click button next to the call sign on the Direct-To list activates a trial planning function that allows the controller to quickly visualize the direct route, choose a different fix if necessary, and automatically input the direct route flight plan amendment to the FAA Host computer. The Direct-To Tool (shown in the figure) was implemented in the Center-TRACON Automation System (CTAS) by adding one additional module to the existing software architecture for the Traffic Management Advisor (TMA).

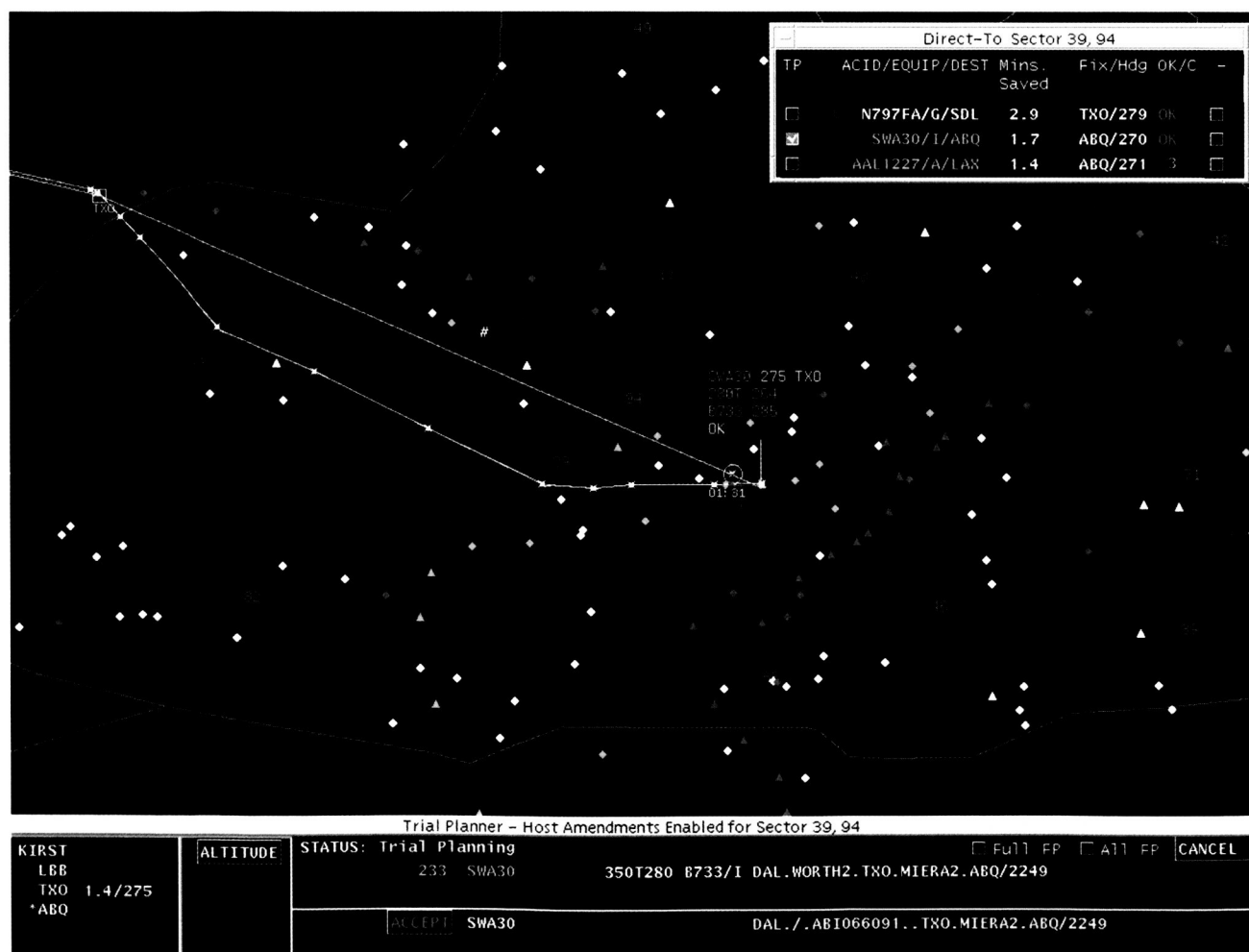


Fig. 1. Direct-To Controller Tool.

Accounting for the wind field is an essential element of the Direct-To algorithm. The CTAS trajectory synthesizer, with its hourly wind update from National Oceanic and Atmospheric Administration's Rapid Update Cycle atmospheric model, compares flying time along the flight plan route and the direct route to identify time-saving routes. Candidate Direct-To fixes are restricted to be within a limit rectangle (1,000 x 600 miles for Fort Worth Center airspace) to prevent aircraft from deviating significantly from planned routes. For large airports within the limit region, where a direct route to the airport is not feasible, Direct-To fixes are limited to an appropriate fix along the arrival route to the airport.

Analysis of Fort Worth Center traffic data shows a potential average saving of 1,800 minutes flying time per day or about 2.5 minutes per Direct-To aircraft. A controller simulation of Direct-To was conducted at Ames in August 1999. Controller feedback was very favorable and the Fort Worth Center controller team felt the tool was ready for field-test evaluation. A functional test of the Direct-To Tool integrated with the Center Host computer was conducted at the FAA Technical Center in June 1999. The point-and-click flight plan amendment capability was demonstrated with only minor changes (three lines of code) to the CTAS/Host interface software. A provisional patent application has been filed. Future plans call for field-test evaluation of the Direct-To Tool at Fort Worth Center.

Point of Contact: D. McNally
(650) 604-5440
dmcnally@mail.arc.nasa.gov

Active Final Approach Spacing Tool Development

John E. Robinson, Cheryl Quinn, Douglas Isaacson

In many highly congested terminal areas, air traffic controllers often do not provide optimal aircraft runway assignment, sequencing, and spacing while maintaining the public's expected level of safety. NASA and the Federal Aviation Administration (FAA) are continuing to design, develop, and deploy a software-based decision support tool (DST), called the Final Approach Spacing Tool (FAST), for terminal-area air traffic management and control of arrival aircraft. FAST incorporates advanced-knowledge engineering algorithms, accurate trajectory prediction, and a specialized graphical-user interface (GUI) to provide detailed schedule information to TRACON traffic management coordinators and commands to TRACON approach controllers. An early version of this DST, known as *Passive FAST* (pFAST), provided a reduced set of advisories, namely runway assignments and landing sequences. These advisories enabled controllers to achieve a more balanced airport, as well as throughput increases of 9%–13%. The follow-on version of this DST, known as *Active FAST* (aFAST), will provide additional tactical advisory information, namely, heading, speed, and altitude commands. These advisories, if followed, allow reduction of excess-in-trail separation between aircraft at touchdown. Continued research is required to enhance FAST so that it can provide this additional advisory information. This research includes the development of advanced scheduling algorithms and automated conflict-resolution schemes and the definition of an appropriate computer-human interface (CHI).

Figure 1 shows the aFAST GUI with a typical set of passive and active advisories. The passive advisories, runway assignment and landing sequence, are presented as yellow text in the aircraft's full datablock (FDB). In this example, AAL1109 is sequenced No. 2 to runway 18R. The active advisories, heading, and speed are presented as cyan and orange map graphics and text in the aircraft's FDB. In figure 1, the controller is being advised to start turning EGF423 to 100 degrees at the filled diamond and to start slowing DAL1105 to 210 knots IAS at the unfilled circle.

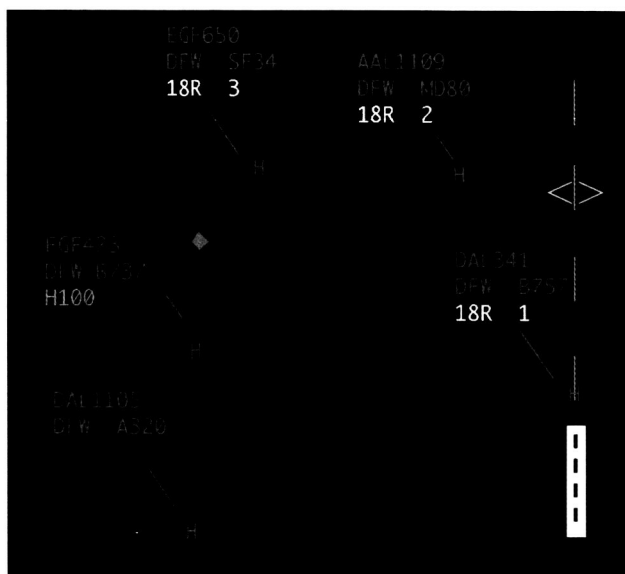


Fig. 1. aFAST graphical-user interface showing typical advisories.

During FY99, a significant amount of the aFAST software infrastructure was completed. The new design addresses several key limitations discovered during the operational testing and deployment of pFAST, and allows easier rapid prototyping of sequencing and conflict resolution logic. In addition, a method for investigating CHI requirements of the aFAST GUI, independent of the aFAST scheduling algorithms, was developed. This approach provided controllers with active advisory information replayed from recorded traffic scenarios. Though the controllers are not actively controlling the aircraft, they issue the advisories and evaluate the user interface. This method decouples the evaluations of the user interface and scheduling algorithms, while maintaining a realistic air traffic environment. A series of "shadow" simulations was conducted to evaluate advisory format, symbols, timing, and use of color. During these simulations, controller reaction times to advisory onset and command issuance were recorded. Following each scenario, questionnaires were administered to assess the usability of and workload associated with aFAST advisories. Results from the study comparing color and monochrome advisory presentation indicate that controllers noticed advisory onset more quickly when those advisories

were presented in color. Controllers also rated the color advisories as producing less screen clutter and lower mental workload.

Point of Contact: J. Robinson
(650) 604-0873
jerobinson@mail.arc.nasa.gov

Distributed Air/Ground Traffic Management

Karl Bilimoria, Steve Green

Distributed Air/Ground Traffic Management (DAG-TM) is an integrated gate-to-gate operational concept in which flight deck crews, air traffic service providers, and aeronautical operational control (AOC) personnel use distributed decision-making to enable user preferences and increase system capacity, while meeting air traffic management requirements (figure 1). The DAG-TM operational concept was developed by NASA (Ames, Langley and Glenn Research Centers) under the Advanced Air Transportation Technologies (AATT) Project, as a detailed instantiation of possible operational modes for Free Flight. It embodies the far-term vision of the AATT Project regarding air traffic operations in the National Airspace System (NAS).

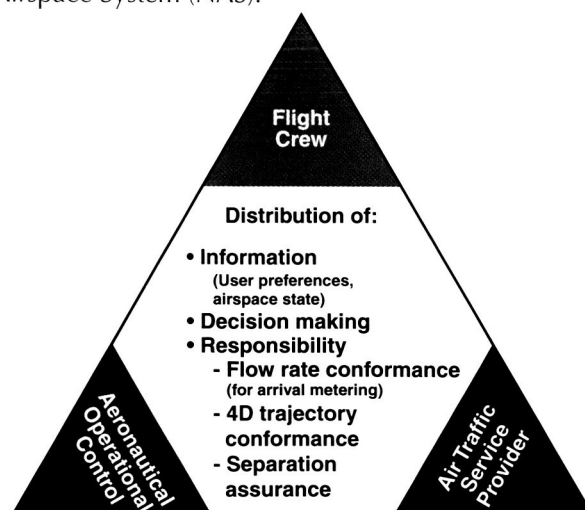


Fig. 1. The DAG-TM triad.

DAG-TM operations will be accomplished with a human-centered operational paradigm enabled by procedural and technological innovations. All user classes (commercial carriers, general aviation, etc.) will be addressed by DAG-TM, with emphasis directed toward ensuring access to airspace resources for the entire user community. Although all users would benefit from DAG-TM, users with higher levels of equipment would benefit even more. Figure 2 depicts some of the airspace problems that arise from dynamic constraints in the NAS; the DAG-TM solutions to these (and other) problems are called concept elements. The DAG-TM operational concept was formulated as a cohesive set of 15 concept elements designed to safely mitigate the extent and effect of dynamic NAS constraints, while maximizing

the flexibility of airspace operations. From these 15 concept elements, 4 were selected for initial studies under the AATT Project. They are (1) En Route Airspace: Collaboration for mitigating local Traffic Flow Management (TFM) constraints; (2) En Route Airspace: Free maneuvering for user-preferred separation and local TFM conformance; (3) En Route Airspace: Trajectory negotiation for user-preferred separation and local TFM conformance; and (4) Terminal Airspace: Self-spacing for merging and in-trail separation of arrivals.

It is noted that Free Maneuvering and Trajectory Negotiation are complementary concept elements that address the problem of inefficient trajectory deviations for separation and local TFM conformance.

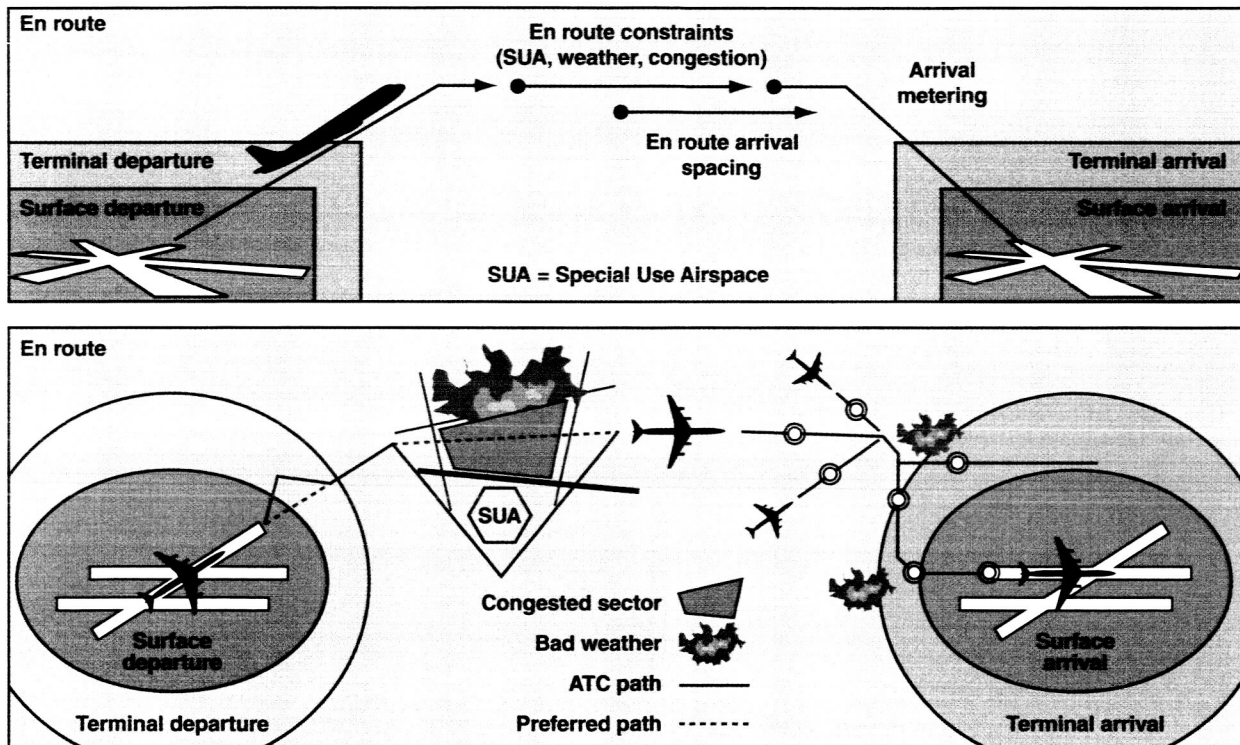


Fig. 2. Examples of airspace problems addressed by Distributed Air-Ground Traffic Management (DAG-TM).

Ongoing research activities under each concept element include concept development, research prototype development, concept validation, cost/benefits assessments, and safety assessments.

Points of Contact: K. Bilimoria/S. Green
(650) 604-1638/5431
kbilimoria@mail.arc.nasa.gov
sgreen@mail.arc.nasa.gov

Information Management for Airline Operations

Roxana Wales, John O'Neill

Ames researchers are investigating airline delays in a collaborative project with United Airlines (UAL). The research team is conducting a systemic study of airline operations and delay situations in United's operations at San Francisco airport in order to identify potential sources of up-to-the-minute, real-time delay information and ways to feed that information, electronically, into the Ames-developed Surface Management System (SMS) technology. Such information will improve traffic movement on the ramp (non-taxiway) area of the airport and increase the overall efficiency of the air traffic system. By collaborating in the project and opening their operations to Ames' researchers, United is benefiting from an increased understanding of their own delay situations, their work-practice procedures, and the ways that information technology and communications systems can be used to better manage their operations and to reduce delays and their effects.

The initial study has focused on United's Shuttle operations. Through a process of intensive fieldwork that includes observations, interviews, and the writing and analysis of field notes, the researchers have identified areas of work procedures that have been analyzed for communication, computer support, and knowledge-management requirements, and for the ways in which these areas organizationally either contribute to or help manage delay situations. Four areas were studied in 1999: (1) the ramp area of the airport where planes are parked at the gate and

where baggage and cargo are loaded and unloaded (see figure 1); (2) the bag room; (3) the station operations center or local control center for operations; and (4) customer service operations.

Additionally, in 1999 the team visited United's operations, data analysis, and scheduling centers at UAL's world headquarters in Chicago to study the larger system environment of UAL and the effect that this environment has on local San Francisco operations.

Preliminary study findings have identified the complex nature of airline delays, problems in teaming structures and the lack of training in procedures, and "disconnects" in information flows across UAL. The study has helped to define a new information environment—one that facilitates information flows and provides the information required for the next generation of decision-making tools at UAL, and one that can also provide delay information to an SMS technology.



Fig. 1. Ramp operations.

Point of Contact: R. Wales
(650) 604-4776
rwales@mail.arc.nasa.gov

Taxiway Navigation and Situation Awareness Operational Integration

Becky Hooey, David C. Foyle, Anthony Andre

The Taxiway Navigation and Situation Awareness (T-NASA) system is a suite of cockpit displays (composed of a head-up display (HUD) and an electronic moving map (EMM) as shown in figure 1) designed in support of the Aero-Space Technology Enterprise research objective to maintain safety while tripling throughput in all weather conditions. The T-NASA taxi HUD uses scene-linked symbology, superimposed on the forward scene, to present taxi route information, situational awareness information, and ground speed. The EMM depicts the cleared taxi route, as well as real-time information about own-ship position, airport traffic, and hold-short locations. The T-NASA system assumes that in the future taxi clearances will be data linked, allowing for both a textual and graphical representation in the cockpit, improved taxi route conformance, and improved traffic flow.

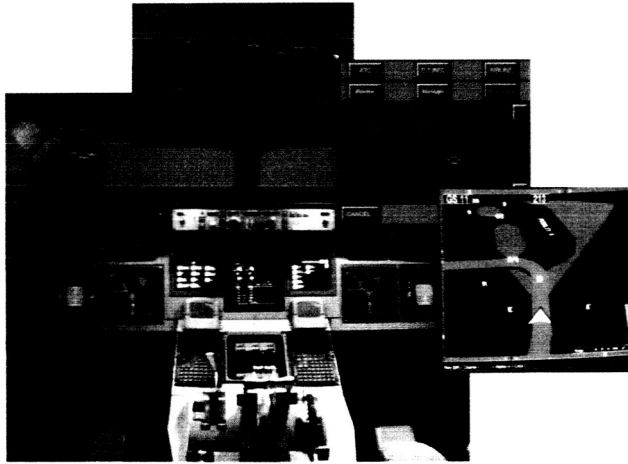


Fig. 1. T-NASA display suite integrated into NASA's Advanced Concept Flight Simulator with insets of the head-up display, data-link display, and electronic moving map.

During FY99, our accomplishments included the development and evaluation of two implementation plans for integrating T-NASA into surface operations. The Transition Implementation, designed to integrate

easily into near-term operations, required minimal procedural and equipment modifications. The most notable modification was the introduction of data-link backup to ATC voice communications. The Future Implementation promised greater efficiency benefits, but required revolutionary modifications to current operations such as the sole use of data link for all routine ATC-pilot communications and the introduction of airborne taxi clearances.

A series of focus groups and a high-fidelity simulation conducted in Ames' Advanced Concept Flight Simulator (ACFS) investigated the operational issues associated with the Transition and Future implementations of the T-NASA displays. The simulation focused on issues raised during the focus groups including the timing and format of taxi clearances, pilot workload, situational awareness, and complacency. Commercial airline crews (18) completed 14 low-visibility (runway visual range (RVR) of 1,000 feet) land-and-taxi scenarios that included both nominal taxi events (such as hold-shorts and route amendments) and off-nominal events (such as near traffic incursions, clearance errors, and display information inconsistencies). All crews completed four baseline scenarios using current standard operations and equipment. In addition, crews completed 10 scenarios with either the Transition Implementation (9 crews) or the Future Implementation package (9 crews).

T-NASA increased taxi speeds by 16% (2.2 knots) over present scenarios while simultaneously eliminating major navigation errors (making a wrong turn, failing to turn) which occurred in 20% of the present scenarios. Further, the revolutionary changes embedded in the Future Implementation package produced large efficiency benefits. Specifically, when taxi clearances were data linked to pilots while airborne (outside outermarker), the time spent stopped after runway turnoff was eliminated (saving approximately 10 seconds per trial), and taxi speeds during this typical bottle-necked phase of taxiing increased by approximately 78% (7.4 knots). Also, the Future Implementation package provided substantial improvements in ATC-pilot communication efficiency by reducing radio congestion and communication errors. These results suggest not only that T-NASA can provide substantial benefits in terms of

the efficiency and safety of surface operations, but that further gains may be realized by incorporating revolutionary changes to surface operations such as the use of data link and airborne taxi clearances.

Point of Contact: D. Foyle
(650) 604-3053
dfoyle@mail.arc.nasa.gov

Hybrid Systems

George Meyer

It is the central tenet of the Free Flight concept that the proper distribution of real-time decision-making between users and air traffic service providers will improve system safety and efficiency. Consequently, it is important to thoroughly understand the trade-off between centralized and decentralized information flow and control for such large systems. Technically such systems are difficult to analyze because they are composed of many objects that interact in a complex and hybrid environment. At present there are no effective analytical tools for use in the design and analysis of such systems. The objective of the present task is to contribute, through university research grants and internal research, to the development of such tools, and to then apply them to the specific case of air traffic management. The participating universities are the University of California at Berkeley, University of Utah, University of Illinois at Chicago, Wayne State University, Case Western Reserve University, and State University of New York at Stony Brook.

One approach that is followed is to try to understand in detail simpler problems and to then generalize the results to the real problem. An example is shown in the figure. The system evolves on a rectangular grid, and only two-dimensional motion along the grid is permitted. There are sources injecting objects representing individual flights into the grid and sinks absorbing the objects. Sources and sinks may represent departure and arrival airports or entry and exit cells at a given flight level. In the figure, the cell at (1,1) is both a sink for gray objects and a source of black objects. Conversely, the cell at (12,14)

absorbs black and injected gray objects, respectively. In the example there are only two colors; in the general case there may be many more. Each object attempts to minimize the total number of steps that it takes to move from source to sink. There are many solutions for each object. Safety dictates that occupation of the same cell or the interchange of cells is forbidden. System cost is the conflict-free total deviation from the sum of individual minima. The following questions are addressed: Does a given departure schedule have a zero-cost solution? Does a given pattern on the grid have a zero-cost solution? In either case if there is a solution, can the solution be constructed with only local information and local rules and decisions, or are global information and central control necessary? If there is no zero-cost solution, then what are the minimum-cost solutions? What is the most efficient modification of the schedule or pattern? The key objective of the research is to obtain answers to these questions analytically and only from the properties of schedules and patterns. Progress has been made in this direction, and theorems have been developed that guarantee local cost-free solutions.

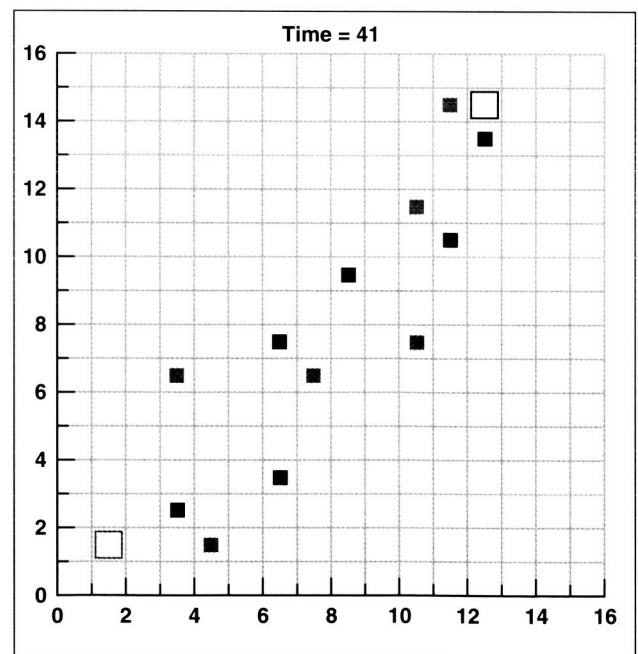


Fig. 1. An example configuration.

For example, according to one theorem, if (1) the source/sink pair is not inline, (2) the pair is separated by a distance that is a multiple of four, (3) the time of departure for one color is a multiple of four, (0, 4, 8,...), and (4) that of the other color is the same but staggered by two, (2, 6, 10,...), then all conflicts are resolvable by local one-one negotiation. Consequently, the pattern in the figure is solvable without central control. On the other hand, several resolvable configurations that require central control have also been found. The objective of the work on this cellular model of air traffic management is to complete the theory for the two-color case, and then extend the results to more colors.

Point of Contact: G. Meyer
(650) 604-5750
gmeyer@mail.arc.nasa.gov

Inflight Activity Breaks Reduce Sleepiness in Pilots

David Neri, Melissa Mallis

Flight operations often result in fatigue, sleep loss, and circadian disruption leading to significant decrements in alertness and performance. These problems can be difficult to detect reliably and to counteract effectively in constrained operational environments such as the flight deck. Left unaddressed, alertness and performance decrements reduce the margin of safety and increase the chances of an incident or accident. One serious challenge facing flight crews is the requirement to maintain vigilance during long, highly automated, and often-uneventful nighttime flights.

Currently there is no system in place to assist flight crews in managing their alertness. Furthermore, strategy choices are severely restricted in the flight deck environment. For example, although previous research has demonstrated the effectiveness of a 26-minute nap in significantly improving subsequent physiological alertness and performance, the FAA does not currently sanction napping on the flight deck. Current Federal Aviation Regulations also mandate that flight crews remain seated ("...each

required flight crewmember on flight deck duty must remain at the assigned duty station with seat belt fastened while the aircraft is taking off or landing, and while it is enroute") with but a few exceptions.

Nevertheless, surveys of flight crews reveal that many use physical activity as a countermeasure during fatiguing flights. Despite this widespread belief by flight crews in the effectiveness of physical activity, there have been no controlled studies of its effect on vigilance, sleepiness, and performance in the aviation environment. This flight simulator study examined whether regularly spaced brief bouts of controlled physical activity (standing up, walking, stretching) combined with social interaction could improve alertness and performance during a long, uneventful, overnight flight requiring extended wakefulness and vigilance. The data obtained from this study support NASA's Aero-Space Technology Enterprise and its objective of reducing the aircraft accident rate.

Fourteen two-man crews flew a 6-hour (2:00-8:00 a.m.) uneventful flight from Seattle to Honolulu in the Ames 747-400 flight simulator. The 14 subjects in the Treatment Group received five short (7-minute) breaks with controlled physical activity and social interaction, spaced hourly during the cruise portion of the flight. An equivalent number in the Control Group received only one 7-minute break in the middle of cruise. Measures of psychomotor vigilance performance, subjective sleepiness, continuous brain wave activity (electroencephalography; EEG), and continuous eye movement activity (electrooculography; EOG) were collected throughout the flight.

Treatment subjects receiving the hourly activity breaks reported significantly greater subjective alertness when it was measured at 5, 15, and 25 minutes post-break, with the strongest effects near the time of the daily circadian trough in alertness (~5:00-6:30 a.m.). The benefit in subjective alertness dissipated by 40 minutes post-break, and there was no evidence of objective vigilance performance improvement when it was sampled from 15 to 25 minutes post-break. There was the expected performance deterioration in both groups because of an elevated sleep drive and the circadian time of day. However, during the latter part of the night, the EEG and EOG measures for the Treatment Group revealed statistically significant post-break reductions relative to the Control Group in slow eye movements, EEG

theta-band activity (two indicators of drowsiness), and episodes of stage 2 and 3 sleep. The figure shows that in the sampled 15-minute periods at 5:40 a.m. and 6:40 a.m., the Control Group pilots were either asleep (stage 2 or 3) or exhibiting significant sleepiness (EEG theta activity) 20%–25% of the time. Conversely, the Treatment Group pilots, who had just received a 7-minute break, fell asleep or exhibited significant sleepiness for less than 5% of the time during the same two periods. Furthermore, higher numbers of Control subjects exhibited sleepy behaviors during these two time periods (12 of 14 subjects) than Treatment subjects (no more than 7 of 13 subjects).

Overall, the physiological data were consistent with subjective reports in indicating that brief, controlled activity breaks were effective in reducing nighttime sleepiness for at least 15 minutes post-break. The breaks provided particular benefits during the early morning hours—the circadian time associated with the greatest vulnerability to fatigue. Furthermore, the breaks continued to mask any underlying sleepiness for up to 25 minutes post-break. The physical activity that occurred as part of the breaks most likely produced enough sympathetic nervous system activation to produce an EEG response characteristic of increased arousal.

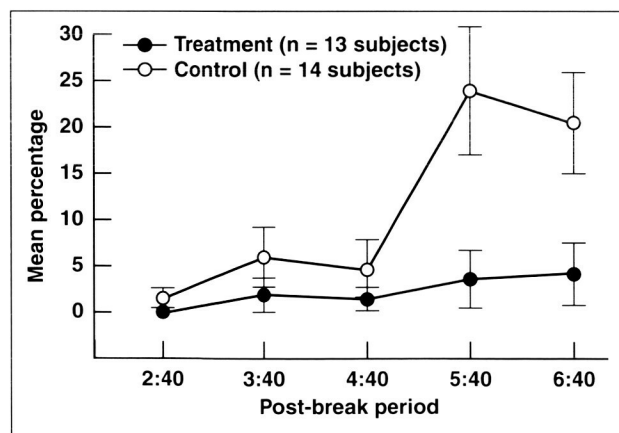


Fig. 1. Mean percentage (± 1 s.e.m.) of combined EEG theta activity and stage 2 or 3 sleep exhibited by pilots on the flight deck during the 15-minute period following a controlled activity break (Treatment Group) or during a corresponding time period (Control Group). The Control Group received only the middle break (ending at 4:40 a.m.).

Controlled activity breaks are not substitutes for adequate sleep, but they do represent a practical, short-term countermeasure to the fatiguing effects of a long nighttime flight, provided appropriate controls are in place to ensure the wakefulness and alertness of the other crewmembers remaining on the flight deck.

Point of Contact: M. Mallis
(650) 604-3654
mmallis@mail.arc.nasa.gov

Communication Strategies for Correcting Errors

J. Orasanu, U. Fischer, C. Van Aken, L. McDonnell

Maintaining safety in high-risk engineered environments like aviation is a team effort that depends crucially on the team members' efficiency in monitoring each other's performance and on their effectiveness in intervening if they consider a decision or action to be unsafe. Unfortunately, analyses of aviation accidents and incidents indicate that pilots, in particular junior pilots, have frequently failed in this important crew function, especially in situations in which their interventions posed a direct challenge to the other crewmember's judgment and decision-making skill. In such situations, junior crewmembers will sometimes only hint at the possibility of a problem rather than tell the captain explicitly to perform a corrective action.

This kind of communication failure has been identified as a "monitoring/challenging error" by the National Transportation Safety Board (NTSB) and was found to occur in over 75 percent of the accidents reviewed. Moreover, monitoring/challenging failures appear to contribute to "plan continuation errors." These are errors in which the crew continues with its planned course of action in the face of cues suggesting that the plan should be reconsidered. The research reported here is an effort to understand communication strategies for correcting crew errors, and looks at differences in strategies as a function of crew position (captain vs. first officer) and of risk and face-threat posed by the problem.

Three studies were conducted to determine (1) what strategies captains and first officers indicate they would use to correct errors in hypothetical situations, (2) what strategies captains and first officers judge most effective in getting them to change their own behavior, and (3) what kinds of communication strategies pilots actually use when confronted with errors in simulated flights. The first two studies were paper and pencil tasks and the third was conducted in a 747-400 simulator.

It was hypothesized that captains would be more direct in correcting first officers than first officers would be in mitigating errors by the captain. However, for both crew positions communications were expected to be more direct during high-risk or emergency situations than during low-risk incidents. In addition to risk, pilots' communications were hypothesized to be sensitive to the degree to which an error implied a threat to the professional "face" of a crewmember. If the other pilot has made an obvious error, calling attention to it may involve a direct challenge to the pilot's status, judgment, or skill. In situations like these, politeness dictates the use of more indirect speech than would be the case in situations that are less face-threatening.

In the first paper and pencil task, participating pilots received descriptions of aviation incidents and were asked to state how they would correct various pilot errors. As predicted, captains were more direct than first officers were: they predominantly used commands, whereas first officers preferred to use hints. The risk level also influenced pilot interventions in the predicted direction: captains and first officers were more direct in high-risk situations. In contrast, pilot responses to varying levels of face-threat of the incidents were not consistent with the predictions made by politeness theory.

The second paper and pencil task examined which types of communication would be most effective in correcting pilot errors. Pilots were asked to rate how effective various communication strategies would be in getting them to carry out the speaker's intent. As shown in figure 1, both captains and first officers favored communications that appealed to a crew concept rather than to any particular status-based model, and consistently rated commands, the most direct communication strategy, as less effective than crew suggestions or preferences.

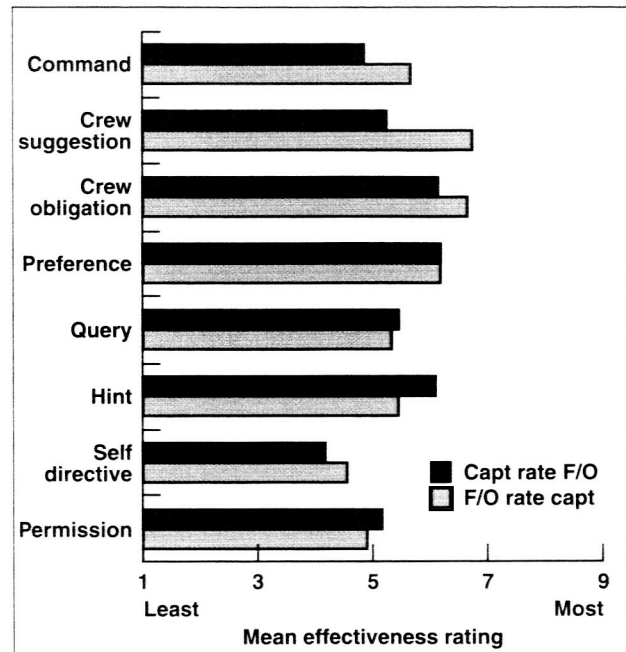


Fig. 1. Captain and first officer mean effectiveness ratings of different communication types.

The third study examined pilot error-challenging strategies during a full-mission simulation study. Errors based on those used in the paper and pencil tasks were scripted into flight scenarios, which participating pilots flew with a research confederate pilot trained to perform the scripted errors. The results of this study indicate that both captains and first officers used error-correcting strategies that supported a positive crew climate, such as strong hints and suggestions. As expected, both captains and first officers were sensitive to risk, and communicated more directly when risk was high. The influence of face-threat was somewhat different for captains and first officers, as expected from their differences in rank.

These findings, which have identified the strategies most effective for mitigating errors in the cockpit, can aid in the development of training under the safety program that helps pilots develop more effective error-correction strategies.

Point of Contact: J. Orasanu
 (650) 604-3404
jorasanu@mail.arc.nasa.gov

Rotor Design Options for Whirl Flutter

C. W. Acree, R. J. Peyran, Wayne Johnson

Coupled wing/rotor whirl-mode aeroelastic instability is the major barrier to increasing tilt-rotor speeds. This research investigated the unusually simple approach of adjusting the chordwise positions of the rotor blade aerodynamic center (a.c.) and center of gravity (c.g.) to improve the stability boundary of the full aircraft. The XV-15 tilt-rotor research aircraft was modeled with the CAMRAD II rotorcraft analysis program; the model was then modified to simulate a thinner wing, which had lower drag but also a lower stability boundary than the baseline wing. Numerous rotor modifications were studied to determine their effects on whirl flutter for the XV-15 with the new wing.

Small stepwise, rearward offsets of the a.c. over 20% of the blade radius created large increases in the stability boundary, in some cases by over 100 knots. The effect grew progressively stronger as the offsets were shifted outboard. Forward offsets of the c.g. had similar but less dramatic effects. An example of a stepped a.c. offset is shown in figure 1, with the unmodified blade for reference. The a.c. offsets were modeled by shifting the entire airfoil section with respect to the elastic axis (EA), as shown in figure 1.

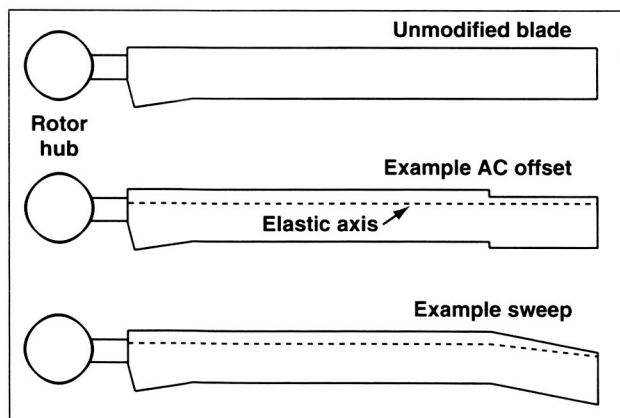


Fig. 1. XV-15 rotor blade planforms: unmodified, stepped offset, and swept (45 degree twist and 1 degree baseline sweep not shown).

The research was extended to include swept blades, which give benefits similar to those of the stepped offsets, but for a much more practical blade configuration. Figure 1 shows an example swept blade with 10-degree a.c. sweep and 5-degree c.g. and a.c. sweep. Although unorthodox, the design is feasible. Control-system (pitch) stiffness was also increased for a further improvement in stability.

Figure 2 summarizes the combined benefits of the example swept blade with doubled control stiffness. Damping of the three unstable whirl modes is plotted against airspeed; the wing/rotor structure is aeroelastically unstable below zero damping. The rotor modifications completely eliminated the instabilities.

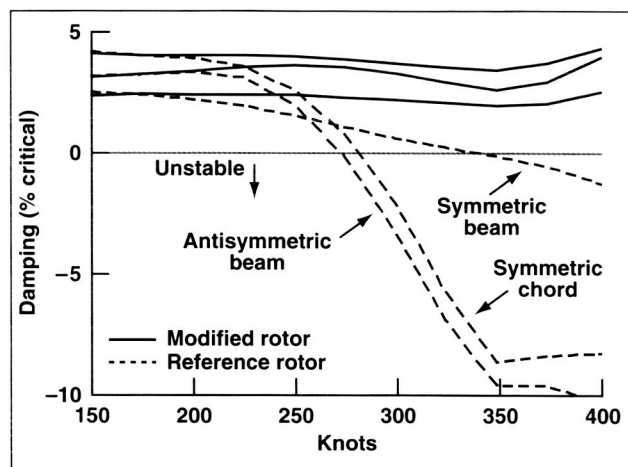


Fig. 2. Whirl-mode damping versus airspeed for the original rotor blade and control system and for the example swept blade with double control-system stiffness. (Modes that were always stable are not shown.)

Point of Contact: C. W. Acree, Jr.
(650) 604-5423
wacree@mail.arc.nasa.gov

Efficient Computational Fluid Dynamics for Rotorcraft Analysis

Frank Caradonna

Airflows over rotorcraft are far more complex and more difficult to predict than those that occur on fixed-wing aircraft. The inability to predict many of these flows is a direct or indirect contributor to the cost, duration, and risk of the rotorcraft development process. For this reason, the application of computational fluid dynamics (CFD) is an important and growing part of the rotorcraft research process. However, rotorcraft aerodynamics is difficult for CFD because the limiting physical problems of rotorcraft differ from those of fixed-wing aircraft for which CFD was originally developed. An example of such a flow is the wake that is shed by the rotor. Such wakes are also generated by conventional aircraft and are made visible in the contrails of high-altitude airliners. The primary difference with rotorcraft is that because of its rotary motion, a rotor never gets far from its shed wake. This adjacent wake strongly determines the performance and acoustics of a rotor. The ability to predict this wake with the required accuracy has been shown to require far greater computational resources (with conventional methods) than is practical for engineering analysis. The objective of this work is to develop new CFD wake-computation methods that are accurate and practical for everyday use.

A new class of CFD methods, specifically designed for engineering analysis, has been developed. The method is a modification of the potential solvers that were an early focus of CFD development. The approach, called "vortex embedding," consists of a means of inserting a freely convecting vortical wake—a capability that such solvers originally lacked. This approach permits the prediction of this wake with a grid system that is orders-of-magnitude smaller (and hence more efficient) than present methods. Until this year, the approach lacked the ability to predict the viscous flow on the rotor surface. This shortcoming has been removed with the development of an overset/hybrid solver that combines the embedding method in the wake region and a Navier-Stokes viscous-flow solver adjacent to the blade surface.

The prediction of tilt-rotor flows is ideal for this method because the high lift of these rotors results in blade-root stall. Recent computations are demonstrating the ability to predict the performance of the XV-15 tilt-rotor performance. The accompanying figure shows experimental and computed figures of merit (a measure of rotor power) for this rotor. It is shown that the figures of merit at higher thrust levels (characteristic of actual operating conditions) is well predicted. The inset in this figure is a visualization of the computed wake that is shed by this rotor.

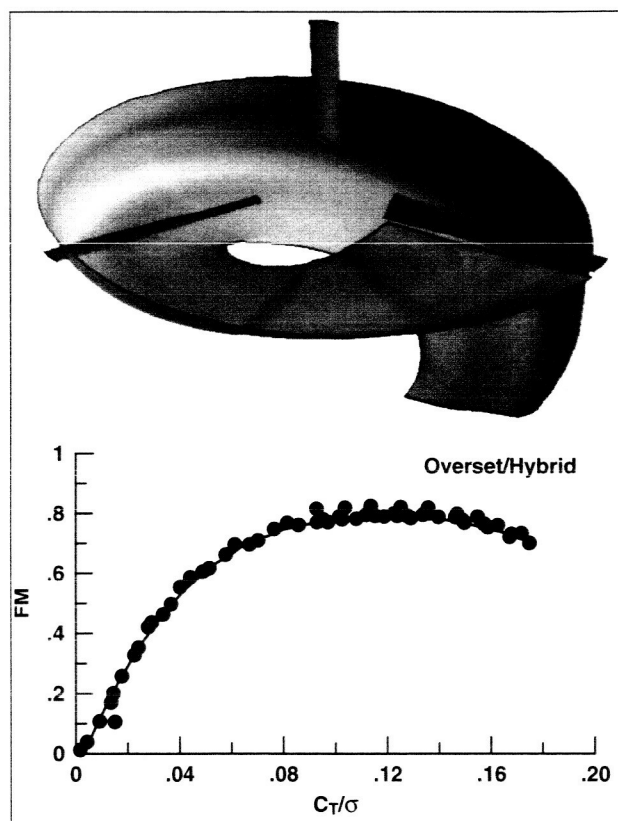


Fig 1. Hybrid overset/imbedded computation of XV-15 hover performance.

Point of Contact: F. Caradonna
(650) 604-5902
fcaradonna@mail.arc.nasa.gov

Analysis of Advanced Rotorcraft Configurations

Wayne Johnson

Advanced rotorcraft configurations are being investigated with the objectives of identifying vehicles that are larger, quieter, and faster than current-generation rotorcraft. A large rotorcraft, carrying perhaps 150 passengers, could do much to alleviate airport capacity limitations, and a quiet rotorcraft is essential for community acceptance of the benefits of VTOL operations. A fast, long-range, long-endurance rotorcraft, notably the tilt-rotor configuration, will improve rotorcraft economics through productivity increases.

A major part of the investigation of advanced rotorcraft configurations consists of conducting comprehensive analyses of vehicle behavior for the purpose of assessing vehicle potential and feasibility, as well as to establish the analytical models required to support the vehicle development. The analytical work of FY99 included applications to tilt-rotor aircraft.

Tilt Rotor Aeroacoustic Model (TRAM) wind tunnel measurements are being compared with calculations performed by using the comprehensive analysis tool (Comprehensive Analytical Model of Rotorcraft Aerodynamics and Dynamics (CAMRAD II)). The objective is to establish the wing and wake aerodynamic models that are required for tilt-rotor analysis and design. The TRAM test in the German-Dutch Wind Tunnel (DNW) produced extensive measurements. This is the first test to encompass air loads, performance, and structural load measurements on tilt rotors, as well as acoustic and flow-visualization data. The correlation of measurements and calculations includes helicopter-mode operation (performance, air loads, and blade structural loads), hover (performance and air loads), and airplane-mode operation (performance). Figure 1 shows an

example of the comparison of TRAM-measured performance with calculations. The figure shows the difference in calculated rotor power obtained by using an aerodynamic model (wing and wake) appropriate for helicopter rotors, instead of a tilt-rotor aerodynamic model. The span loading and wake formation are very different on tilt rotors and helicopters, so it is essential to use model features specific to tilt rotors in order to adequately predict the behavior. Future analyses will be concerned with TRAM tests in the Ames 40- by 80-Foot Wind Tunnel, which will produce data over a much larger operating envelope for two rotors and the airframe, including advanced flow-visualization results, and with XV-15 rotor tests in the Ames 80- by 120-Foot Tunnel in order to obtain tilt-rotor data at a larger scale (although no air loads data) with different blade planform and twist.

The quad tilt-rotor configuration has been proposed in order to meet the objective of a large rotorcraft; it is hoped there will be fewer difficulties

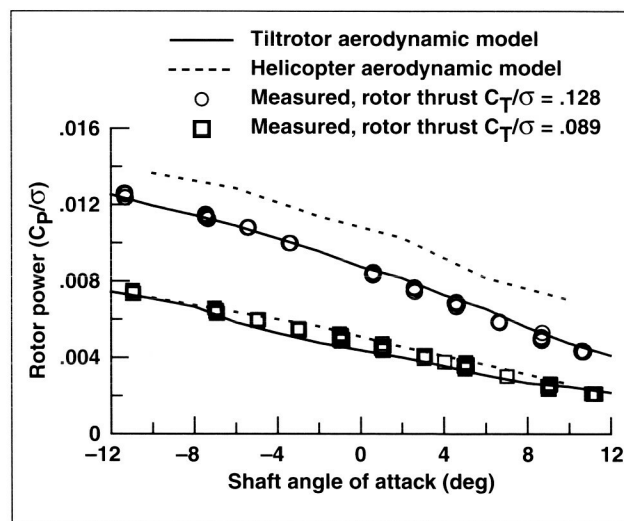


Fig. 1. Comparison of measured and calculated tilt-rotor power; helicopter-mode operation, at wind tunnel speed = 0.15 times rotor-tip speed.

associated with scaling the rotors to large size (since there are four rather than two rotors to lift the gross weight). The technical issues in the development of quad tilt rotors include aerodynamic interference (performance, control, and handling qualities; wing-to-wing, rotor-to-wing, and wing-to-rotor); vibration and blade loads; and whirl flutter. Figure 2 shows results from CAMRAD II calculations for a quad tilt rotor, illustrating the aerodynamic interference issues. The calculations were performed with a rigid airframe and a free-wake model (for 2 wings, and 12 blades on 4 rotors).

The views in figure 2 are from forward/port, for two rotor azimuth angles. Shown are the wing section lift, the rotor blade section thrust, and the wing and rotor-tip vortices. The wing-to-wing aerodynamic interference is evident in the influence of the front-wing tip vortices on the rear-wing span loading, producing an increased loading at the rear-wing tip; this interference will affect efficiency and handling qualities. The rotor-to-wing interference is evident in the loading at midspan of the rear wing. Three-per-revolution loading variation is produced by the rotor-tip vortices, hence the different loading in the two pictures. This interference will produce increased vibration and structural loads. The wing-to-rotor interference is evident in the loading on the rotor blades when in front of the wing, compared to outside the wing, as in the two pictures; this interference will affect prop rotor efficiency, vibration, and blade loads. Also of concern is whirl flutter (coupled aeroelastic stability of the rotor on the flexible wings), since the rear wing has a larger span than the front wing, and thus lower frequencies and less stability if the two wings have the same sectional stiffnesses. Investigations being conducted at Ames Research Center promise design solutions other than stiffer and heavier wings as a means to produce an acceptable level of whirl flutter stability.

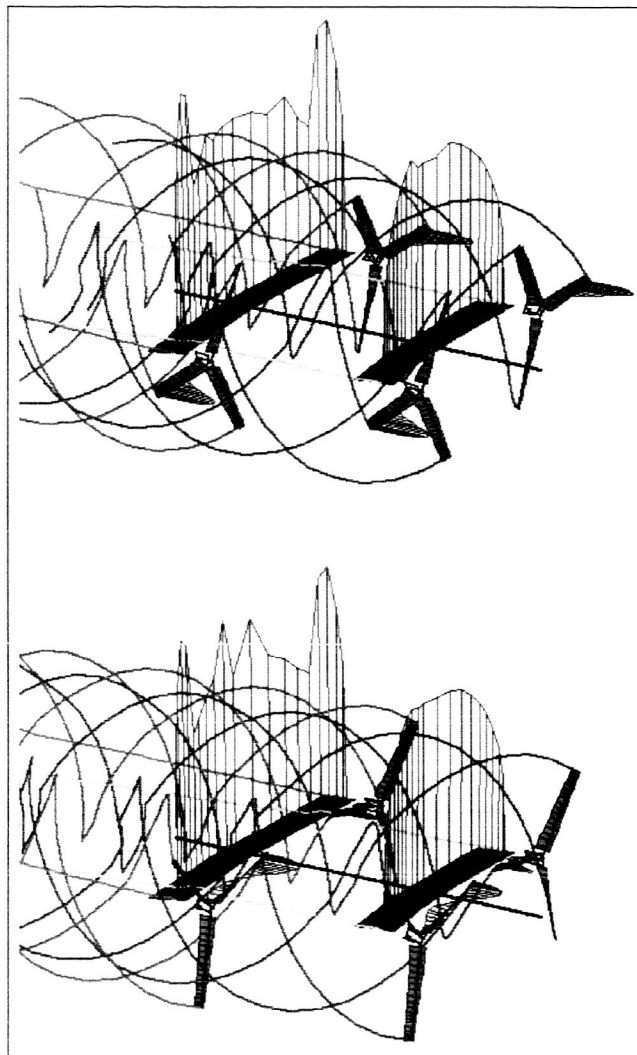


Fig. 2. Analysis of quad tilt-rotor aerodynamic interference (98,000 lb gross weight; flight speed, 250 knots).

Point of Contact: W. Johnson
(650) 604-2242
wjohnson@mail.arc.nasa.gov

Prediction of Rotorcraft Pitch-Link Loads

Sesi Kottapalli

The pitch links of rotor blades are essential hardware that provide direct control to rotorcraft. The pitch-link loads undergo large changes in magnitude as a result of flight conditions that range from those of relatively benign level flight to those associated with severe, complex maneuvers. In the present study, a "complex" maneuver was defined as one that involved simultaneous non-zero aircraft angle of bank (associated with turns) and aircraft pitch rate (associated with a pull-up or a push-over). Also, since a typical rotor blade pitch link operates in a highly dynamic environment, the pitch-link loads obtained from flight tests have associated with them a greater degree of uncertainty. Analytical prediction of pitch-link loads is thus difficult, and methods that provide accurate results are highly desirable. The objectives were (1) to obtain physical insights into the nature of complex maneuvers and (2) to apply neural networks to efficiently characterize maneuver-related rotorcraft blade pitch-link loads. The NASA/Army UH-60A Airloads Program database was used.

Since existing load factors do not represent the above-defined complex maneuvers, a new physics-based parameter, the maneuver-load-factor (MLF) was derived and used. The MLF includes both the aircraft angle of bank and pitch rate, resulting in a single parameter. Figure 1 shows the MLF and the pitch-link loads variations with forward speed. Approximately 80 test data points (with pitch-link loads greater than 1,000 pounds) were considered. The associated neural network application involved five inputs, namely, the MLF and four standard parameters. The neural network output was the peak oscillatory pitch-link load. Figure 2 shows the presently obtained finer correlation (± 400 pounds error-band). This correlation was obtained using a single-hidden-layer, back-propagation neural network with 10 processing elements; it was trained for 600,000 iterations and had a final root-mean-square error of 0.07.

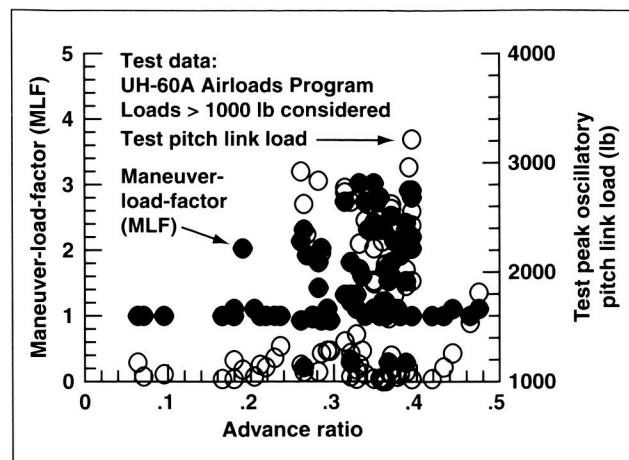


Fig. 1. Maneuver-load-factor and pitch-link load variations with speed (advance ratio).

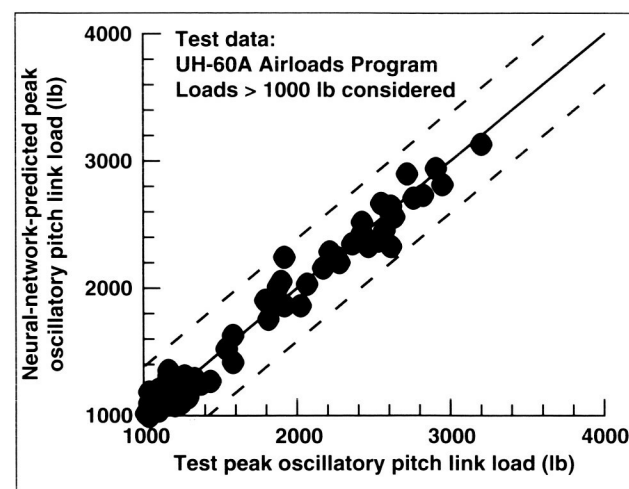


Fig. 2. Pitch-link load correlation using physics- and neural-network-based approach.

Point of Contact: S. Kottapalli
 (650) 604-3092
skotapalli@mail.arc.nasa.gov

Model Hingeless Rotor Dynamics Program

Thomas H. Maier

A wind tunnel experiment was conducted to measure the aeroelastic stability of a soft in-plane hingeless rotor with swept-tip blades. The data from this experiment will be used to assess current helicopter analytical tools and to guide future improvements to these codes. Aeroelastic and aeromechanical stability are important elements in the design of helicopters. Poor design, in this regard, can lead to the loss of prototype aircraft and loads problems, and can limit cyclic annoyances. For this reason it is important for helicopter designers to have analytical tools that accurately predict such phenomena.

The development of accurate analytical methods requires careful comparison of calculations with experimental measurements. These methods, particularly at an early stage in their development, benefit

from test data obtained with simplified rotor models whose properties are accurately characterized. Two such tests have been completed at Ames Research Center. The first test, completed in 1995, was conducted using a rotor with straight blades. The second test was completed in 1999 using a rotor with swept-tip blades. The swept-tip geometry introduces additional bending/torsion coupling and provides data that amplify the importance of the air loading at the tip of the blade. Both types of rotor blades and the swept-tip rotor installed in the wind tunnel are shown in figure 1. Stability of the lag mode is measured by exciting this mode and measuring the decay with the Moving-Block analysis after the excitation is terminated. The excitation is achieved by oscillating the blades root pitch at the regressive lag frequency by using hydraulic actuators in the nonrotating system. Both rotors were tested over a range of forward flight conditions on an essentially rigid test stand in one of the Ames 7- by 10-Foot Wind Tunnels.

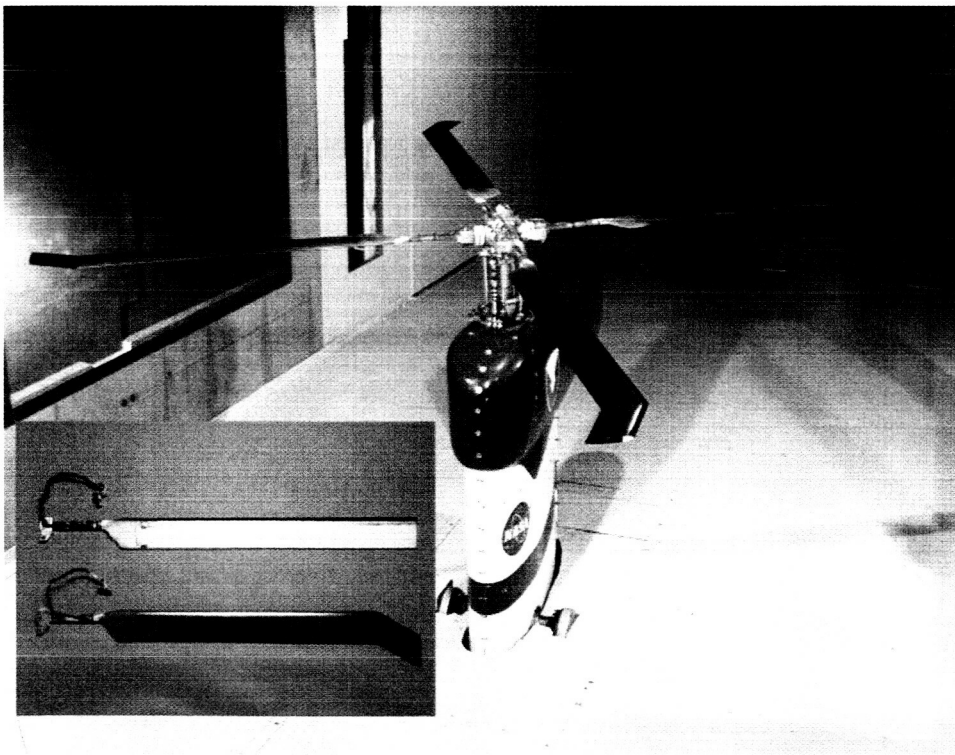


Fig. 1. Isolated rotor aeroelastic stability model with swept-tip rotor in the Army/NASA 7- by 10- Foot Wind Tunnel; straight and swept-tip rotor blades.

In addition to the wind tunnel test, calculations were made with a comprehensive rotorcraft analytical tool, CAMRAD II, to demonstrate current analytical capability. The second figure shows damping measurements of the regressing lag mode for the swept-tip rotor and CAMRAD II calculations. In the figure the damping coefficient, or exponent, is plotted versus the advance ratio (a measure of airspeed, $\mu = V/WR$) for five collective pitch angles. The agreement between analysis and experiment is good for the lowest collective pitch angles; however, the analysis overpredicts damping as the collective pitch angle is increased. Further, the calculations do not capture the up-down-up character of the measurements with increasing advance ratio. An analytical study has been initiated to look at the sensitivity of damping to various physical model parameters and analytical model sophistication.

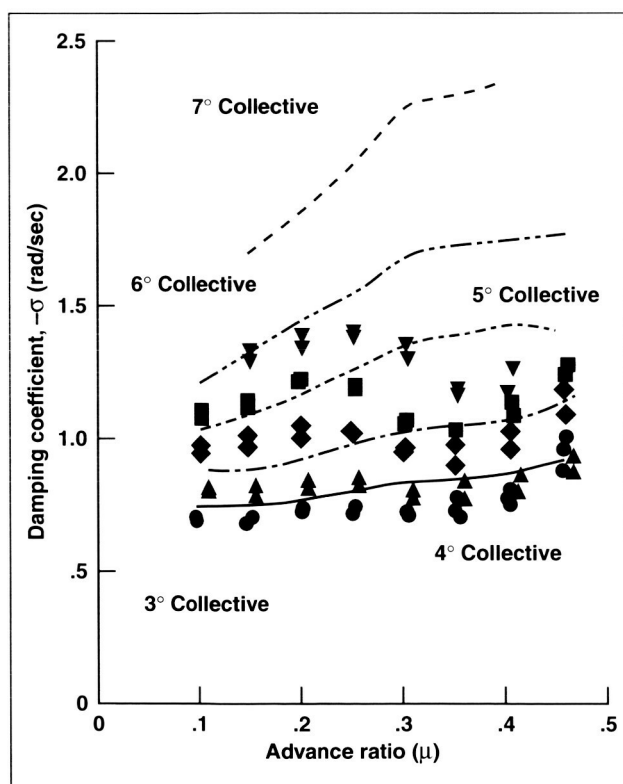


Fig. 2. A comparison of theory and experiment for the swept-tip rotor regressing lag mode stability in forward flight for various collective pitch angles.

Point of Contact: T. Maier
 (650) 604-3643
tmaier@mail.arc.nasa.gov

Active Control of Stall on Helicopter Rotors

Khanh Q. Nguyen

In an effort to expand helicopter flight envelopes, this analytical study explores the potential of using higher harmonic blade pitch to reduce the adverse effects of dynamic stall on rotor blades. Since excessive stall-induced loads can damage rotor structural components, stall severely restricts helicopter maximum speed and loading capabilities. On the other hand, successful control of stall can enhance the utility of helicopters.

The rotorcraft analysis code UMARC (University of Maryland Advanced Rotorcraft Code) was modified for a stall suppression investigation of the UH-60A rotor. At a severe stalled condition, the analysis predicts three distinct stall events spreading over the retreating side of the rotor disk. Prescribed 2-per-rev input can reduce stall moderately, as shown in the figure, where the lift excess is used as a measure of stall; the other input harmonics are less effective. Stall responses to individual input harmonics exhibit highly nonlinear behaviors, rendering the closed-loop controller ineffective in suppressing stall and the combined effects of individual harmonics non-additive.

Point of Contact: K. Nguyen
 (650) 604-5043
knguyen@mail.arc.nasa.gov

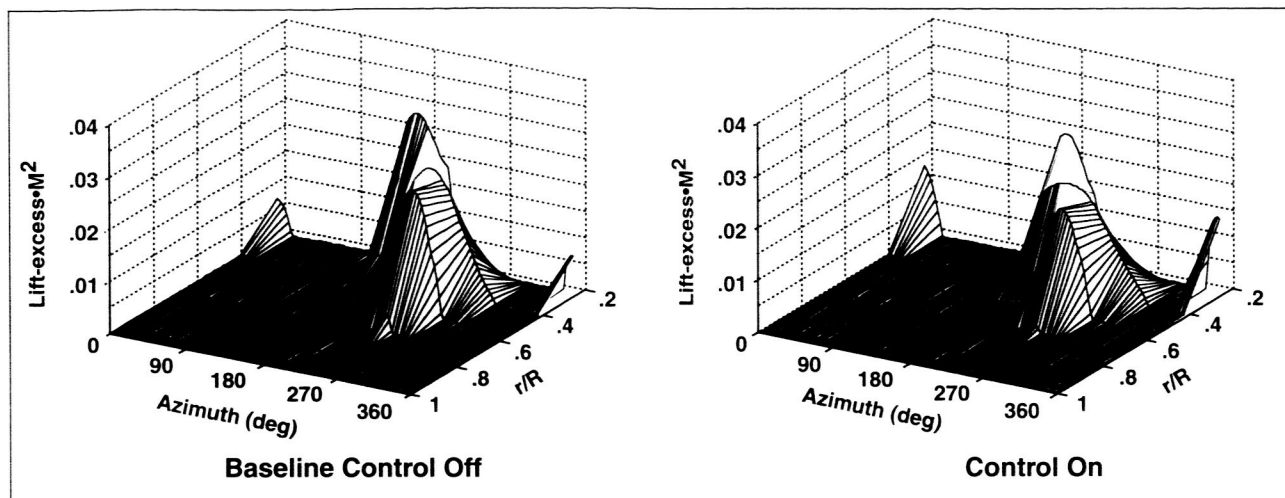


Fig. 1. Effect of higher harmonic input on rotor stall: baseline (left), with 2-per-rev input (right), 102 knots, blade loading C_T/σ 0.13.

Large-Rotor Research Program

Thomas R. Norman, Patrick M. Shinoda,
Stephen A. Jacklin

As part of its Rotorcraft Program, NASA is committed to providing the experimental data necessary to (1) validate newly developed predictive capabilities and (2) provide physical insight into those areas where accurate predictive capability does not yet exist. To make the acquisition of these data possible for large-scale rotor systems, NASA and the U.S. Army have developed a new wind tunnel test stand, the Large Rotor Test Apparatus (LRTA). The LRTA (see figure 1) is designed for testing moderate-to-large helicopter blades and tilt rotors up to 50,000 pounds of thrust and 6,000 horsepower and provides unique capabilities that will support both industry and government rotorcraft test programs.

During the past year, two major milestones were reached in the development of the LRTA. The first was the successful calibration of the LRTA rotor balance, following fabrication and assembly of the LRTA rotor balance calibration facility (figure 2). This calibration effort demonstrated the capability of the LRTA balance design to measure rotor hub loads to

better than 0.5% full-scale. This level of load measurement accuracy is critical to the successful wind tunnel testing of large rotor systems.

The second milestone reached in FY99 was the design, fabrication, and integration of a state-of-the-art digital rotor-control console for use with the LRTA. This new console provides the digital commands and feedback controls necessary to safely "fly" a rotor system in the wind tunnel. In addition, it provides the capability to control the LRTA dynamic

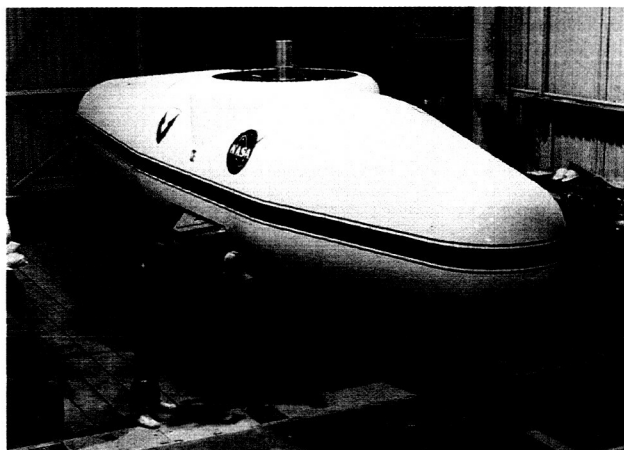


Fig. 1. Large Rotor Test Apparatus.

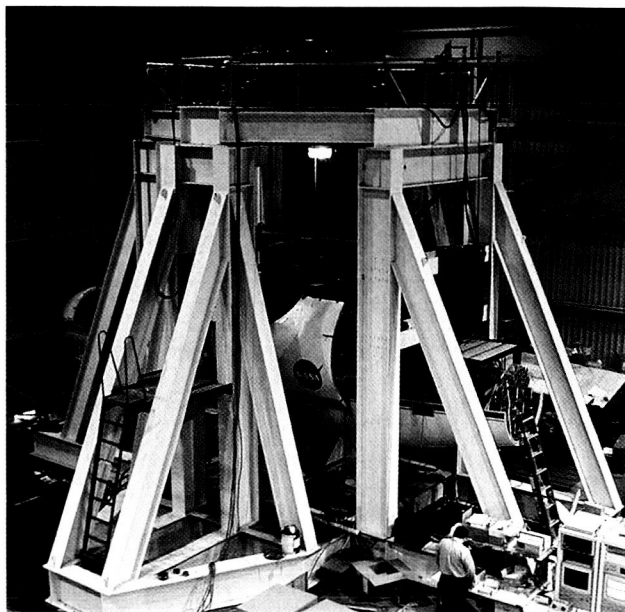


Fig. 2. LRTA rotor balance calibration facility.

actuators, allowing for dynamic high-frequency blade pitch control up to 30 hertz.

With these major milestones met, the LRTA is now ready to become the workhorse facility for NASA's large-rotor experimental programs.

Point of Contact: T. Norman
(650) 604-6653
tnorman@mail.arc.nasa.gov

A Study of Dynamic Stall Using Two-Dimensional Oscillating Wing Experimental Data

Myung Rhee

Dynamic stall produces a significant limitation on the operation and performance of rotorcraft at high-speed. To understand this complex and unsteady aerodynamic phenomenon, a number of studies have been performed to obtain and analyze test data from nonrotating oscillating wings in wind tunnels. Many of these experiments have failed to generate sufficient information to capture the complicated aerodynamic flow characteristics occurring during the dynamic stall process. However, data from one test are now available that afford an opportunity for detailed analysis.

The Army Aeroflightdynamics Directorate performed the test at Ames Research Center in a 7-by 10-foot wind tunnel. The objective of the experiment was to produce high quality data of two-dimensional (2-D) and three-dimensional (3-D) dynamic stall on a semi-span and full-span wing undergoing pitching motions designed to simulate typical rotor blade motions. The airfoil section, a NACA 0015, was tested at a Mach number of 0.3. Various tests were performed for a combination of parameters such as pitch oscillation amplitudes and reduced frequencies. Results from this experiment included the integrated measurements from pressure transducer arrays in the form of lift, drag, and pitching moment coefficients at various wing span locations. Instantaneous pressure distributions have now been made available as a part of the present work; examples are shown in figures 1 and 2.

The initial work here has focused on the 2-D data of the Army experiment to study the vortex development during the dynamic stall process under different test conditions. Detailed analysis has been completed to better understand the flow characteristics of the NACA 0015 airfoil undergoing dynamic motion during dynamic stall. Additionally, the flow behavior data of the NACA 0015 airfoil in this experiment has been compared with NACA 0012 airfoil data previously obtained under similar operating conditions in the same 7- by 10-foot wind tunnel.

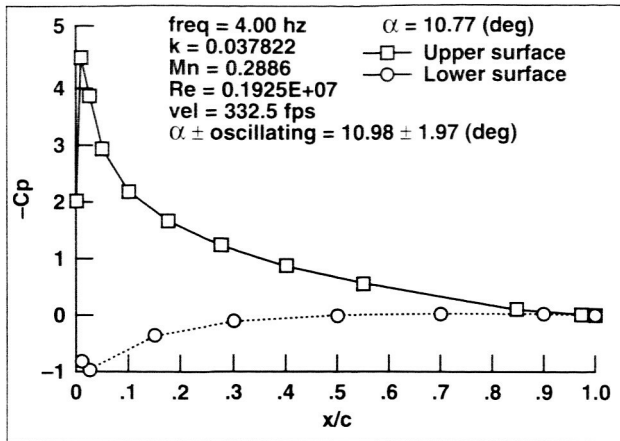


Fig. 1. AFDD 2-D and 3-D oscillating wing experiment upper and lower surface pressures versus chord location (50.0% span).

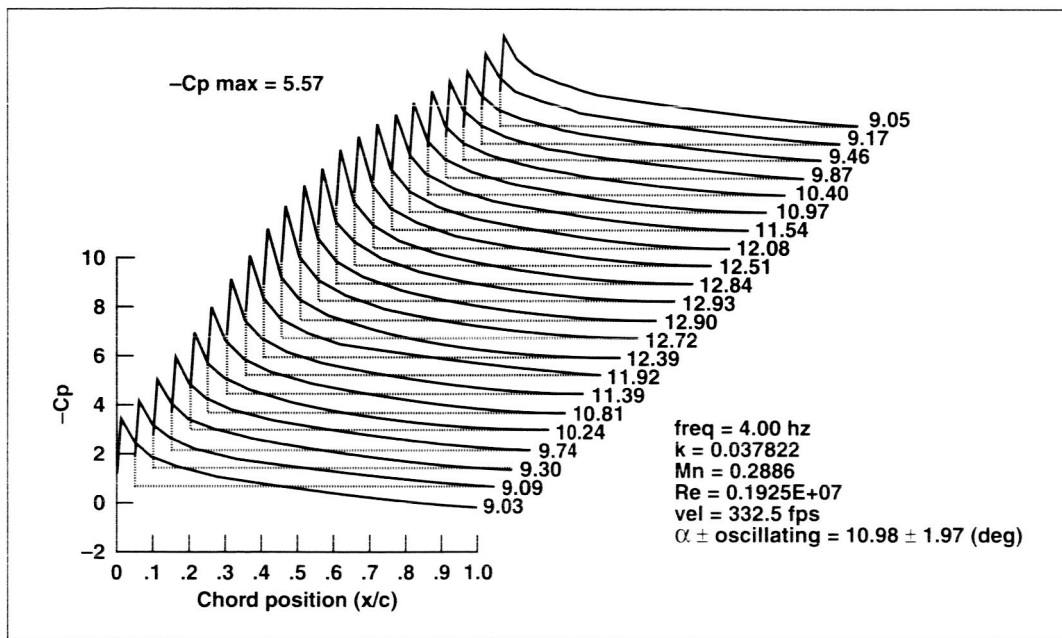


Fig. 2. AFDD 2-D and 3-D oscillating wing experiment upper surface pressure versus chord location with pitch angle during prescribed pitch motion (50.0% span).

Point of Contact: M. Rhee
 (650) 604-3646
 mrhee@mail.arc.nasa.gov

Rotor Blade Analysis Using the Mixed Finite-Element Method

Gene Ruzicka, Dewey H. Hodges

Accurate and efficient analysis of rotorcraft blades has long been a challenge. Using classic finite-element methods, it is possible to model blades of geometry, but a high price is paid for this capability in the form of large models with correspondingly large computational costs. It is possible in many applications to reduce computational costs by employing a technique called *modal reduction*, which seeks to collapse the analytical model to a handful of coordinates. Unfortunately, the modal reduction process is often ineffective for a rotor blade composed of finite elements that parameterize all unknown quantities as displacements. The reason is that the blade's axial force, which is the most critical factor in determining the blade's bending stiffness, is composed of contributions that nearly cancel, one from the axial displacement, and one from the bending displacements. Thus, the error in the axial force can be expected to be significantly larger than the error in either of the contributions; this is an example of the classic "small difference of large quantities" conundrum that often confronts numerical analysts.

One approach to modally reducing rotor blades is to express the blade's axial displacement in terms of the axial force. This eliminates the error-prone step of summing contributions that nearly cancel to the axial force, but does so at the expense of imposing restrictions on the blade geometry that can be modeled. An alternative approach, and one that has been the subject of this research, is to represent the axial force *and* the axial displacement in the blade model. Such an analytical procedure, which represents displacements as well as forces, is referred to as a *mixed method*. In addition to the anticipated improvement modal reduction accuracy, numerical analysts have long known that mixed methods bring about a synergy that results in better accuracy, for a given number of model degrees of freedom, than could be obtained with methods that employ only displacements or only forces. Apart from these accuracy considerations, mixed finite elements have several important analytical advantages: for example, they can be used in software developed for the more

commonly used displacement elements, and they can be coupled to displacement elements.

FY99 saw the completion of a software prototype for studying the modal reduction properties of mixed finite elements. This task applied a mixed treatment, in the axial direction only, to the principal rotor-blade modeling component, the Nonlinear Beam Element, of the Second Comprehensive Helicopter Analysis System (2GCHAS). A preliminary evaluation of the element's modal reduction accuracy was conducted by studying the periodic solution of an articulated blade. Figure 1 compares the blade's flap response when calculated in modal and in finite-element coordinates. Note that the finite-element model has 92 degrees of freedom, whereas the two sets of modal coordinates employ only one each or two each of the bending, axial, and torsion eigenmodes. It may be seen that the modal results are nearly identical to the finite-element results when only two each of the eigenmodes are employed as model coordinates.

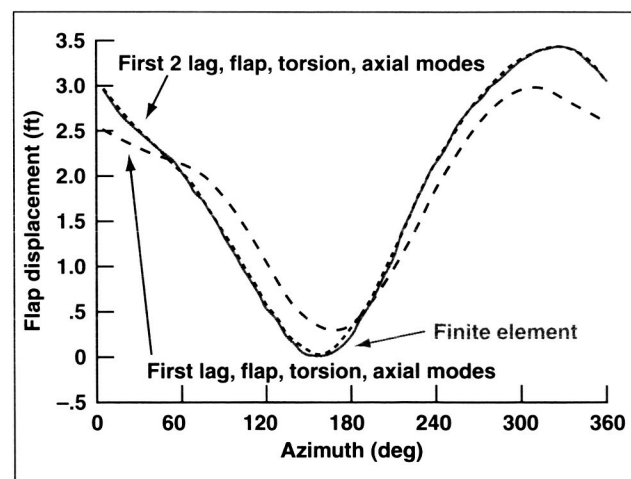


Fig. 1. Comparison of blade-tip response using finite-element and modal coordinates.

Point of Contact: G. C. Ruzicka
(650) 604-3919
gruzicka@mail.arc.nasa.gov

Three-Component Velocity Measurements in the Wake of a Rotor in Hover

Alan J. Wadcock, Gloria K. Yamauchi,
James T. Heineck

Improved rotorcraft aeroacoustic and performance analyses are highly dependent on the accurate modeling of the rotor wake structure, in particular, the strength and size of the blade-tip vortex. Particle image velocimetry (PIV) can provide these structural wake measurements very efficiently. The present investigation represents the first three-component PIV measurements acquired in a rotor wake by NASA.

The objective was to acquire three-component velocity fields in the wake of a hovering, two-bladed, untwisted rotor and determine the vortex size and strength as a function of wake age. A 7.5-foot-diameter rotor with a constant chord of 7.5 inches was selected for the study. The rotor was operated at a tip speed of 342 feet per second with the rotor thrusting downward (wake up) to minimize recirculation; 500 PIV stereo image pairs were acquired for each wake age, which ranged from 0 to 270 degrees.

Figure 1 shows an *instantaneous* in-plane velocity field with associated contours of vorticity. The vorticity map clearly identifies the location of the vortices shed from the rotor blade tip. The wake age of the vortex in the lower left corner is approximately

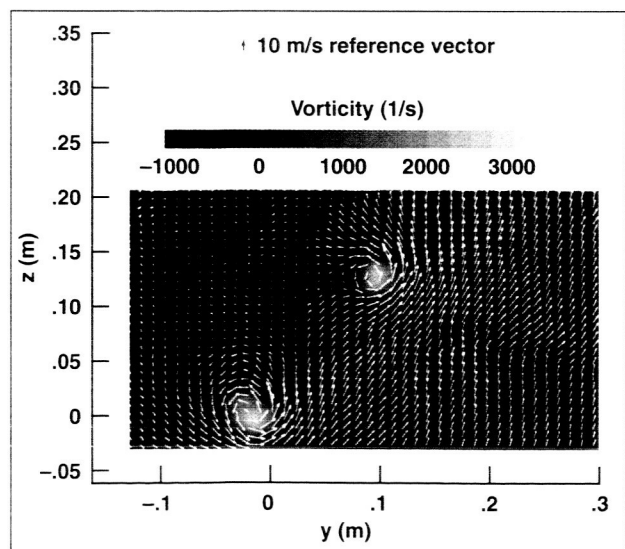


Fig. 1. Instantaneous in-plane velocity field with vorticity map.

30 degrees. The upper vortex was generated by the preceding blade and has a wake age of approximately 210 degrees. For clarity, only alternate rows and columns of velocity vectors are shown (1/4 the total number of vectors). Figure 2 shows the *same* instantaneous in-plane velocity field with associated contours of out-of-plane velocity. The out-of-plane velocity map helps identify the wake trailed from the inboard part of the blade. The direction of positive out-of-plane velocity is out of the paper. This is also the direction of blade motion.

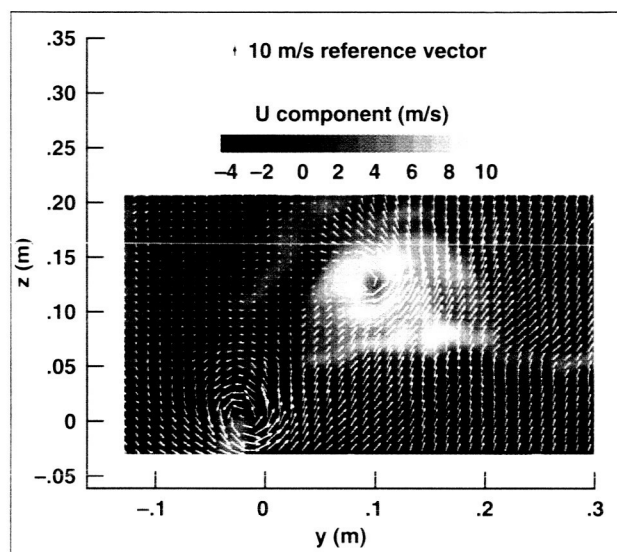


Fig. 2. Instantaneous in-plane velocity field without vorticity map.

Vortex-wander effects necessarily contaminate measurements of vortex wakes that rely on point measurement techniques. Whole flow-field techniques like PIV allow us to mitigate such effects by averaging in a coordinate system fixed with respect to the vortex. Such an average retains the vortex structure despite vortex wander and provides a better estimate for the mean vortex structure.

These results clearly demonstrate the feasibility of using three-component PIV for rotor wake measurements in hover, and this technique will be extended to the study of rotors in forward flight.

Point of Contact: A. Wadcock
(650) 604-4573
awadcock@mail.arc.nasa.gov

Evaluation of Aeronautical Design Standard-33 Using a UH-60A Black Hawk

Christopher L. Blanken, David R. Arterburn,
Luigi S. Cicolani

The U.S. Army's Aeronautical Design Standard-33 (ADS-33D-PRF) is a rotorcraft handling-qualities specification that was developed at Ames. Because this specification was initially applied in the RAH-66 Comanche helicopter program, the requirements generally related more to scout and attack rotorcraft. Recently, Ames expanded its handling-qualities research work to include utility rotorcraft, with and without externally slung loads. As part of this research, an 80-hour flight-test assessment of ADS-33D-PRF was conducted at Ames using an instrumented UH-60A Black Hawk, the Army's primary utility helicopter. The trial was performed (1) to assess the required compliance testing and to evaluate the requirements in a good visual environment; (2) to tailor the existing flight-test maneuvers and develop new maneuvers specifically designed to adequately evaluate the handling-qualities of utility helicopters, with and without externally slung loads; (3) to correlate the results from the quantitative testing with those from the qualitative evaluations; and (4) to establish a handling-qualities baseline of the UH-60A in terms of ADS-33 against which the effects of future modifications to the aircraft may be better quantified.

The 80-hour flight test was performed in three phases. Six pilots participated in Phase 1, the purpose of which was to tailor the existing ADS-33D-PRF flight-test maneuvers and to develop new ones. As shown in figure 1, course cueing for these flight-test maneuvers was constructed and refined to provide sufficient cues such that the evaluation pilots could determine "Desired" and "Adequate" maneuver performance standards. Eight experimental test pilots participated in the Phase 2 formal handling-qualities evaluations of the Black Hawk for these maneuvers and for three aircraft configurations: empty (approximate average weight = 13,500 pounds); with an internal ballast (17,300 pounds); and empty but with a 6,000-pound externally slung load (total operating weight 19,300 pounds). Data were collected in calm (<5 knots) and light wind conditions (7-15 knots). During Phase 3, the empty and internal ballast

configurations were used to assess the compliance testing and criteria from the quantitative requirements in ADS-33D-PRF at hover and in forward flight.

Selected flight-test maneuvers from ADS-33D-PRF and from a CH-47D cargo helicopter assessment were refined for the utility mission. The maneuver performance standards were generally aligned with those developed in the cargo helicopter flight test. The addition of light winds (7-15 knots) tended to degrade the handling-qualities for some maneuvers more so than others. From the internal ballast configuration, the qualitative results for calm conditions (shown in figure 2) suggest that except for the Hover Turn and the Pirouette maneuvers, the average Handling Quality Rating (HQR) for the UH-60A, as tested, is close to the Level 1-2 boundary. The Phase 3 results showed that with real-time monitoring of the control inputs and aircraft response, the frequency-sweep testing and the steps, doublets, and pulse control inputs were performed in a routine and efficient manner. The initial lessons learned and results from this flight-test assessment of ADS-33D-PRF using a UH-60A Black Hawk helicopter will be instrumental in expanding the D-version of ADS-33 into an E-version that includes a first-cut at criteria suitable for utility rotorcraft, with and without externally slung loads.

Point of Contact: C. L. Blanken
(650) 604-5836
cblanken@mail.arc.nasa.gov



Fig. 1. UH-60A Black Hawk with externally slung load performing maneuver assessment.

requirements for these parameters are based on decades of experience with cathode-ray tube (CRT) displays, and not necessarily on perception science.

High-information-content imagery requires broad information channel capacity to the device in order to display fine detail, subtle shading, full color, and continuous motion. However, excess channel capacity for one of these parameters can often be used to compensate for a lack in another. A well-known example of this is the halftones used in printing, where some spatial resolution is sacrificed to enhance tone reproduction.

For several years, Ames has been developing a display optimization tool set known as Visual Display Engineering and Optimization System (VIDEOS). In the investigation of the gray-scale/resolution trade-off for displays, it was found that without dithering, there was no trade-off; there was both a minimum spatial resolution and a minimum number of gray levels required in order to produce an image indistinguishable from a photo-quality version. With dithering, an important trade-off region emerged that corresponds to parameter values achievable by microdisplays being developed for helmet-mounted systems. A summary graph for these results is shown in figure 1. Plot coordinates are spatial resolution (abscissa) and number of gray levels (ordinate). The shaded upper-right-hand regions are below threshold for discrimination. Data points are the threshold results for three observers in the psychophysical study; continuous contours were generated by the computational study using the human vision model and a just noticeable difference $JND = 1$ for the threshold. Figure 1a shows the results for non-dithered images: the rectangular shape of the below-threshold region indicates the lack of a gray-scale/resolution trade-off. The triangular portion of the contour in figure 1b demarcates the trade-off region for the dithered images. When color dither for displays was investigated, it was found that a considerable savings in computational power could be achieved by dithering in the digital, instead of the luminance, representation of the image, as long as at least six levels of each color were used. These six levels could correspond to what is known as the "browser-safe" palette commonly used for image compression on the Internet.

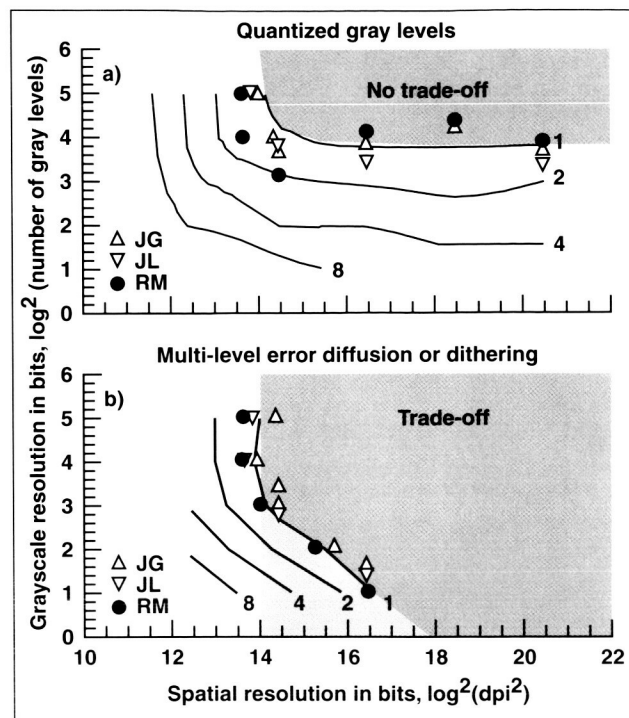


Fig. 1. Threshold contour plots for distinguishing a lower-resolution image from a photo-quality version.

The broad information channel capacity required for high-information content imagery also requires high power outlays to support the device communication needs and to rapidly switch data onto the display device. The ViDEOS team is developing methods for reducing these requirements without sacrificing the visual quality of the images presented to the user. Because these devices act essentially as random access memory units, they provide new opportunities to save communication channel capacity, power, and, ultimately, weight. The unique feature of the Ames approach to this technology problem is that the information quality of the images drives the optimization of the display system. The ultimate goal is to provide new venues of visual information to the pilot thereby improving safety and efficiency.

Figure 2 shows a commercially available near-to-eye display system, suitable for avionics. This lightweight unit can be connected to a flight helmet or even to a baseball cap. This display was manufactured by LitEye™ Microdisplay Systems.

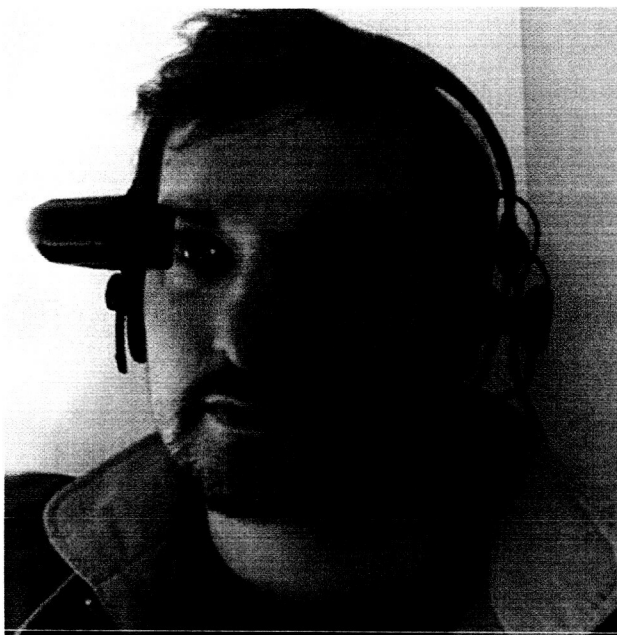


Fig. 2. A near-to-eye display system in use.

Point of Contact: J. O. Larimer
 (650) 604-5185
 jlarimer@mail.arc.nasa.gov

Human Factors Field Evaluation of Cockpit Display of Traffic Information (CDTI)

Rose Ashford, Vernol Battiste

Cockpit Display of Traffic Information (CDTI) is a major departure from traditional ground-based air traffic control and will markedly improve air traffic safety and efficiency, as well as facilitate modernization of the National Airspace System. A prototype CDTI was installed on 12 aircraft (8 Boeing 727's and 4 DC-9's) belonging to the member airlines of the Cargo Airline Association. This initial CDTI (figure 1) displays proximate aircraft relative to their own-ship, assisting flight crews in sighting and identifying traffic "out the window." NASA provided a human factors evaluation of the CDTI to demonstrate whether it would be safe and effective for these initial visual applications, and to provide preliminary results supporting future CDTI applications involving aircraft that are sharing separation responsibility.

Flight scenarios were developed to evaluate flight crew workload, situational awareness, and effectiveness of the CDTI as an aid to visual acquisition and visual approaches. Additional scenarios were developed to demonstrate aircraft station-keeping capabilities assisted by the CDTI. A data collection program was developed and implemented, including the recruiting and training of NASA observers for each flight, and developing protocols for collecting data from the flight deck during the flight scenarios, and for debriefing the flight crews afterward. The evaluation focused on examining the CDTI's effects on flight crew workload and attention, and how normal cockpit procedures were affected by its use.

The planned flight scenarios were flown at Airborne Airpark in Wilmington, Ohio, on July 10, 1999. Results from the evaluation indicate that the CDTI provides significant benefits in flight crew situational awareness, that it aids visual acquisition of traffic, and that it enhances visual approaches. Flight crews found the CDTI easy to use, and they were very positive regarding CDTI as an aid to visually acquiring traffic and determining how close to follow when making a visual approach to a runway. They thought the CDTI helped them maintain awareness of several targets and to reacquire previously sighted traffic, both common requirements in busy terminal airspace. Analysis of the aircraft track data also indicates that the CDTI enhances approach efficiency, although there is much variability in those data, a direct result of the real flight environment. Flight crews were able to manage the station-keeping task satisfactorily.

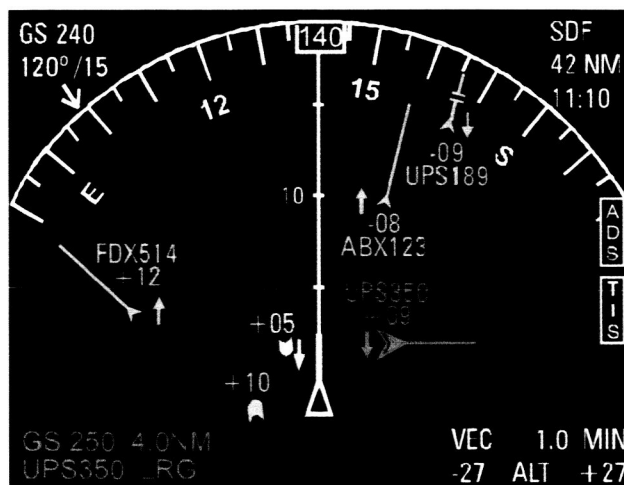


Fig. 1. Cockpit display of traffic information.

The results of this investigation are being used to support further development of the CDTI and its eventual installation in many more aircraft. Additionally, evaluation of this prototype is contributing to future CDTI designs and their applications toward free-flight for all aircraft. This has significant implications for future aviation capacity and safety enhancements, and supports the Aerospace Technologies Enterprise goal of tripling throughput while maintaining safety in the National Airspace System.

Point of Contact: R. Ashford
(650) 604-0914
rashford@mail.arc.nasa.gov

Rotorcraft Uninhabited Aerial Vehicle (RUAV) System Identification, Modeling, and Flight Control System Development

**Mark B. Tischler, Luigi S. Cicolani,
 Jason D. Colbourne, Chad R. Frost**

A new challenge to industry and the government alike is the trend toward highly compressed schedules for rotorcraft uninhabited aerial vehicle (RUAV) development and system fielding. Current RUAV proposals and development programs are on 6- to 9-month schedules, in contrast to the 6- to 10-year schedules common to most recent piloted rotorcraft systems. This year, the Army/NASA Rotorcraft Division launched a new initiative: COnTrol and Simulation Technologies for Autonomous Rotorcraft (COSTAR) which seeks to develop key enabling technologies for the control and simulation of RUAVs.

The COSTAR initiative refines technologies originally developed for manned rotorcraft for application to the RUAV problem, and seeks to increase technology integration sufficiently to realize the desired reduction in design cycle time. Key elements of COSTAR include accurate flight-mechanics modeling using system identification (CIFER[®]), control system design optimization for multiple objectives (CONDUIT), and real-time workstation-based simulation (RIPTIDE). COSTAR technologies are central to three ongoing cooperative

projects, in which university and industry RUAV developers have teamed with the Army/NASA Rotorcraft Division's Flight Control Technology Group.

In one such cooperative activity, Army/NASA personnel worked under direct contract to Northrop Grumman, supporting development of the U.S. Navy's Vertical Takeoff UAV (VTUAV) (figure 1). Ames personnel participated in flight testing, followed by extensive system identification of the aircraft dynamic models (using CIFER[®]), and flight control analysis/optimization (using CONDUIT). Ames was also responsible for developing the detailed flight control preliminary design, including the determination of a comprehensive set of "Aeronautical Design Standard-33 (ADS-33) like" design requirements for use in CONDUIT. This close working relationship resulted in a successful autonomous flight of the demonstrator aircraft. The Flight Control Technology Group is currently under contract to Northrop Grumman to support system identification of forward flight models, and flight control law optimization for the full flight envelope.

Another joint venture involves model identification, control system design, and flight testing of a fully instrumented model-scale unmanned helicopter (a Yamaha R-50 with 10-foot-diameter rotor). In conjunction with Carnegie-Mellon University, the CIFER[®] system identification techniques developed for full-size helicopters were applied to the R-50. An accurate, high-bandwidth, linear state-space model was derived for the hover condition. A conclusion of this study was that small helicopters seem to be particularly well suited to identification, in part because of the dominance of the rotor in their dynamics. This is illustrated by the exceptionally clean frequency-sweep time responses shown in figure 2. The R-50 was shown to be dynamically similar to a scaled UH-1H, although the R-50 is proportionally heavier. Preliminary control system designs have been studied using CONDUIT, and evaluated using the RIPTIDE simulation environment for remotely piloted operations.

Army/NASA personnel and technology have also been instrumental in Kaman Aerospace's development of the Broad-area Unmanned Responsive Resupply Operations (BURRO) aircraft for the U.S. Marine Corps. The BURRO program adapts the existing K-MAX piloted external-lift helicopter for

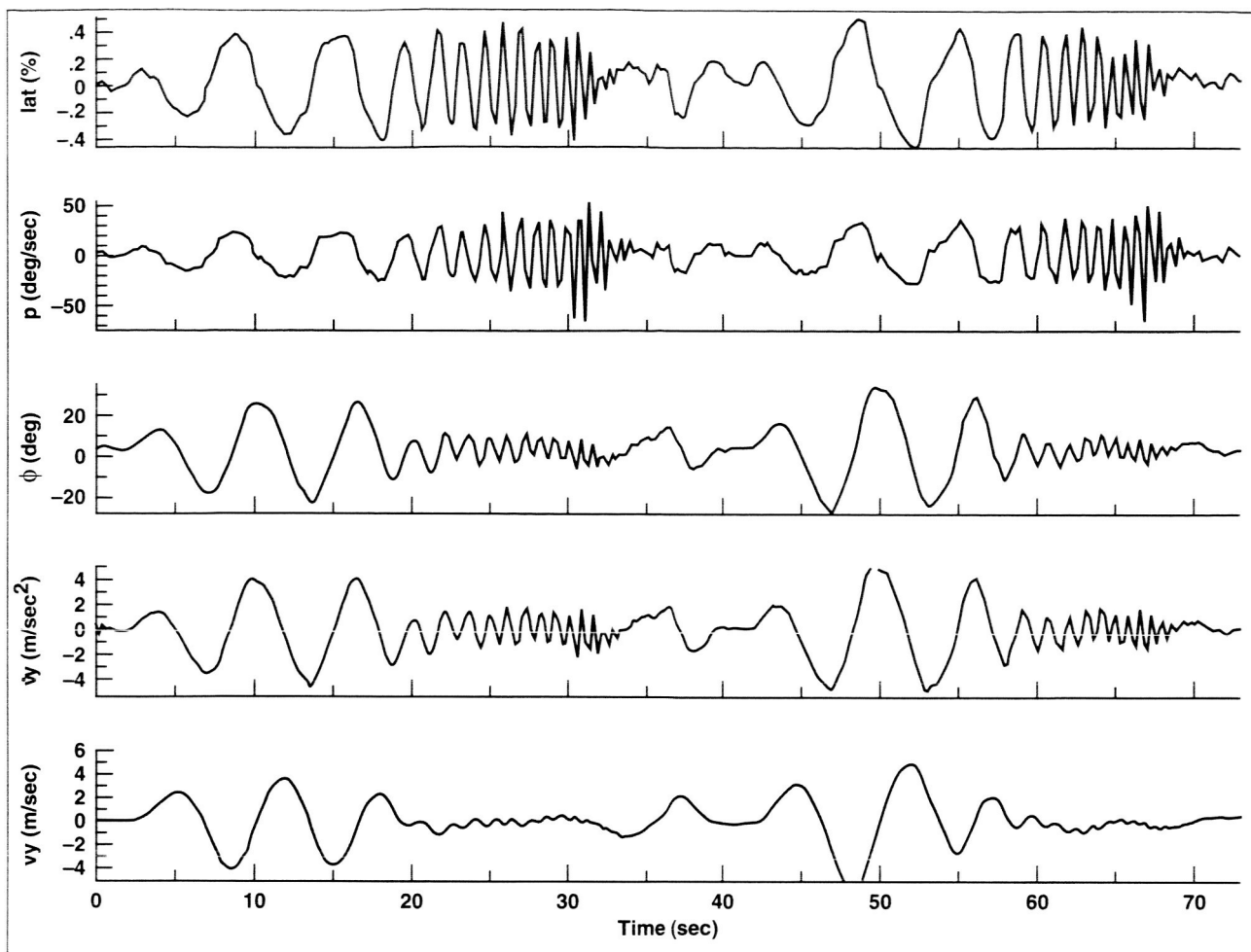


Fig. 1. Frequency sweeps collected for R-50 identification.

remotely piloted flight and autonomous way-point navigation. CIPHER[®] was used to identify linear math models for unloaded and loaded flight at hover and at 50 and 80 knots; this is the first time that system identification has been used to extract a coupled aircraft-plus-slung load model. The resulting linear models were used to design and tune a flight control system in the CONDUIT environment—19 design parameters were tuned to meet 41 handling-quality and performance specifications, which were based on the ADS-33 manned rotorcraft requirements. This work led to a successful flight demonstration of the K-MAX BURRO UAV for the Marine Corps. Follow-on work will expand the range and capabilities of the demonstrator aircraft.

Point of Contact: M. B. Tischler
 (650) 604-5563
mtischler@mail.arc.nasa.gov

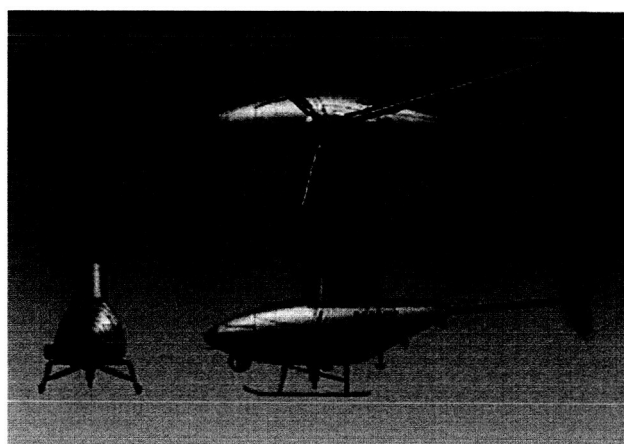


Fig. 2. VTUAV aircraft.

Piloted Simulation Investigation of Helicopter Flight Envelope Tactile Cueing

Matthew S. Whalley

Two ground-based piloted simulation trials of helicopter flight envelope tactile cueing have been conducted. The objective of the trials was to develop methods of helping the pilot to observe flight envelope limits while conducting precise and demanding evaluation tasks. In one trial, large-displacement conventional inceptors were used; in the other, short displacement sidesticks. The inceptors in both trials were programmable and active.

Figure 1 shows the algorithm that was used to estimate the inceptor position corresponding to a vehicle limit. A polynomial neural network (PNN) provided lead estimate of the limit variable, which was then adjusted using a simple adaptation algorithm before being compared with the preset limit to determine the corresponding inceptor position. A tactile force breakout which the pilot could override (softstop) was then driven to the inceptor location corresponding to the limit. The simulated limits were time-varying in nature.

Figure 2 shows four time-histories of torque, collective position, and collective force for the four active sidestick test configurations. The movement of the transient/do-not-exceed boundary can be seen as the torque value transitioned above and below the continuous limit of 80 percent. The pilots were required to respect the limit using the instrument cues and the tactile cues. For the configurations with

tactile cueing, the softstop movement associated with the transient/do-not-exceed boundary can be seen. The pilot's input tracked the softstop as it moved downward in accordance with the cueing algorithm. The collective force contributed by the softstop is indicated. Typically, 2–3 times the friction force was held when riding against the softstop. Maintaining this force in order to achieve maximum performance was associated with improved pilot acceptance and task performance.

The following major points were noted. The programmable nature of the active sidesticks enabled implementation of all conventional inceptor functionality including trim follow-up, beep trim, and trim release, and yielded favorable pilot commentary regarding posture, feel characteristics, and controllability. With tactile cueing, conventional inceptors and the sidesticks yielded nearly equivalent performance. For both types of inceptors, tactile cueing significantly reduced the time required to reach the envelope limit, increased the dwell time at the limit, reduced exceedances, and improved pilot opinion. Tactile cueing enabled the pilots to easily track and respect notional dynamic limits designed to account for accumulated fatigue damage. Tactile cueing enabled the pilots to easily track both torque and rotor stall limits simultaneously while performing an aggressive turning task with their attention focused entirely outside the cockpit.

Point of Contact: M. Whalley
(650) 604-3505
mwhalley@mail.arc.nasa.gov

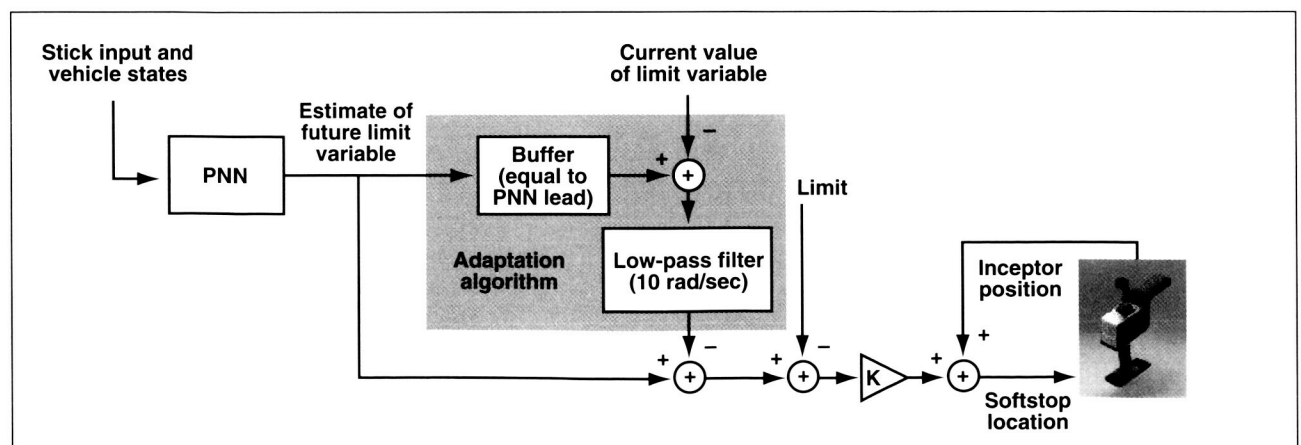


Fig. 1. Softstop location calculation using PNN.

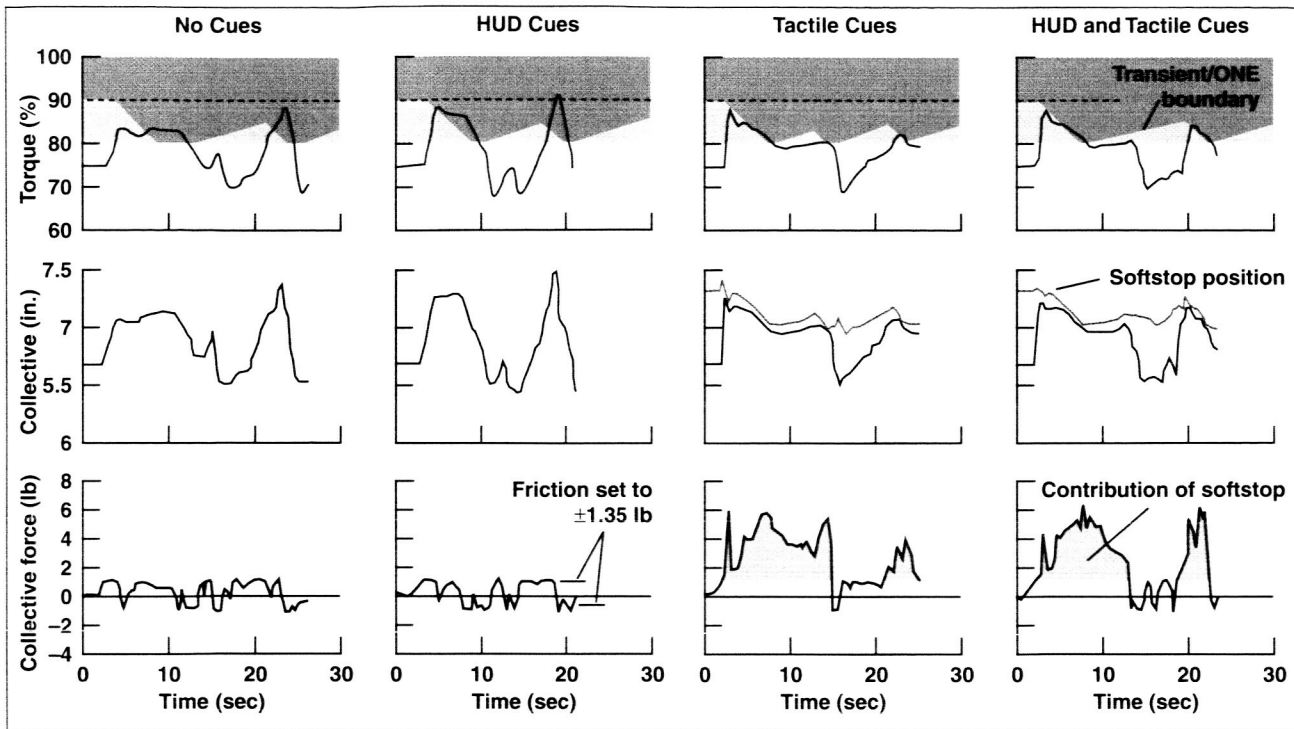


Fig. 2. Sample time-histories from the bob-up task using the active sidestick.

Tilt-Rotor Noise Reduction

Mark D. Betzina, Cahit Kitaplioglu,
Khanh Q. Nguyen

Reducing tilt-rotor noise by 12 decibels was a major goal of the Short Haul Civil Tiltrotor (SHCT) program. Blade vortex interaction (BVI) noise reduction was considered a key enabling technology that would allow tilt rotors to land in populated areas such as city centers, thereby relieving congestion at major airports. One of the SHCT objectives was to investigate BVI noise reduction techniques using an isolated, full-scale XV-15 tilt rotor in approach flight conditions in the Ames 80- by 120-Foot Wind Tunnel.

Figure 1 shows two contour plots of noise levels measured on a horizontal plane below and forward of the advancing side of the rotor. This measurement area was chosen to capture the highest BVI noise levels. The center of the rotor is located at the origin,

and the arc in the lower left corner represents the location of the rotor blade tips. The left-hand plot shows noise measurements at a high BVI noise condition. The highest noise level, near the center of the measurement area, is 118.5 decibels. The right-hand plot shows the result achieved by tilting the rotor tip-path-plane forward from +3 degrees (aft tilt) to -3 degrees (forward tilt) and applying higher harmonic control (HHC). An HHC system provides high-frequency inputs to the rotor controls, resulting in blade-pitch oscillations at two, three, and four times per revolution on the three-bladed rotor. By making these inputs at the proper phase relative to the blade azimuth position, a large reduction in the rotor's noise signature is produced. The highest noise level for this condition is 102.0 decibels, at a point located near the upper left corner of the measurement area.

Therefore, the peak noise within the measurement area was reduced by 16.5 decibels, surpassing the SHCT program goal of 12 decibels. This noise

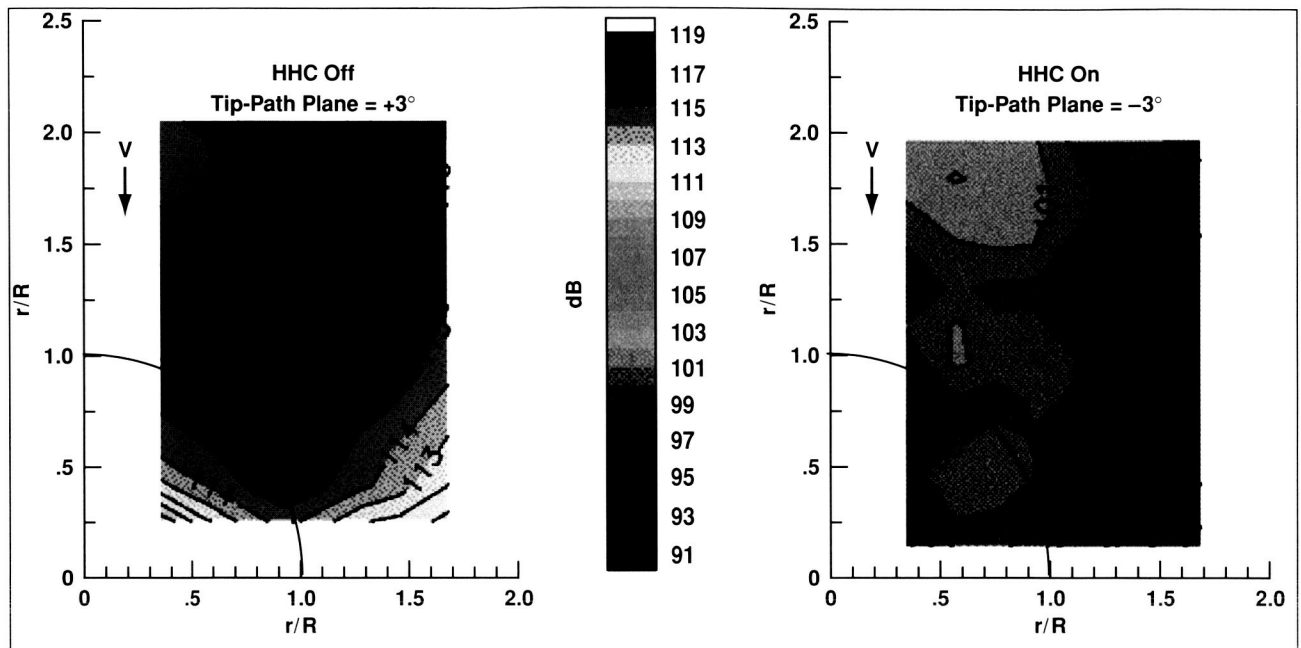


Fig. 1. Noise reduction on a horizontal plane below rotor: velocity = 69 knots, thrust = 5,500 pounds.

reduction was achieved by utilizing a combination of HHC and by changing the rotor's tip-path-plane angle-of-attack. The rotor tip-path-plane angle of a tilt-rotor aircraft can be changed in flight by varying the nacelle tilt angle, wing flap position, and

approach glideslope, thus producing a slightly different approach flight condition.

Point of Contact: M. Betzina
 (650) 604-5106
 mbetzina@mail.arc.nasa.gov

A Numerical and Experimental Study of Wind Turbine Unsteady Aerodynamics

Earl Duque, Robert Kufeld

Accurate, reliable, and robust numerical predictions of the power required to turn the main rotor blades of a rotorcraft remain a challenge to the industry. Although various numerical methods do exist and have been used in the design of many different aircraft, there still remain some questions regarding the prediction of the maximum power required. Many of the existing theories do not work well in this flight regime. One possible flaw is our lack of understanding of how a rotor blade stalls along the inboard radial locations.

To address this lack of understanding, NASA has formed a collaborative effort with the Department of Energy's (DoE) National Renewable Energy Laboratory (NREL) to investigate the unsteady aerodynamics of a horizontal axis wind turbine (HAWT). The main purpose of this project is to gain a better understanding of a wind turbine's unsteady aerodynamics. By improving our understanding of this machine's aerodynamic environment, we simultaneously improve our capability to properly model rotorcraft rotor blades.

In this effort, researchers use advanced rotorcraft computational fluid dynamics (CFD) methods to simulate the wind turbine. Solutions based on the Reynolds-averaged Navier-Stokes equations have been obtained as illustrated in figure 1. Concurrently,

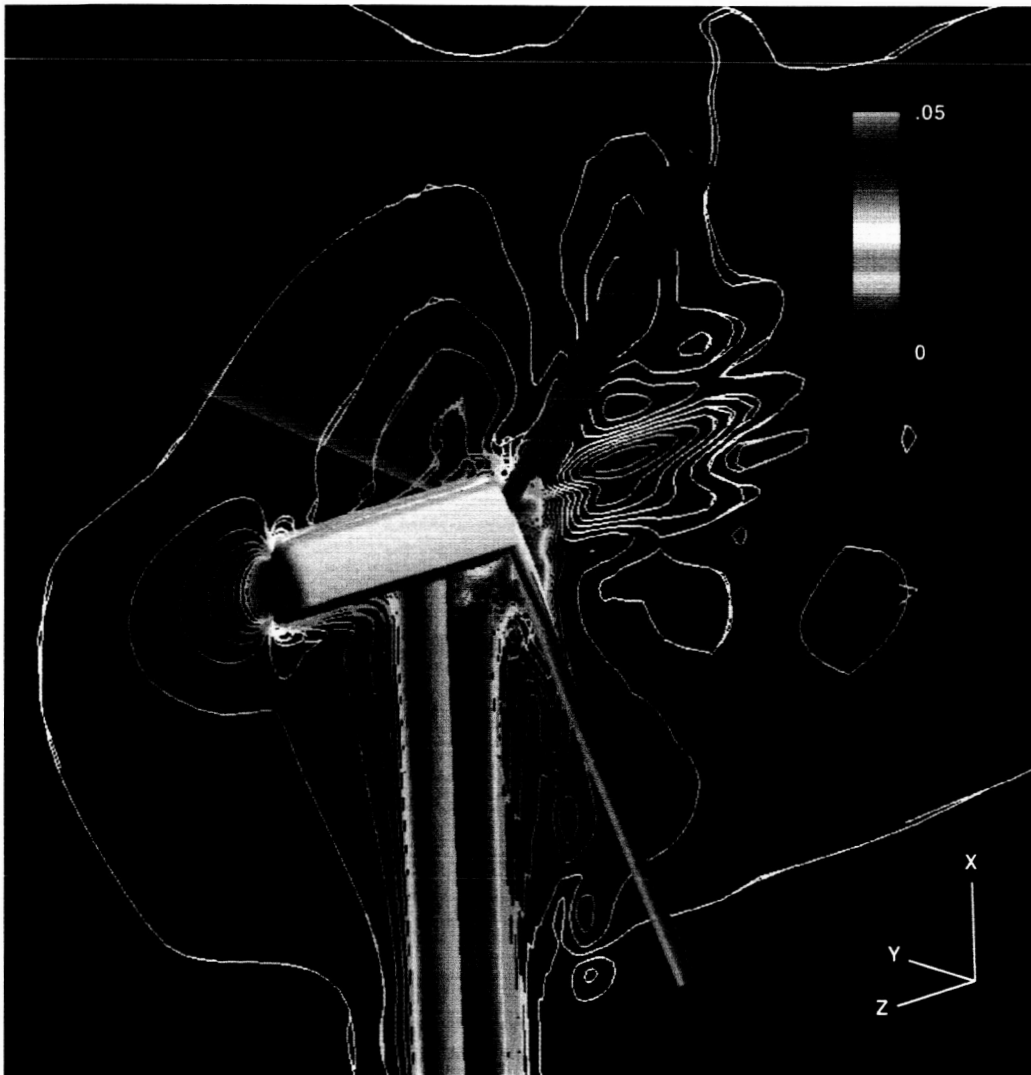


Fig. 1. Computed velocity contours on the NREL Phase 2 Unsteady Aerodynamics Experiment.

NREL has installed and will test their Unsteady Aerodynamics Experiment in NASA's 80- by 120-Foot Wind Tunnel. This test is the largest and most comprehensive wind tunnel test of an HAWT in the world. It will provide extensive unsteady data regarding, for example, pressure, air loads, and dynamic blade response. The information gathered from the experimental data, combined with the knowledge obtained through the computations, forms the nucleus for the development of more accurate semi-empirical rotor design methods. In addition, the knowledge gained through this collaborative program will have a major effect on the understanding of other rotary flow fields such as those of tilt rotors and helicopters.

This collaborative effort directly addresses aerodynamic issues relevant to both rotorcraft and wind turbines. By utilizing scientific resources from both NREL and NASA, we have been able to advance

our understanding of the aerodynamic behavior of rotor blades to the benefit of both industries.

Point of Contact: E. Duque
(650) 604-4489
eduque@mail.arc.nasa.gov

Analysis of On-Blade Control

Mark V. Fulton

Because high levels of helicopter vibration are bothersome to pilots, passengers, and on-board equipment, efforts are under way to develop improved active rotor concepts for vibration control. In an effort to explore the benefits of on-blade controls, a small-scale active rotor was previously tested in the Army/NASA 7- by 10-Foot Wind Tunnel. The rotor shown in the figure contained one elevon (or control surface) per blade which was actuated by piezoceramic bimorph actuators to reduce vibratory blade loads. Previous reports have described the test in detail along with preliminary 2GCHAS (Second Generation Comprehensive Helicopter Analysis System) calculations used for data correlation and for explaining the observed aeroelastic phenomenon. More recently, CAMRAD II (Comprehensive Analytical Model of Rotorcraft Aerodynamics and Dynamics) calculations were made to study several model features, including tip loss and elevon dynamics, and to allow further forward flight vibratory loads comparisons. In all cases, the control consisted of elevon deflection, and the response consisted of blade root bending and torsion moments.

In hover, the predictions captured the basic aeroelastic effects evident in the data, including elevon reversal and aeroelastic resonant peaks. For some cases, however, the magnitude of the predictions significantly differed from the experimental measurements. For example, the calculated peak torsion moment response (to elevon deflection) was only 60% of the experimental peak response for a nominal hover condition. A parameter found to be rather effective in changing the torsion resonant peak was tip loss—ignoring the aerodynamic loads for the outboard 2% of the blade increased the torsion peak



Fig. 2. NREL Phase 6 Unsteady Aerodynamics Experiment installed in 80- by 120-foot wind tunnel test section.

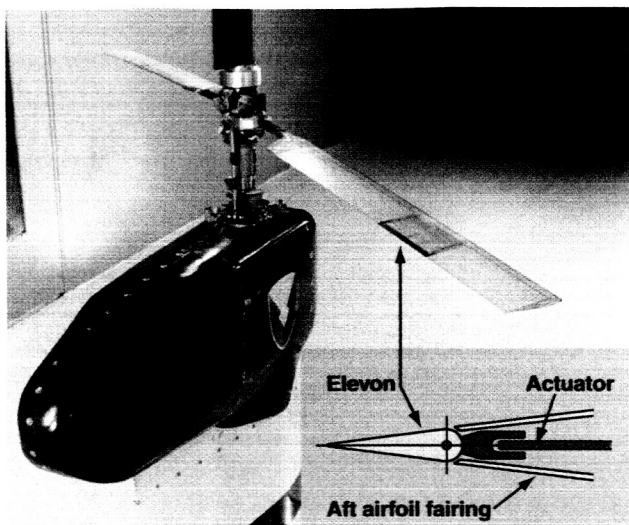


Fig. 1. Active rotor with on-blade elevons in the Ames 7- by 10-Foot Wind Tunnel.

by 13%. A tip loss for lift can be predicted by conventional lifting-line theory when nonuniform inflow exists. This approach, however, does not work for pitching moment, suggesting that the incorporation of an advanced lifting-line model may be warranted. Less significant was the inclusion of a model of elevon dynamics, which increased the torsion peak response by 6% and also caused a coupling between blade response and elevon motion. Results from forward flight tended to confirm the hover results, but suffered from the conventional problems of vibratory load prediction for helicopter rotors—the general trends were captured, but significant differences existed. For example, a correlation plot of the 2–5 per-revolution flap bending moment harmonics was produced for four wind tunnel speeds. A least-squares curve fit yielded a correlation coefficient of 0.56, indicating a low level of correlation between the analysis and the test data.

Point of Contact: M. Fulton
(650) 604-0102
mfulton@mail.arc.nasa.gov

Full-Span Tilt-Rotor Aeroacoustic Model

Megan S. McCluer, Jeffrey L. Johnson

Tilt rotors are a new breed of subsonic aircraft developed for both military and civil aviation. The current production of the military V-22 Osprey and the launch decision of the BA-609 civil tilt rotor will certainly enhance the U.S. military and economic competitive status in the international aviation arena. In addition, civil tilt rotors have the potential to increase air transportation throughput in congested airports by off-loading busy runways. To support the U.S. civil tilt-rotor development, NASA created the Short Haul Civil Tiltrotor project (SHCT) from the Aviation Systems Capacity program.

The SHCT program addresses critical enabling technologies for civil tilt rotors that include low-noise tilt rotors. NASA Ames and Langley Research Centers, the U.S. Army Aeroflightdynamics Directorate, and the U.S. rotorcraft industry, have jointly developed an aeroacoustic research program aimed at accomplishing the SHCT goals. One of the major milestones of the program is to validate aeroacoustic analyses for low-noise tilt-rotor designs. The primary objective of the Tilt-Rotor Aeroacoustic Model (TRAM) project is to provide a comprehensive database for code validation.

The TRAM is a quarter-scale V-22 model with two configurations: an isolated rotor configuration and a full-span, dual-rotor aircraft configuration. The TRAM isolated rotor was tested in the Duits-Nederlandse Wind Tunnel in the spring of 1998. The Full-Span TRAM (FS TRAM), shown in the figure, was installed and will be tested in the NASA Ames 40- by 80-Foot Wind Tunnel to provide aeroacoustic data for the complete aircraft configuration.

The FS TRAM is a highly complex aircraft model designed to accommodate many aspects of tilt-rotor research. The model has two rotor balances, one per rotor, and a fuselage balance. The pressure-instrumented blades provide high-frequency air-load measurements, and wing-mounted pressure tabs provide data about rotor-wing interaction effects. In addition, both wings and blades are instrumented with strain gauges for safety-of-flight monitoring and structural load measurements. The data generated from the FS TRAM wind tunnel test will be a unique

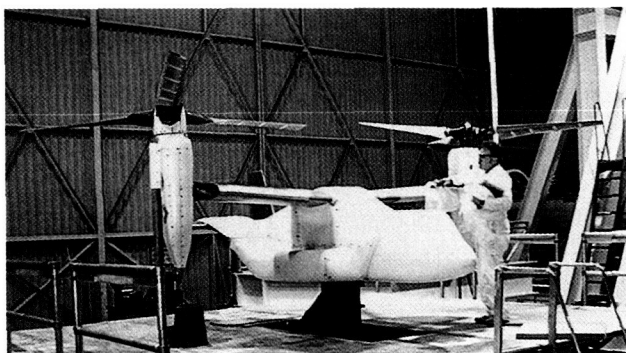


Fig. 1. Full-span TRAM under development at NASA Ames Research Center.

and valuable asset in the development of aero-acoustic analyses for advanced tilt-rotor designs.

In addition to the intensive hardware and instrumentation build-up, significant progress has been made on the FS TRAM, including the complete checkout of two new electromagnetic motors, the left rotor drive system, and the new control system. A 700-channel slip ring was completely wired, and the new rotor hubs were installed. Furthermore, modifications made to the existing microphone traverse system will allow measurements of the acoustic directivity of both rotors. Significant preparations are under way to install a particle image velocimetry system for detailed flow measurements and a laser light sheet system for flow visualization of the rotor wakes.

Point of Contact: M. McCluer
 (650) 604-0010
mmccluer@mail.arc.nasa.gov

Active Control of Tilt-Rotor Aeroacoustics

Khanh Q. Nguyen, Doug L. Lillie

Tilt-rotor aircraft have great potential to relieve air traffic congestion by ferrying passengers directly to and from vertiports located near urban areas. Since these aircraft operate like helicopters during landing, the tilt rotors produce highly impulsive noise owing to blade-vortex interactions (BVI). Thus, reducing BVI noise is a key enabling technology that will allow tilt rotors to operate in populated areas. Higher harmonic control (HHC) was shown to be highly effective in reducing BVI noise on tilt rotors. For a three-bladed rotor, an HHC system generates low-amplitude blade-pitch oscillations two, three, and four times per rotor revolution that are superimposed with the primary control input for trim. In addition, practical applications of HHC to tilt rotors require the development of suitable signal processing techniques to identify the radiated BVI noise for feedback control. A method using pressure sensors mounted on the blades for identification and control of BVI noise was demonstrated in an 80- by 120-foot wind tunnel test of a full-scale XV-15 tilt rotor. The controller successfully reduced the BVI noise level by more than 5 decibels, as indicated by the measured noise contours under the rotor shown in the figure on the following page.

Point of Contact: K. Nguyen
 (650) 604-5043
knguyen@mail.arc.nasa.gov

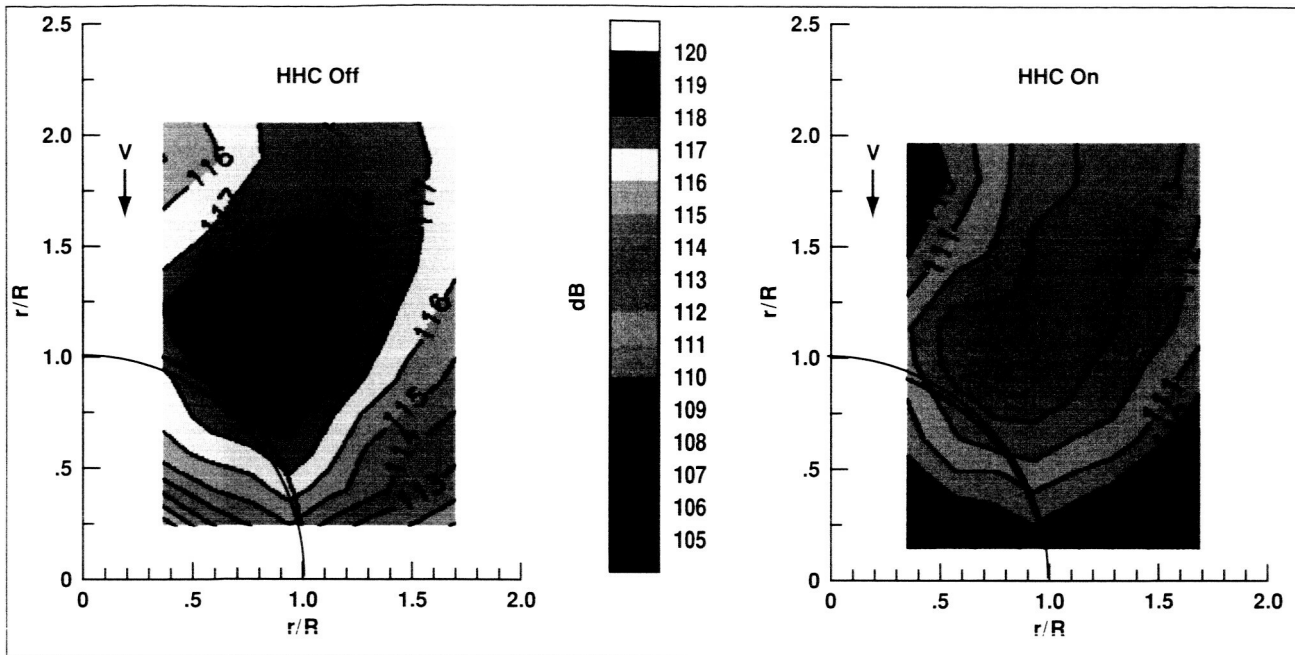


Fig. 1. Noise controller reduces noise measured on a plane under the XV-15 rotor: tunnel speed 69 knots, rotor thrust 5,500 pounds.

Tilt-Rotor Noise Reduction Study

Thomas R. Norman

The successful introduction of the civil tilt rotor into the national airspace system relies heavily on its community acceptance. In particular, a tilt rotor with reduced noise emissions is critical. Various approaches are being considered to address this problem. One such approach, the application of remotely adjustable on-blade control elements to rotor blades, is receiving considerable attention. This research effort is an attempt to better define the on-blade requirements and ultimately to identify a feasible design implementation.

The objective of this effort, performed by Continuum Dynamics, Inc. under an SBIR (Small Business Innovation Research) Phase I contract, was to determine a mix of on-blade control-surface deflection or in-flight twist change to produce significant payload and range enhancement and blade vortex interaction (BVI) noise reduction for a representative civil tilt rotor. In addition, they were to establish preliminary

designs for adjusting blade twist in a rotating environment using smart structures.

Through the combination of a comprehensive analysis and noise prediction code, BVI noise was predicted for various levels of tilt-rotor blade washout (see figure 1). These results demonstrate that if an

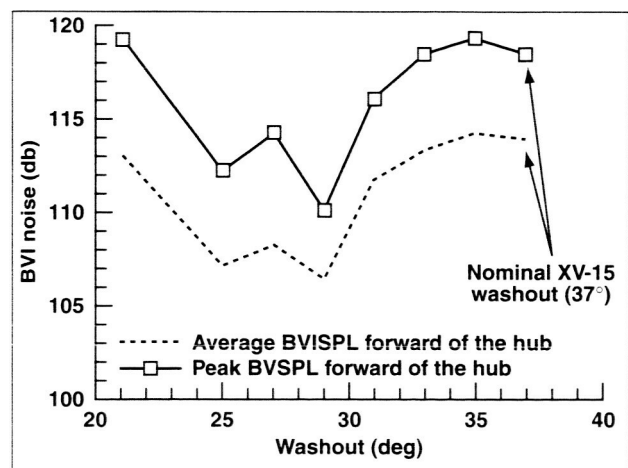


Fig. 1. Effect of blade washout on blade vortex interaction noise.

on-blade device can be developed to decrease blade washout, the BVI noise level in front of the tilt-rotor hub can be reduced by as much as 6 decibels. A noise-reduction strategy combining both on-blade deployment and nacelle tilt could reduce BVI noise levels by as much as 12 decibels. These noise reductions are consistent with NASA's 10- and 20-year goals and, if realized, could significantly accelerate the acceptance of tilt rotors into our national airspace system. In conjunction with this analytical work, various concepts were identified and considered as means to implement the necessary blade twist changes.

Point of Contact: T. Norman
(650) 604-6653
tnorman@mail.arc.nasa.gov

Isolated Tilt-Rotor Aeroacoustics

Gloria Yamauchi, Larry Young, Earl Booth

As part of the Short Haul Civil Tiltrotor (SHCT) project, an element of the Aviation Systems Capacity program, a test of an isolated tilt rotor was conducted in the Duits-Nederlandse Windtunnel (DNW) open-jet test section in April-May 1998. The model was the isolated configuration of the Tilt-Rotor Aeroacoustic Model (TRAM) and consists of a 0.25-scale V-22 right-hand rotor and nacelle. Aeroacoustic data and rotor wake measurements were acquired for a range of conditions in which blade-vortex interaction (BVI) occurs. The test was led by NASA Ames Research Center in partnership with the U.S. Army, NASA Langley, and the Boeing Company.

Unlike conventional helicopter rotor blades, proprotor blades are highly twisted and can generate negative loading over a large area of the rotor disk. The negative loading causes multiple vortices (of opposite sign) to be shed, thereby increasing the complexity of the wake. Hence, modeling tilt-rotor wakes and predicting tilt-rotor aeroacoustics are very challenging tasks.

The positions of wake segments relative to the rotor blade were acquired for a range of thrust and shaft angles, and the rotation sense of the wake

segments was determined. Figure 1 shows a single video frame depicting a counterrotating vortex pair upstream of one of the three TRAM blades. Two-dimensional velocity measurements were also obtained using the particle image velocimetry (PIV) technique. Three methods for averaging the PIV velocity data were investigated with two of the methods accounting for vortex wander. The core size and core circulation of the negative vortices were found to be smaller than the positive circulation vortices. Figure 2 shows the air-loads distribution for the same BVI condition as that shown in figure 1. Note that the blade-tip region is negatively loaded over a substantial region of the advancing side. This kind of loading is much different from that on conventional helicopter blades, where only a small region may be negatively loaded depending on the tip twist. Figure 3 shows the resulting BVI directivity pattern. BVI metric levels were found to increase with rotor-shaft angle for constant advance ratio and rotor thrust coefficient. The maximum BVI levels were found at a much higher shaft angle than would be the case for a typical helicopter.

Data have also been distributed to NASA's SHCT industry partners for enabling an improved understanding and a better prediction of tilt-rotor rotor-noise mechanisms. The isolated TRAM-DNW data will complement the full-span (dual rotors with complete 0.25-scale V-22 airframe representation) TRAM data that will soon be acquired in the Ames National Full-scale Aerodynamics Complex 40- by 80-Foot Wind Tunnel in FY00. By comparing the data from the two tests, an improved understanding of the interactional aerodynamics and acoustics for tilt-rotor aircraft will be achieved.

Points of Contact: G. Yamauchi/L. Young/E. Booth
(650) 604-6719/4022/3627
gyamauchi@mail.arc.nasa.gov
layoung@mail.arc.nasa.gov
e.r.booth@larc.nasa.gov

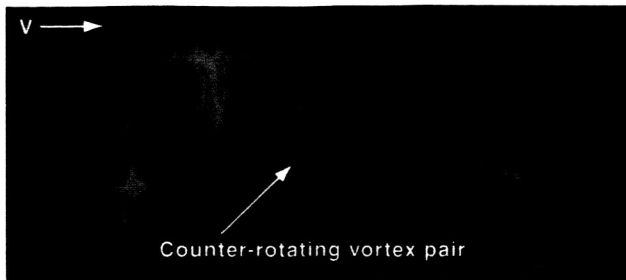


Fig. 1. Counter-rotating vortex pair for a blade-vortex interaction (BVI) test condition.

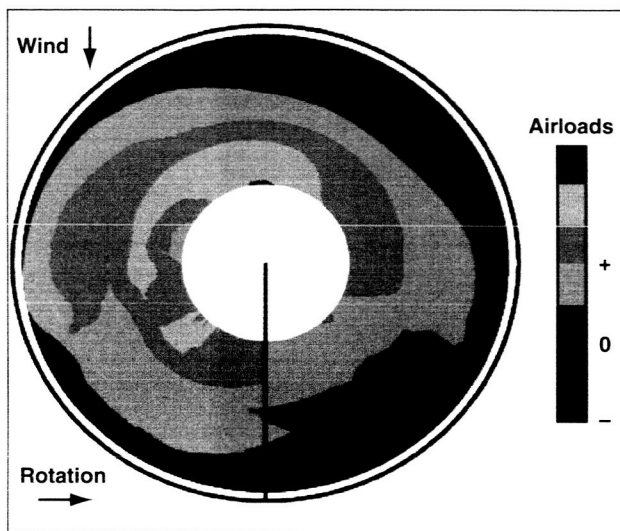


Fig. 2. Air-loads distribution for BVI condition.

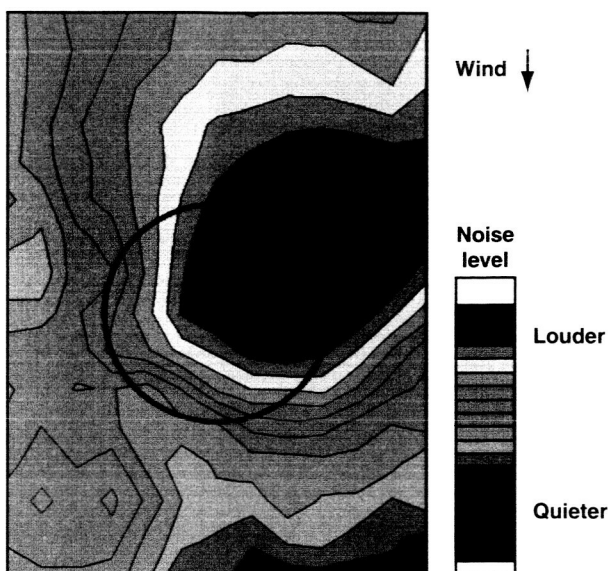


Fig. 3. BVI noise directivity map.

Single-Point and Multi-Point Aerodynamic Shape Optimization of a High Speed Civil Transport

Susan Cliff

The focus of this work was to develop and apply high-fidelity numerical design optimization techniques to the aerodynamic design of High Speed Civil Transport (HSCT) configurations for the purpose of substantially improving their aerodynamic performance, in an effort to develop an economically feasible concept. It was sponsored by the High Speed Research (HSR) program in direct support of Goal 2, Objective 6: "Reduce the travel time to the Far East and Europe by 50% within 20 years," A direct consequence of this effort was the rapid acceleration of the development of high-fidelity aerodynamic design optimization methods within NASA and industry, applicable to the entire spectrum of flight vehicles. Such methods represent the next generation of design tools and hence directly support Goal 2, Objective 8: "Provide next-generation design tools...."

Single-point and multi-point aerodynamic-shape optimization methods at Ames were developed and demonstrated for the design of an advanced HSCT referred to as the Technology Concept Airplane (TCA). A large variety of software methods were integrated to yield an efficient and productive design/optimization process. This integrated set of tools is referred to as the Aerodynamic Shape Optimization (ASO) Library. The tools consisted of flow solvers, grid-generation and perturbation tools, design variable and geometric constraint implementation tools, gradient computation methods, and numerical optimization methods. Some of the tools were commercially available, others were developed in-house, and still others were modifications of commercial software.

Both single and multiple grid-block Euler optimization methods were developed and applied. The single-block method was used solely for the cruise-point design of wing-body-nacelle configurations, and the multi-block method was used for the multi-point designs of full configurations. Both optimization methods were coupled to constrained and unconstrained optimization algorithms, which employ sequential quadratic programming methods. These

methods allow for a single objective function and multiple linear and nonlinear constraints. The objective function gradients are with respect to a user-specified set of design variables. The gradients are calculated using either finite differences or, more efficiently, with the adjoint method. The adjoint method results in over an order-of-magnitude reduction in computational time relative to the use of finite differences. Consequently, a much larger set of design variables can be employed with the adjoint approach. The single-block method was run exclusively on the CRAY C-90; the multi-block method was parallelized and run on a variety of platforms.

A number of analytical tools were used to provide higher fidelity analysis of the optimized configurations than provided by the design methods. Intermediate and final configuration analyses were carried out by use of the AIRPLANE Euler code and two Navier-Stokes codes. AIRPLANE uses an unstructured tetrahedral mesh and is therefore capable of computations about arbitrarily complex configurations. Navier-Stokes analyses were performed with OVERFLOW and UPS. OVERFLOW was used to analyze the wing/body/nacelle/diverter configurations, and UPS was restricted to wing/body configurations. The UPS code uses an upwind marching

scheme and was used to validate previous Ames HSR designs; it was found to produce very accurate solutions.

The TCA baseline configuration, which was the subject of the optimization effort and is shown in the figure, was developed by the Boeing Company in support of the NASA HSR program, using linear-theory-based methods and extensive multidisciplinary system analysis. The design was subject to an extensive set of geometric constraints generated as part of the conceptual design of the aircraft.

The configuration consisted of a wing, body, four nacelles and boundary-layer diverters for the single cruise-point (Mach 2.4) design. For the multi-point design, the configuration was expanded to include leading and trailing edge wing flaps for improving transonic performance and a canard and empennage for longitudinal trim. Multi-point optimization was performed at three design points: supersonic cruise, transonic cruise, and transonic acceleration, corresponding to Mach 2.40, 0.90, and 1.10, respectively.

Cruise-point optimization using the single-block approach was followed by two forms of multi-point design: (1) sequential design (design at the cruise-flight condition followed by flap and canard/tail incidence angle optimization at the two transonic

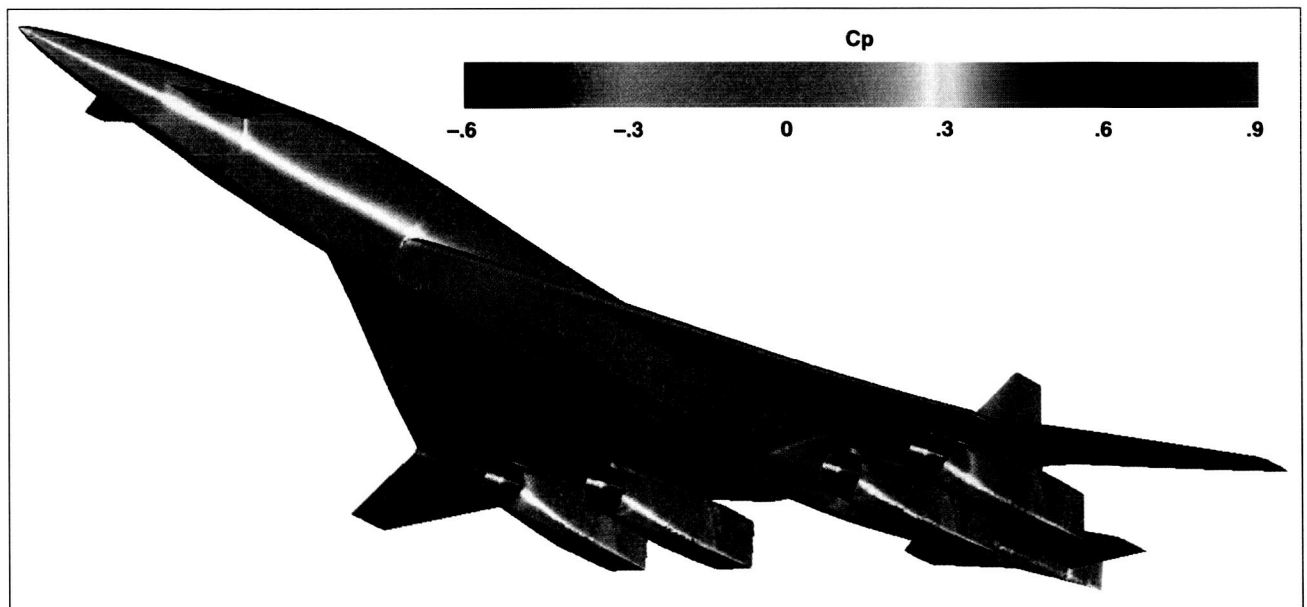


Fig. 1. AIRPLANE computation of the TCA configuration at the transonic acceleration design condition, $M = 1.1$, angle of attack = 3.5 degrees.

conditions), and (2) multi-point design (simultaneous design at the three flight conditions via a composite objective function). The single-point approach produced the bulk of the performance benefits, lowering the weighted-composite required thrust by 4.28 counts after trimming the full configuration at the three design points. (A 7.0 count drag reduction was achieved at cruise for the vehicle without trimming surfaces.) The sequential and multi-point methods achieved 6.03 and 7.55 counts of thrust reduction, respectively. These performance gains are significant, since a single drag count reduction at cruise reduces the takeoff weight of current designs by approximately 8,000 pounds.

Point of Contact: S. Cliff
(650) 604-3907
scliff@mail.arc.nasa.gov

Resound Microphone Wind Noise Reduction

Clifton Horne, Paul T. Soderman

ReSound Corp. in Redwood City, California, has developed a miniature, ear-mounted, hands-free, microphone/receiver for use by technicians, police, firefighters, or others who need an unobtrusive communication system. When used in the field, however, wind-induced noise tended to mask voice communication. A foam covering reduced the noise, but was bulky and obtrusive. Through a Reimbursable Space Act Agreement, ReSound collaborated with the Experimental Physics Branch personnel to mitigate the wind-induced noise without resorting to bulky foam coverings.

To achieve the objective, an artificial head was installed in a ducted fan flow in the AIP acoustics laboratory (figure 1), and a series of experiments was conducted on wind-induced noise of the baseline ReSound microphone over a 3-month period. Using technology developed at Ames for measurement of aircraft model noise in wind tunnels, a screen-covered forebody was designed that protected the microphone sensor yet conformed to the shape and

size of the ear-mounted device (figure 2). The forebody had an aerodynamic shape to minimize flow perturbations; the screen inhibited unsteady pressures at the sensors while passing sound waves. New information was acquired on the baseline and on improved microphone designs regarding effects of turbulence, wind speed, head-tilt angle, and yaw angle. The fluid-mechanic sources of wind noise were isolated. Turbulence, airspeed, and noise were measured in the fan flow, in the free-wind outdoors, in a moving truck in calm air, and in the low turbulence 7- by 10-foot wind tunnel. Results showed that the new wind screen gave improved noise reduction

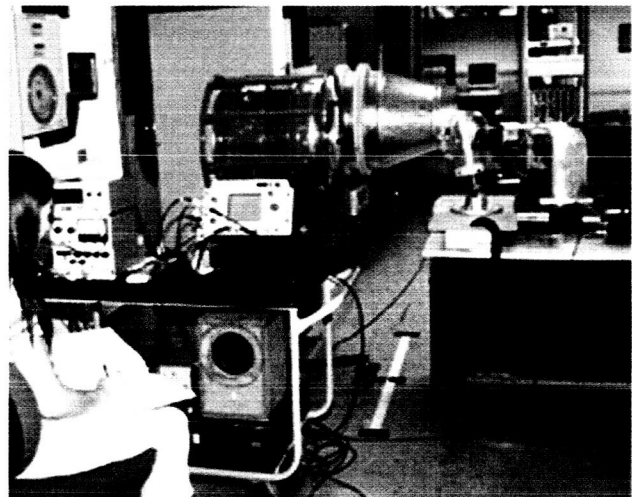


Fig. 1. Experimental set-up in acoustic lab with artificial head model, wind simulator, and instrumentation for measuring flow characteristics and microphone noise.

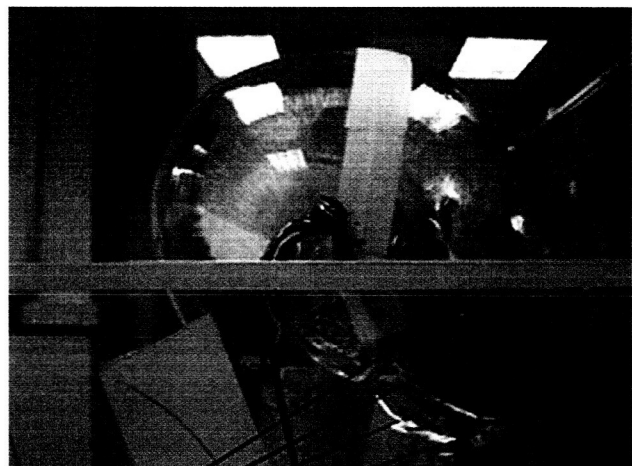


Fig. 2. Close-up detail of artificial head model with ear-mounted microphone and alignment template.

relative to the ReSound baseline with foam covering and that it has a more robust, streamlined shape that lends itself to unobtrusive operation by the user. Microphone response was carefully correlated with flow parameters such as turbulence, airspeed, and flow angle so that future changes can be evaluated using the database.

Further improvements in the design may be possible by optimizing the screen impedance and the forebody shape.

Points of Contact: C. Horne/ P. Soderman
(650) 604-4571/6675
chorne@mail.arc.nasa.gov
psoderman@mail.arc.nasa.gov

Stealth Technology Reduces Airframe Noise

Paul T. Soderman

Recent airframe noise studies at Ames Research Center and elsewhere have identified flap side-edge noise as an important component of aircraft landing noise. During aerodynamic tests of an Air Force stealth fighter design (called SHARC) in the Ames 40- by 80-Foot Wind Tunnel, it came to our attention that stealth technology might have acoustic attributes. Specifically, the Continuous Moldline Technology (CMT) developed for SHARC eliminates flap side edges by blending the flap and wing trailing edges with a flexible material that is load bearing. This led to a 7- by 10-foot wind tunnel aeroacoustic test of a two-dimensional airfoil with a simple hinged flap with and without a CMT modification (figure 1).

To investigate CMT performance, a 70-element phased microphone array technology (PMAT) acoustic system was installed in the Ames 7- by 10-Foot Wind Tunnel test section wall. The array is designed for visualization of noise sources and determination of their individual strengths. Noise radiation from the vertically mounted wing/flap model revealed a virtual elimination of the side-edge

noise in the flyover direction. Because of the large noise reduction, it was necessary to recess the microphones in order to reduce flow-induced noise and increase the signal-to-noise ratio. A strong Kevlar cloth covered the recess. With this array geometry, noise levels that were 20 decibels below the wind tunnel background noise could be identified.

With the new array, it was found that the CMT flap was at least 6–8 decibels quieter than the simple hinged flap, as shown by the phased array images of figure 2. Background noise made it impossible to identify noise sources below that level. Previous work indicates that the simple hinged flap is quieter than the conventional Fowler flap used on current air transports. Hence, new aircraft designs such as the Blended Wind Body, which can operate with a simple high lift system, would benefit from the low noise of simple hinged or CMT flap systems. Aerodynamic performance data were acquired simultaneously with the acoustic data.

Point of Contact: P. Soderman
(650) 604-6675
psoderman@mail.arc.nasa.gov

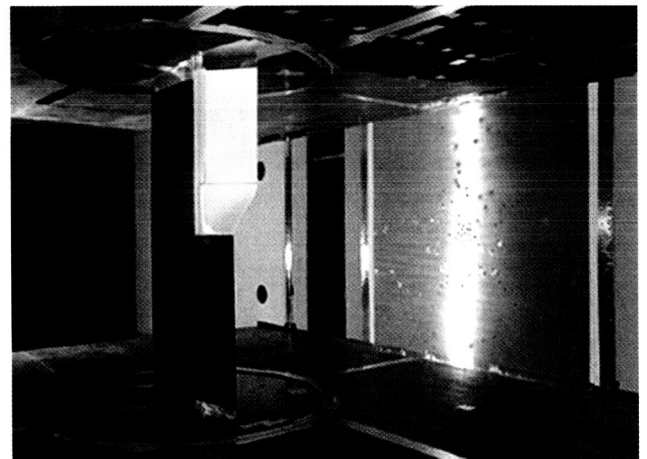


Fig. 1. Upstream view of airfoil model with simple flap (upper white) blended to wing by CMT section. Phased microphone array is mounted on test section right wall.

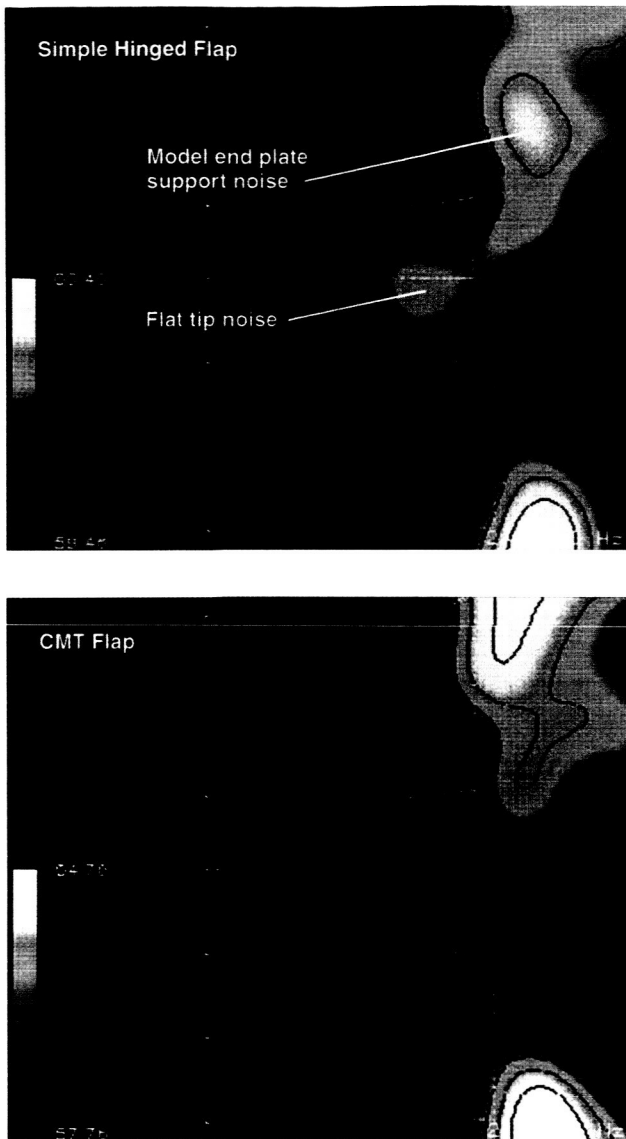


Fig. 2. Noise source images at simple flap tip (upper) eliminated by CMT flap (lower).

REVOLUTIONARY TECHNOLOGY

Improved Rotorcraft Airfoil Designs Using Genetic Algorithms

David W. Fanjoy, William A. Crossley,
Anastasios Lyrintzis, Sesi Kottapalli

Genetic algorithms (GAs) are an optimal search technique based on "evolutionary programming" techniques that mimic Darwin's idea of "natural selection." Ongoing research has demonstrated that GAs are useful tools in aerospace design. Recent research has centered on using GA-based-methods for airfoil design. A "practical" problem of rotorcraft industry origin that involved the vertical tail (NACA 63-418 airfoil section) of a current Army helicopter was considered. The vertical tail was experiencing buffeting within its normal flight envelope, and excessive flow separation at moderate angles of attack was a suspected cause. The objective of this effort was to design a new GA-based vertical tail airfoil section that maintained attached flow. The associated shape-design problem was as follows: minimize airfoil drag while retaining the thickness, lift, and moment of the NACA 63-418 airfoil. An additional constraint ensured that the new airfoil design retained attached flow at three flight conditions (at angles of attack of -2, 4, and 12 degrees, and at a Mach number of 0.06). A simplified aerodynamic analysis, the panel method, was to be used to keep computational expense low.

Compared to the NACA 63-418 airfoil, the new GA-based airfoil (figure 1) featured a maximum thickness location that was farther forward; it also had a more complex camber distribution. Results showed that the new GA-based airfoil exhibited similar lift, a smaller pitching moment, and less flow separation than the NACA 63-418. Figure 2 shows that at an angle of attack of 12 degrees, the separation location improvement for the new GA-based airfoil was 18% of the chord. Further analysis using two more advanced codes (Ames' ARC2D and the Massachusetts Institute of Technology's XFOIL) confirmed the above improvement (however, the

three codes predicted different improvement levels). To summarize, it is believed that the present GA-based procedure can be used for solving rotorcraft-related problems of a practical nature.

Point of Contact: S. Kottapalli
(650) 604-3092
skottapalli@mail.arc.nasa.gov

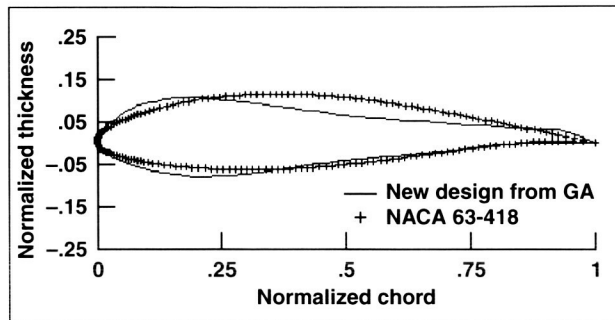


Fig. 1. NACA 63-418 design and new, genetic-algorithm-based design.

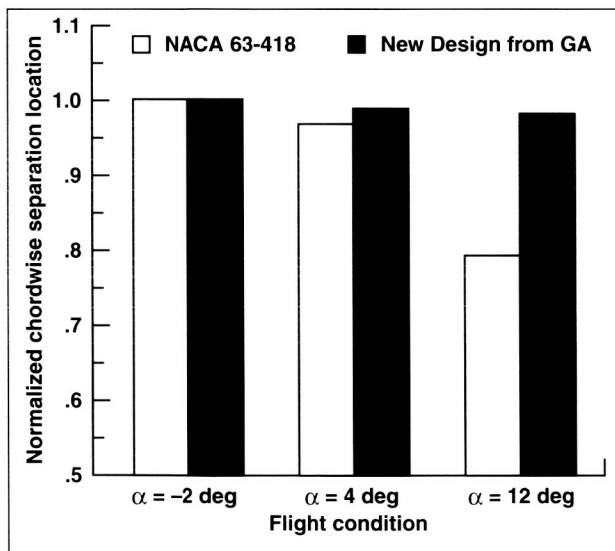


Fig. 2. Upper surface separation locations: angle of attack = 12 degrees (NACA 63-418 design and new design).

Overset Structured Grids for Unsteady Aerodynamics

Robert L. Meakin

The Department of Defense is supporting the development of robust adaptive refinement methods for unsteady geometrically complex moving body problems by means of the High Performance Computing Modernization Program (HPCMP) Initiative known as CHSSI. The object of the work is to exploit the computational advantages inherent in structured data to solve this important class of problems on parallel scalable computer platforms.

The physical domain of complex problems is decomposed into near-body and off-body regions. The near-body domain is discretized with "Chimera" overset grids that need extend only a short distance into the field. The off-body domain is discretized with overset structured Cartesian grids (uniform) of varying levels of refinement. The near-body grids resolve viscous boundary layers and other flow features expected to develop near body surfaces. Off-body grids automatically adapt to the proximity of near-body components and evolving flow features. The adaptation scheme automatically maintains solution accuracy at the resolution capacity of the near-body system of grids. The approach is computationally efficient and has high potential for scalability. Grid components are automatically organized into groups of equal size, which facilitates parallel scale-up on the number of groups requested. The method has been implemented in the computer program known as OVERFLOW-D.

For example, OVERFLOW-D was used in FY99 to obtain a time-accurate simulation of the V-22 tilt-rotor aircraft in high-speed cruise conditions. Temporal resolution of the simulation provided 2,000 time-steps per revolution of the rotor blades. Nearly 30 million grid points are used to spatially resolve the problem domain. An important result of the simulation is the capture of the rotor-tip vortices as part of the solution. As indicated in the figure, the vortices are evident in the field a full body length downstream of rotors. The simulation was carried out using 65 processors on an IBM-SP. Post-process analysis of the large unsteady data set was carried out on an SGI Origin 2000.

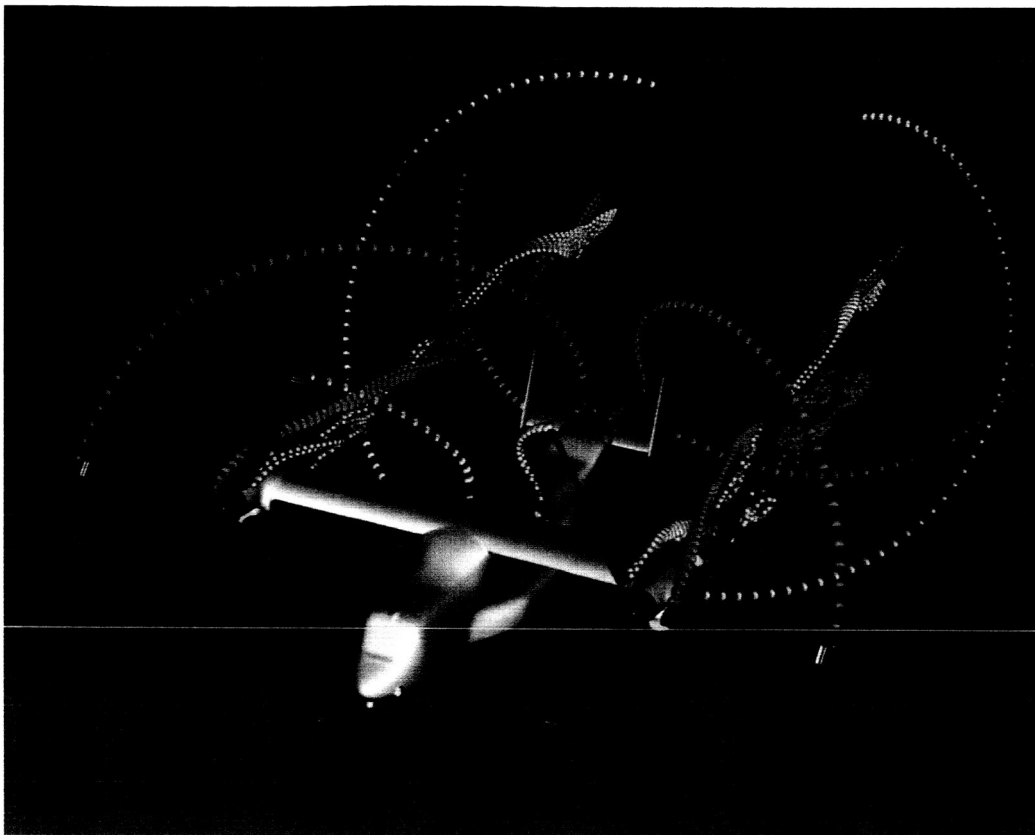


Fig. 1. The V-22 rotor-wake system is visualized in a post process where filaments of particles are released from inboard and outboard blade tips every 25 time-steps.

The V-22 result is significant in several respects. Accurate simulation of the rotor wake system is important in predicting rotor-airframe interactional dynamics, as well as aircraft acoustics. Combined with existing flight data and scheduled tunnel data, the result provides the basis for demonstrating design-to-flight analysis capability for general tilt-rotor aircraft. The result is a high-fidelity baseline data-set that can be used to evaluate future tilt-rotor concepts

such as variable-diameter tilt rotors, quadrotors, and future defense transport tilt rotor configurations. The capabilities illustrated by this simulation support important defense and civil priorities relating to rotary-wing aircraft.

Point of Contact: R. Meakin
(650) 604-3969
bmeakin@mail.arc.nasa.gov

Planar Doppler Velocimetry: Three-Component Velocity Measurements in a Full-Scale Rotor Flow Field

Michael S. Reinath, Robert L. McKenzie

Planar Doppler velocimetry (PDV) is an optical, laser-based flow-field measurement technique that is being developed for the large wind tunnels at Ames Research Center. The PDV technique measures the Doppler shift of light that is scattered from aerosol particles that are added to the flow and illuminated by a pulsed laser sheet. Images of the planar measurement region are acquired with scientific-grade digital cameras and then processed to yield instantaneous, three-dimensional (3-D) velocity maps, which are limited in size only by the field of view of the cameras and any requirement to meet a particular spatial resolution.

The PDV concept is based on the sensitive frequency discrimination that occurs when the scattered laser light is viewed through an optical filter cell containing iodine vapor. Particles moving with the flow pass through the laser sheet and scatter light that is shifted in frequency according to the Doppler effect. Some of this light is collected to form an image that records intensity variations not caused by the Doppler effect. These variations are caused primarily by nonuniform aerosol distribution and nonuniform illumination. Simultaneously, some of the light is collected and imaged through the optical filter cell containing the iodine vapor. This cell acts as a sharp spectral filter at the laser frequency. Because the Doppler-shifted laser light has a narrower bandwidth than the spectral range of the iodine absorption feature edge, Doppler shifts of the collected light are converted to variations in recorded image intensity as the frequency moves on the filter edge. In its full implementation, pairs of filtered and unfiltered images are simultaneously acquired during each laser pulse by using three camera systems that view the laser sheet from three different locations. The filtered images are normalized by the unfiltered images to eliminate the variations in intensity that are not related to the Doppler effect. These normalized images are processed and become quantitative velocity map images of three separate, instantaneous

velocity-field components. An algebraic transformation yields the complete 3-D orthogonal velocity vector field.

At Ames Research Center, the PDV technique, along with its related optical hardware and data analysis software, has been shown in the laboratory to be capable of resolving instantaneous velocities as low as 2 meters per second from a single pulse and to be applicable at ranges exceeding 40 meters. These capabilities, in addition to the minimal requirements of PDV on the optical and density properties of the aerosols that must be added to the flow, make it particularly attractive as a means of measuring 3-D velocity vector fields in time-dependent flows in large-scale facilities where full-scale rotor tests are conducted and velocity vector-field measurements between turning rotor blades are of interest.

The PDV system was first used in the wind tunnel environment during the XV-15 rotor test in the Ames 80- by 120-Foot Wind Tunnel. That test was conducted to determine fundamental differences in blade vortex interaction (BVI) noise for this tilt rotor in approach flight configuration. The first figure shows a diagram of the test section and measurement geometry. The three camera locations are shown along with the respective measured velocity vector directions. The camera field of view is indicated by the square region in the laser sheet. Measurements were acquired at various stations behind the rotor blade using a variable time delay to synchronize the laser pulses and camera shutters with the rotor azimuth. The second figure shows the computed, single-pulse 3-D orthogonal velocity vector field. The view is normal to the measurement plane; in-plane velocities are shown as vectors, and out-of-plane velocities are shown as color contours. Also shown is the position of the rotor blade, which is 22.6 degrees upstream of the measurement plane in this case. Free-stream velocity, rotor-shaft angle, and advance ratio simulate the tilt-rotor approach configuration.

Point of Contact: M. Reinath
(650) 604-6680
mreinath@mail.arc.nasa.gov

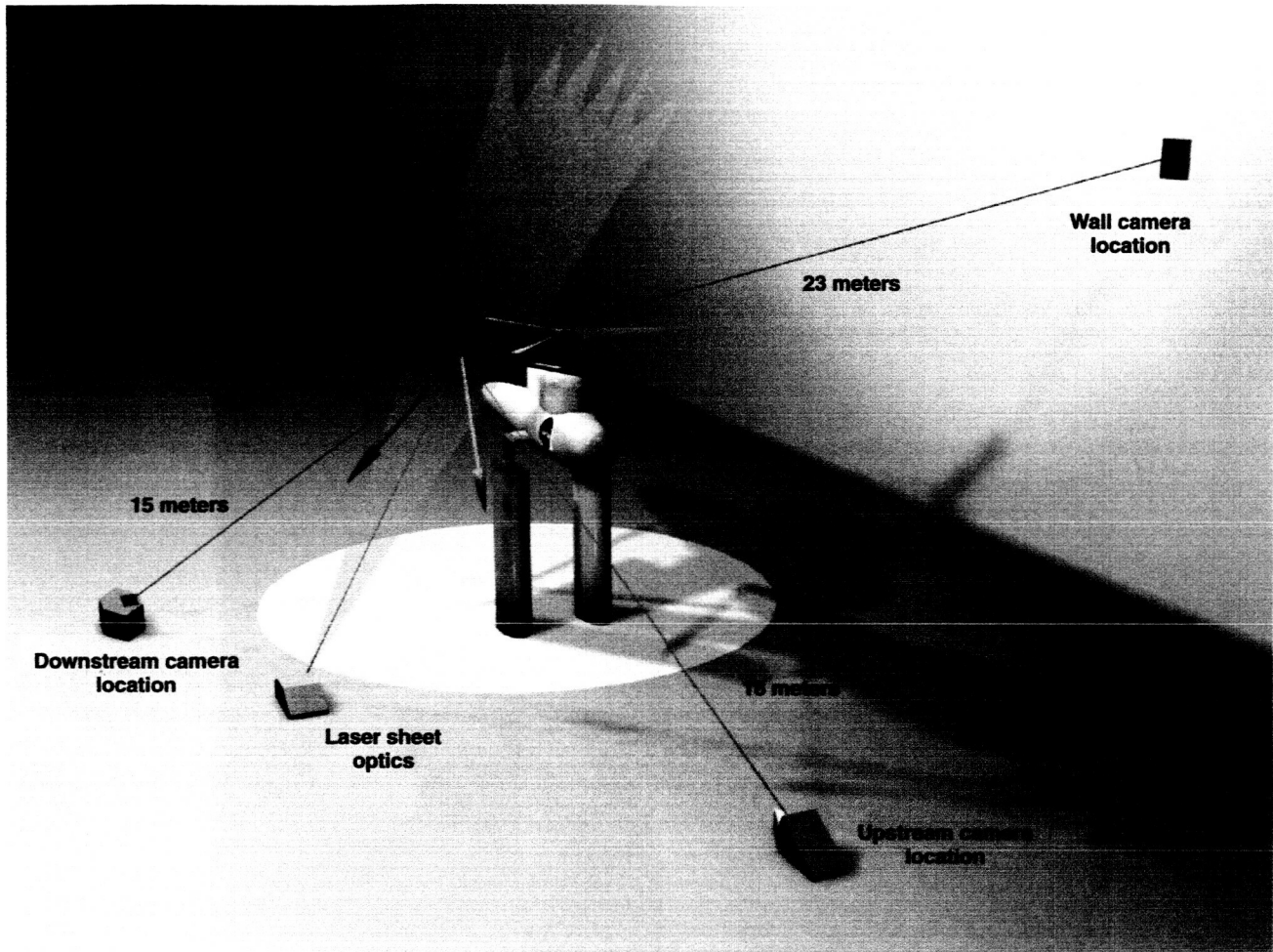


Fig. 1. XV-15 rotor and PDV system configuration in the Ames 80- by 120-Foot Wind Tunnel; vectors indicate the respective measured velocity component directions.

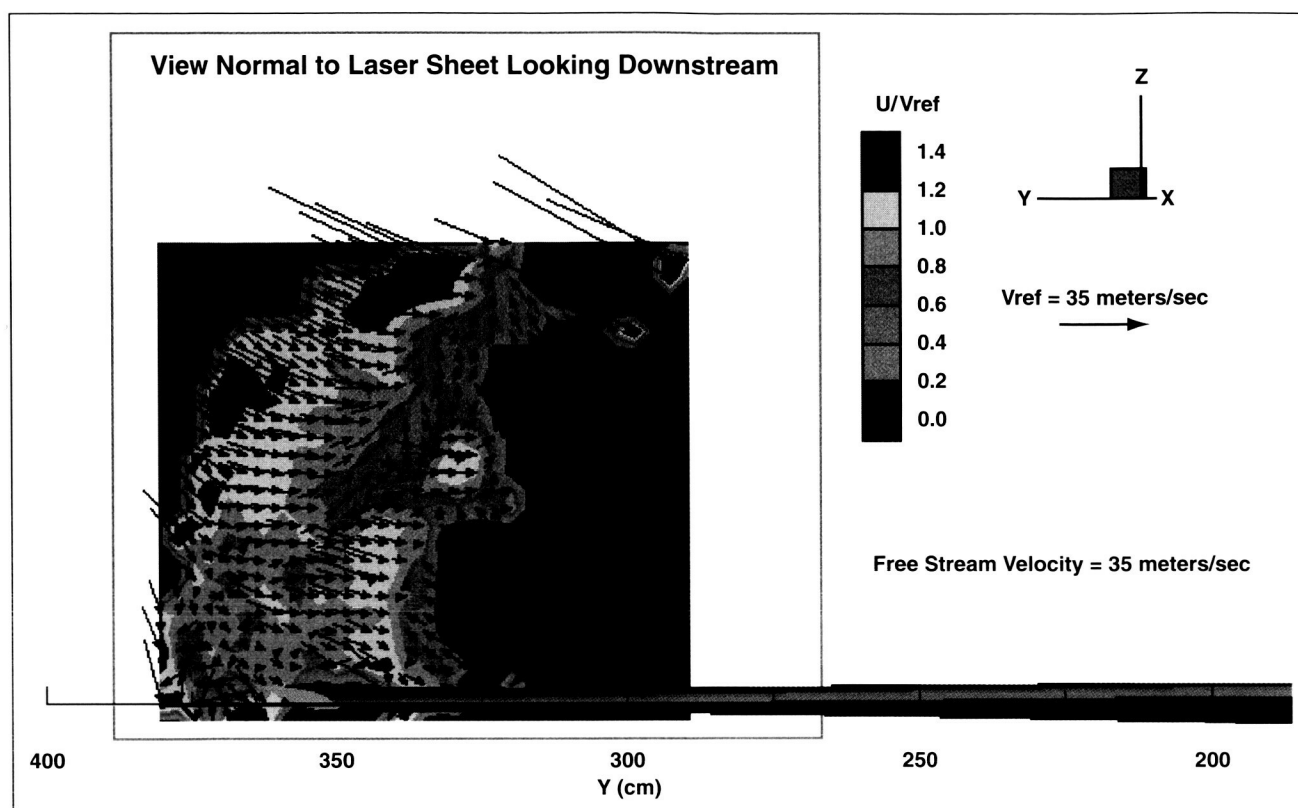


Fig 2. Orthogonal velocity vector field processed from a single-pulse measurement (view is normal to the measurement plane looking downstream).

Photonic Switching Using Light Bullets

Peter M. Goorjian

The objective of this work was to develop a faster, more efficient data switch for use in optical communications networks and optical signal processing systems. An optical device has been developed to perform ultrafast, all-optical switching by using light bullets to switch light bullets. This invention was granted U.S. Patents 5,651,079, July 22, 1997 and 5,963,683, October 5, 1999; it was based on computer simulations of the interactions of light bullets.

The rapid proliferation of information technology in commerce, finance, education, health, government, security, and entertainment, together with the ever-increasing power of computers and data storage devices, is fueling a potentially massive demand for network interconnections, especially broadband

services. Switching is an essential operation of all communications networks and digital computers and signal processing systems. Switching is presently a limiting factor in the speed of operation of optical communications and computing, because most commercial devices must use electrical forms of switching, and in the longer term electronic systems will become increasingly complex and costly. Network designers will turn increasingly to photonic transport and switching technologies. An all-optical switch would have the inherent advantages of higher speed and higher efficiency.

One such all-optical switch has been designed at Ames Research Center. In the NASA switch configuration, light bullets propagate through, and interact nonlinearly with, each other within a planar slab waveguide to selectively change each other's directions of propagation into predetermined output

channels. The resulting performance should enable low-power, high-speed switching in a small device.

Possible materials include nonlinear glasses, semiconductor crystals, and multiple quantum-well semiconductors. The patents describe the necessary material parameters, including negative group velocity dispersion, nonlinear index of refraction, and wavelength of light, that are required in order for the light bullets to interact and selectively change each other's direction of propagation.

The figure shows the results of a computer simulation of two counter-propagating light bullets at four instants in time. As they collide with each other, they deflect each other through attraction. This deflection is the basis of a light switch, that is, where light switches light.

Point of Contact: P. Goorjian
(650) 604-5547
goorjian@nas.nasa.gov

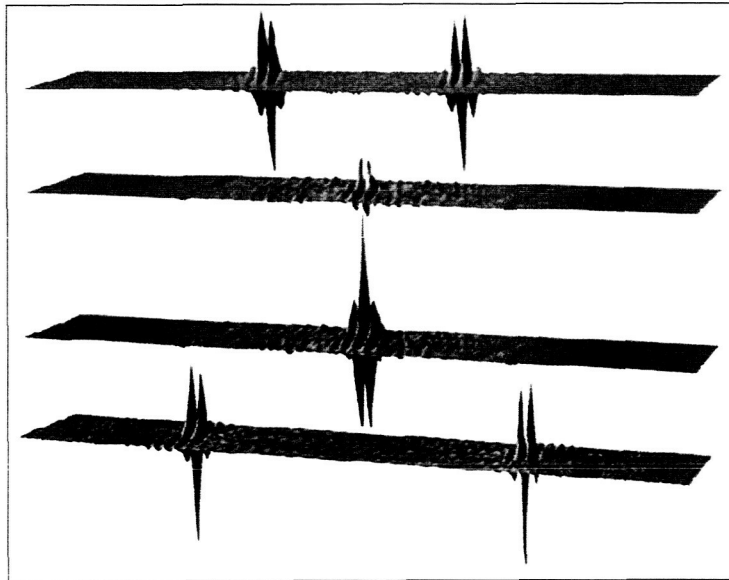


Fig. 1. Collision of two counter-propagating light bullets.

A Computational Model of Situational Awareness

Robert J. Shively

Situational awareness (SA) is a term that has great intuitive appeal, especially in aviation. Although often invoked in a descriptive manner, SA is difficult to precisely define. As a result, a computational, mathematically defined model of SA has been developed. The goal of the modeling effort was to enhance researcher communication and to advance

efforts to improve pilot SA and performance through improved display design or aircrew procedures.

The Computational Situational Awareness (CSA) model is composed of two essential features: situational elements and situation-specific nodes. Situational elements (SEs) are relevant information in the environment that define the circumstances (for example, other aircraft, obstacles, way points, own-ship parameters). The pilot experiences these elements through perception, experience, or a preflight briefing. Each SE has a mathematical weight based upon its importance in the situation and a

mathematical value based upon one of four levels of awareness (detection, recognition, identification, and comprehension). These four levels of awareness provide a means of quantifying an operator's perception of the situational elements.

Situation-sensitive nodes are semantically related collections of SE's. The nodes are defined by the context of a given task and are weighted by the overall importance of the node in determining the level of SA. If the situation changes, then the weights on the nodes, or the nodes themselves, may change to reflect accurately the level of SA. SA is the weighted average of knowledge that the pilot has in each node, and thus is a measure of the pilot's perceived SA. The CSA model then subtracts an error component, based on misidentified SE's or unknown elements in the environment.

The computational model of situational awareness was designed to be embedded in an existing model of human performance, the Man-Machine Design and Analysis System (MIDAS). MIDAS has very detailed representations for the two major components of human-systems integration: (1) the human operator, and (2) the system, or environment under study. The human model consists of perception, and cognitive processes such as working memory, scheduling, decision making, and long-term memory. Output measures from the aggregation of models include task execution time lines, operator workload, and the aforementioned situation-awareness construct.

The systems model includes the cockpit, or workstation, the environment, and the human figure model. The environmental model consists of elements in the world with which the simulated operator or crew station interacts, for example, trees, other aircraft, tanks, or air traffic control. The human anthropometric model is Jack®, developed by the University of Pennsylvania.

The CSA model was developed, integrated into MIDAS, and tested in simulation. A recent study evaluated the validity of the CSA when compared with pilots in a manned simulation with very favorable results. As shown in figures 1 and 2, both subjective ratings of SA (Subjective Awareness Rating Technique: SART) and performance measures of SA (RMSE altitude) are highly correlated with the predicted SA levels.

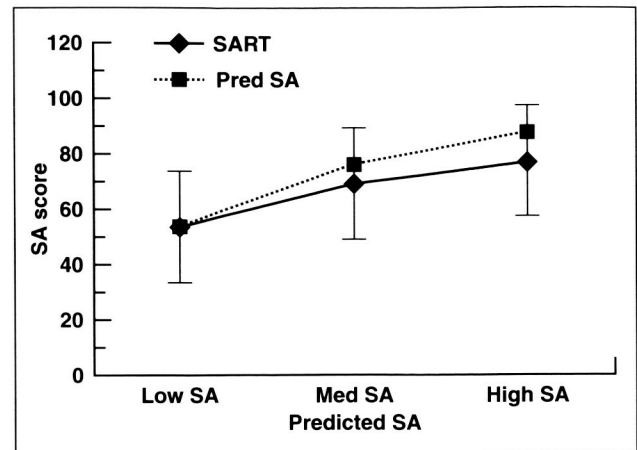


Fig. 1. SART versus predictions.

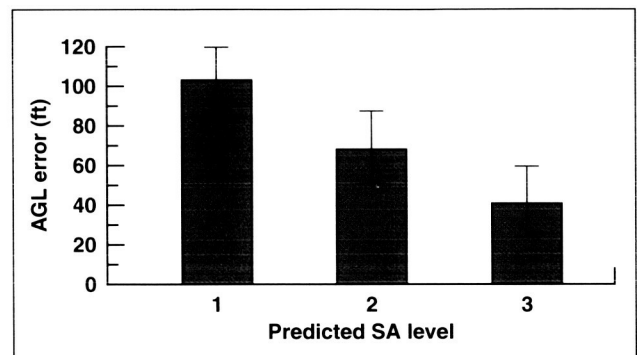


Fig. 2. RMSE altitude versus predictions.

Point of Contact: R. Shively
(650) 604-6249
jshively@mail.arc.nasa.gov

A Computational Tool for Rotor Design

Roger Strawn

Helicopter and tilt-rotor blades produce complex vortical flow fields that interact with the nacelles, wings, fuselage, and the ground. Rotorcraft designers need an efficient computational tool that can model these vortical flow fields and accurately predict the aerodynamic performance of rotary-wing vehicles. The purpose of this project is to develop a computational tool with which to model the complex flow fields around rotors and bodies. In an industry design environment, turnaround time must be reduced to a level at which design cycles can be conducted within schedule and cost. Therefore, the computational tool must be efficient and easy to use.

With Ames' funding, Sukra Helitek Inc. developed a software tool called Rot3DC, which simulates the flow field around rotary-wing vehicles. The method employs a graphical user interface to model either isolated rotors or rotor and fuselage problems, including ground interference. Rot3DC solves the Navier-Stokes equations on unstructured grids with a simple, but effective, momentum-source representation for the rotor blades. This momentum-source rotor-blade model allows for highly efficient solutions of rotor flow fields.

Figure 1 shows a sample aerodynamic solution from the Rot3DC code for a V-22 tilt-rotor landing on the deck of an aircraft carrier. This figure demonstrates the complicated interactions between the rotor downwash, the wings of the V-22, and the deck of the ship. Despite these complex flow-field features, the Rot3DC code can model these solutions in a matter of hours on a high-end personal computer. This rapid turnaround and simplified problem setup make Rot3DC well-suited for helicopter design applications. Indeed, the Boeing Company has licensed Rot3DC and is using it to model the Comanche helicopter and V-22 tilt rotor.

Sukra Helitek Inc. plans to upgrade the Rot3DC computer code to include a higher-fidelity unsteady rotor model and solution-adaptive grids for improved modeling of rotor wakes. These modifications should improve the overall analytical accuracy while retaining the ease of use and rapid turnaround of the original Rot3DC software package.

Point of Contact: R. Strawn
(650) 604-4510
rstrawn@mail.arc.nasa.gov

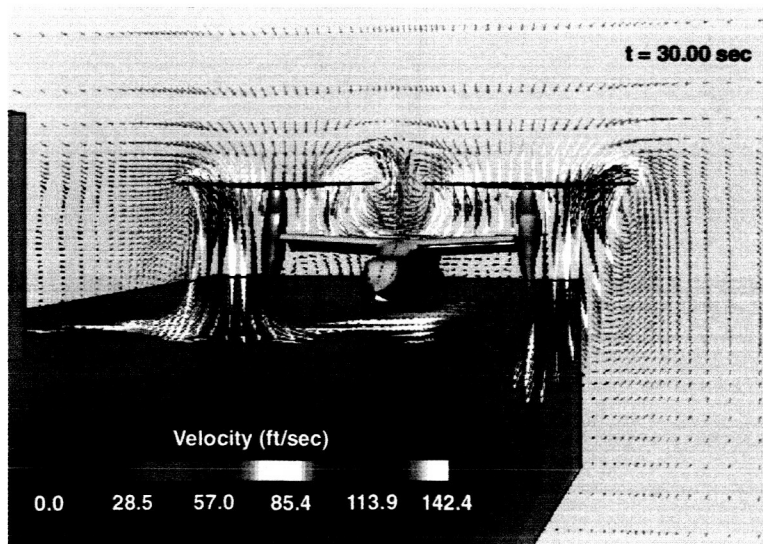


Fig. 1. Computed velocity flow field for the V-22 tilt rotor during a shipboard landing.

Java Pathfinder: A Tool for Verifying and Validating Software

Guillaume Brat, Klaus Havelund, Seungjoon Park, Willem Visser

Software, particularly systems capable of autonomous operation, is fast becoming a major enabling technology at NASA. Unfortunately, the cost savings of autonomous software systems can easily be offset by the risk of in-flight failure of the software. Although rigorous testing of software before deployment can increase the confidence of its correctness, the tendency of in-flight software to be multi-threaded makes it hard to find subtle errors caused by the unforeseen interaction of concurrently executing components. The Java PathFinder project developed two versions of a tool that augments traditional testing techniques in order to find subtle errors in multi-threaded programs.

As can be deduced from the name, the current focus is on finding errors in programs written in Java, but future work will also focus on C and C++ as well as on design notations such as the Unified Modeling Language (UML). Specifically, Java Pathfinder uses a technique called model checking that allows all possible executions of a Java program to be analyzed in order to find errors. Typical errors being targeted include deadlocks and mutual exclusion and assertion violations.

The Java PathFinder project was initiated after a practical experiment in 1997 in which part of the Remote Agent, an artificial-intelligence-based software component of the Deep Space 1 spacecraft, was analyzed as an experiment. The analysis identified five classic multi-threading errors that had not been caught by normal testing. One of these errors is illustrated in the figure which describes a situation in which two threads executing in parallel interact in an unexpected manner. The analysis was done by hand translating part of the Remote Agent code into the language of an existing model-checking tool. This was a time-consuming task. The first version of Java PathFinder, JPF1, finished in August 1999, automated this process by translating from Java to an existing model checker. For the first time, JPF1 demonstrated the feasibility of model-checking Java source code directly without human interaction. JPF1 was applied

to two software systems developed at NASA: a satellite file exchange module developed at Goddard Space Center, and a ground control module for the Space Shuttle Launch facility at Kennedy Space Center.

Although demonstrating feasibility, JPF1 had some drawbacks. First, Java is traditionally compiled into byte code (a low-level machine-oriented language) before execution, and libraries often come as byte code rather than as source code. Hence, JPF1 could not handle libraries. Second, since SPIN was used as the model checking engine, and since SPIN is not easily modifiable, it was not possible to experiment with alternative search strategies in order to deal efficiently with large programs. Hence, a new version of Java PathFinder, JPF2, was developed (in Java), which model checks Java byte code directly. Subsequently, advanced testing techniques have been integrated into JPF2, which has been used to find an intricate, but known, error in the real-time operating system DEOS used by Honeywell in business aircraft.

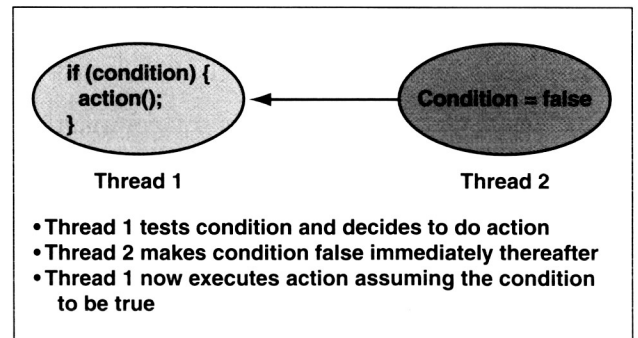


Fig. 1. Error pattern found in remote agent.

Point of Contact: K. Havelund
(650) 604-3366
havelund@ptolemy.arc.nasa.gov

An Electromagnetic Actuator for Helicopter Rotor Active Control

Brent Wellman, Robert A. Ormiston

There is considerable interest in the potential of active rotor control as a means of improving rotorcraft loads, vibration, noise, and performance by using various approaches including individual blade control, on-blade controls, and active twist. Smart materials and actuators figure prominently in many of these approaches, but at present this technology is limited with respect to actuation force and displacement capability, as well as maturity level of the underlying technologies.

With these considerations in mind, the U.S. Army Aeroflightdynamics Directorate (AFDD) investigated alternative technologies for individual blade control surface actuation, and solicited proposals under the Small Business Innovative Research (SBIR) program.

The Heliflap™ is an electromagnetic actuator and trailing-edge control surface developed for helicopter rotor active-control applications. It is a rugged, compact system with no external linkages and no moving parts except the flap itself. It has excellent force, deflection, and frequency characteristics, as well as good power and thermal dissipation characteristics. The flap amplitude and frequency are controlled by modulation of the electrical current to the actuators. The net installed weight for the non-optimized prototype is 9.6 pounds. The design and development of the Heliflap has been completed including bench testing and preliminary whirl testing on a full-scale OH-58 helicopter rotor (figure 1) at rotor speeds up to 81% of normal operations and at low collective pitch settings.

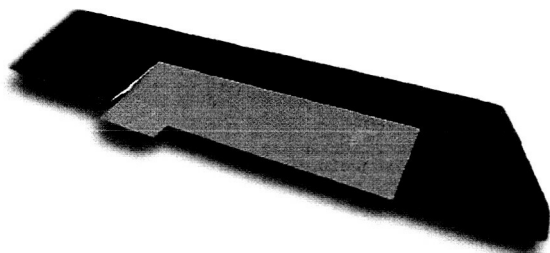


Fig. 1. Prototype Heliflap™ installed in an OH-58 rotor blade.

Test results compare favorably with design predictions from the Heliflap analytical model. Bench testing demonstrated 35.6 foot-pounds static torque for 100 amperes, ± 8 -degree deflections, and operation from 0–37 hertz. Whirl testing of the 6- by 24-inch prototype at 81% nominal rotor speed demonstrated ± 6 -degree deflections at 21 hertz (4.4 times per rotor revolution) requiring a total average electrical power of 220 watts. The actuator appears to be well suited for active control for rotor vibration reduction and may have significant potential for application to rotor primary flight control as well. A comparison of test results with computer predictions of the actuator performance is shown in figure 2.

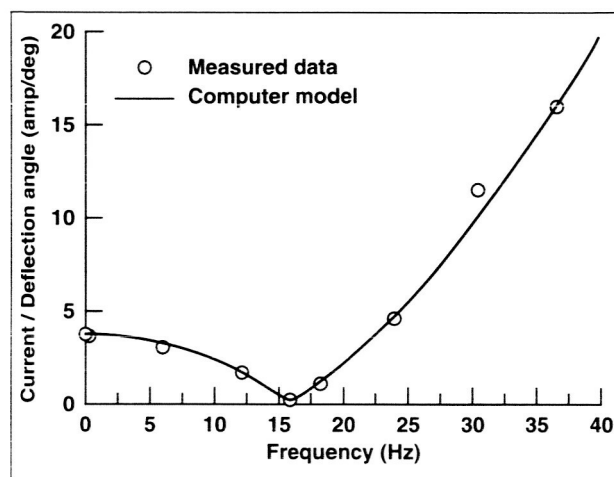


Fig. 2. Current required per degree of deflection versus frequency for a nonrotating blade.

Points of Contact: B. Wellman/R. Ormiston
(650) 604-3645/5835
bwellman@mail.arc.nasa.gov
rormiston@mail.arc.nasa.gov

MATRIX_x Automated Testing Tool

Ann Patterson-Hine, Joel Henry

This research program has focused on developing tools and techniques that can automate the process of testing and troubleshooting complex control systems that are implemented using an autocoder. Significant increases in software complexity and sophistication have made software more difficult to test and troubleshoot. Historically, the cost of debugging has been the most time-consuming and expensive aspect of large-scale software development. In order to increase software production efficiency, many real-time systems and controllers are being implemented with the code generated by automatic code generators, such as the MATRIX_x SystemBuild from Integrated Systems, Inc. and SIMULINK Real Time Workshop from The Mathworks, Inc.

The MATRIX_x Automated Testing Tool (MATT) was developed at East Tennessee State University to aid in the verification of systems implemented in the MATRIX_x environment. The tool targets automation of black box techniques such as critical value testing, random input testing, cyclic value testing, and floating-point accuracy testing. MATT supports automated testing of MATRIX_x models, at the superblock level, through a user friendly interface for both the Solaris and Windows platforms. This tool provides powerful support for the generation of test matrices, launching of simulation, capturing simulation results, and analyzing these results. Graphing is supported, as well as the ability to save test data for later reuse and save simulation results for regression analysis. MATT can literally generate thousands of tests, simulate those tests, and capture results in minutes. More than 20 test types are provided in addition to the ability to import user-created test data. A user simply selects a MATRIX_x model, chooses a superblock, selects the number of tests, selects the test type for each input variable, creates an input matrix, launches a simulation, and analyzes the results through MATT Results and Summary screens. Graphs are easily created as well by simply choosing the input or output variables to graph and creating the graph in MATT.

In an era of highly ambitious technological goals critically dependent on real-time software, well-planned and effective testing strategies based on

automation are needed to meet these goals. The MATT tool supports specification of a set of test types, strategies for applying these test types, and automated support for testing real-time systems built using MATRIX_x.

Point of Contact: A. Patterson-Hine
(650) 604-4178
apatterson-hine@mail.arc.nasa.gov

Nanoelectronics Modeling

M. P. Anantram, Liu Yang, T. R. Govindan, Jie Han, Alexei Svizhenko

Nanoelectronics research at Ames encompasses topics in molecular devices and miniaturization of conventional semiconductor devices. The objective is to acquire the knowledge necessary to build future generations of computing devices and sensors to fulfill NASA's challenges in aerospace transport and space missions. There were three significant accomplishments in FY99. First, we modeled electron transport in capped carbon nanotubes and gleaned the effect of caps and defects on electron emission, which is important in the use of the nanotubes as probe tips and wires. Second, through modeling and analysis we related conductance to mechanical deformation of carbon nanotubes, which is important in the use of nanotubes as sensors. Third, we developed a simulator for quantum mechanical transport in semiconductor devices, which provides important capability to study future generations of ultrasmall devices. A brief description of each follows.

The large length-to-diameter ratio of carbon nanotubes makes them good candidates for molecular wires and field emitters, and for use in probe-tip applications where electron emission from the tip of the capped tube is important. The results show that transmission probability mimics the behavior of the electronic density of states at all energies except the localized energy levels of a polyhedral cap (figure 1). The close proximity of a substrate causes hybridization of the localized state. As a result, subtle quantum interference between various transmission paths gives

rise to antiresonances in the transmission probability, at energies of the localized states (figure 1). Our observations indicate that by appropriately engineering the location of defects, these antiresonances can be transformed to huge transmission resonances. This is especially useful because these resonances offer a way to obtain a large current density in a narrow energy window around the localized energy level.

A potential application of carbon nanotubes as sensors is exploiting the relationship between mechanical deformation and electronic properties of the tubes. Our work provides fundamental insights into this relationship by providing detailed answers for the band-gap variation with tensile and torsional strain as a function of nanotube chirality, diameter, and magnitude of strain. The electronic properties of a nanotube in equilibrium are determined by indices (n, m) , which define the chirality and diameter. The significant results are that (1) the magnitude of slope of band gap versus strain has an almost universal behavior that depends only on the chiral angle, and (2) the sign of slope depends only on the value of $(n - m) \bmod 3$. Figure 2 demonstrates these results for the case of tensile strain. For example, $(6,5)$ and $(6,4)$ nanotubes have chiral angles close to each other but the slope of band gap versus strain has opposite signs.

As devices continue to be miniaturized, modeling tools based on quantum physics become increasingly important. The difficulty in building such a simulator lies in developing a set of physical approximations that enable solutions on available supercomputers. We have developed such a two-dimensional device simulator which solves the nonequilibrium Green's function equations and Poisson's equation self-consistently on a nonuniform spatial grid. Figure 3 shows the self-consistently calculated charge density for one such case. The simulation predicts the expected small electron density close to the gate ($x = 0$ nm) at the large potential barrier created by the gate oxide.

Point of Contact: M. Anantram
(650) 604-1852
anan@nas.nasa.gov

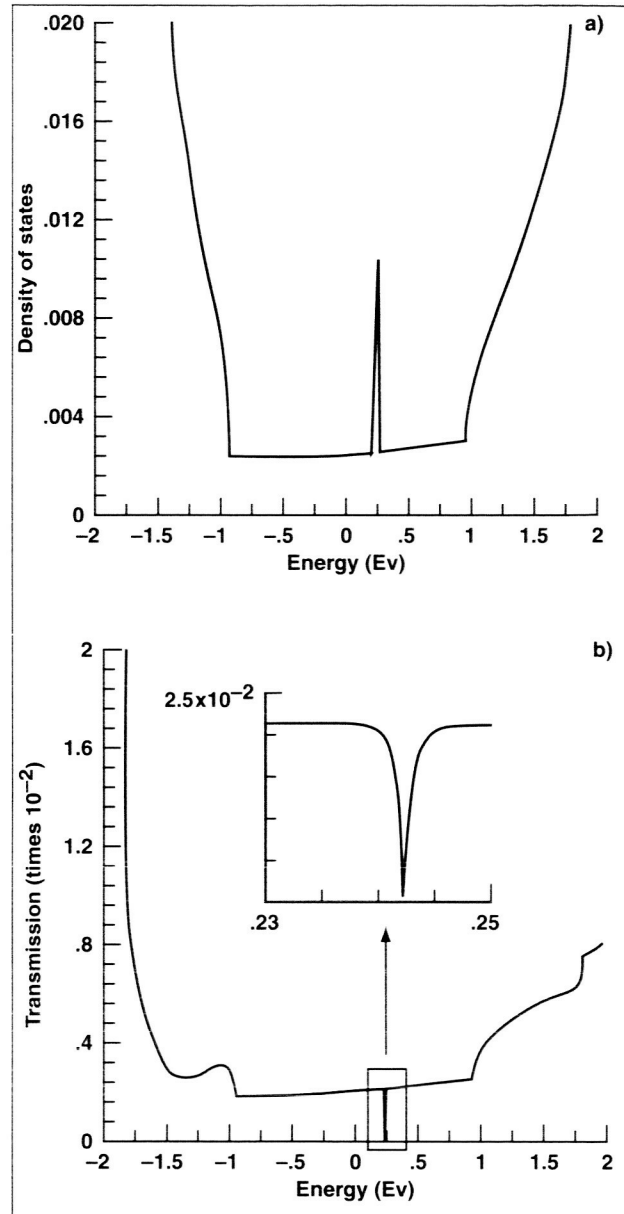


Fig. 1. (a) Density of states (DOS) versus energy in the cap region of a $(10,10)$ nanotube with a polyhedral cap. The peak in DOS corresponds to localized energy levels in the cap. (b) The transmission antiresonances correspond to the DOS peaks in (a). The inset shows an expanded region of one antiresonance. In the presence of appropriate defects these transmission antiresonances are converted to resonances capable of carrying large currents when compared to the background energies.

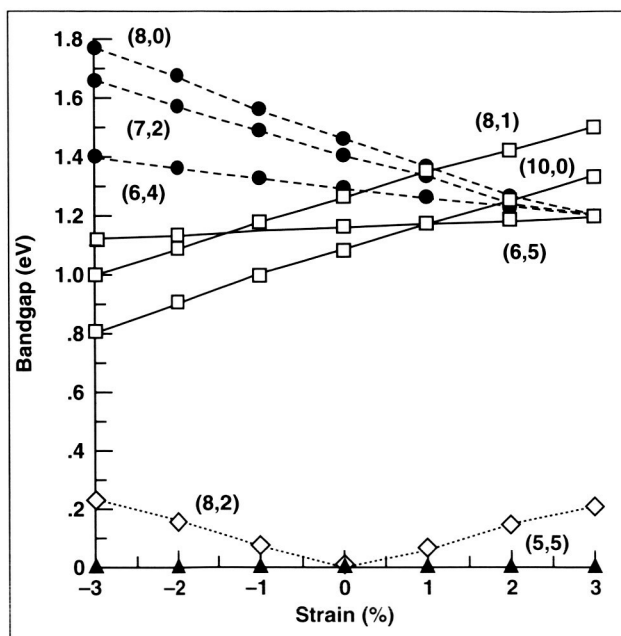


Fig. 2. Band gap versus tensile strain: for semiconducting tubes, the sign of slope of band gap versus strain depends only on the value of $(n - m) \bmod 3$ values of 1, -1 and 0, respectively.

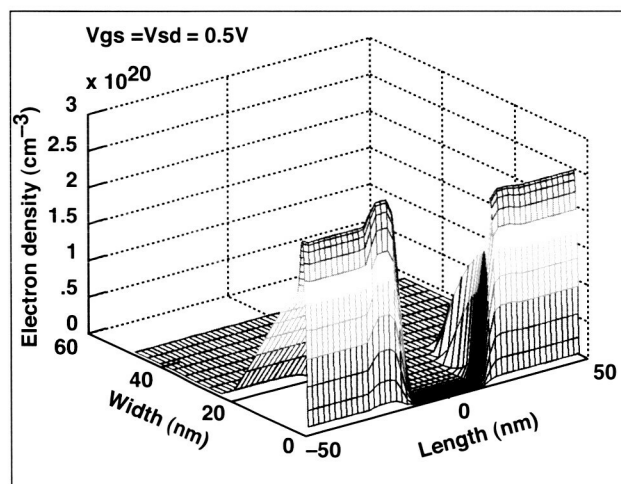


Fig. 3. Self-consistently calculated charge density when the gate and drain bias is equal to 0.5 V. The grid spacing is about an Angstrom near the gate ($x = 0$ nm), and 10 times larger near the substrate ($x = 120$ nm). The x-axis is perpendicular to the gate (from gate to substrate) and the y-axis is along the transport direction (from source to drain). X and Y are in units of nm, and density is in units of cm^{-3} .

Plasticity and Kinky Chemistry of Carbon Nanotubes

Deepak Srivastava, Fedor Dzegilenko

Since their discovery in 1991, carbon nanotubes have been the subject of intense research interest based on early predictions of their unique mechanical, electronic, and chemical properties. Materials with the predicted unique properties of carbon nanotubes are of great interest for use in future generations of aerospace vehicles. For their structural properties, carbon nanotubes could be used as reinforcing fibers in ultralight multifunctional composites. For their electronic properties, carbon nanotubes offer the potential of very high-speed, low-power computing elements, high-density data storage, and unique sensors. In a continuing effort to model and predict the properties of carbon nanotubes, Ames accomplished three significant results during FY99. First, accurate values of the nanomechanics and plasticity of carbon nanotubes based on quantum molecular dynamics simulations were computed. Second, the concept of mechanical deformation catalyzed—kinky—chemistry as a means to control local chemistry of nanotubes was discovered. Third, the ease of nano-indentation of silicon surfaces with carbon nanotubes was established.

The elastic response and plastic failure mechanisms of single-wall nanotubes were investigated by means of quantum molecular dynamics simulations. Working with researchers from Stanford University and the University of Kentucky, it was found that the elastic limit of thin carbon nanotubes under axial compression is significantly lower than earlier predictions based on classic molecular dynamics investigations. A novel mechanism of nanoscale plasticity is observed in which bonding geometry collapses from a graphitic to a localized diamond-like reconstruction. Figure 1 shows a compressed nanotube collapsed near the two edges by plastic deformation. The bonding geometry shown in figure 1(b) reveals a diamond-like structure at the location of the collapse. The computed critical stress (approximately 153 gigapascals) for the collapse and the shape of the resulting deformation are in good agreement with recent experimental observations of compressed nanotubes in polymer composites. These

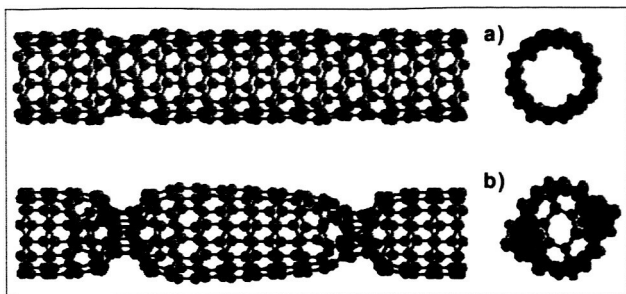


Fig. 1. (a) Compressed nanotube collapsed near the two edges by plastic deformation. (b) A diamond-like structure at the location of the collapse.

results are a first step in the accurate characterization of isolated nanotubes for their potential application in ultralight structural composites for aerospace applications.

The relationship between mechanical deformation and chemical reactivity (mechano- or kinky-chemistry) of carbon nanotubes was investigated in a collaborative effort between Ames, North Carolina State University, and the University of Washington at St. Louis. The sidewalls of pure nanotubes are relatively inert, whereas the end-caps are reactive. However, for many applications selective sidewall functionalization or reactivity of carbon nanotubes is highly desired. It is shown that such reactivity could be enhanced and controlled by mechanical deformations. When a mechanically twisted or kinked tube is exposed to an environment of reactant, the reactant specifically functionalizes (adsorbs) or etches the twist or kink. Figure 2(a) shows a twisted nanotube that has flattened into a ribbon-like structure with sharp edges. Figure 2(b) shows the preferential adsorption of atomic H at the strained edges of the twisted nanotube. For the first time, computational prediction of the kinky chemistry of nanotubes has been experimentally verified in a proof-of-principle experiment at University of Washington at St. Louis.

Indentation of diamond and silicon surfaces with carbon nanotubes used as atomic force microscope (AFM) tips was simulated. Indentation of a diamond surface by a nanotube causes buckling and collapse of the tube. However, a nanotube very easily indents a silicon surface. Thus, this technique can be used for making nanoscale holes on silicon surfaces with potential applications in high-density data storage, or nanolithography of silicon surfaces for electronics applications.

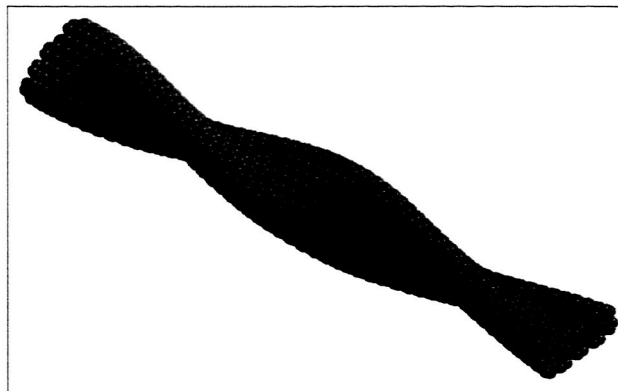


Fig. 2(a). Twisted nanotube that has flattened into a ribbon-like structure with sharp edges.

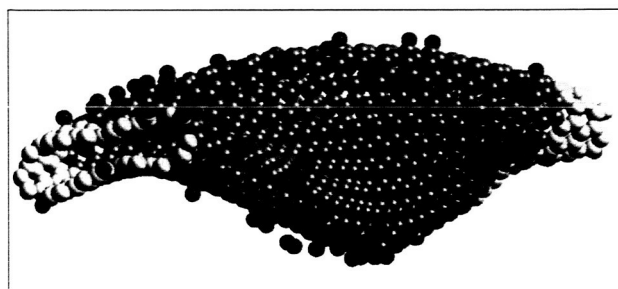


Fig. 2(b). Preferential adsorption of atomic H at the strained edges of the twisted nanotube.

Point of Contact: D. Srivastava
(650) 604-3486
deepak@nas.nasa.gov

Characterization of Carbon Nanotubes under Deformation

Richard L. Jaffe, Liu Yang, Jie Han, M. P. Anantram

Ongoing nanotechnology research at Ames Research Center is aimed at developing revolutionary small-scale electronic devices and sensors to meet the requirements of future NASA missions. Carbon Nanotubes (CNT) are hollow cylinders of graphitic carbon atoms; the cylinders have diameters of ~ 0.001 microns and lengths of up to several microns (more than 100 times smaller than the components of today's microprocessors). Depending on the orientation of the hexagonal carbon rings in the tube surface, some CNTs have metallic properties (that is, the band gap is zero) and others are semiconductors (that is, the band gap is finite, but less than 1 electron volt).

Because of their varying electronic properties and very small size, CNT components are expected to have an important role in the development of future electronic devices. In addition, CNTs have extraordinarily large tensile modulus and tensile strength, which places them among the strongest materials known. These attributes make them promising candidates for reinforcing fibers and for microelectronic-mechanical sensors (MEMS). Single-CNT transistors (shown schematically in figure 1) have been fabricated and tested under ideal laboratory conditions, but it is not known whether they will function under typical operating conditions of integrated circuits. Previously, modeling studies were carried out to characterize idealized CNT electronic devices. This year, research focused on characterizing electronic devices and sensors under realistic operating conditions where the CNTs are bent, flattened, and twisted by their interactions with substrates, metal contacts, and other devices.

Electronic properties of stretched, compressed, and bent CNTs have been studied, using a full-valence electron tight-binding model to calculate the electronic density of states (DOS), bandgap and conductance. Selected results for stretched and compressed nanotubes are illustrated in figure 2.

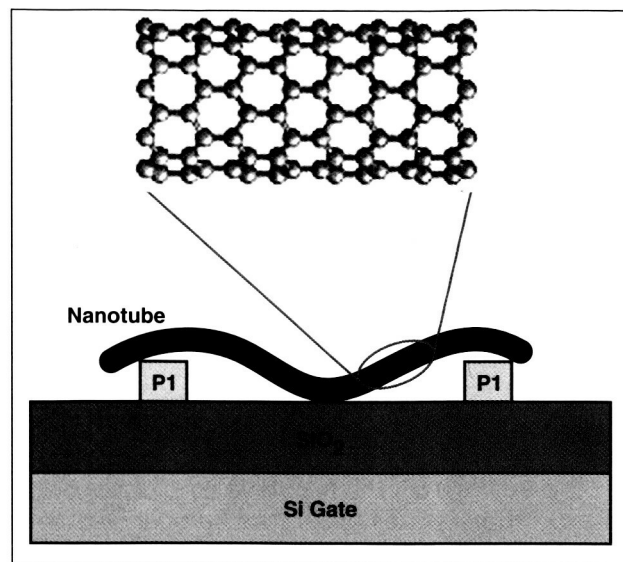


Fig. 1. Schematic diagram of a single carbon nanotube transistor. The source and drain potentials are applied at the platinum contacts, and the gate voltage from the underlying silicon controls the operation of the device.

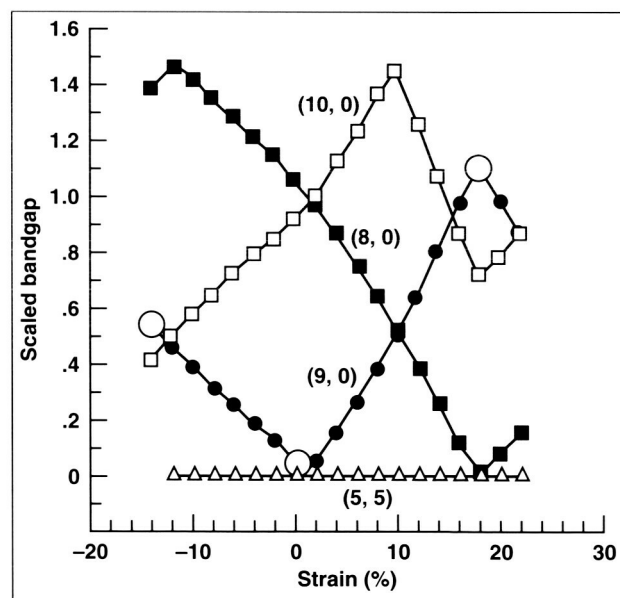


Fig. 2. Variation of computed band gap as a function of tensile strain for several different carbon nanotubes; negative strain represents compression, and positive strain represents tension.

Similar results have been found for other deformations. We find that some metallic-like nanotubes (labeled 5,5) remain conducting even when subjected to large compressive or tensile strain, as evidenced by their bandgaps remaining zero. However, other conducting tubes (labeled 9,0) develop sizeable band gaps under these conditions. Finally the band gaps of semiconducting tubes (8,0 and 10,0) are found to be very sensitive to the applied strain. Metallic nanotubes, such as the (5,5), retain their electronic properties even when subjected to large deformations; as a result, they are promising candidates for use in CNT-based electronic devices. On the other hand, other conducting tubes, such as the (9,0), are good candidates for MEMS devices, because their conductivity decreases markedly with increasing tensile strain. Optimal performance of CNT devices and sensors will be achieved by selecting the correct type of nanotube for the particular application.

Point of Contact: R. Jaffe

(650) 604-6458

rjaffe@mail.arc.nasa.gov

Computational Quantum Optoelectronics for Information Technology

C. Z. Ning, S. C. Cheung, P. M. Goorjian, J. Li, A. Liu

The interaction between laser light and semiconductor nanostructures is the basis for current and future optoelectronics-based information technology. The objective of the Computational Quantum Optoelectronics (CQP) project at Ames Research Center is to explore new optoelectronic devices, to study speed and size limits imposed by fundamental physics principles, and to design and optimize the performance of existing devices to meet NASA's needs in information technology. During FY99 the project made significant accomplishments in three areas: comprehensive semiconductor laser simulation, ultrafast laser modulation with a terahertz

heating field, and terahertz wave generation in semiconductor quantum wells.

In terms of comprehensive laser simulation, the focus in FY99 was on the so-called vertical-cavity surface-emitting laser (VCSEL). Ames researchers have developed a comprehensive simulation code using finite-difference methods in time and two-dimensional space domain. The model takes into account the quantum-well structure information and the material composition of a given VCSEL structure design. The effects of the detailed Coulomb interactions of charged carriers are also included. Since researchers directly solve the resulting partial differential equations numerically, VCSELs of different designs are treated with the same ease, such as those with gain confinement or index confinement, or devices of different current contact shapes. Also, time-evolution of VCSEL spatial modes on a picosecond scale are resolved. This type of space-time-resolved simulation is especially important when VCSELs are subject to injection current modulation, as is the case in VCSEL-based interconnects. Figure 1 shows the output laser intensity patterns at four different pumping levels for a VCSEL with an annular current contact.

In the area of ultrafast laser modulation, researchers have investigated the possibility of increasing the communication bandwidth by utilizing the much faster process of heating the electron-hole gas in a semiconductor with an electrical field. Detailed investigation has shown the feasibility and limitations of using such an approach. Researchers have investigated the underlying physical processes of electron-hole plasma interacting with semiconductor lattice vibrations when heated by an applied electrical field with frequency up to a few terahertz. They developed a detailed model to study laser modulation under such a terahertz-heating field. The results show that this method allows a modulation of semiconductor lasers at frequencies from tens of gigahertz (10^9 Hz) to 1 terahertz (10^{12} Hz). Even though it is a theoretical result at this stage, the approach indicates some fundamental advantages of this new modulation strategy over existing approaches.

Another closely related area of research in the overall effort in quantum optoelectronics is terahertz generation. We have investigated two possibilities using carefully designed quantum-well structures for

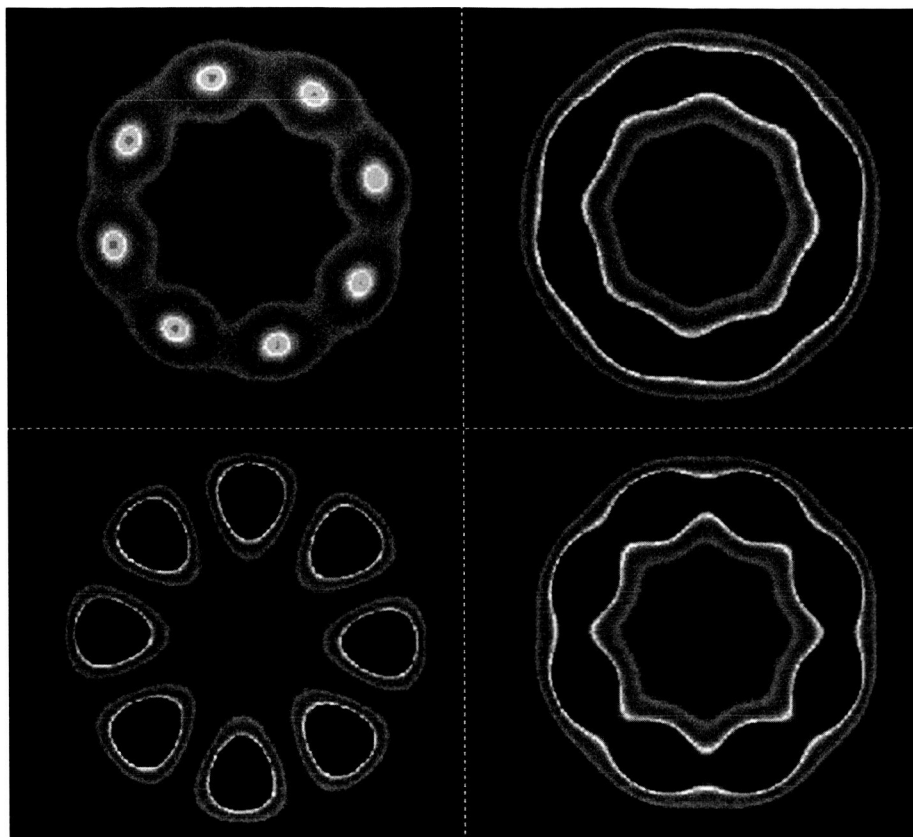


Fig. 1. The figure shows an example of the space-time-resolved computer simulation of the laser intensity pattern across the output facet. The four images show snapshots of the laser intensity at different times for a VCSEL with a current contact of the annular shape.

achieving terahertz emission through optical pumping by another laser. The first possibility is an optically pumped terahertz laser. The second approach is based on nonlinear optical wave mixing. Ames researchers have developed a theoretical model and computer simulation code that allows them to optimize the quantum-well structure design to achieve maximum nonlinear optical coefficients. Systematic theoretical and numerical simulation has shown the feasibility of generating radiation at a few terahertz by using this approach. This frequency is critical for the Earth Science Enterprise's atmosphere spectroscopy program and in far-infrared astronomy for the Space Science Enterprise. Efficient and compact terahertz sources will also find many commercial applications.

Point of Contact: C. Ning
(650) 604-3983
cning@nas.nasa.gov

A Liquifier for Mars Surface Applications

Louis J. Salerno, Ben Helvensteijn, Peter Kittel

NASA is planning an extensive set of robotic and human exploration missions that will make extensive use of cryogenic propellants. In-situ-consumable-production (ISCP) will reduce the mass launched from Earth by manufacturing propellant gases on the Mars surface. NASA's Exploration programs will benefit significantly from ISCP, providing that low cost, lightweight methods of propellant gas liquefaction are available to make exploration financially feasible.

The objective was to demonstrate that the planned 2003 Mars surface oxygen gas liquefaction requirement could be met with an existing, off-the-shelf tactical cryogenic cooler and a simple heat exchanger. The requirement is that oxygen gas produced during the daytime on the Mars surface

(typical temperature environment of 240 K) be liquefied at a rate of 12.6 grams per hour (g/hr) and stored at a pressure of 0.2 atmospheres (atm) (0.2 megapascals (MPa)).

Figure 1 shows a schematic of the test setup. Using nitrogen as a surrogate test gas (for safety reasons), N_2 gas at room temperature was supplied to a liquefier in an environmental chamber nominally maintained at 240 K. System pressure was 2 atm (0.2 MPa). An average liquefaction rate of 9.1 g/hr of nitrogen was realized over a 3.55-hour period. The equivalent oxygen liquefaction rate is obtained by considering both the increase in refrigeration capacity of the cooler at the higher oxygen liquefaction temperature and the ratio between the total enthalpy changes of oxygen and nitrogen when cooled from room temperature and liquefied. It follows that liquefying nitrogen at a rate of 9.1 g/hr corresponds to an oxygen liquefaction rate of 12.9 g/hr. This exceeds the planned demonstrations for the 2003 Mars mission goal by 2%.

The more formidable challenge remains to demonstrate that the 2,500 g/hr requirement for the later human missions can be met with an economically feasible package.

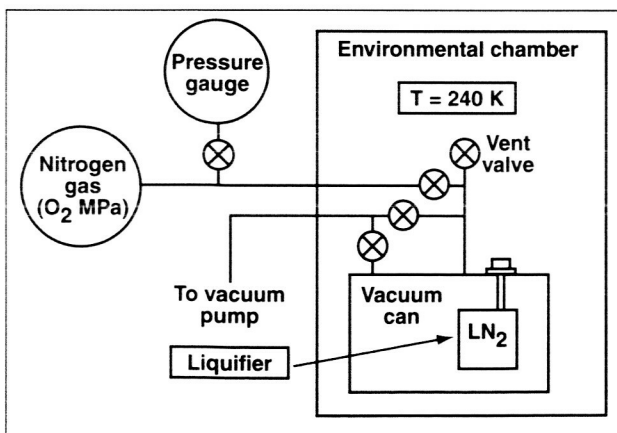


Fig. 1. Liquefier test setup.

Point of Contact: L. Salerno
(650) 604-3189
lsalerno@mail.arc.nasa.gov

Integration of Pressure-Sensitive Paint Data to Obtain Loads

James Bell

A primary reason for developing pressure-sensitive paint (PSP) for wind tunnel testing has been the desire to use PSP in measuring aircraft loads. This would obviate the need for a separate loads model and test, as well as make loads data available much earlier in the design cycle than is presently the case. However, the ability of PSP to deliver accurate loads data cannot be validated until integrated pressures from PSP have been shown to give accurate force and moment values.

The main objective was to modify the current PSP data reduction code to support integration of pressure data over a model surface grid and to compare PSP-derived force and moment measurements with those obtained from the balance.

The current PSP data reduction code already produces pressure maps that are projected onto a model surface grid. This code was modified to produce integrated force and moment values by summing the mean pressure on each surface panel and multiplying it by the panel area. To verify the method, forces were computed from PSP data taken during a test of a semispan wing in the Ames Unitary Wind Tunnel in October 1993. Figure 1 shows a view of surface pressures on the wind tunnel model, together with the surface grid. This test was chosen because of the relatively simple model geometry, and because PSP data were available over the top and bottom of the wing.

The integrated PSP data are compared to balance data in figure 2, which shows lift coefficient computed using both methods. Values agree to within less than 3% except at the high positive and negative angles of attack. At these angles the model half-body, which was not coated with PSP and is thus not included in the pressure integration, begins to contribute substantially to the lift.

It remains to extend the pressure integration method to calculating moments, and to calculations for more complex aerodynamic shapes.

Point of Contact: J. Bell
(650) 604-4142
jhbelle@mail.arc.nasa.gov

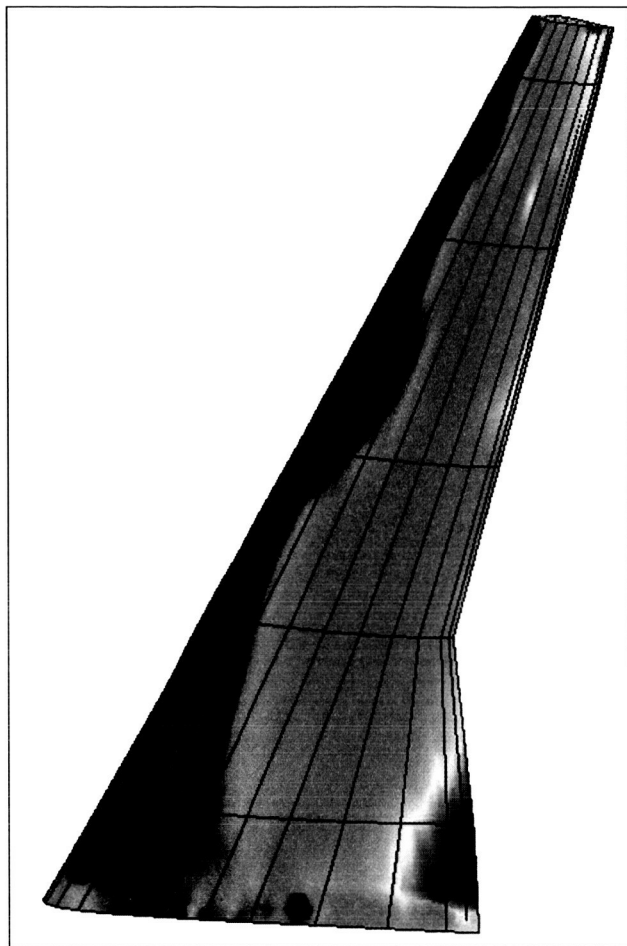


Fig. 1. PSP-derived pressures and grid lines on the suction surface of a transonic wing.

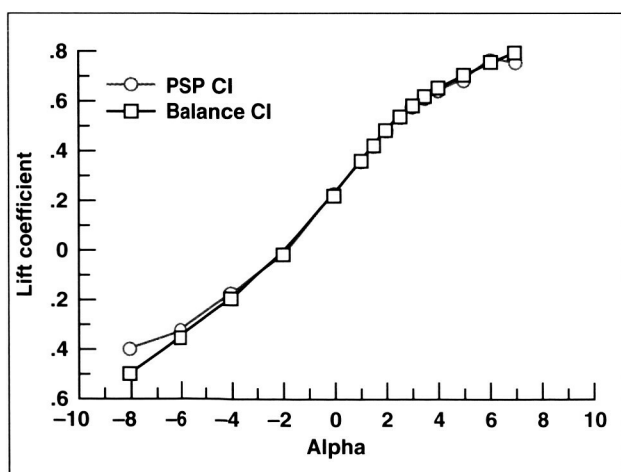


Fig. 2. Lift coefficient determined from balance data and PSP data.

Wind Tunnel Testing with Fast Time-Response PSP

Edward Schairer, James Bell

Although proven successful for steady pressure measurements, extension of the pressure-sensitive paint (PSP) technique to unsteady flows, especially for rotorcraft, is considered quite difficult. This is partly because of the complex chemistry of a pressure-sensitive paint which has both fast time-response (greater than 1 kilohertz (kHz) as opposed to a typical PSP time response of 1 hertz (Hz)) and a self-referencing capability (often provided by adding a second pressure-insensitive luminescent dye to produce a biluminophore paint). Also, there is the problem of developing a camera coupled to a flash illumination system that is fast enough to stop the motion of the rotor model. Unsteady PSP would allow full pressure measurements on helicopter rotors, which would be of great benefit because rotors are extremely difficult to instrument with conventional pressure sensors.

The objective is to set up an oscillating-wing wind tunnel facility for PSP measurements using flash illumination and to use it to test candidate fast biluminophore paints. The oscillating-wing rig is simpler and more convenient than a rotor model, but it contains most of the model's essential elements: a moving wing and the requirement for measurements over a large surface area.

Two candidate fast biluminophore paints were tested. One was provided by researchers from TsAGI. The second paint was developed under NASA contract by ISSI, Inc. Only the results from the ISSI paint are discussed here. Figure 1 shows a PSP image of the wing upper surface at an 8 degree (deg) pitch angle, showing the suction peak produced by the NACA 0012 airfoil. Figure 2 shows the pressure level along a chordwise line at midspan, again at an 8 deg pitch angle, for the static case as well as for two different oscillation rates. The suction values reported by the PSP decrease significantly in the dynamic cases. This is in conflict with theory, which predicts only a slight change in pressure at the 2-Hz and 5-Hz oscillation rates. These data suggest that the PSP's time response is not sufficient to capture the fluctuating pressures over the airfoil.

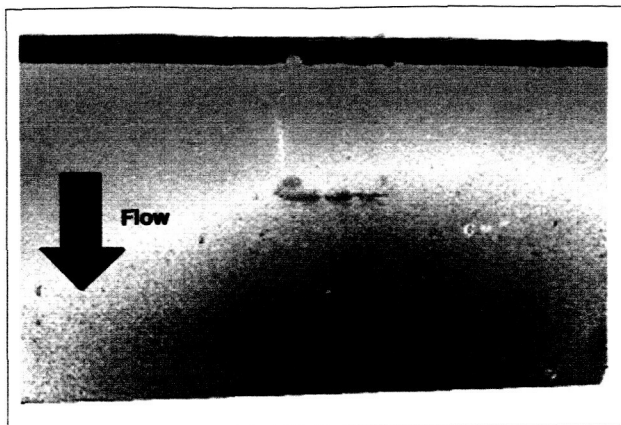


Fig. 1. PSP data on upper surface at 8 deg pitch angle (steady).

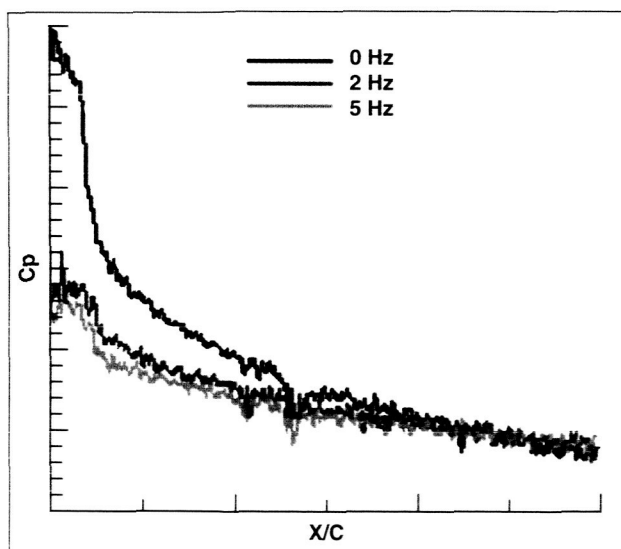


Fig. 2. Comparison of PSP-derived pressure distributions: steady (0 Hz) versus unsteady (2, 5 Hz).

Reformulated versions of the ISSI paint are currently being prepared. A new oscillating airfoil is being fabricated which contains unsteady pressure transducers for direct comparison with the PSP data. New flash units have been obtained which will provide higher brightness with a much shorter flash duration. A second round of testing is to be conducted.

Point of Contact: E. Schairer
 (650) 604-6925
eschairer@mail.arc.nasa.gov

Distributed Remote Management of Aerospace Data

Joan D. Walton, David J. Korsmeyer

The DARWIN system provides web-based remote access to the integrated knowledge generated from advanced wind-tunnel instrumentation suites and by sophisticated numerical simulation codes. Every year at Ames Research Center, these independent sources generate large volumes of high-quality data on flight vehicles. However, these data are only valuable to the design process if they can be readily accessed, analyzed, and applied by aerospace engineers. The DARWIN system has been developed in conjunction with new computational and experimental test technologies to enhance design-cycle productivity by providing design engineers with faster and better access to these valuable data.

DARWIN allows engineers to securely access and analyze these aerospace data from remote locations. Once engineers have been provided with a DARWIN account, they can use a web browser to visit the DARWIN secure web site and log in. The DARWIN web pages present data from only those tests for which users have been granted access (see figure 1). After logging in users can browse through the tests or query the database for specific information. Data from wind tunnel tests in progress can be viewed on a "live" screen that updates its displays in near real time to reflect the most recent results. Both live and archival data are displayed in user-configurable tables and plots. Once the user has retrieved a set of data and adjusted the tables and plots as desired, the work can be saved as a DARWIN data set. All the user's data sets are stored in a hierarchical "folder tree," which operates similarly to a Macintosh or Windows desktop. The user can add or delete DARWIN data sets, post files (such as text documents or spreadsheets or images), make links to other web sites, and create folders to organize them all. Unlike a PC, however, the folder tree is available to the user via a web browser from whatever machine and location the user chooses.

DARWIN has been deployed at Ames since 1997 as a tool for remotely accessing wind tunnel data. It has been popular with engineers for its live monitoring capabilities and its cross-test comparison features.

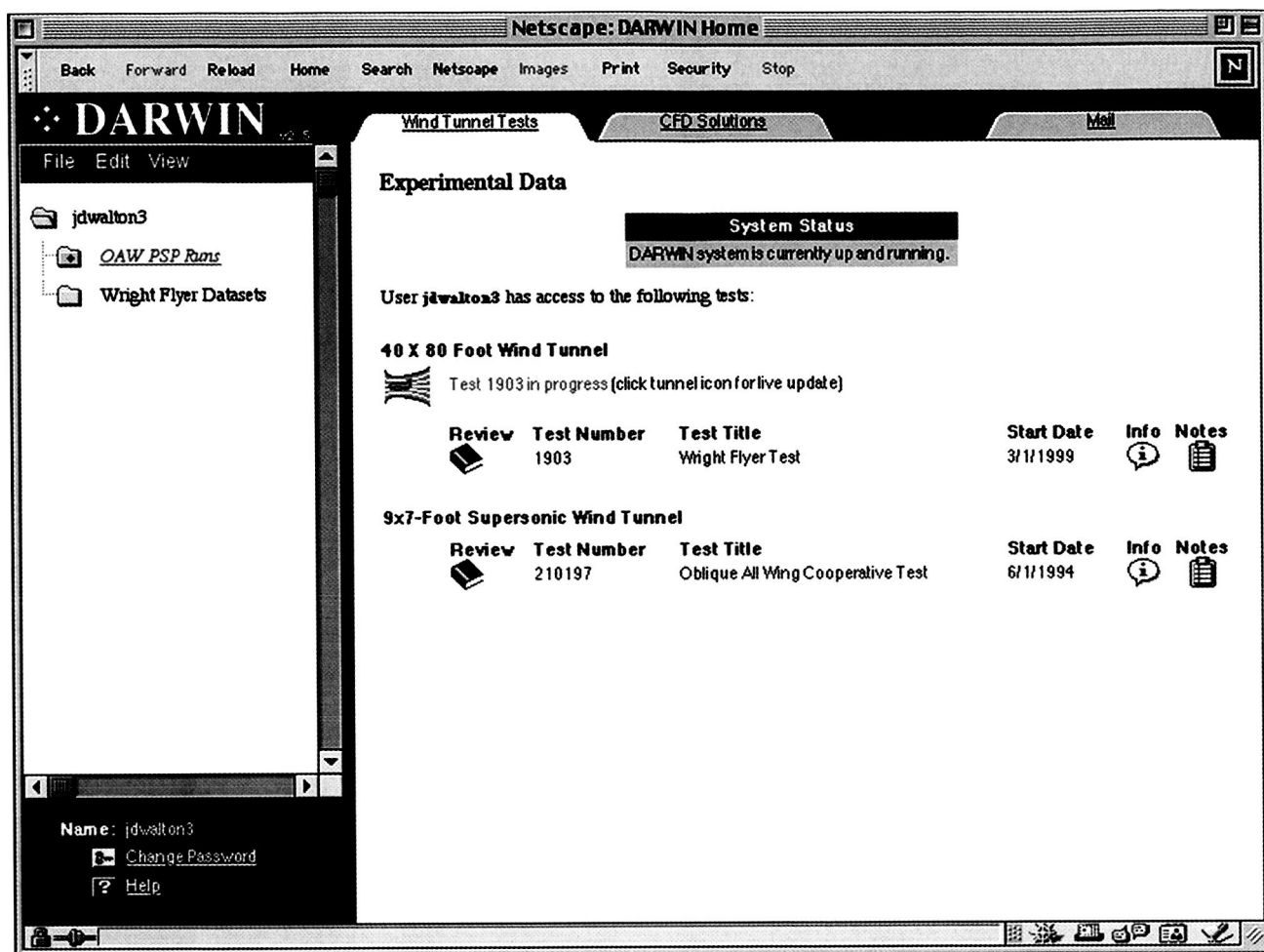


Fig. 1. The DARWIN web application.

In 1999 significant advances were made in broadening the DARWIN system to capture the results of computational fluid dynamics (CFD) simulations as well as test data from the tunnels. A major limitation of the system was its restriction to 241 variables, 31 of which were fixed and always required. Although these variables were pertinent to certain types of wind tunnel tests, they were not always germane to CFD results or to spacecraft models. Thus, the first major step in this process was redesigning the DARWIN database so that it could capture any type and number of variables associated with the data. The user interface software was rewritten to take advantage of the new database model and to provide displays that were custom-tailored to CFD requirements. The second step involved generalizing the DARWIN loading routines to accept input files from a variety of systems, not just from the Ames wind

tunnels. With these advances in place, DARWIN is well on its way to becoming a general data management tool for the Aero-Space Enterprise.

Point of Contact: J. Walton
(650) 604-2005
jdwalton@mail.arc.nasa.gov

Release of Distributed Collaborative Virtual Wind Tunnel

Steve Bryson, Bryan Green, David Whitney, Sandy Johan, Leslie Keely, Michael Gerald-Yamasaki, Creon Levit

The Distributed, Collaborative Virtual Wind Tunnel (DCVWT) is an immersive virtual-reality-based system for use in the investigation of simulated airflow by geographically distributed, collaborative teams (figure 1). Participants in the DCVWT interact with the airflow simulation as if they were in the same room interacting with a model, even if they are in fact spread across the country. Simulations ranging from ocean temperature through commercial aircraft to the Reusable Launch Vehicle can be examined in the DCVWT. The DCVWT plays two roles, providing an immersive environment for collaborative design, as well as acting as a test bed for developing new methods. In addition to the Office of Aero-Space Technology, the results of the DCVWT effort also benefit the Human Exploration and Development of Space and the Earth Sciences Enterprises. Programs like the Intelligent Synthesis Environment Program use technology and techniques pioneered in the DCVWT in the development of distributed, collaborative design environments.

The DCVWT is based on a client-server model, in which the data to be examined resides on a single

server. Various representations of these data, such as particle traces in the flow or surfaces of constant temperature are computed on the server as three-dimensional graphical objects. Multiple-user clients receive these graphical objects, which are drawn by the client from a point of view determined by the user (figure 2). In this way each user can have his own view of the same data. Each user can interact with the data representations, for example, moving a particle trace source, and all users will see the result. All users are "peers," each able to interact with the data, showing things to the other users. Interaction is performed via a "direct manipulation" paradigm, where each user can directly "pick up" a data analysis tool via a three-dimensional interface. Such a direct manipulation interface requires very high performance in order to give the sense of the data analysis tool moving in response to the user's motions. Such interaction involves information traveling from the user client to the server, computation of the new data analysis representation on the server, sending the new representation to all the clients, and drawing from all the clients. Because the complete round trip must occur in about one-tenth of a second, careful system design and a high-performance network are required.

The DCVWT presents a new paradigm in collaborative design. Rather than all participants seeing the same "master" view controlled by one user, all participants in the DCVWT have equal status, each with his own view of the same three-dimensional data. When one person changes the data representations, all participants see the result from their own points of view. This is how the DCVWT creates the effect of all participants being in the same room even though they may be actually widely geographically distributed. The DCVWT supports a variety of interface hardware, ranging from conventional workstation and mouse to immersive virtual reality interfaces, allowing each client to tailor its display to requirements or budget.

The DCVWT has been demonstrated in cross-country operation, with four user clients, two in Washington, D.C., at NASA Headquarters, and two at Ames. The server for this demonstration was at Ames. The performance was very satisfactory, with very good responsiveness, giving a sense of moving objects in virtual space.



Fig. 1. The Distributed Collaborative Virtual Wind Tunnel, using the Responsive Workbench virtual reality display, showing an analysis of simulated airflow around the Space Shuttle.

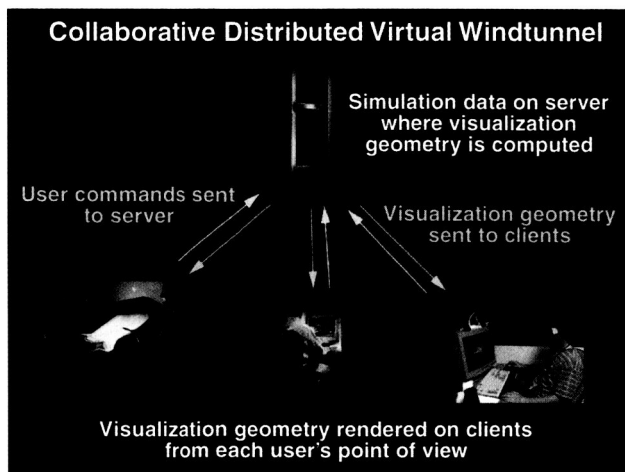


Fig. 2. The Client-Server architecture of Distributed Collaborative Virtual Wind Tunnel. Simulation data reside on the server (top), where visualization geometry is computed and sent to multiple-user clients (bottom). User commands are sent from each client, causing new visualization geometry to be computed by the server, which is then sent to all clients. Note that the clients can have different types of display and each sees the data from his own point of view.

Point of Contact: S. Bryson
 (650) 604-4524
 bryson@nas.nasa.gov

The main objective was to devise an experiment to study wake flow under conditions of adverse pressure gradient for the purpose of obtaining data useful in assessing and improving turbulence models for high-lift systems. Other objectives included obtaining laser Doppler velocimeter (LDV) measurements of velocity and turbulent Reynolds stress in a wake with reversed flow and studying the sensitivity of the wake to pressure gradient (flow divergence), asymmetry, and Reynolds number.

Experiments were performed in the High Reynolds Channel 1 wind tunnel at Ames. Wake flow behind a splitter plate was subjected to an adverse pressure gradient by passing the flow through a divergent wall test section. Boundary layers on the wind tunnel walls were prevented from separating with tangential blowing. High Reynolds number flows ($Re_c = 10$ million) were achieved by pressurizing the wind tunnel to 6 atmospheres. Two component LDV measurements of velocity and Reynolds stress were obtained for several test cases including separation. The figure shows the tunnel geometry with streamlines (derived from the velocity measurements) superimposed for a case with reversed flow along the centerline of the wake. Also shown are the measurements of the $-uv$ turbulent Reynolds stress for the upper half of the channel. The flow was remarkably stable and repeatable with good spanwise uniformity.

Point of Contact: D. Driver
 (650) 604-5396
 ddriver@mail.arc.nasa.gov

Wake Flow in Adverse Pressure Gradient

Dave Driver

High lift developed by multi-element airfoils can be limited by flow reversals in the wake of the main element. Turbulent mixing in the wake controls the growth of the wake and dictates the extent to which the wake experiences flow reversal. Consequently, subtle differences in turbulence models make a significant difference in the prediction of wake growth. The AST program, in an effort to improve predictions of high-lift systems, provided funding for basic experiments that would provide data for guiding turbulence model development.

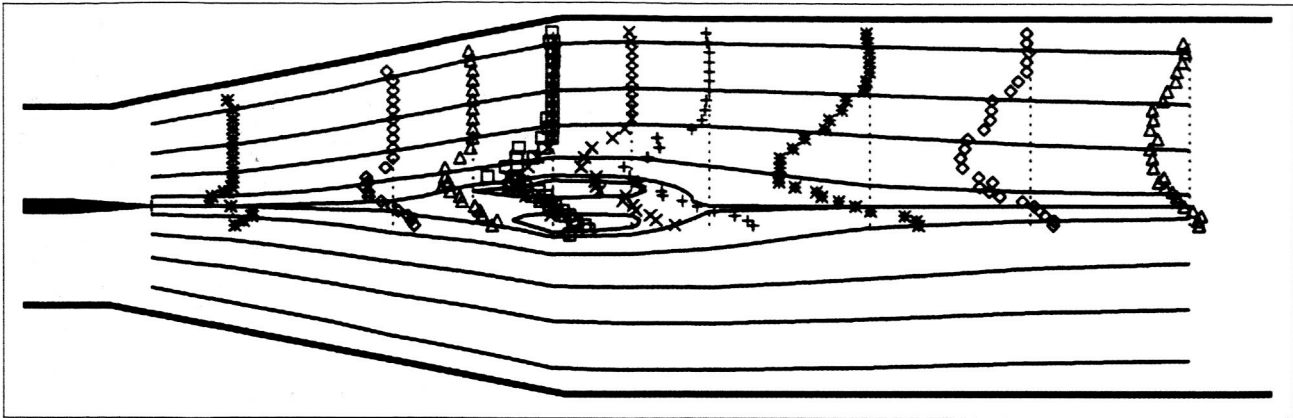


Fig. 1. Test section geometry with streamlines and uv Reynolds stress profiles overlaid.

V-22 Osprey Shipboard Interactional Aerodynamics Investigation

Kurt Long, Greg Zilliac

The U.S. Navy is currently conducting an extensive land-based and shipboard flight test program to evaluate the V-22 Osprey tilt-rotor aircraft. During shipboard tests aboard USS SAIPAN (LHA 2), V-22 test pilots experienced a roll anomaly while descending from hover. This anomaly consisted of uncommanded roll oscillation of approximately a 90-degree amplitude. Postflight analysis revealed that the roll was consistent with factors that might include an aberration in the aircraft's flight control systems logic, or air-load asymmetries caused by vehicle/ship interactional aerodynamics. Based on related ongoing shipboard air-wake measurement efforts at the Fluid Mechanics Lab (FML), the Navy requested FML support in investigating possible aerodynamic causes for the incident.

In an attempt to identify the cause of this anomaly, a 1/120-scale model of the V-22 Osprey's side-by-side, three-bladed, counterrotating twin rotor system was designed, constructed, and installed in the FML 32- by 48-inch wind tunnel (figure 1). Significant full-scale incident conditions were duplicated in the wind tunnel, including relative wind speed and direction, and deck spotting

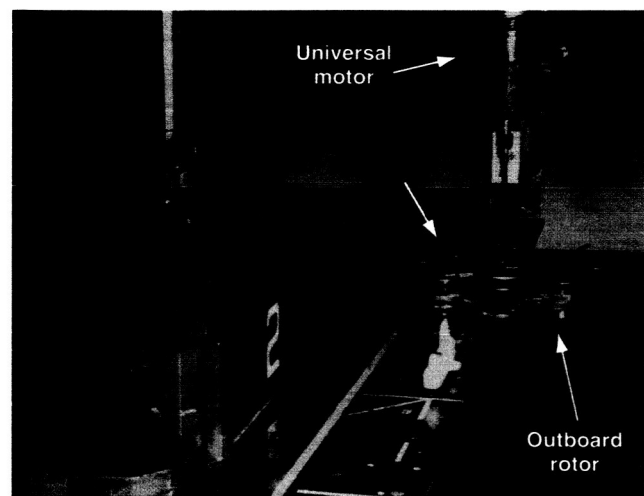


Fig. 1. 1/120-scale LHA and V-22 models..

location, and the presence of the upwind parked H-46 helicopter. To facilitate smoke (laser sheet and ambient illumination) and tuft-flow visualization, the tunnel was operated at approximately 40 feet per second. To ensure the correct ratio of rotor downwash to incoming ambient wind velocities, the rotors were spun at approximately 20,000 revolutions per minute, producing average downwash velocities of 60 feet per second. A 1.5-horsepower universal motor, speed-governed by a feedback controller, powered the rotors via a system of gears and belts. The rotors and motor were mounted to an

instrumented roll pivot, which was able to record roll moment variations, by means of a strain gage, as the model was moved to various locations over the deck. This assembly was mounted on an automated traversing and data collection system, enabling precise positioning and measurements around the ship deck.

The tests investigated flow patterns in the vicinity of each rotor disk. Flow-field pattern variations with height demonstrated clearly that a large ground vortex (figure 2) forms upwind of the inboard rotor at very low wheel heights above deck. The presence of this ground vortex is consistent with prior full-scale tests and with video from the actual incident. When the rotor system was moved laterally, the vortex tended to vary in size and location, depending on model proximity to the deck edge. The effects of ship superstructure on flow asymmetries showed that the port-side superstructure tends to trap the upwind ground vortex, whereas superstructure removal produced smaller upwind vortices and flow asymmetries.

The tests also investigated the effect of deck proximity on the vehicle roll moment. When the rotor system was moved laterally from a position outboard of the deck edge inwards to a position over

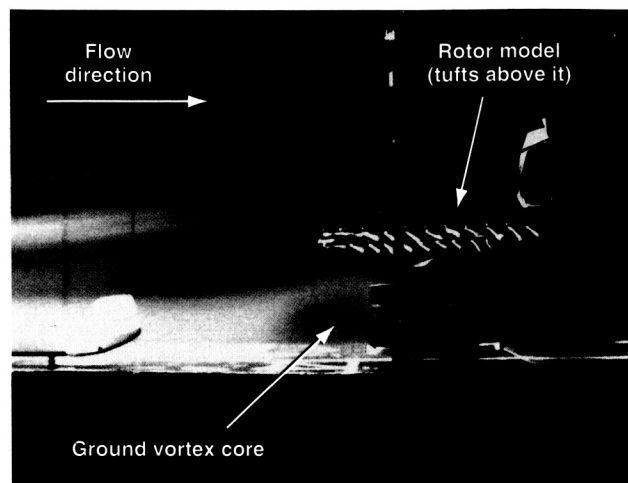


Fig. 2. Side view of upwind ground vortex.

the desired landing spot (figure 3), the roll moment was found to vary significantly, further substantiating the flow-visualization findings. The roll moment was found to also vary with traverse height, providing further insight into the complicated shipboard rotorcraft interactional environment.

Point of Contact: G. Zilliac
 (650) 604-0613
 gzilliac@mail.arc.nasa.gov

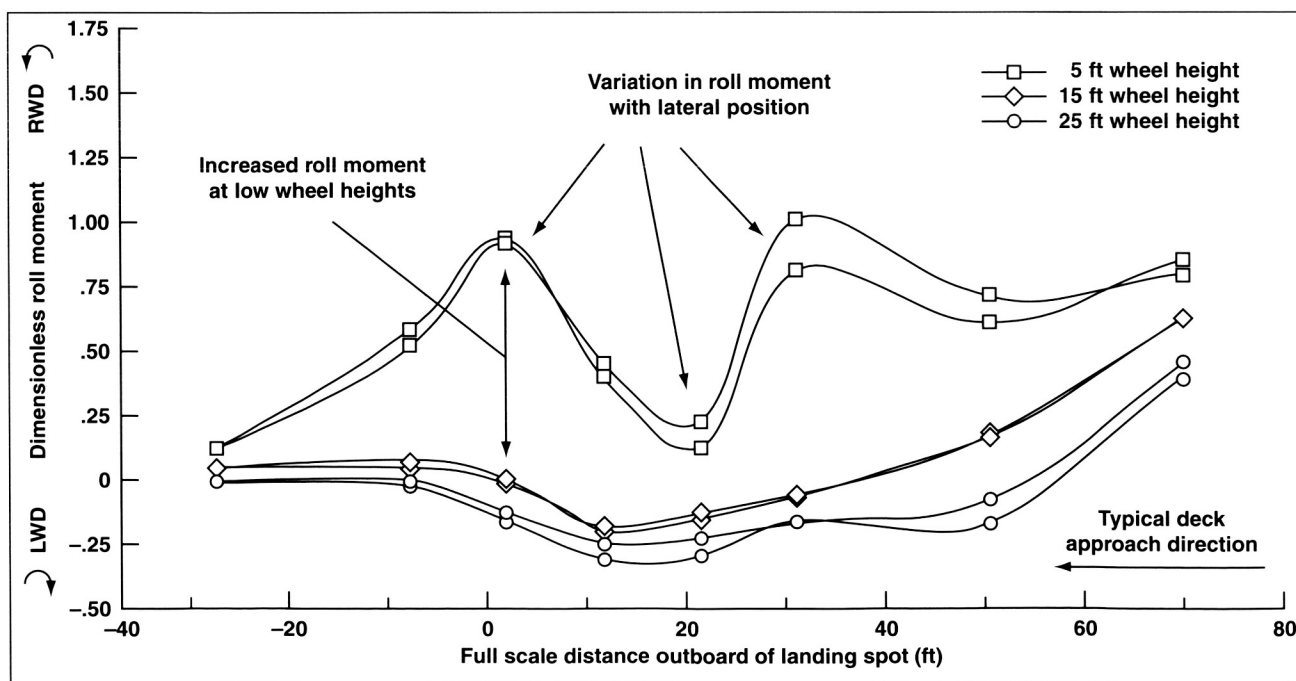


Fig. 3. Steady-state roll moment variation with height.

Distortion and Elevated Growth of Instabilities by Vortices Induced by Free-Stream Nonuniformity

Johnathan H. Watmuff

The objective of this effort is to study the interaction between streamwise vorticity and Tollmien-Schlichting (TS) waves in an effort to gain new insights into the physical processes responsible for bypass transition. Transition by means of amplification and nonlinear breakdown of initially small-amplitude TS waves is only observed for low free-stream turbulence (FST) levels. "Bypass" of TS instability mechanisms has been hypothesized for higher FST levels. However, recent observations demonstrate that TS waves still play an active role at moderate FST levels. Elevated FST levels also appear to be associated with streamwise vorticity within the layer that originates at the leading edge. Therefore, the influence of streamwise vortices on TS waves may provide new insights into bypass transition, which has remained a mystery since the 1930s.

Free stream nonuniformity (FSN) is deliberately introduced into an otherwise highly uniform free stream. The FSN is in the form of a laminar wake from a fine wire ($d = 0.002$ inch, $R_d = 16$) located $7,250d$ upstream of the leading edge of a flat plate. Interaction of the wake with the leading edge results in a pair of weak counterrotating vortices embedded within the Blasius boundary layer. The characteristics of two-dimensional TS waves generated by a vibrating ribbon have been determined with extensive hot-wire measurements, both with and without the presence of the vortices.

The ribbon is located just upstream of Branch I of the neutral stability diagram ($F = 60 \times 10^{-6}$, $R = 485$) and it is active over the full span of the test section thereby allowing the wave behavior to be studied over large streamwise distances. The wave amplitude grows by almost two orders-of-magnitude between Branch I and Branch II for this operating point. The development of peak root-mean-square (rms) wave amplitude with streamwise distance conforms with predictions from linear stability theory. However, large variations in the rms wave amplitude emerge in the spanwise direction despite the relatively small wave amplitude ($u/U_1 \approx 0.5\%$). Spanwise profiles (not shown) of the rms wave amplitude have the same

form of peak-valley splitting initially observed in 1962. The phenomenon is now known as K-type secondary instability and it has been subject to extensive theoretical study.

The vortices introduce considerable phase distortion of the TS waves as shown in Figure 1. Initially, the rms wave amplitude is *reduced* in the vicinity of the vortices for a substantial streamwise distance, as shown in Figure 2(a). A remarkable feature has been captured in the contours for $R = 914$, shown in Figure 2(b), that is, the appearance of two small regions at $y \approx 1.5$ mm with exceptionally low rms amplitude. This point marks a critical change in the wave behavior since a small increase in Reynolds number leads to a completely different distribution in which the maximum wave amplitude now occurs between the vortices, as shown in figure 2(c). A further increase in Reynolds number

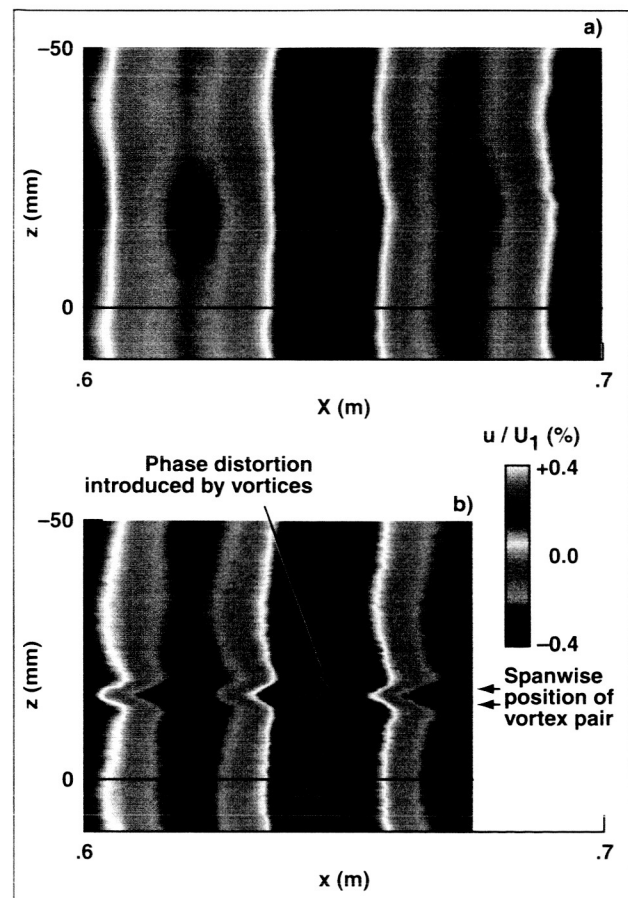


Fig. 1. Hot-wire data in horizontal plane showing phase distortion of Tollmien-Schlichting waves by FSN induced streamwise vortices embedded in the layer. (a) Without vortices, (b) with vortices.

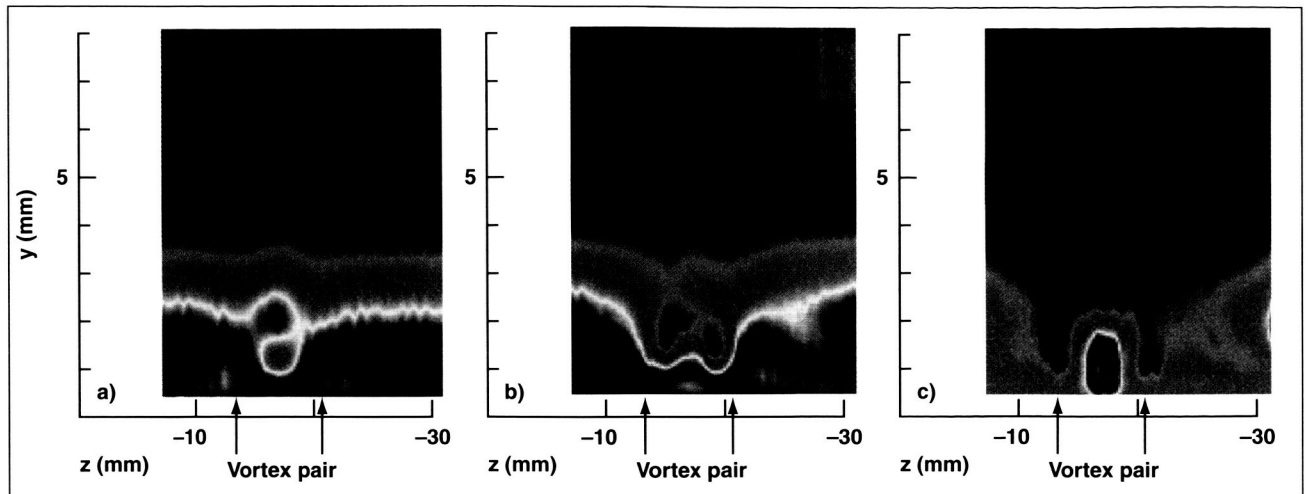


Fig. 2. Distortion of Tollmien-Schlichting wave amplitude in three spanwise planes downstream of the vibrating ribbon for the case with the FSN induced streamwise vortices embedded in the layer. (a) $x = 1.15$ m, $R = 876$ ($= R_x^{1/2}$); (b) $x = 1.25$ m, $R = 914$; (c) $x = 1.35$ m, $R = 950$.

results in rapid growth in amplitude (e.g., $u/U_1 \approx 10\%$ for $R = 984$) and in the onset of random behavior, which is a characteristic of the final approach to breakdown to turbulence.

A different type of secondary instability mechanism appears to be associated with the vortices, which leads to transition at a lower Reynolds number. The results help explain the adverse effects of wind tunnel flow quality on tests concerning bodies with substantial regions of laminar flow.

Point of Contact: J. Watmuff
 (650) 604-4150
jwatmuff@mail.arc.nasa.gov

The Effects of Thin Paint Coatings on the Aerodynamics of Semi-Span Wings

Edward Schairer, Rabi Mehta, Mike Olsen

The objective of this research was to measure the effect of pressure-sensitive paint (PSP) on the aerodynamic performance of high-aspect-ratio, semi-span wings at transonic cruise and landing conditions. The PSP technique for measuring pressure distributions on wind-tunnel models requires coating the surface of the model with special paint that luminesces when illuminated by light of appropriate frequency. The technique has the potential to eliminate the need for pressure taps in wind tunnel models while yielding pressure information over entire surfaces rather than just at discrete points. The presence of paint on a model, however, can alter the flow (that is, it can become "intrusive") by adding thickness to the model or by changing the roughness of the model and thus altering the development of the boundary layer. Changes in surface roughness are likely to be most critical at high Reynolds numbers where boundary layers are thinner.

Two models were tested: (1) a single-element, supercritical wing at transonic cruise conditions in High Reynolds Number Channel 2 (HRC-2); and (2) a multi-element wing-body model complete with slats, flaps, and engine pylon and nacelle at landing

conditions in the Ames 12-Foot Pressure Wind Tunnel. The effect of the paint was determined by comparing pressure-tap data (both models) and balance data (high-lift model only) from runs with and without paint on the models.

Paint intrusiveness was measured on both models. The shock wave on the cruise model was displaced slightly upstream when the model was painted relative to when it was not painted. This occurred at all Reynolds numbers (7.3 million to 13.6 million) even after the paint had been polished to a "hydraulically smooth" finish. The stall angle of the high-lift model at the highest Reynolds number (6.7 million) was nearly 4° lower when there was unpolished paint on the leading-edge slats compared to when the model was unpainted (figure 1). Polishing the paint on the slats restored the stall to its

paint-off behavior. Applying paint to other parts of the wing had very little effect. Even before being polished, the paint was hydraulically smooth at all Reynolds numbers (3.4 to 6.7 million).

These experiments demonstrated that pressure paints applied to wind tunnel models must be very smooth. The roughness of paint along the leading edges of high-lift models is especially important. Accepted roughness criteria developed for simplified geometries may not apply to complex, three-dimensional configurations. This research shows the importance of assessing the intrusiveness of pressure paint whenever it is used.

Point of Contact: E. Schairer
(650) 604-6925
eschairer@mail.arc.nasa.gov

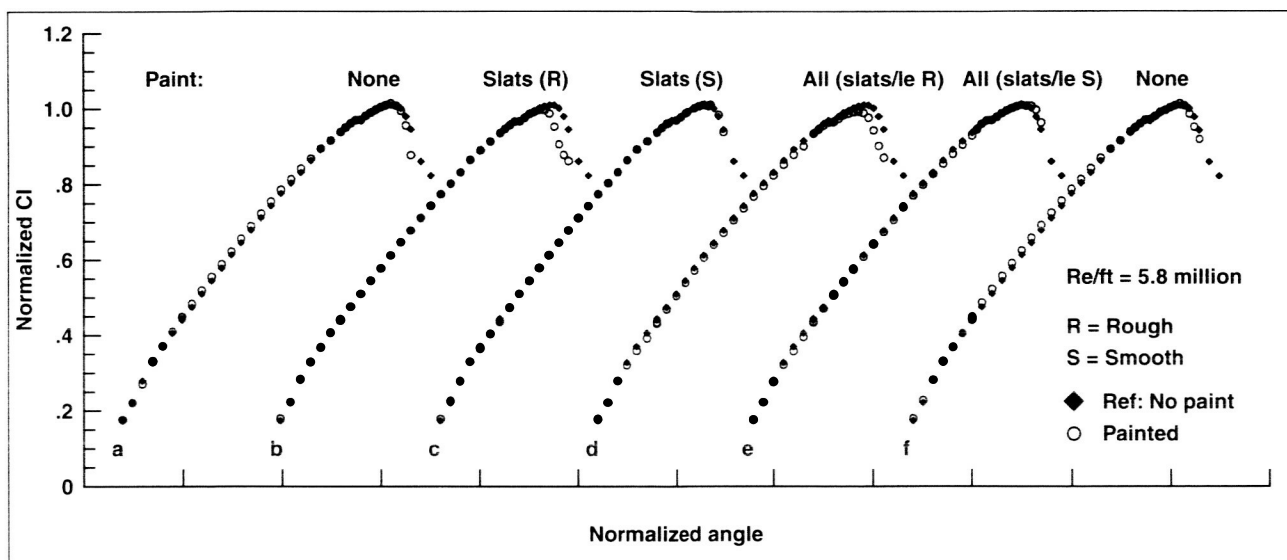


Fig. 1. Comparison of paint-off and paint-on lift curves of high-lift wing at maximum Reynolds number (6.7 million).

Three Degree-of-Freedom Architecture for Hand-Controllers and Robots

Bernard D. Adelstein, Peter Ho

The goal of this work was to develop a new mechanical architecture—for actively powered haptic (“force-feel”) hand-controllers and robotic manipulators—that offers enhanced performance in terms of combined work-space size, position and force control accuracy, and payload. For hand-controllers, these attributes have obvious impact on the subjectively perceived “feel” of interactions with virtual or telemanipulated environments.

The moving structural components of a hand-controller or manipulator form the mechanical linkage that couples force and motion between the device’s actuators (motors) and end-effector. Thus, the linkage’s architecture directly determines not only the work space but also transmission characteristics such as dynamic range (comparing maximum usable force to friction) and bandwidth (frequency content of deliverable force and motion) that define control accuracy and contribute to payload capacity.

A novel three-degree-of-freedom (DOF) linkage architecture was devised, offering significant improvement over prior technology with respect to the above listed performance criteria. The innovative architecture (figure 1) is a mechanism composed of 10 rigid links that connect 12 single-DOF rotary joints. The links and joints are arranged in three loops that couple a handgrip or robot end-effector (D) to three rotary actuators (A, B, and C). The moving links do not carry actuator weight and inertia since A, B, and C are all mounted on a common base (unlabeled link 1). This frees more of the actuator force budget for useful work, that is, payload. Because the base link does not move, more powerful and typically heavier actuators can be used without the need for more massive moving support structures. This lower inertia improves acceleration response and expands structural bandwidth for better control at high frequencies.

The architecture requires no belt, cable, pulley, or screw transmission elements, all of which can be backlash-, friction-, or compliance-prone and that would therefore compromise end-effector force and position control. The actuators can be embodied by COTS (commercial, off-the-shelf) rotary electric

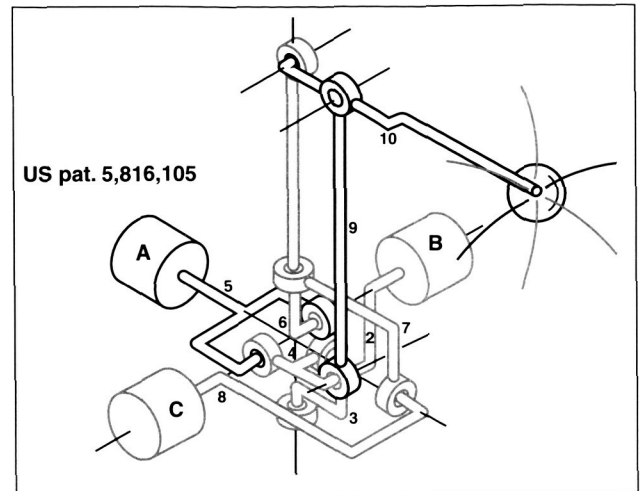


Fig. 1. Three-DOF parallel mechanism.

motors and the other joints by COTS backlash-free, low-friction ball bearings. Enhancing usable human and actuator force levels while minimizing losses to friction increases dynamic force range and is critical for back-drivability and the feel of hand-controllers.

The multiple-loop configuration of the linkage forms a so-called “parallel” mechanism, universally acknowledged as being structurally stiffer than competing “serial” designs. Greater stiffness is key to enhanced structural and control bandwidth, as well as improved position control accuracy.

The linkage work-space volume is correspondingly larger than that of prior three-DOF parallel configurations, approaching the work space of serial devices. This new architecture’s work space is bounded by the singularity at the sphere of maximum reach typical of all arm-like devices and by singularities in the sphere’s equator—the plane defined by the three actuator axes. In general, work-space singularities correspond to locations at which the linkage loses its ability either to move or to apply force in one or more directions.

The linkage is composed of the minimum number of links and rotary joints in which all three actuators can be supported on a common base, giving the architecture fewer component parts than other three-DOF, spatial, all-rotary joint mechanisms. Fabrication and assembly constraints for the linkage are relatively simple: only the intersection of joint axes within two of the mechanism loops and the parallelism of joint axes in the third loop are mandatory. A closed-form potential energy analysis

demonstrates that, in theory, the linkage can be statically balanced for all base link orientations and also provides a three-step link mass-distribution procedure to achieve the balance. Perfect static balance obviates the need for actuator or external forces to support unbalanced linkage weight for any pose, freeing up more force for useful work.

Finally, the three-DOF architecture is scalable from large crane-sized construction and material-

handling equipment down to micro-machines for use in applications such as minimally invasive surgery. Arm- and finger-scale three-DOF force-feel joysticks (figure 2) demonstrate a portion of this scalability.

Point of Contact: B. Adelstein
(650) 604-3922
dadelstein@mail.arc.nasa.gov

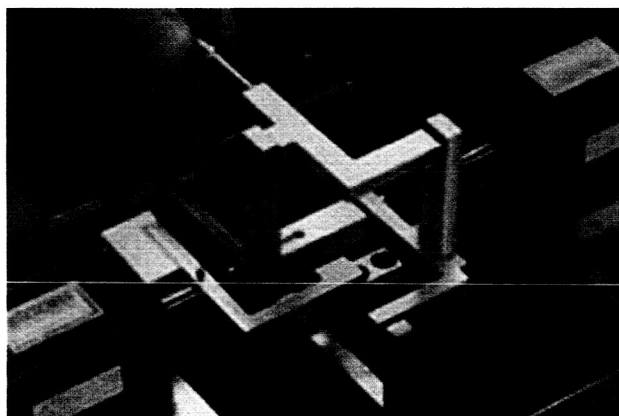
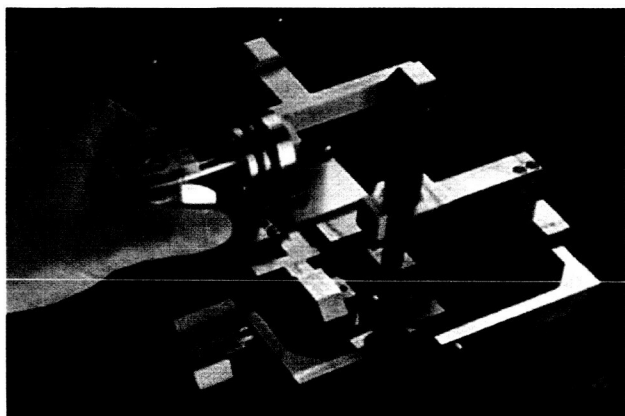


Fig. 2. Arm- and finger-scale force-feel hand-controllers.

Performance of the COSMOS Multi-Level Parallelism Molecular Dynamics Code on the 512 CPU Origin System

James R. Taft

Ames recently purchased an SGI 512 CPU Origin 2000 system. The system has been named Lomax, after the late celebrated Ames researcher Harvard Lomax. The Lomax system is the largest single shared-memory multi-processor system in the world (see figure 1). It is the result of an Ames-driven partnership with SGI to push the limits of single-system shared memory designs. It is believed that large CPU count single-system designs offer many potential advantages in those research areas that require very high levels of parallel computational performance. This system has demonstrated over 60 billion floating-point operations per second (60 GFLOP/sec) of sustained performance for the

production computational fluid dynamics (CFD) code OVERFLOW-MLP (13 times that of a 16 CPU C90 system). This system offers even higher performance potential for molecular dynamics simulations.

Recently, the Lomax system was used as the parallelization testbed for the COSMOS ab initio

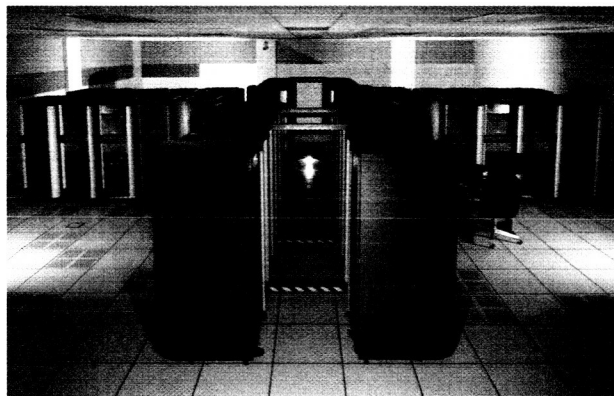


Fig. 1. The Ames 512 CPU SGI Origin 2000 system.

molecular dynamics model used in NASA’s astrobiology research effort. The COSMOS code is often used to perform protein-folding simulations. Historically, many important problems involving 20,000-30,000 atoms have not scaled well on “clustered” parallel systems. This lack of performance is due to the small amount of work performed by each CPU relative to the time spent transferring data between CPUs.

The single-system approach of the SGI Origin 2000 architecture, and the large CPU count Lomax system in particular, offers an ideal platform for such computations. The Origin design supports very fast and low latency memory access times from any processor to any memory module. This low latency and high performance are essential for parallel scaling to the hundreds of CPUs necessary to execute problems in a timely manner.

The optimization effort is focused on inserting the highly efficient Ames-developed multi-level parallelism (MLP) approach into COSMOS. At this point the two major time-consuming routines have been converted with highly encouraging results. The first routine computes its zones between all water molecules in the system (WATNLS1). The second (MPFGATHER) gathers the forces for subsequent molecular movement. The results are summarized in Table 1.

Table 1. A comparison of COSMOS and COSMOS-MLP execution times.

<u>COSMOS (32 CPUs)</u>	<u>COSMOS-MLP (343 CPUs)</u>
Module Summary	Module Summary
WATNLS1: 56.66	WATNLS1: 0.94 (60x)
MPFGATHER: 42.13	MPFGATHER: 0.11 (383x)
BARRIER: 0.08	BARRIER: 1.97
Totals: 98.87	Totals: 2.92 (36x)

As the table shows, the MLP modifications dramatically improve the code performance on the two most time-dominating routines. The speedup arises from the much higher scaling efficiencies

found in the MLP based parallel algorithm, coupled to a greater reuse of encached data. It is this expanded cache reuse that fuels the observed dramatic superlinear speedup over the old code executing at its parallel limit of 32 CPUs.

Current efforts indicate that COSMOS-MLP executions on Lomax will be some of the fastest ever achieved in this field. The results of this research have far-ranging implications in the commercial world, for the advanced numerical techniques developed under this effort are generally applicable to a number of industry standard models used by the university and drug research communities in the United States.

Points of Contact:
J. Taft (COSMOS-MLP)/A. Pohorille (COSMOS)
(650) 604-0704/5759
jtaft@nas.nasa.gov
pohorille@raphael.arc.nasa.gov

Space Technology and CFD Applied to the Development of the DeBakey Heart Assist Device

Cetin Kiris, Dochan Kwak

Approximately 20 million people worldwide suffer annually from heart failure, a quarter of them in America alone. In the United States, only 2,500 donor hearts are available each year. The DeBakey Ventricular Assist Device (VAD) prolongs life until a suitable transplant heart is available, and is used to boost blood flow in patients suffering from hemodynamic deterioration, that is, loss of blood pressure and lowered cardiac output.

The use of computational fluid dynamics (CFD) technology led to major design improvements in the heart assist device, enabling its human implantation. The DeBakey VAD is a miniaturized heart pump designed to increase blood circulation in heart-failure patients awaiting a transplant. A ventricular assist device has to be small and efficient, generating a 5-liter-per-minute blood flow rate against

100 mm Hg pressure. Because blood is the operating fluid, the design of a VAD requires that it propel the blood gently, that is, it must minimize damage to the red blood cells. In order to reduce red blood cell damage, the pumping device must be designed to avoid regions of high shear stress and separated flow in the pump. In addition, the blood must be properly washed out of the pump since the formation of blood clots may appear within stagnation regions as a result of previously damaged blood cells. Since the device is small and the operating conditions severe, instrumentation for making necessary flow measurements is extremely difficult to design. Therefore it became necessary to look at the flow by computational means. The detailed computational flow analysis now affords VAD designers with a view of the complicated fluid dynamic processes inside their devices.

Through the collaborative efforts of MicroMed Technology Inc., Ames Research Center, and the Johnson Space Center, the device has evolved from early versions of the DeBakey VAD, which caused thrombus formation (blood clotting) and hemolysis (red blood cell damage). To solve these problems, Ames scientists employed shuttle main engine technology and CFD modeling capabilities, coupled with high-performance computing technology, to make several design modifications that vastly improved the VAD's performance. A three-dimensional, viscous, incompressible Navier-Stokes code (INS3D) was used to analyze the flow. Several design iterations were performed in order to increase the hydrodynamic performances of this axial pump. The research team investigated seven designs, altering cavity shapes, blade curvature, inlet cannula shapes, and impeller tip clearance size. They then suggested three major design modifications to solve the problems of cell damage resulting from their exposure to high shear stress and interrupted regions of blood flow in the DeBakey VAD (see figures 1 and 2).

The first improvement was the addition of an inducer that spins with the impeller, drawing the blood in and out of the device, thus preventing a back flow. Additionally, the inducer provides enough pressure rise to eliminate back flow in the impeller hub region. The front edges of the blades were slanted forward, allowing blood to flow at the correct angle with the impeller, thereby increasing the

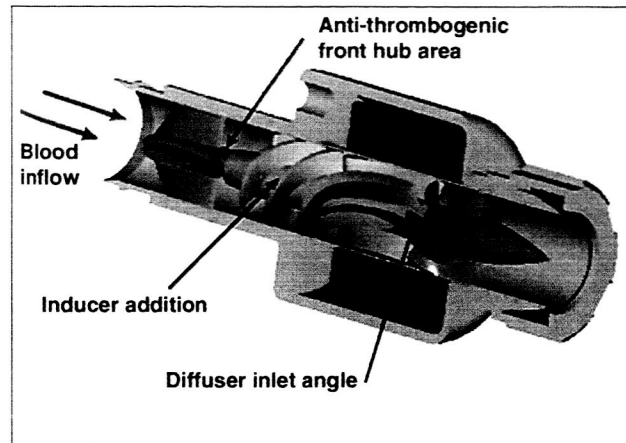


Fig. 1. Using CFD analysis, three major design modifications were made.

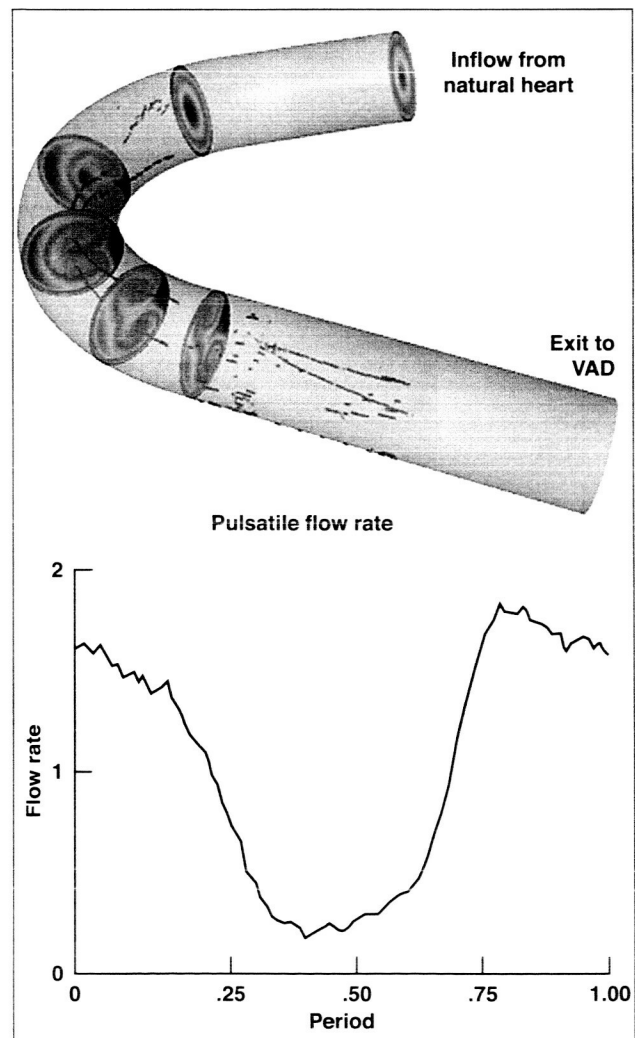


Fig. 2. Particle traces and velocity contours in the inlet cannula.

	Baseline design	New design
Hemolysis index	0.02	0.002
Thrombus formation	yes	no
Test run time	2 days	30+days

Fig. 3. Performance of the new VAD design.

efficiency of flow through the device. Second, CFD results suggested that the original design of the device caused clotting in the front bearing area where the blood passes over the flow straightener and meets the impeller blades. Expanding the hub area's width increased the circulation of blood, eliminating stagnant sections where clotting was known to occur. Additionally, researchers tapered the hub surface, accelerating blood flow, and thus creating good wall washing. And third, the exiting flow angle of the blood was examined and the diffuser angle was repositioned. Changing the diffuser blade angle aligns it with the blood flowing through the device, creating a smoother transition of blood over pump surfaces, and reducing the shear stress that causes cell damage.

Clinical tests conducted by MicroMed Technology and Baylor College of Medicine have confirmed the improvement in performance—hemolysis was decreased tenfold (figure 3). In collaboration with designers at MicroMed Technology, modifications made through the use of CFD analysis have resulted in a device that can perform for more than 100 days. The longest successful trial period to date in a human was 110 days, after which a donor heart was transplanted. The team's ultimate goal is to make the VAD a permanent alternative to heart transplant surgery. Successful European trials of the device in humans suggest its ability to provide long-term ventricular assistance.

Point of Contact: C. Kiris
(650) 604-4485
ckiris@mail.arc.nasa.gov

ACCESS TO SPACE

Application of Rotary-Wing Technologies to Planetary Science Missions

Larry A. Young

The next few years promise a unique convergence of NASA aeronautics and space programs. NASA planetary science missions are becoming increasingly more sophisticated and this will ultimately culminate, in part, in the development of planetary aerial vehicles (PAVs). Early work in this area has principally focused on conceptual design of fixed-wing aircraft configurations for Martian exploration. However, autonomous vertical-lift vehicles—and rotary-wing technologies in general—hold considerable potential for supporting planetary science and exploration missions.

For planetary science missions to Venus, Mars, and Titan, vertical-lift vehicles (using rotors as the means of propulsion) could potentially be developed and flown to support robotic science missions to these two planets and Saturn's moon (figure 1). For missions to Jupiter, Saturn, Uranus, and Neptune, vertical-lift capability is not required for PAVs supporting scientific investigations of the gas-giant planets. However, rotary-wing technologies, such as aeromechanics for PAV propeller design, could still be applicable for vehicles developed for these planets.

Autonomous vertical-lift PAVs would have the following advantages and capabilities when used for planetary exploration:

1. Their hover and low-speed flight capability would enable detailed and panoramic surveys of remote sites.
2. They would enable remote-site sample return to lander platforms or precision placement of scientific probes or both.
3. Soft landing capability would enable vehicle reuse (that is, lander refueling and multiple sorties) or remote-site monitoring and exploration.
4. Hover and soft landing provide good fail-safe "hold" modes for autonomous operation of PAVs.

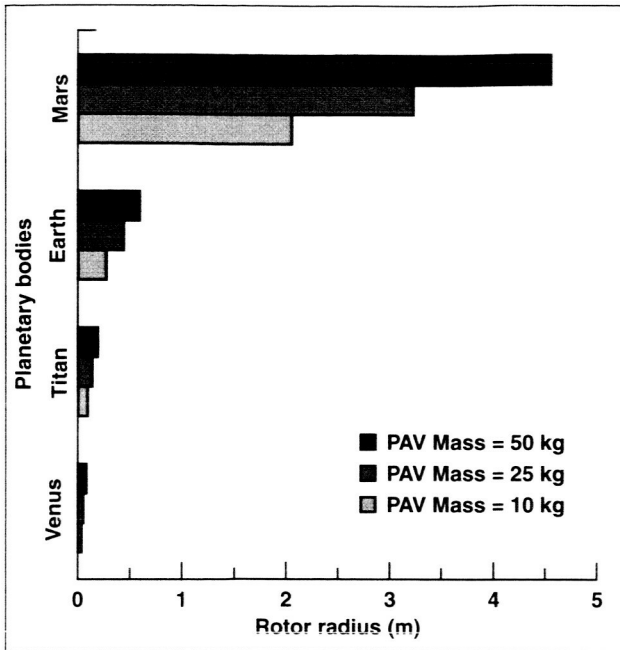


Fig. 1. Comparison of rotors sized for hover (for equivalent values of tip Mach number, solidity, and mean lift coefficient).

5. They would provide greater range, speed, and access to hazardous terrain than a surface rover.

6. They would provide greater resolution of surface details or observation of atmospheric phenomena than an orbiter.

The objective of the work being performed is to assess the feasibility of developing vertical-lift planetary aerial vehicles. Work to date has focussed on a conceptual design study of a Martian Autonomous Rotorcraft for Science (MARS). Given the thin, carbon-dioxide-based Martian atmosphere, developing a rotorcraft that can fly in that planetary environment will be very challenging. A university grant has been initiated to develop a conceptual design of a mission and flight-control computer architecture.

Point of Contact: L. Young
 (650) 604-4022
layoung@mail.arc.nasa.gov

Ballistic Range Tests Verify Stability of a Loaf-Shaped Entry Vehicle

Peter Gage, Gary Allen, Chul Park, Jeff Brown, Paul Wercinski, Tim Tam

An entry vehicle whose shape resembles that of a loaf of bread has been proposed for missions to be flown as secondary payloads on the Ariane V launch vehicle. This shape conforms well within the volume available inside the Ariane structure for auxiliary payloads, and provides a much more efficient and larger internal packaging capability for the given launch-vehicle constraints than the conventional sphere-cone geometry (such as that of the Mars-Pathfinder entry vehicle). Because aerodynamic stability for this new class of vehicles must be evaluated, initial ballistic range testing was conducted to assess the supersonic behavior of loaf-shape vehicles. Figure 1 shows a shadowgraph image of the ballistic range model flying at supersonic speeds.

The loaf-shaped model for the ballistic range tests is sized to be launched from a 1.75-inch-bore gun. The model has geometry and mass properties that are similar to those being considered for the mission. Model dimensions are 1.15 x 0.78 x 0.66 inches and

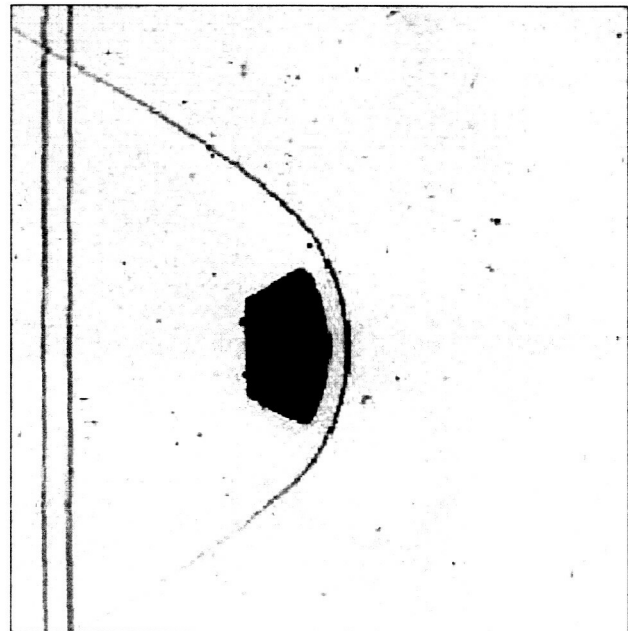


Fig. 1. Sample shadowgraph from aeroballistic testing of loaf-shaped entry vehicle.

the center of gravity is at 39% of the length (measured from the nose). An ambient density of 0.18 kilogram per cubic meter of carbon dioxide (CO_2) is chosen so that the Reynolds number will be consistent with that for the full-scale entry body at Mars. A nominal launch velocity of 680 meters per second ensures Mach numbers ranging from 2.5 down to 2 as the model decelerates along the length of the test section.

Four tests were conducted at consistent conditions in order to reduce uncertainty in the estimated aerodynamic parameters. The results summarized in Table 1 confirm the stable behavior of the loaf-shaped vehicle. The experimental value of drag coefficient is lower than the computational fluid dynamic (CFD) estimate because it includes wake effects. Pitch and yaw coefficients also indicate a discrepancy that is up to 20% of the CFD estimate, which confirms that analysis of the forebody alone does not adequately predict aerodynamic behavior at low supersonic speeds. Uncertainty in lift coefficient is relatively high because the angle-of-attack variation was small in some tests.

Table 1. Aerodynamic parameters of bread-loaf geometry in supersonic speed range.

Parameter	Forebody CFD estimate	Ballistic range estimate
CD_0	1.6	1.381 ± 0.002
Cm_α	-0.208	-0.18 ± 0.01
Cn_β	-0.235	-0.28 ± 0.02
CL_α	-1.07	-0.80 ± 0.19

The results of this study indicate the feasibility of using a loaf-shaped entry vehicle which maximizes packaging capability for the Ariane V launch vehicle. If this shape is selected for future missions, additional tests and full-body CFD analysis should be performed to model the detailed flow more accurately and to reliably define the vehicle aerodynamic coefficients.

Point of Contact: P. Gage
(650) 604-0193
pgage@mail.arc.nasa.gov

Aerothermal Analysis of X-33 Elevon Control Surface Deflection

Dean Kontinos, Dinesh Prabhu

As the X-33 nears final construction, the analytical emphasis has been redirected from generating design data to mitigating flight risk. Computational simulation of the flow field surrounding deflected elevon control surfaces has been performed to verify engineering estimates of the heating levels that the canted fin must be designed to withstand. This analysis serves to reaffirm design assumptions and reduce uncertainty, thus decreasing flight risk.

In previous simulations, surface heating predictions were based on the assumption of a smooth body. In reality, the body surface has both protuberances, such as steps and gaps formed between seals or tiles, and control-surface deflections that divert the flow from its nominal path. These surface irregularities and control-surface deflections trigger local fluid mechanical interactions that increase the heat transfer in some zone of influence on the surface. The thermal protection system is designed to account for these local effects by applying multiplicative scale factors, derived through empiricism and theory that augment the baseline smooth-body heating levels.

To validate the design correlations, computational fluid dynamics (CFD) techniques have been used to simulate the flow field around deflected elevon control surfaces. The geometric model includes the gap between the elevon control surface and the main body, the gap between the elevon surfaces, and the abbreviated edge of the elevon at the tip of the canted fin. Figure 1 shows radiative equilibrium surface temperature contours on the windward side of the X-33, along with an expanded view of the deflected elevon surfaces. The flow conditions are Mach 10, an angle of attack of 30 degrees, an altitude of 180,000 feet, and elevon control-surface deflection of 25 degrees. Evident in the figure is the increased heating on the face of the elevon generated by its deflection into the hypersonic flow field. Also discernible is increased heating on the sides of the elevon caused by the flow accelerating around the edges of the control surface. The maximum elevon surface temperature occurs in the gap region. These results are being used to verify the suitability of the design.

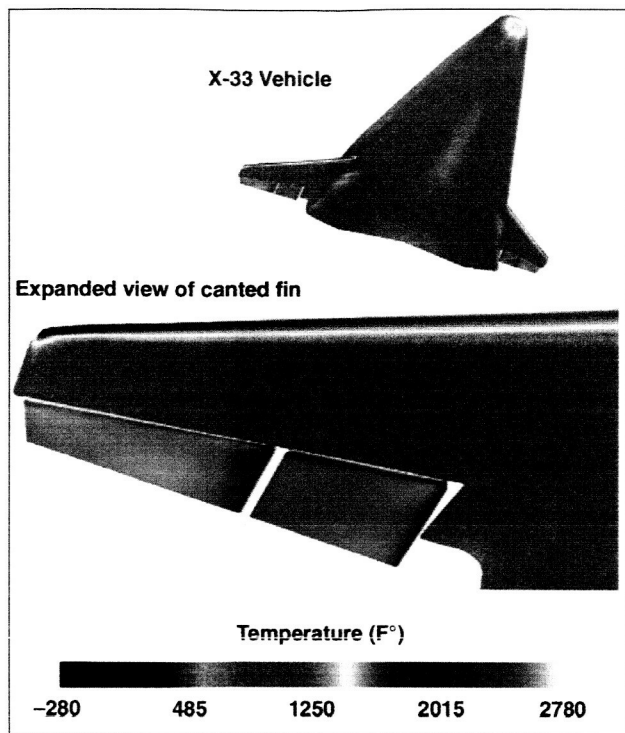


Fig. 1. Computed radiative equilibrium surface temperature contours on the X-33 vehicle with the elevon control surface deflected 25 degrees at Mach 9, an angle of attack of 30 degrees, and an altitude of 180,000 feet.

Point of Contact: D. Kontinos
 (650) 604-4283
 dkontinos@mail.arc.nasa.gov

CFD Analysis of Arc-Jet and Flight Environments for the B-2 Flight Experiment

Mark Loomis, Grant Palmer

Ames Research Center has been developing new ultrahigh temperature ceramics (UHTC) for potential use in the sharp leading edges of future space vehicles. These materials have been developed and tested in ground-based arc-jet facilities, and a flight test program called SHARP (slender hypervelocity research aerothermodynamic research probes) has

been initiated. The first flight demonstration, SHARP-B1, incorporated a 0.141-inch-radius UHTC nose-tip on a U.S. Air Force reentry vehicle in collaboration with Sandia National Laboratory; it was successfully flown in May 1997. The second flight test, SHARP-B2, incorporates four instrumented UHTC strakes mounted on the side of the entry vehicle; it is scheduled to fly in June 2000. The goal of these flight tests is to assess the performance of the materials under realistic entry conditions.

Computational fluid dynamics (CFD) simulations of the flight environment have been performed to aid in the design of the test hardware and instrumentation, and simulations of critical qualifying ground tests in the arc-heated wind tunnels have been performed to aid in test interpretation and instrument checkout, and to show traceability of the ground-test environment to flight.

Figure 1 shows computed heat-transfer profiles on the surface of the flight vehicle and the test article in the arc-heated wind tunnel. Although simulation of the complex-flow physics in the arc-heated wind tunnel is difficult, the goal of the simulations is to understand the flow environment well enough that the similarities and differences in the flight conditions can be assessed. Initial comparisons between the CFD and arc-jet data are generally within 40% for heat transfer and 5% for pressure, giving some confidence in the predictive method. The CFD predictions will be compared with flight results once they are available.

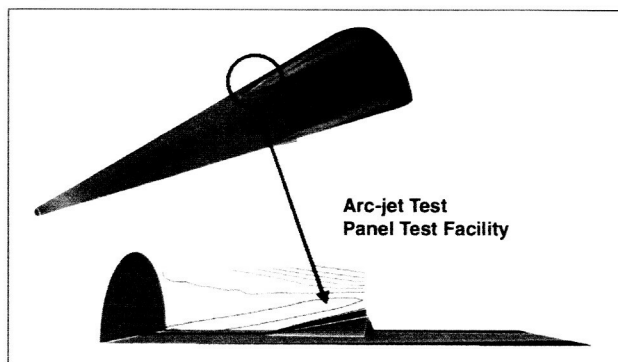


Fig. 1. Heat-transfer profiles for flight vehicle and test article. Flight: Modified MK-12 RV launched on Minuteman III.

Point of Contact: M. Loomis
 (650) 604-6578
 mloomis@mail.arc.nasa.gov


Web-Based Analyses for Vehicle Engineering

Michael Wright, Peter Gage, Dinesh Prabhu,
Periklis Papadopoulos, Joe Olejniczak, Dave Olynick

The preliminary design of an aerospace vehicle is a complex task, one that requires the collaborative effort of a group of engineers using many different engineering analysis software packages. During the early stages, the design goes through frequent changes from the original baseline, each change requiring parametric modifications to the computational models. Typically, no single person is proficient in the use of all of the required software, which means that the resident experts in each software package are tasked to spend considerable time making small, repetitive changes to the baseline models. In this project we seek to automate this process by building a Hypertext Markup Language (HTML) based user interface called WAVE (web-based analyses for vehicle engineering) which ties a subset of the capabilities of a set of engineering

analysis tools into a straightforward uniform package that can be used by a design engineer who is not familiar with the details of the analysis software.


Using this method, the software experts first build parameterized models of the vehicle systems and environment, and then determine the best solution procedure for the given task. A customized interface is then built for the vehicle within WAVE that ties all of the analytical tools together. During the design process, the end user is presented with a subset of the capabilities of the original analysis software, consisting of only those parameters that have been chosen to vary during preliminary design. For example, in figure 1 the complexity of a computational fluid dynamics (CFD) code input deck with more than 100 input quantities has been reduced to an HTML form with eight parameters that define the free-stream conditions for the simulation. Similar reductions in complexity are made for each of the analysis packages. In this manner a single designer can quickly examine parametric variations about the baseline without the help of a team of software experts. Of course, expert help would still be required to go



GEM Geometry Input

Model Name:

a_outer_max (in)	<input type="text" value="1.15"/>
a_inner_max (in)	<input type="text" value=".8"/>
b_outer_max (in)	<input type="text" value=".78"/>
b_inner_max (in)	<input type="text" value=".4"/>
a_outer_base (in)	<input type="text" value=".72"/>
a_inner_base (in)	<input type="text" value=".6"/>
b_outer_base (in)	<input type="text" value=".48"/>
b_inner_base (in)	<input type="text" value=".3"/>
L_fore (in)	<input type="text" value=".22"/>
L_aft (in)	<input type="text" value=".44"/>
R_max (in)	<input type="text" value=".01"/>
R_base (in)	<input type="text" value=".01"/>



Case Builder Input GEM (mod1)

Case Tag	mod1
Velocity (m/s)	<input type="text" value="0"/>
Angle of Attack (Degrees)	<input type="text" value="0"/>
Sideslip Angle (Degrees)	<input type="text" value="0"/>
Density (kg/m ³)	<input type="text" value="0"/>
Temperature (Kelvin)	<input type="text" value="0"/>
Cutoff Reynolds Number (1/m)	<input type="text" value="1.056"/>
Mixture Gas Constant (x)	<input type="text" value="287.1"/>
Mixture Ratio of Specific Heats	<input type="text" value="1.4"/>

Fig. 1. Sample forms from WAVE interface.

beyond the boundaries of the original parametric models, but this would be an infrequent occurrence if the models were set up with sufficient flexibility.

In the test case shown here, we have automated the use of CFD for preliminary design by linking together a computer aided design (CAD) package (Pro-Engineer), grid generation software (Grid-Pro), a CFD code (GASP), and a post-processing tool (Tecplot). Sample HTML forms are shown in figure 1 for the CAD and CFD portions of the analysis. By stepping through each of the packages in turn the designer can make parametric changes to the baseline vehicle shape, generate appropriate volume grids, run CFD analyses, and view selected results, all

from within a single web-based interface. At each step of the analysis, quality checking is performed, and questionable results are highlighted. Figure 2 shows the results of such a quality check on a volume grid. Cut-planes through the grid are shown, with questionable areas highlighted in yellow. The data resulting from this design process can then be moved offline for more detailed analysis, or archived for future use.

Point of Contact: M. Wright
(650) 604-4210
mjwright@mail.arc.nasa.gov

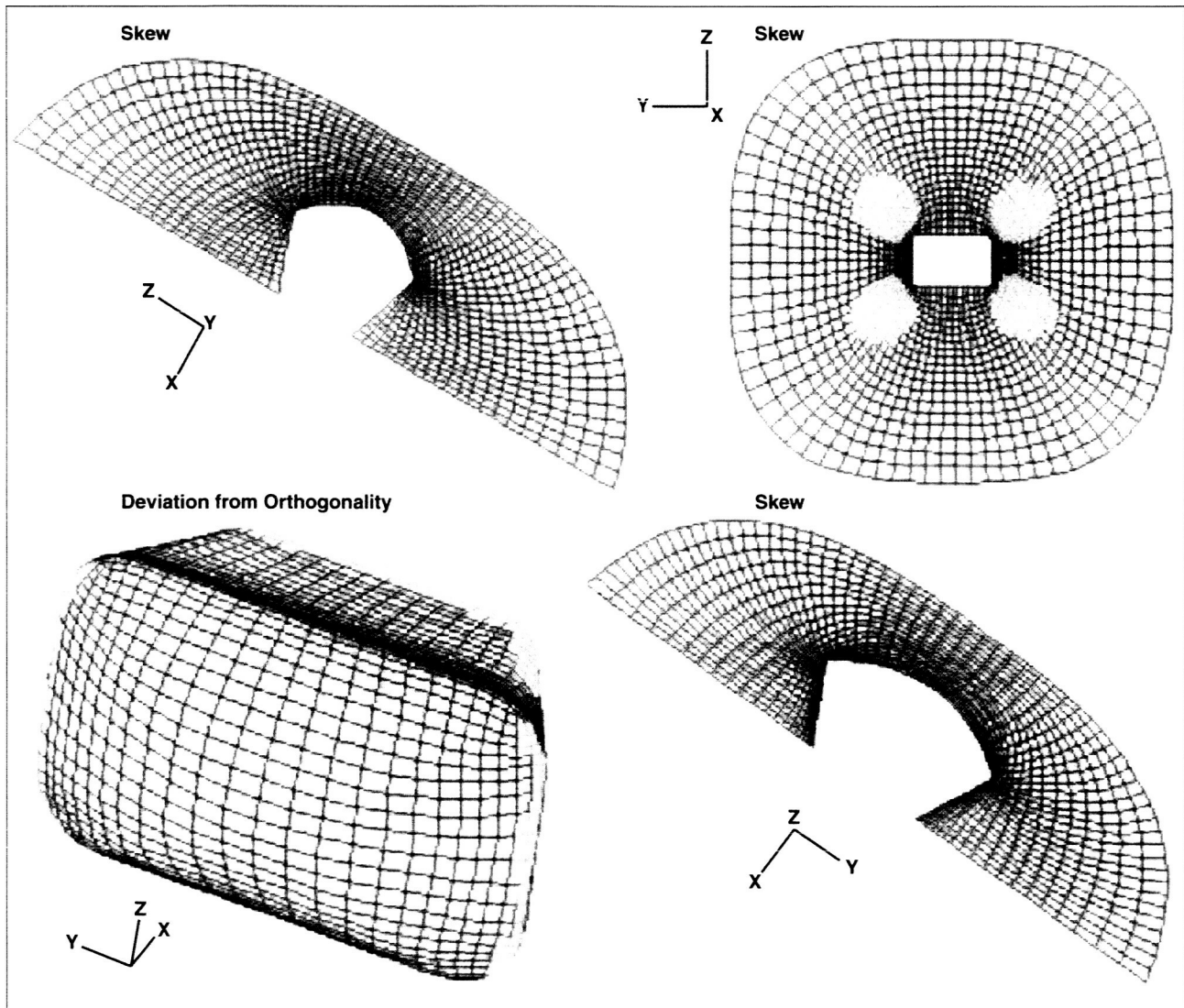


Fig. 2. Sample results from grid quality analysis.

Aerodynamic Shape Optimization of the X-37 Configuration for Improved Stability and Performance

Susan Cliff

The objective of this work was to apply numerical shape optimizations to the X-37 in order to improve its longitudinal stability and performance during descent. Wind tunnel test results for this vehicle, which were designed by Boeing at Seal Beach, California, showed longitudinal instability at Mach numbers between 0.6 and 1.5 and at moderate to high angles of attack. The instability was attributed to flow separation from the wing and tails. As part of the X-37 development program, Ames was requested to assist in refining this configuration through the use of numerical-optimization techniques developed under the High Speed Research Program.

The X-37 configuration is shown in the figure. It has an all-moving canted tail and a low-mounted wing, which is coincident with the lower surface of the fuselage. Optimization efforts were limited to supersonic conditions for the configuration with an aft extension to smoothly close the fuselage since the subsonic solution accuracy was questionable with the large blunt base. The design goals were to improve the longitudinal stability by increasing the lift coefficient for which the pitching-moment curve

slope was greater than 0.025 for Mach numbers between 0.8 and 1.5, and to improve the subsonic/transonic aerodynamic performance. The geometric constraints provided by Boeing included a fixed airfoil thickness along the wing flap hinge line, wing and ruddervator minimum thickness, and a leading-edge bluntness constraint. Wing twist and dihedral angle constraints were also provided along with ruddervator-sweep and dihedral-angle constraints.

The optimization tools employed in this design activity are embodied in the Ames Aerodynamic Shape Optimization (ASO) Library. The tools consisted of flow solvers, grid-generation and perturbation tools, design-variable and geometric constraint implementation tools, gradient computation methods, and numerical optimization methods. Some of the tools were commercially available, others were developed in-house; still others were modifications of commercial software. The basic optimization tool is the commercially available SYN107 multiblock code which consists of both a Euler flow solver and an adjoint solver, coupled to a constrained-optimization algorithm. The use of an adjoint solver provides efficient gradient information at a computational cost that is nearly independent of the number of design variables and of the convergence level of the flow solver. Geometric improvements to the wing and fuselage are obtained by optimizing the coefficients of analytic shape functions added to the surfaces.

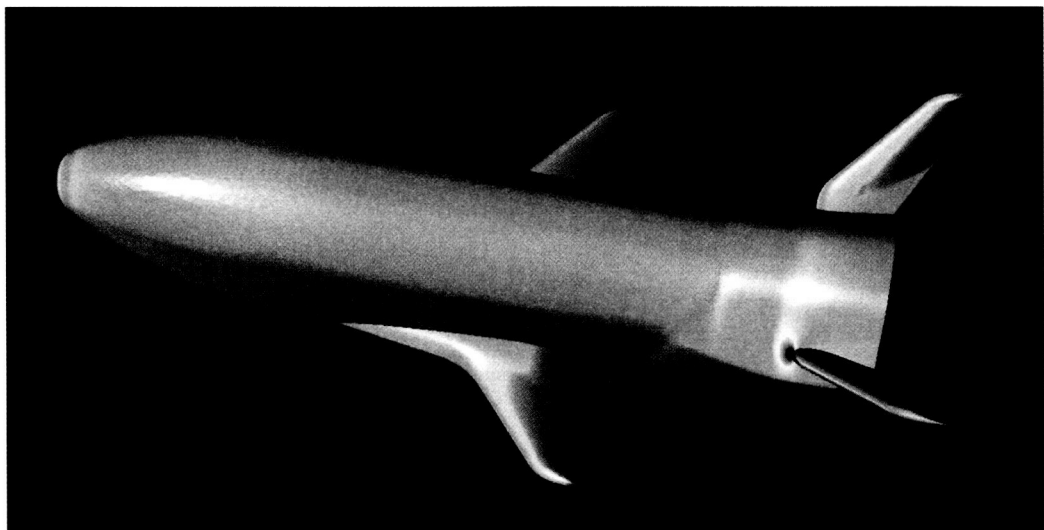


Fig. 1. AIRPLANE computation of the X-37 configuration, colored pressure coefficient contours at Mach = 1.2, angle of attack = 10 degrees.

High-fidelity analyses were obtained through the use of the AIRPLANE code, an unstructured tetrahedral Euler method. The unstructured grid method handles arbitrary geometries without incurring large increases in time or difficulty for increased geometric complexity.

Euler-based numerical optimization and hand design methods were used to modify the wing, body, and ruddervator of the configuration to improve stability and performance. Several parametric studies of the wing and ruddervator such as the wing fore and aft positions, ruddervator dihedral angle, span, vertical position, sweep and twist modifications were also performed. Several different objective functions were used to address the stability problem, both single-point design with a target pitching moment, and composite multipoint objectives to directly modify the slope of the pitching-moment curve between two angles of attack. However, minimizing a weighted drag/lift objective function at a fixed Mach number of 1.2 and an angle of attack of 10 degrees was the most effective objective for both stability and performance. This lent credibility to the presumption that reducing the pressure drag reduces or delays the shock-induced flow separation, thereby improving performance and stability.

AIRPLANE analyses of the optimized design predicted improved stability over the Mach number range of 0.8 to 4.75. All geometric constraints were satisfied, including the additional constraint of no lower-surface leading-edge droop. In addition, significant performance improvements were achieved for the redesigned configuration at Mach numbers of 0.8, 1.2, 1.5, 1.8, 3.0, and 4.75. An 8% total drag reduction representing approximately 330 counts was obtained at the design Mach number of 1.2. In addition, a 10% reduction in drag was obtained at the secondary design Mach number of 0.8.

Many of the parametric modifications to the ruddervator (dihedral angle, span, vertical position, twist, and sweep angle) and wing (fore and aft position) made significant improvements to the longitudinal stability, but they were not included in the final design because the changes could adversely affect other mission requirements.

Point of Contact: S. Cliff
(650) 604-3907
scliff@mail.arc.nasa.gov

Space Science Enterprise



Overview

Scientists in NASA's Space Science Enterprise seek to answer fundamental questions about the origin and evolution of life and of celestial objects (planets, planetary systems, stars, galaxies, etc.) in the Universe. Ames is recognized as a world leader in astrobiology, the study of life in the Universe and the chemical and physical forces and adaptations that influence life's origin, evolution, and destiny. In pursuing its primary mission in astrobiology, Ames performs pioneering basic research and technology development to advance our fundamental knowledge about the origin, evolution, and distribution of life within the context of cosmic processes. For example, research and technology development are currently conducted for the following purposes.

- To study the mechanisms of the origin, evolution, and distribution of life in the universe
- To determine the abundance and distribution of the biogenic compounds that are conducive to the origin of life

Image MOC2-242 taken of Mars recently by the orbiting Mars Observer Camera (MOC). This image shows texturing on the walls of a small crater located on Mars in the southwestern quarter of the much larger Newton Crater (near 41.1°S, 159.8°W). The image is an excellent example of the stunning high-resolution images of erosion features that are being revealed by the MOC. It is hypothesized that these erosion features were formed by flowing water and debris. Assuming these features share many characteristics with debris flows on Earth, conservative estimates suggest that ~2.5 million liters (660,000 gallons) of water were involved in each event. This is enough water to supply 20 people with their water needs for a year. The presence of liquid water on Mars is of great interest to those who study the origins of life as well as the future of life in the solar system.

(Photo Credit: MOC2-242 NASA/JPL/MSSS).

- To identify locations on bodies within our solar system at which conditions conducive to life exist or have existed
- To explore the other bodies (planets, comets, asteroids) of our solar system
- To locate planets and planet-forming regions around other stars
- To study extra-solar matter such as interstellar gas and dust

Exobiology

Ames' Exobiology Program is a key element of NASA's Astrobiology Initiative and Ames serves as NASA's Lead Center in exobiology. Research in exobiology at Ames ranges from studying the mechanisms of the origin of living systems to the processes governing the evolution of life to the distribution of life on other planets. When coupled with Ames' pioneering research on the dynamics of galaxies, molecular gases and clouds, planetary systems, and the solar system, our study of life is facilitated by understanding the cosmic environment within which life originates and evolves.

Molecules of exobiological significance are ubiquitous in the Universe. It is important to understand the sources and interactions of these Cosmic building blocks and how living systems emerge from prebiotic molecular chaos.

Studies of the following subjects are highlighted here.

- Rates and conditions under which trace gases are emitted or consumed by microbial mats and stromatolites
- Synthesis of organic molecules that are made during meteorite impacts on the surface of Europa
- Chemical evolution of organic matter as a result of heat and pressure generated by asteroid and meteorite impacts
- Photosynthetic microbial mats to understand the role played by their ancient counterparts on Earth
- The origin of oxygenic photosynthesis
- The nature of cometary debris and the significance of meteors as a seeding mechanism for organics on young planets
- Evolution of protocells with small proteins—rather than nucleic acids—performing cellular functions
- How reduced nitrogen, an essential element for the origin of life, may have been available on early Earth
- The upper temperature limits for macroscopic eukarya in the hot springs in Yellowstone National Park
- Peptides as good candidates for the first replicating molecules on primitive Earth

Planetary Systems

Scientists in the Space Science Enterprise are interested in how and where in the Universe planets form, and the geophysical, geochemical, and atmospheric processes that occur over the lifetime of a planet. Further, understanding the dynamics between planetary processes and the origin and evolution of life will help us understand the distribution of life in the Universe.

Studies of the following are highlighted in this report.

- Gaseous disks around young solar-mass stars to provide insight into the development of our own planetary system
- The frequency of the occurrence of extrasolar planets and their properties
- Hydrocarbon dust in the diffuse interstellar medium
- Planetary rings for understanding properties of colliding particles relevant to the accretion of planets
- Primitive objects in the meteorite record that represent the first large bodies to accumulate in the protoplanetary nebula
- Properties and emergent spectra of extrasolar giant planets and brown dwarfs
- Investigation of star and planet formation processes conducted by a consortium of scientists undertaking a coordinated program of theoretical research
- Global atmospheric circulation of Mars to improve our knowledge of the dynamics of the present and past environment
- Properties of the multiple planets discovered around a Sun-like star
- Extraterrestrial sources of nitriles and hydrocarbons identified in dense clouds and their relevance to the origin of life

- How the presence of an atmosphere can strongly affect impact cratering on planetary bodies

Astrophysics

As NASA's lead in airborne astronomy, scientists at Ames pioneered the field of astrophysics. Study topics range from star-forming regions and processes to interstellar photochemistry to protoplanetary disks. Understanding cosmic processes—the evolution of the Universe itself—is a vital part of the Origins initiative.

Ames' astronomers and astrophysicists use a wide variety of study methods. Ground-based telescopes, such as the Keck and Mount Lemmon Observatories, are regularly employed for observations of celestial objects and processes. Development continues on the Stratospheric Observatory for Infrared Astronomy (SOFIA), an infrared telescope to be carried aboard a Boeing 747 aircraft specially modified for the task. Space-based observations are also made by instruments such as the Hubble Space Telescope (HST) and by other observatories and missions. Computer modeling and laboratory analogs of chemical processes enhance these observational astronomy techniques.

The following astrophysical studies are highlighted in this report.

- The Nstars database developed at Ames as a web-accessible source of data on stars for the use of the astronomical community
- Detection of extrasolar planets by the star-transit method that can also provide planetary masses and radii
- Spectroscopic data related to complex organic matter found on solid bodies in the outer solar system
- The AIRES (Airborne InfraRed Echelle Spectrometer) being developed as a facility-class spectrometer for the SOFIA airborne observatory
- The scientific instrumentation that will be needed for NGST (Next Generation Space Telescope) observations of galaxies, stars, and planets
- The infrared properties of the SOFIA telescope surfaces as they might contribute to background noise
- Design of the water vapor monitor for SOFIA
- Chemical processes that occur in dense interstellar clouds and that are simulated in the laboratory

Space Technology

In support of the Space Science Enterprise in conducting future space science and exploration missions, Ames scientists and engineers develop and validate technologies and instruments, develop calculation-based and modeling algorithms, and refine analytical methods.

This report highlights the following Ames space technology work.

- Increasing the flexibility and robustness of Mars rovers by developing onboard autonomy and contingency planning
- The application of evolutionary search techniques to the process of automated engineering design
- Ways to make statistical data analysis easier and more accessible to scientists by synthesizing efficient data analysis programs from statistical models
- A tool to provide a centralized project information resource that is accessible to an entire scientific team over the World Wide Web
- Technologies for rigorously verifying requirements for the software models used in autonomous controllers for space devices
- Technologies for cryogenic propellants to support human missions to Mars
- How the requirements for liquefying the surface oxygen on Mars can best be met using off-the-shelf cryogenic coolers and simple heat exchangers
- The potential for rotary-wing technologies to support missions of planetary science and exploration

Trace-Gas Production and Consumption in Microbial Mats

Brad M. Bebout

The Ames Microbial Ecology/Biogeochemistry Research Lab has made contributions to determining the rates and conditions under which various trace gases are emitted and/or consumed by microbial mats and stromatolites. The most promising search strategy for the detection of life on extrasolar planets is the detection of possibly biogenic gases using infrared spectrometry. Space-based interferometers, such as the Terrestrial Planet Finder, should be able to resolve the spectra of several biologically important trace gases in the atmospheres of extrasolar planets, possibly within 10 to 15 years. Therefore, it is important to provide a conceptual framework for the interpretation of the possible biogenicity of these gases.

Measurements of the production and consumption of reduced gases have been made under current conditions on the Earth, and conditions that are not present now but have existed in Earth's past. To date these measurements indicate that: (1) there is a significant escape of a variety of reduced gases from these communities, and (2) there is significant oxidation, but also significant production, of these gases in the surface (oxidized) layers of these communities. Of particular note is the finding of significant rates of methane production in the aerobic zone of microbial mats, because methanogenesis is thought to be an anaerobic process.

Measurements of trace-gas production and consumption have been made in field-incubated microbial mats, in stromatolites, and in samples returned to Ames. Over the past year, the capability to incubate mats under natural conditions has been significantly enhanced with the modification of a greenhouse on the roof of Building N239. This greenhouse has been fitted with ultraviolet-radiation-transparent acrylic to accommodate the importance of ultraviolet (UV) rays in the ecology of these communities. This greenhouse offers the capability to incubate mats under natural solar illumination,

realistic water flows and temperatures, and atmospheres of variable gas composition.

In conjunction with the activities of the Early Microbial Ecosystems Module of the Ames Astrobiology Institute Team, the Biogeochemistry/Microbial Ecology Research Laboratory has participated in numerous field expeditions. Measurements of numerous important biogeochemical processes in microbial mats were made on these trips, including oxygenic photosynthesis, nutrient cycling, and nitrogen fixation.

Technology development continues to center on microsensor technology. In order to be able to better measure light (specifically plane irradiance) within photosynthetic microbial mats, a novel fiber-optic microsensor capable of making these measurements even within lithified (hard) microbial mats and stromatolites was developed.

Point of Contact: B. Bebout
(650) 604-3227
bbebout@mail.arc.nasa.gov

Synthesis of Organic Molecules in the Fracture Zone of Meteorite Impacts on Europa

Jerome G. Borucki, Bishun N. Khare

This work studies the synthesis of organic molecules that occurs as a result of meteorite impacts into planets with icy surfaces, such as Europa. Meteorite impacts into icy surfaces cause a large zone of fracturing under the impact crater. Very large voltages are generated during this fracturing, and that energy is, in effect, "stored" in the ice as electrostatic charges spread over a large area of the ice for substantial periods of time. Over time, the electrostatic charges can accumulate until a critical level ("the breakdown potential of ice") is reached, at which time electrical arcing occurs. In the presence of water-ice, methane, and ammonia, this arcing

serves as the energy source for the synthesis of organic molecules. Spark experiments performed on ices that simulate conditions on Europa have produced large organic molecules, which have become semiconducting.

The classic experimental apparatus for spark-discharge experiments designed by Miller/Urey/Sagan/Khare consisted of a glass sphere with two electrodes connected to an external high-voltage source protruding into its cavity. The sphere cavity was filled with ammonia, methane, and water vapors, and an electrical arc was induced between the electrodes. This simple system generated complex molecules known as tholins. Experiments with extending this model to simulated meteorite impacts into ice have shown that impacts can generate voltages sufficiently high to serve as the energy source for the synthesis of organics in ice.

An ice cylinder (25 by 61 centimeters (cm) long) is formed in a Teflon tube. The thick-walled (2.5 cm) Teflon contains the ice from exploding sideways at impact and cushions the ice, thus simulating a larger ice field. Four electrodes are embedded in the ice cylinder at 5, 20, 38, and 53 cm from the top surface of the ice. Three magnetic coils are wound on the circumference of the tube, and a photodiode monitor is placed about 15 cm from the top of the ice. A quarter-inch-diameter solid aluminum sphere serves as the simulated "meteor."

The Ames Vertical Gun Facility was used to launch the sphere at 5.6 kilometers per second (km/sec) into the ice cylinder cooled to -150 degrees Centigrade ($^{\circ}\text{C}$). Recent test results from this system showed that the voltage created in the ice at the uppermost electrode was greater than 300 volts (the channel saturated). Additionally, several saturated spikes were noted in the oscilloscope trace, indicating that arcing was occurring in the ice during the impact. Large oscillatory (10-kilohertz) magnet signals occurred in the same time frame as the impact, showing that large currents were flowing in the ice, in turn suggesting that the ice became conductive at impact of the projectile.

The second series of experiments had photodiodes monitoring the ice both from the top and from the side about 15 cm down from the top through a light pipe. The impact velocity of eighth- to quarter-inch aluminum spheres was 5 to 6 km/sec, and the energy of the projectile from 200 to 3000 joules with

the ice at a temperature of -170 $^{\circ}\text{C}$. At projectile impact, light emission, high voltage, and a large magnetic field that lasted about 5 milliseconds (ms) were recorded; then after a pause of 280 ms, a secondary light, voltage, and magnetic field occurred. The voltage and light had four spikes in a 10-ms timeframe, and the emissions correlated with each other, indicating that arcing was occurring in the fracture zone under the impact.

The fracture zone under a meteorite impact can be thought of as having two regions (like the plates of a capacitor) that will be charged either positive or negative. The charging of the two regions or plates occurs because of the breaking of molecular bonds in the fracture zone and/or crystalline ice that is subjected to the piezoelectric effect. Breaking of molecular bonds would produce free electrons and positive and negative ions, which would produce the large electrostatic charge imbalances, and would result in the formation of new organic molecules.

Another recent ice experiment was conducted in the laboratory using an ice block with two electrodes imbedded in the ice organic mixture at -200 $^{\circ}\text{C}$. The results showed that the organics were generated and the ice mixture became semiconducting. The semiconducting organics caused the spark to cease, and the ice mixture became liquid at an outside temperature of -200 $^{\circ}\text{C}$. Identification of the organics produced is under way.

The result of the above experiments have shown that large (tholin type) organic molecules can be formed in the fracture zones produced by meteorite impacts on the ice surface of Europa.

Point of Contact: B. Khare
(650) 604-2465
bkhare@mail.arc.nasa.gov

Impacts and Meteorite Organic Compounds

George Cooper, Friedrich Horz, Alanna Oleary,
Sherwood Chang

The majority of meteorites that contain organic compounds are thought to originate in the asteroid belt. Impacts among asteroids and impacts between asteroids and comets with the planets generate heat and pressure that may have altered or destroyed preexisting organic matter (depending upon impact velocities). Very little is known about the impact-related chemical evolution of organic matter relevant to this stage of the cosmic history of biogenic elements and compounds. At Ames Research Center, research continues in an effort to understand the effects of impacts on organic compounds.

One experimental approach is to subject mixtures of organic compounds, embedded in the matrix of a meteorite, to simulated hypervelocity impacts using a vertical gun. By choice of suitable targets and projectile materials, the compounds are subjected to simulated impacts, resulting in various pressures in the range of 100 to 400 kilobar. Each pressure can then be converted by mathematical equations into the corresponding impact velocity that an actual asteroid or meteorite would have experienced. Most of these velocities are too high to obtain in the laboratory. After the laboratory impacts, the products are analyzed to determine the degree of survival of the organic compounds.

Four classes of organic compounds, known to be indigenous to carbonaceous meteorites, have been studied: organic sulfur, organic phosphorous, polyaromatic hydrocarbons, and amino acids. The sulfur compounds were sulfonic acids containing one to four carbons. The phosphorous compounds were phosphonic acids, also containing one to four carbons.

Results show that over the range of pressures the general trend is that the survival rates of compounds are inversely proportional to impact pressure (impact velocity). However, at lower pressures, 100 to 200 kilobar (approximately 1 to 2 kilometers per second (km/sec)), the sulfonic acids containing only one or two carbons show nearly complete survival. There was a significant drop in survival rates at approximately 300 kilobar for all organic sulfur and

phosphorous compounds. Pressures of 300 to 400 kilobar (4 to 5 km/sec) resulted in survival rates of approximately 20 to 30% for all one- and two-carbon compounds, while the three- and four-carbon compounds survived at rates of approximately 0 to 10%. In the case of polyaromatic hydrocarbons and amino acids, a similar trend of decreasing survival rates with increasing pressure was observed. However, these two groups were less stable than the sulfur compounds at lower pressures.

These results indicate that significant amounts of meteoritic organic compounds would have survived impacts within the asteroid belt throughout solar-system history. In the context of asteroid impacts on Earth, the results also suggest that most of organic compounds would have survived in objects that experienced impact velocities near or below 4 to 5 km/sec.

Point of Contact: G. Cooper
(650) 604-5968
gcooper@mail.arc.nasa.gov

Biogeochemistry of Early Earth Photosynthetic Ecosystems: Production of Hydrogen and Carbon Monoxide

Tori M. Hoehler, Brad M. Bebout,
David J. DesMarais

For the first three-quarters of its history, Earth's biosphere consisted exclusively of microbial life. Most of this period was dominated by photosynthetic microbial mats, highly complex and organized communities of microorganisms that once covered the Earth. For two billion years, these mats were the primary biologic agents of global environmental change (for example, the oxygenation of the atmosphere) and the crucible for evolution of the complex macroscopic life forms we know today. Ames' Early Microbial Ecosystems Research Group studies the biology, chemistry, and geology of closely related modern microbial mats in order to better understand the important role played by their ancient counterparts.

A key focus is to understand how the chemistry of the mat influences, and is influenced by, the collective activities of the constituent bacteria. The sunlit surface layer of the mat harbors the highest population of active bacteria, is the most productive, and has the most direct interaction with the outside environment. Within this layer, concentrations of two gaseous products of microbial metabolism, hydrogen and carbon monoxide, vary in dramatic fashion during the course of one day (as shown in figure 1). The light-driven liberation of carbon monoxide has not been previously observed in mat communities. Given the widespread distribution of mats on early Earth, this light-driven liberation of carbon monoxide could have represented a significant but unrecognized contribution to the ancient atmosphere. Hydrogen concentrations in the mat vary by a factor of 10,000 or more during one day/night cycle. This variation is much greater than the variation that the Earth's surface environment on the whole has experienced during its entire history.

This variation in hydrogen is especially important in the context of the microbiology and chemistry of the mat. Many of the bacteria in the mat utilize hydrogen as an essential means of transferring chemical energy and "information" to one another. The dramatic daily variations in hydrogen may extensively influence the way in which these organisms interact and function as a collective whole. An important key to global change in the ancient environment, and to half of the evolution of life on Earth, may thus lie in the roller-coaster chemistry of microbial mats.

Point of Contact: T. Hoehler
(650) 604-1355
thoehler@mail.arc.nasa.gov

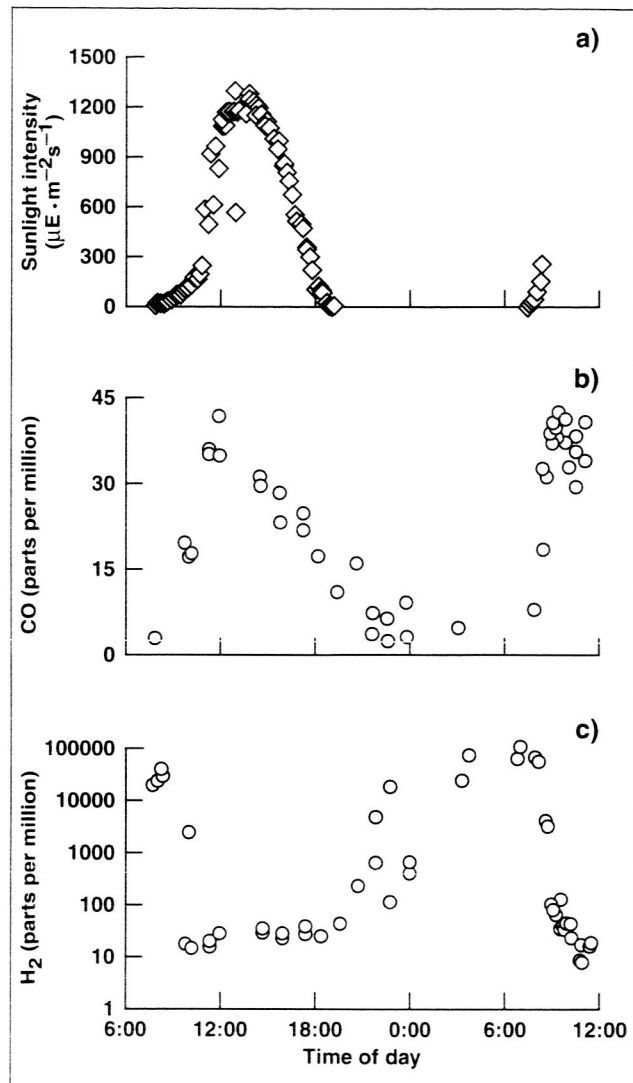


Fig. 1. Light intensity (a), carbon monoxide concentration (b), and hydrogen concentration (c) at the surface of a microbial mat from Baja, Mexico, during the course of one diel (24-hour day/night cycle). These graphs illustrate the dramatic light-driven chemistry generated by bacteria within the microbial mat. The chemical environment shown here experiences a greatly more substantial shift in conditions over a few hours than the Earth's atmosphere has during its entire history.

Evolutionary Relationships of Stromatolite-Building Cyanobacteria

Linda Jahnke, Kenneth Cullings, Detlev Vogler, Harold P. Klein

Stromatolites are one of the most abundant fossils in Precambrian rocks, and as such, provide valuable information about Earth's earliest biosphere. The microfossil record in stromatolites traces Earth's history since the oldest life over 3.5 billion years ago. Modern stromatolite structures are formed by sediment trapping and/or mineral precipitation of microbial mat communities living in shallow-water environments. Microbial mats are "living" stromatolites—modern-day analogs that provide an opportunity to study the way ancient microbial communities lived and evolved. Though direct evidence is lacking, fossil stromatolite diversity appears to be under the direct influence of microbial species diversity. Most modern microbial mats are constructed by cyanobacteria, but this may not have been the case for the earliest fossil stromatolites. Oxygenic photosynthesis first evolved in the cyanobacteria, so understanding the relationship between cyanobacterial and stromatolite morphology is crucial to determining the biotype of these early stromatolites and the timing of this crucial evolutionary event.

This study focuses on a type of modern coniform stromatolite constructed in the thermal springs of Yellowstone National Park by a fine filamentous cyanobacterium called *Phormidium*. These mats are considered the best analog for the fossil conophyton that are one of the most distinctive groups of Precambrian stromatolites, with a fossil record dating back to 3.5 billion years. A variety of stable organic compounds, generally referred to as "chemical fossils" or "biomarkers," have been extracted from these coniform mats, in particular the 2-methylhopanoids. The 2-methylhopanoids are considered a biomarker for the cyanobacteria, and detection of its fossil

equivalent in 2.7-billion-year-old sedimentary rocks has established a minimum age for the evolution of oxygenic photosynthesis. Understanding the relationships among the source of this important biomarker, stromatolite morphology, and cyanobacterial biodiversity provides essential clues in deciphering the identity of the original mat-building community and establishing the antiquity of *Phormidium* conophyton stromatolites.

A variety of morphologically similar *Phormidium* stromatolites have been isolated from the Yellowstone coniform mats. They form three distinct groups based on lipid biomarker composition. Two of the *Phormidium* groups synthesize hopanoids, but only one of these, represented by *Phormidium* OSS, synthesizes the cyanobacterial specific 2-methylhopanoids. The third group, represented by *Phormidium* RCO, synthesizes no hopanoids. A variety of molecular tools (denaturing gradient gel electrophoresis, DNA sequencing, and molecular phylogenetics) have been used to characterize the evolutionary relationship among these coniform-mat, *Phormidium* isolates. Phylogenetic analysis supports the three groups based on lipid biomarker composition (figure 1). Further, the cyanobacteria isolated thus far form a monophyletic group, indicating a single origin. This moderately thermophilic, coniform *Phormidium* clade is as well supported as several other well-established cyanobacterial clusters such as the *Microcystis* or halotolerant *Eubacterium*. Such close phylogenetic relatedness suggests a common evolutionary path within a close microbial community, giving rise to coniform biodiversity.

Point of Contact: L. Jahnke
(650) 604-3221
ljahnke@mail.arc.nasa.gov

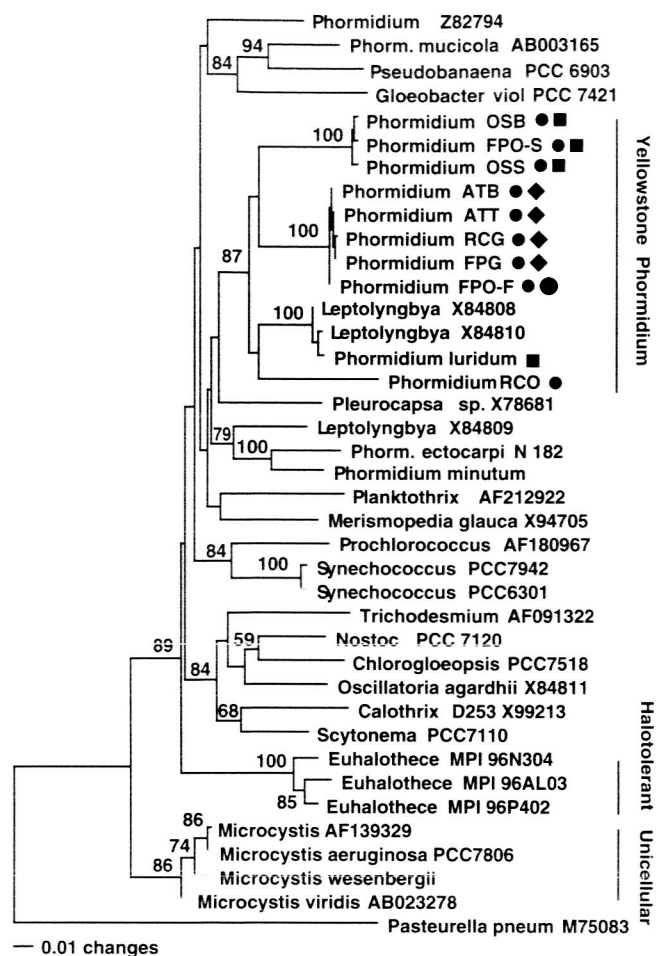


Fig. 1. Phylogenetic tree constructed using the DNA sequences for the 16S ribosome of Yellowstone *Phormidium* isolates (l), and cyanobacterial species chosen from GenBank to represent major clades showing *Phormidium* group synthesizing 2-methylhopanoids (n), and the group synthesizing only nonmethylated hopanoids (u).

Astrobiology Leonid Meteor Shower Mission

Peter Jenniskens, Steven J. Butow, Mark Fonda

The anticipated 1999 Leonid meteor storm provided a unique opportunity to study the nature and composition of meteoroids. Because the timing and intensity of the Leonid showers can be determined to within acceptable parameters to plan observing campaigns, NASA Ames Research Center and the United States Air Force (USAF) jointly sponsored the Leonid Multi-Instrument Aircraft Campaign (Leonid MAC). The airborne campaign produced a wealth of data, images, and spectra that will result in new insights on the nature of cometary debris and the significance of meteors as a seeding mechanism for organics on young planets.

The Leonid meteor storm begins its long journey as cometary ejecta from a periodic comet named 55P/Tempel-Tuttle. Comets are known to contain both simple and complex organics that predate the evolution of the solar system. The complex organics are thought to remain part of the meteoroids after ejection when the cometary ices have evaporated. Each year our present day Earth passes through an estimated 40,000 tons of such meteoric debris. At the time of the origin of life, about 4 billion years ago, that influx was a hundredfold larger. Earth was void of the basic organic compounds necessary for the origins of life. Many have postulated differing theories ranging from complex, time-dependent geochemistry to singular catastrophic impact events to account for the source of organics. Meteors provide a potential alternative pathway for their introduction.

The 1999 mission had two principal objectives: (a) to provide insight into the origins of life on Earth; and (b) to assess the impact threat of a meteor storm to satellites orbiting the Earth. It followed a successful NASA-sponsored mission in 1998. The NASA and USAF partnership provided 35 scientists from seven different nations two platforms for stereoscopic observations under the best possible observing conditions right under the peak of the shower. The Flying Infrared Signature Technology Aircraft (FISTA) and the Airborne Ranging and Instrument Aircraft (ARIA) were operated by the USAF.

Techniques employed included: state-of-the-art high-definition TV technology, near real-time flux measurements using intensified video cameras (the results of which are shown in figure 1), and spectroscopic measurements of meteors and persistent trains at wavelengths spanning from the near ultraviolet to the midinfrared (mid-IR). Results include the first spectroscopic record of the afterglow of a meteor fireball, shown in figure 2, and the first near- and mid-IR spectra of meteor trains. The first video record of a meteor storm also shows lightning near the horizon, and it may contain clues to whether meteors trigger "sprites" and "elves."

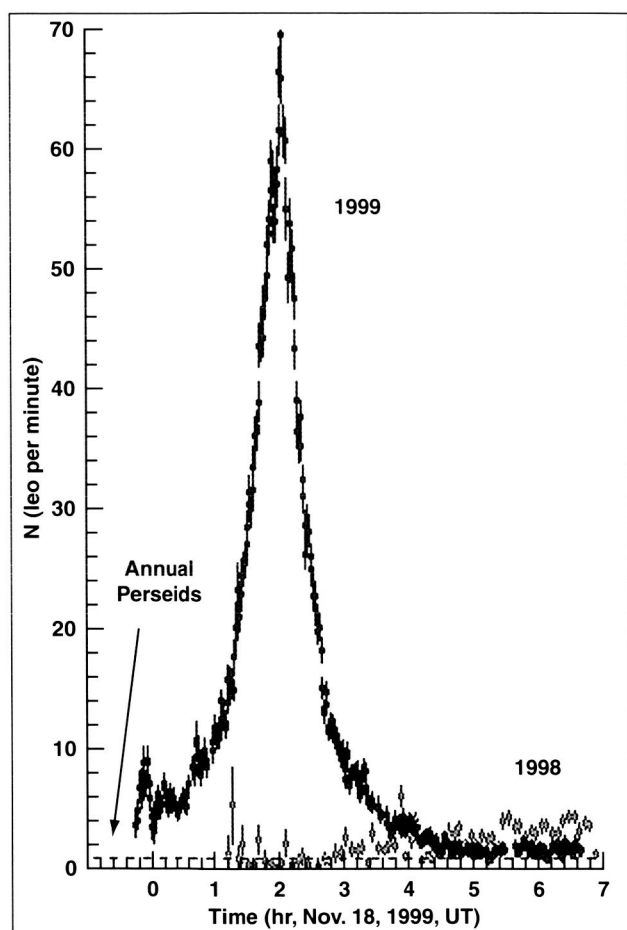


Fig. 1. Rate of Leonid meteors in 1998 and 1999 compared to that during the annual summer Perseid shower (dashed line at the bottom).

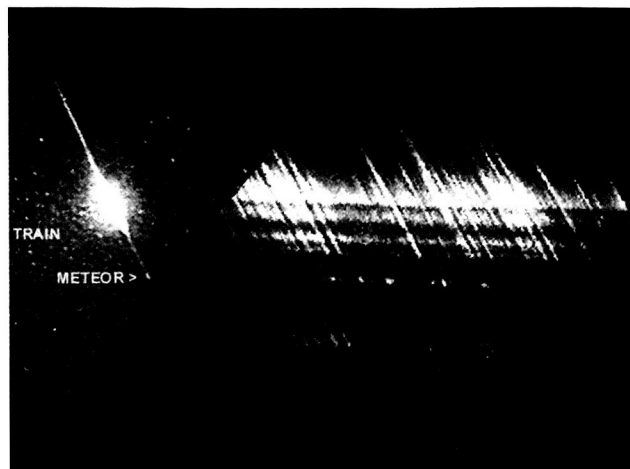


Fig. 2. The meteor and afterglow of the 04:00:29 UT Leonid fireball of Nov. 18, 1999, was detected by an Ames' slitless LLLTV spectrograph in the wavelength range from 0.4 to 0.9 micron.

Ames contributed to this mission new and highly successful approaches to meteor and meteor train spectroscopy at visual wavelengths. Interplane meteor targeting and spotting software were deployed to facilitate stereoscopic location and observation of significant meteor events for the first time. The mission also demonstrated a virtual mission-control concept, where aircraft tracking, status, and telemetry were all accessible through an internet browser. An INMARSAT datalink from the ARIA aircraft was combined with local-area network architecture on both aircraft to create the first airborne extranet connected with NASA Ames Research Center and other ground-based scientists and observatories for near-real-time flux reporting.

Point of Contact: P. Jenniskens
 (650) 604-3086
 peter@max.arc.nasa.gov

Exploring Evolution Without a Genome

Michael H. New, Andrew Pohorille

In modern organisms, many essential life functions are performed by proteins, which are synthesized using information encoded in a nucleic acid genome. Darwinian evolution proceeds through small, random changes in the genome of an organism. If the proteins produced by an altered genome improve the ability of the organism to survive, then that organism is more likely to reproduce and distribute the altered genome to future generations. Thus, the functioning and evolution of living organisms require both proteins and nucleic acids. It is, however, unlikely that both proteins and nucleic acids arose simultaneously on the early Earth, and immediately became interconnected. How, then, did the earliest living organisms, protocells, perform essential life functions, grow, and evolve?

This study proposes that protocells initially functioned and evolved without nucleic acids and, instead, small proteins, called peptides, performed cellular functions. Since amino acids, the building blocks of peptides, cannot pair precisely as do nucleic acid bases, the transfer of information between generations via the exact replication of peptides is not possible. Thus a new concept of evolution independent of coded information storage—*nongenomic evolution*—is required.

Central to this concept is the emergence of ligases, proto-enzymes that form the peptide bonds that link amino acids in a peptide. Initially, these ligases were very weak, nonspecific catalysts producing peptides of various lengths and sequences. A few of the peptides so generated could have been better catalysts of peptide bond formation than the proto-enzymes that formed them, thereby generating even more peptides and increasing the chances of producing functional ones. Some of these functional peptides were proteases, proto-enzymes that cut peptide bonds. Since proteases cleave unstructured peptides more rapidly than structured ones, and since functional peptides have some degree of ordered structure, proteases would preferentially destroy nonfunctional peptides. Occasionally, the newly

produced peptides would be capable of performing novel functions. If these novel peptides integrated into the protocellular metabolism, they could increase the capabilities of the protocell. Eventually, this process could lead to the emergence (or utilization) of nucleic acids and their coupling with peptides into a genomic system.

To examine the evolutionary potential of a nongenomic system, a simple, computationally tractable model that is capable of capturing the essential biochemical features of the real system was developed. In the simplest implementation of the model, only two catalyzed reactions were considered: the formation (polymerization) and destruction (hydrolysis) of peptide bonds. Thus, a peptide can play a double role: as a substrate for polymerization or hydrolysis or as a catalyst of these chemical reactions. The properties of the products of these reactions are related to the properties of the reactants. To underscore this relationship, the model is called an inherited efficiencies model.

Computer simulations of the inherited efficiencies model were performed, and for many choices of model parameters, the overall catalytic efficiency of a test protocell was observed to increase. Two properties strongly affected the ability of the protocell to evolve: the balance between the probability that a peptide is an efficient protease and the probability that it is an efficient ligase, and the strength of the preference toward the hydrolysis of unstructured peptides. These results are demonstrated in the figures, both of which show the average catalytic efficiency of ligases in a test protocell as the simulations progress for two different realizations of the inherited efficiencies model. The first figure displays the results of lowering the probability that a peptide is an efficient ligase relative to a reference model (solid line). Although in both models the overall catalytic capabilities of the test protocell increase, when the probability of forming efficient ligases is reduced (dashed line), so is the final catalytic capability of the protocell.

A similar effect can be seen in the second figure. In this figure, almost all improvement in the catalytic capabilities of the test protocell is eliminated when the preference for the hydrolysis of unstructured

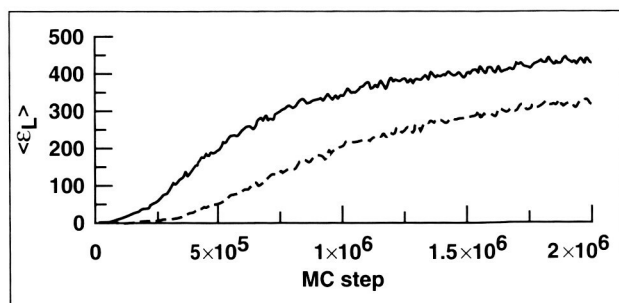


Fig. 1. Average catalytic efficiency of the ligases in the test protocell over the course of a simulation. The solid line represents the results of a reference model, in which the probability of forming an efficient ligase was slightly less than the probability of forming an efficient protease; there was a strong preference for the hydrolysis of unstructured peptides. The dashed line displays the results of a simulation in which the probability of forming an efficient ligase has been lowered.

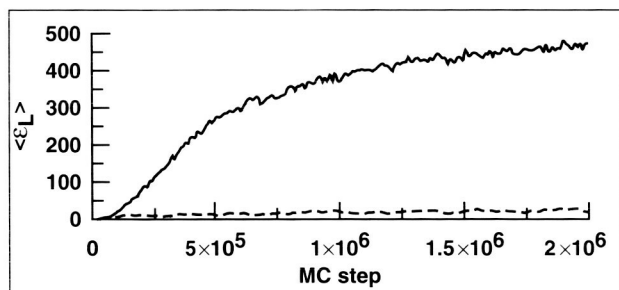


Fig. 2. Average catalytic efficiency of the ligases in the test protocell over the course of a simulation. The solid line displays the same reference model as in figure 1. The dashed line displays the results of a simulation in which the preference for the hydrolysis of unstructured peptides has been reduced slightly.

peptides is reduced slightly (dashed line) relative to the reference model (solid line). When efficient proteases are easy to form, or when there is little preference for the hydrolysis of unstructured peptides, any long and highly efficient peptides will be destroyed before they can greatly affect the population of peptides within the protocell. Therefore, the rate at which the protocell generates new, and possibly efficient, peptides will be slow.

The results presented here demonstrate the possibility of a novel mechanism of early

protocellular evolution. This mechanism does not require the presence of a genome, nor does it rely on any form of sequence complementarity or the exact replication of proteins. It is the preservation of cellular functions and their interrelationships that must be maintained during this early stage of evolution, not the identity of the actors performing those functions.

Point of Contact: M. New
(650) 604-4762
mnew@mail.arc.nasa.gov

Reduced Nitrogen for an Acidic Early Ocean

David P. Summers

This project studies how reduced nitrogen (nitrogen with a low oxidation state) may have been available for the origin of life on the Earth (and potentially on other planets such as Mars). Life today uses nitrogen in a relatively reduced state. Organisms produce that nitrogen biochemically. However, at the time of the origin of life, those biochemical mechanisms were not yet in place. Therefore, there must have been a nonbiological mechanism to produce such nitrogen. Without the availability of reduced nitrogen for the formation of species such as amino and nucleic acids, life could not have started.

One important form of fixed and reduced nitrogen is ammonia. However, current geochemical evidence points to an atmosphere on the early Earth that contained elemental nitrogen (N_2) instead of ammonia. The lighting that would have produced, ultimately, amino acids under a methane/ammonia atmosphere produced only nitrogen monoxide (NO). However, this NO can be converted into nitrite (NO_2^-) and nitrate (NO_3^-) by atmospheric and aqueous processes. Work at Ames has previously shown that one source of ammonia involves the reduction of nitrite to ammonia by the aqueous ferrous iron (iron in the +2 oxidation state; in this case the Fe^{+2} ion), which was common on the early Earth. However, this reaction doesn't form ammonia

at acidic pHs (<7.3). The early Earth is thought to have had a carbon dioxide atmosphere, and since carbon dioxide is acidic, an acidic early ocean is a distinct possibility.

This work has found that a form of ferrous iron, FeS (one form of iron sulfide), will reduce nitrite and nitrate to ammonia under acidic conditions. With regard to nitrite (NO_2^-), figure 1 shows how the concentration of ammonium changes with time when nitrite is added to a suspension of FeS under acidic conditions (pH 6.3). Ammonia is formed at pH 6.3 and, in fact, at all pHs studied. As the pH becomes more acidic, the yield of ammonia (the amount of nitrite that is converted to ammonia) increases from 18% to 53%. This increase is thought to be due to the fact that, under carbon dioxide, less bicarbonate (an ion that is a neutralized form of carbon dioxide) is present in more acidic solutions, and bicarbonate interferes with the reactions. Similarly, it was found that there is a small, but noticeable, decrease in the yield of ammonia when chloride and sulfate ions are added. Presumably these ions tend to block the surface of the FeS particles, preventing the nitrite ion from getting in to react. A phosphate ion has an even bigger effect, cutting the yield by two-thirds.

FeS also reduces nitrate (NO_3^-) under acidic conditions. Yields from nitrate are much lower, typically 7% in a more acid solution (pH <5), and no ammonia is formed at any neutral pHs. Similarly, the reduction of nitrate is much more sensitive to the presence of added species. No ammonia was produced in the presence of chloride, sulfate, or phosphate ions. It appears as if nitrate is much more sensitive to the presence of blocking ions. Perhaps nitrate is more easily blocked from the surface. The reduction of nitrate was observed with Fe^{+2} , but the reaction was never found to be reproducible (different yields were obtained when the reaction was run under what apparently were the same conditions). The lack of reproducibility of nitrate reduction by Fe^{+2} (which also showed a similar effect) might be related to the ease with which the reaction is poisoned.

After reactions, analysis of the surface composition by a scanning electron microscope with a light element detector did not indicate the formation of any iron oxide (see figure 2). However, iron was found dissolved in the solution. Thus, oxidation of the FeS during the reduction of nitrite proceeds by

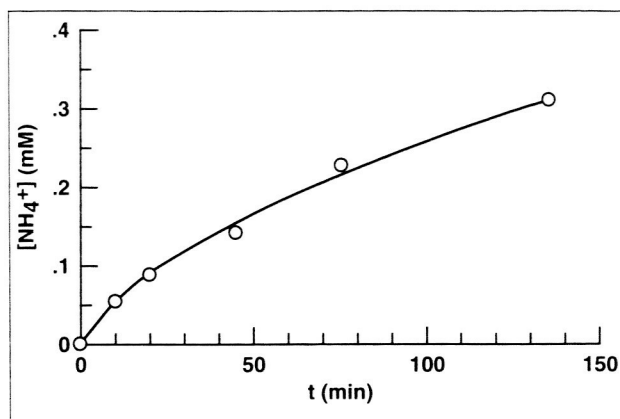


Fig. 1. Ammonium concentration versus time in the reduction of nitrite by FeS under carbon dioxide at pH 6.3.

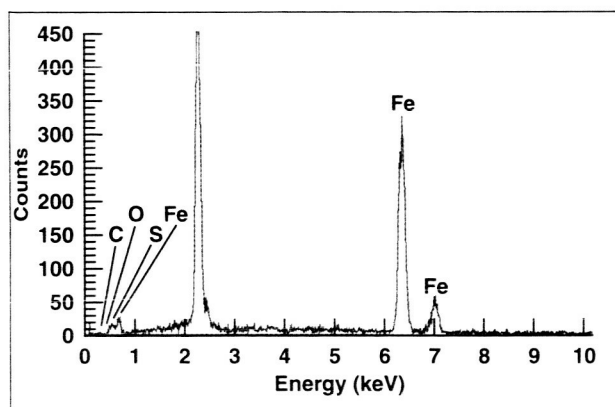


Fig. 2. Surface composition of a particle of FeS after reaction with nitrite.

the formation of FeS_2 at the surface and Fe^{+3} in solution.

Clearly, FeS is a good reductant for the conversion of nitrite and nitrate to ammonia. The reaction occurs under acidic conditions, meaning that such reduction would have been a viable source of ammonia, even if the early oceans were acidic. The reduction of nitrite tolerates the presence of many of the salts that would likely have been present in an early ocean, though some drop in yield is seen. The reduction of nitrate is more sensitive.

Point of Contact: D. Summers
(650) 604-6206
dsummers@mail.arc.nasa.gov

Search for the Upper Temperature Limit of Multicellular Organisms Not Seen by Traditional Environmental Researchers (MONSTERS)

Jonathan Trent

Until fairly recently, it was widely believed that the highest temperature to which life on Earth could possibly adapt was about 60 degrees Centigrade (°C). Above this temperature, it was assumed, essential biomolecules would be destroyed, and life of any kind would, therefore, also be destroyed. In the last two decades, however, this assumption has been proved to be wrong. Many new species of bacteria and archaea have been discovered in a wide range of habitats that have ambient temperatures well above 60 °C. These organisms, known as "thermophiles" (heat lovers), are thriving in hot springs around the world. The hottest of them are living in submarine hot springs that may reach temperatures of 113 °C (hydrostatic pressure prevents boiling). The discovery of these hyperthermophilic microbes has had important scientific and practical consequences. Scientifically, it has expanded our knowledge of the diversity of organisms on Earth, and it has provided important insights into mechanisms for thermostabilization of essential biomolecules. This information is of interest to the NASA Astrobiology program goals of "establishing the limits for life in environments that provide analogues for conditions on other worlds" and "how life evolves on the molecular, organismic, and ecosystem levels."

While many new species of hyperthermophilic bacteria and archaea have been discovered in the last 20 years, few species of thermophilic Eukarya have been discovered. One of the three major branches on the tree of life, Eukarya includes all of the more familiar life forms (figure 1). For Eukarya, the upper temperature limit remains about 60 °C, a level set by some species of fungi found living in self-heating compost piles. Figure 2 shows the current estimates for the temperature range in the universe, the range

in which life as we know it exists, and the ranges to which each of the three major divisions of life have adapted. It is not yet clear, however, if the unimpressive upper temperature limits of Eukarya reflect an inability of these organisms to adapt to high-temperature habitats or the inability of scientists so far to find Eukarya living in these habitats. The scientific objective of this study was to answer the fundamental question: What are the upper temperature limits for macroscopic Eukarya on Earth?

To answer this question, researchers at Ames used a small, robust, submersible video camera and lighting system to hunt for macroscopic Eukarya in the hot springs of Yellowstone National Park. The temperatures of these springs ranged from 31 to 120 °C. It seems likely that there are many undiscovered thermophilic Eukarya lurking in the depths of these hot springs. Like other NASA systems probing distant planets, NASA's video system allows observations in otherwise inaccessible habitats. To date, Eukarya have been observed in springs up to 40 °C, but the search continues for higher temperatures. Ultimately, thermophilic Eukarya will be trapped and brought under scrutiny in the laboratory. It seems likely that new species of extremely thermophilic Eukarya will reveal molecular adaptations to high temperatures that have not been observed in the microbial systems currently being investigated. Such adaptations will expand our view of how complex organisms cope with extreme environments and provide insights into what kinds of organisms may inhabit the hypothetical hydrothermal communities in the subsurface on Mars or the oceans of Europa. For Astrobiology, the search for thermophilic Eukarya will provide guidance for search strategies for life elsewhere in the universe, and their discovery here will raise some intriguing possibilities for finding complex life in hydrothermal systems beyond Earth.

Point of Contact: J. Trent
(650) 604-3686
jtrent@mail.arc.nasa.gov

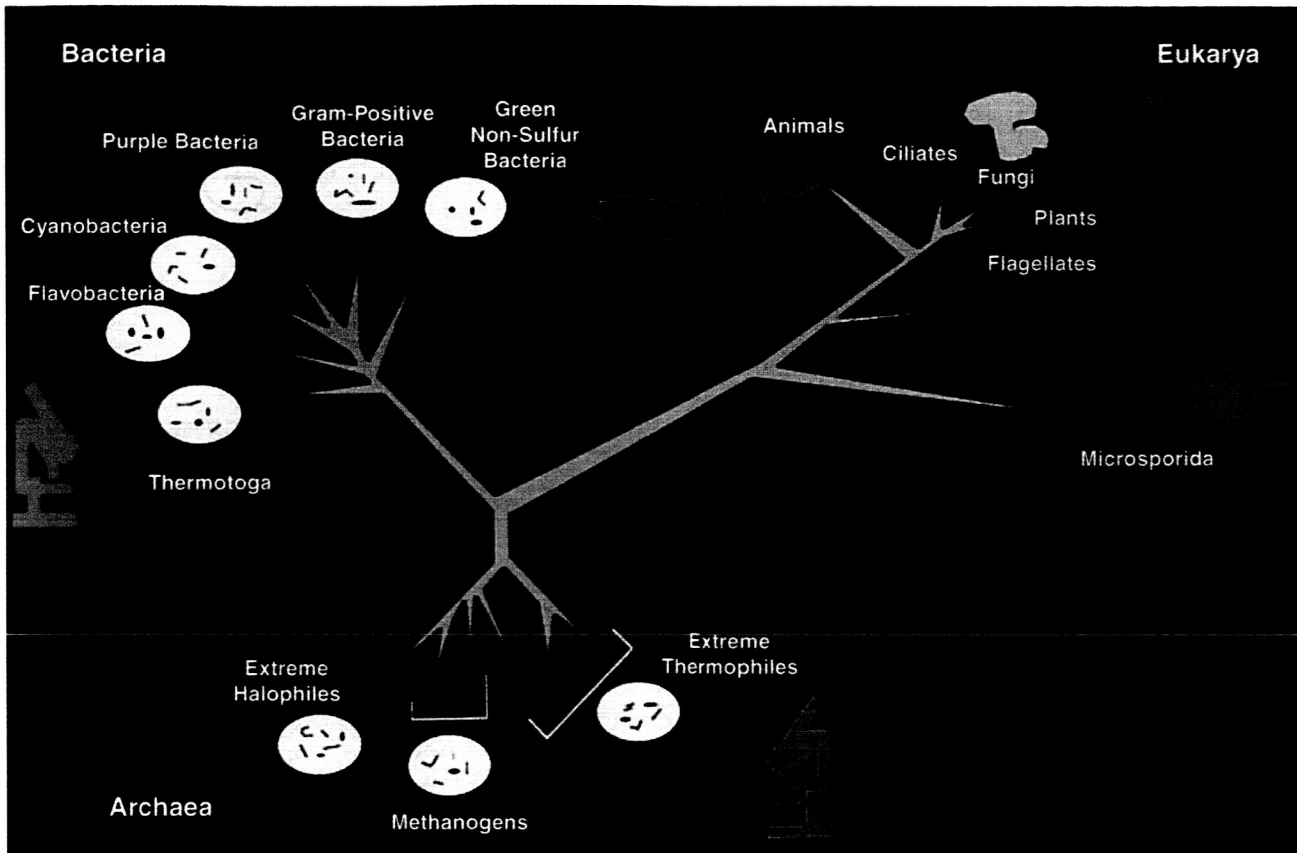


Fig. 1. A stylized representation of the three groups that make up the tree of life, indicating the differences in cell types (background), and showing that bacteria and archaea are microscopic single-celled organisms (balloons), while most Eukarya are macroscopic multicellular organisms. Note: Bacteria and archaea used to be classified together as "prokaryotes" based on structural features of their cells, but recent analysis of critical biomolecules indicates that dividing "prokaryotes" into two separate groups gives a more accurate representation of phylogeny. By both cell structure and molecular criteria, bacteria and archaea are distinct from Eukarya.

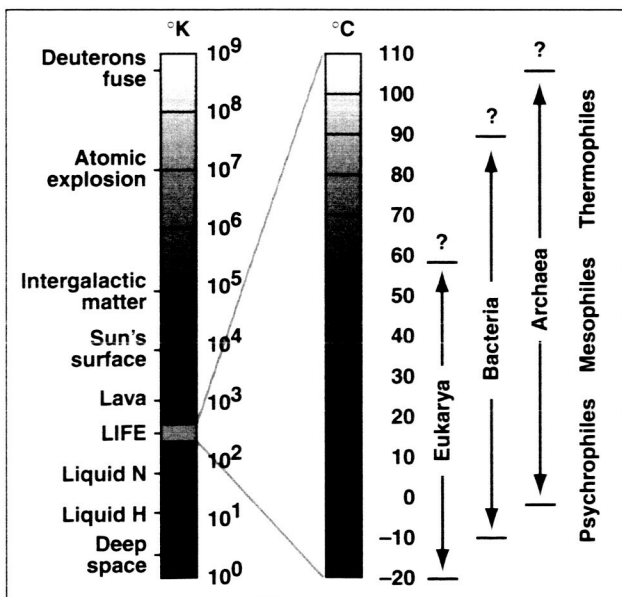


Fig. 2. The temperature range which terrestrial life forms prefer is just a small portion of the complete known temperature range (shown in degrees kelvin on the far left) in the universe. The temperature range in which the three major divisions of terrestrial life forms (eukarya, bacteria, and archaea) have been found living is shown in degrees centigrade on the right in the box. This narrow range is divided into three, based on where organisms have optimal growth; organisms are then categorized according to their preferred range: psychrophiles prefer <15 °C; mesophiles between 15-50 °C; and thermophiles >50 °C. The question marks indicate that we do not yet know the upper limits at which organisms can live.

Prebiotic Peptide Synthesis

Arthur L. Weber

Chemical processes occurring on the primitive Earth about four billion years ago yielded molecules that had the ability to make copies of themselves or replicate. These rudimentary replicating molecules eventually developed into contemporary life that uses both protein and DNA molecules for replication. Since the DNA of contemporary life appears to be too complex to have been chemically made on the primitive Earth, the first replicating systems may have been composed solely of small proteins—called peptides. Peptides are good candidates for the first replicating molecules because they are constructed from very simple building blocks—activated amino acid molecules—which could have been made by chemical processes on the primitive Earth.

To understand how peptides that are necessary for the origin of life could have been synthesized on the primitive Earth four billion years ago, a model chemical process was investigated. This model process has the potential to make peptides from very simple chemical ingredients—formaldehyde, ammonia, and hydrogen sulfide. So far, studies of this process have shown that reaction of formaldehyde, glycolaldehyde (a formaldehyde dimer), and ammonia in the presence of a thiol yields amino acids via activated amino acid thioesters capable of forming peptides. In addition to activated amino acids, the process also generates important biochemical intermediates (such as pyruvate and glyoxylate), and other products that catalyze their own synthesis (such as amino acids, thiols, and imidazoles). The ability of the process to generate catalytic products gives it the potential to be artificially “evolved” to a higher level of chemical activity made possible by the action of its catalytic products.

A peptide catalyst of the model process, polylysine, was confined to a small semipermeable container (a small dialysis unit), suspended in a much larger solution of triose sugar substrate. This reaction system functioned as a catalytic flow reactor. It continually pulled new substrate molecules into the dialysis unit to replace those that had been

catalytically converted to product (pyruvaldehyde), as the product molecules diffused out of the dialysis unit back into the surrounding substrate solution.

In some respects, this chemical flow reactor resembles fermentation by microorganisms that take in and catalytically convert sugars to products (ethyl alcohol or lactic acid) that eventually diffuse out of the cell back into the surrounding medium. The pathway for peptide synthesis, from formaldehyde to activated amino acids, is an attractive model of an early stage in the origin of life. The model generates products in a single-reaction vessel from simple substrates that catalyze reactions involved in their own synthesis.

In contemporary life, metabolic pathways transform organic substrates into useful biomolecules—amino acids, lipids, etc. The energy required to drive metabolism comes from the transfer of high-energy electron pairs in organic substrates to lower energy states, in numerous biochemical end products. Organic substrates are capable of donating the greatest number of high-energy electron pairs, and they have the potential to drive the greatest number of carbon group transformations; the optimal biosynthetic substrate would contain the largest possible number of high-energy electron pairs per carbon atom. Viewed this way, the optimal biosubstrate functions like an optimal battery by generating the largest number of high-energy electrons per unit mass of storage material. The biosynthetic ability of a carbon substrate is determined mainly by the number of high-energy electron pairs per carbon atom. Nevertheless, the optimal biosubstrate would also contain any chemical group that strongly facilitates its conversion to a variety of metabolic intermediates of different size and composition. Since the carbonyl group is the only carbon group that strongly facilitates the synthesis of metabolic intermediates of varying size, the optimal biosubstrate would certainly contain one carbonyl group. Based on the foregoing considerations, this study found sugars to be the optimal biosynthetic substrate of life. They contain the largest number of high-energy electrons per carbon atom, and possess one carbonyl group that facilitates their conversion to a variety of biosynthetic intermediates. This conclusion applies to aqueous life

throughout the universe, because it is based on invariant aqueous carbon chemistry—primarily the universal reduction potentials of carbon groups.

Point of Contact: A. Weber
(650) 604-3226
aweber@mail.arc.nasa.gov

ASTROPHYSICS

The Nearby Stars (NStars) Project

Dana E. Backman

NStars is a project based at Ames to produce a comprehensive Web-accessible database on stars closer than 80 light years to Earth and to promote further observations of those stars by the astronomical community. This effort supports present and future NASA Origins missions such as the Space Infrared Telescope Facility (SIRTF), Stratospheric Observatory for Infrared Astronomy (SOFIA), and the Terrestrial Planet Finder (TPF). For example, TPF is planned as an array of infrared space telescopes capable of detecting Earth-like planets orbiting our nearest neighbor stars. This task is so technically difficult that TPF will not be able to survey all stars within its distance range during a reasonable mission lifetime. NStars is intended to help select a subset of target stars for TPF that have the best chance of harboring an Earth-like planet.

During FY99, a preliminary version of the database was demonstrated to participants in a special Ames workshop on nearby stars. Capabilities to help users examine data over the Web and define subset lists of interesting stars for further investigation were demonstrated. A substantial number of comments from the researchers attending the workshop were collected for further improvement of the database and its user interfaces.

The Nearby Stars workshop was held over three days in June 1999, organized and hosted by the NStars project scientists. The format involved a small number of invited speakers plus poster presentations. The invited talks addressed major topics in astrophysical research on nearby stars. The invited talks,

posters, and notes from discussion sessions will be published as a NASA conference publication in 2000.

NStars project scientist Dana Backman addressed the SIRTF Science Working Group in March 1999 about the NStars project and its support for definition of SIRTF observing programs. Backman also gave a talk at the SOFIA Star Formation workshop in Santa Cruz, California, in July 1999 on possible SOFIA key projects investigating nearby stars.

Five undergraduate students (Avi Mandell, Aaron Burgman, Emma Roberts, Mike Connelley, and Pete Nothstein) worked as research assistants during 1999 on projects connected to NStars. Their projects included: (a) comparison of techniques for determining ages of stars; (b) surveys for variability of solar-type stars using a robotic telescope; and (c) compilation of archived astronomical data to prepare for SIRTF observing programs. Software, database, and Web page development for NStars involved part-time employment of Symtech personnel Sarah West, Eric Vacin, Mick Storm, and Peter Mariani.

Point of Contact: T. Greene
(650) 604-5528
tgreene@mail.arc.nasa.gov

Observations of Extrasolar Planets

Tim Castellano

In the last several years, more than 30 planets have been discovered orbiting other stars. All discoveries to date have been by the radial velocity method whereby extremely small variations in the speed of the star relative to Earth are used to infer the presence of an unseen orbiting companion. More than 20% of the planets discovered orbit their parent stars for periods of less than a week. For these short-period orbits, 10% will be oriented such that the planet will periodically pass in front of the star as seen from Earth. An alternate method of detecting extrasolar planets employing high-precision measurements of the brightness of the stars can confirm the existence of the planet and obtain its mass and radius. This technique was convincingly demonstrated when the

first-ever measurement of the dimming of a star (HD 209458) because of the passage of an orbiting planet occurred in late 1999. This "extrasolar planetary transit" was discovered independently by two groups and widely reported in the news media.

Soon after the announcement, Ames conducted an archival search of the brightness data of the star HD 209458. The data, collected by the European Hipparcos satellite between 1989 and 1992, revealed a photometric dimming consistent with the observed radial-velocity measurements and ground-based transit observations. The long baseline in time between the Hipparcos measurements and the present allowed a precise determination of the orbital period of the planet. These results will be published in the *Astrophysical Journal Letters*. The successful confirmation of an extrasolar planetary transit in the Hipparcos data suggests that it may be possible to discover more extrasolar planets around sun-like stars using data from the Hipparcos satellite or NASA's planned Full Sky Astrometric Explorer (FAME) satellite.

A novel method for obtaining high-precision photometric measurements of bright stars using a spot filter and charge coupled device detectors on ground-based telescopes has been developed. A demonstration of the technique was performed on the sun-like star HD 187123 in the fall of 1999. Although no transit of an extrasolar planet was seen, the required precision was achieved, as shown in figure 1. Additional observations were made of the stars bearing extrasolar planets HD 217107, 51 Pegasi, Upsilon Andromedae, and Tau Bootes, without result.

Point of Contact: T. Castellano
(650) 604-4716
tcastellano@mail.arc.nasa.gov

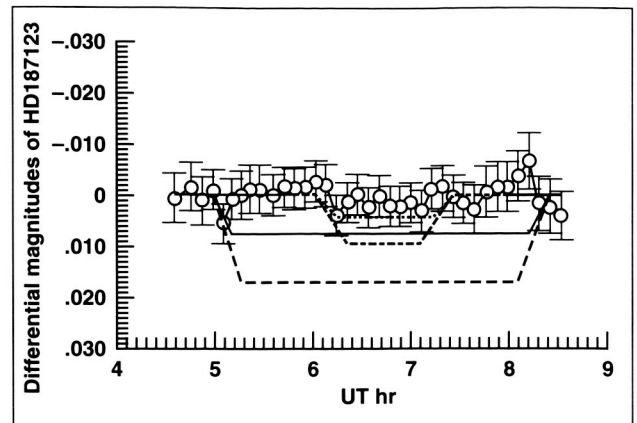


Fig. 1. A sample of data for the star HD 187123 compared to a range of simulated possible transit signals produced by Jupiter-like planets passing in front of a solar-like star.

Composition of Dust Along the Line of Sight Toward the Galactic Center

Jean Chiar, Alexander Tielens, Douglas Whittet

The composition of dust and ice along the line of sight to the galactic center (GC) has been investigated through analysis of midinfrared spectra (2-13 microns) from the Short Wavelength Spectrometer on the Infrared Space Observatory (ISO). The path to the GC samples both diffuse interstellar matter and dense molecular cloud environments by performing a phenomenological comparison with well-studied sightlines known to sample these distinct environments. We have been able to separate spectral absorption features arising in these components toward the GC. Dust absorption features along the lines of sight toward Sagittarius A* (Sgr A*) and the Quintuplet sources (GCS3 and GCS4) are the primary targets in this endeavor. Molecular cloud material is unevenly distributed across the GC. Measurements of absorption features due to abundant solid-state species, such as water/ice and carbon dioxide, reveal that there is more molecular cloud material along the line of sight toward Sgr A* than toward the Quintuplet sources. The Sgr A* sightline has a rich, solid-state infrared

spectrum that also reveals strong evidence for the presence of solid methane, ammonia, and formic acid in the molecular cloud ices.

Hydrocarbon dust in the diffuse interstellar medium along the line of sight to the GC is characterized by absorption features centered at 3.4, 6.8, and 7.3 microns. Ground-based studies have identified the 3.4-micron feature with the C-H stretch vibration mode of aliphatic (chain-like) hydrocarbons. Prevailing theories regarding the production of this robust organic interstellar grain component assume energetic processing of simple interstellar ices (water, carbon monoxide, methane, and ammonia) present in dense molecular clouds. ISO observations have provided the first meaningful observations of the corresponding modes of these hydrocarbons at longer wavelengths, enabling us to rule out some laboratory analogs and, therefore, the production routes of these organics. The integrated strengths of the three observed absorption features suggest that some form

of hydrogenated amorphous carbon (HAC), rather than processed ices, may be their carrier. Figure 1 shows an impressive match to the observed absorption features with a HAC produced in the laboratory by Douglas Furton (Rhode Island College). An absorption feature that is centered at 3.28 microns in the GCS3 spectrum is attributed to the C-H stretch of aromatic (ring-like) hydrocarbons. Since this was the only feature detected, as well as its C-C stretch counterpart (at 6.2 microns), toward the Quintuplet region, but not toward Sgr A*, one of the key questions that now arises is whether aromatic hydrocarbons are a widespread component of the general diffuse interstellar medium, analogous to aliphatic hydrocarbons.

Point of Contact: J. Chiar

(650) 604-0324

chiar@misty.arc.nasa.gov

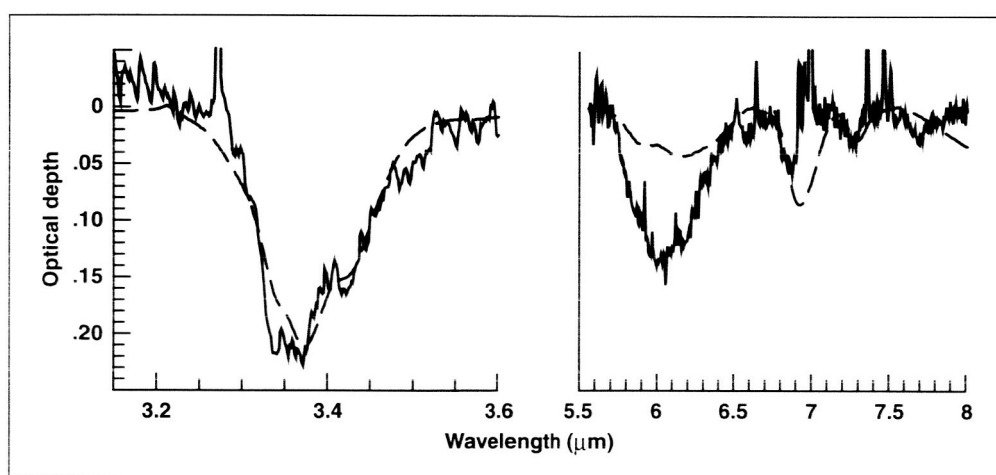


Fig. 1. Midinfrared spectrum of Sagittarius A* (solid line) compared with a laboratory HAC analog from Furton (dashed line). The HAC spectrum is representative of the interstellar absorption features at 3.4, 6.8, and 7.3 microns.

Organic Matter in the Outer Solar System

**Dale P. Cruikshank, Ted L. Roush,
Yvonne J. Pendleton, Cristina Dalle Ore,
Tobias C. Owen, Thomas R. Geballe,
Catherine de Bergh, Bishun N. Khare**

Many solid bodies in the outer solar system are covered with ices of various compositions, including water, carbon dioxide, methane, nitrogen, and other molecules that are solid at the low temperatures that prevail there. These ices have all been detected by remote sensing observations made with telescopes on Earth, or more recently, spacecraft in orbit (notably Galileo at Jupiter). The data also reveal other solid materials that could be minerals or complex carbon-bearing organic molecules. A study in progress using large ground-based telescopes to acquire infrared spectroscopic data, and laboratory results on the optical properties of complex organic matter, seeks to identify the nonicy materials on several satellites of Saturn, Uranus, and Neptune. The work on the satellites of Saturn is in part preparatory to the Cassini spacecraft investigation of the Saturn system, which will begin in 2004 and extend for four years.

One of the Saturn satellites, Iapetus, exhibits a unique exposure of nonice surface material that has very low reflectivity, causing the surface to appear entirely black at certain positions in its orbit around the planet. The infrared spectrum of this black surface of Iapetus has been extended into new wavelength regions in the current study, exploring a part of the spectrum that has not heretofore been seen.

In addition to other characteristics of the spectrum of Iapetus, a very strong absorption band at 3 micrometers wavelength has been revealed clearly for the first time in the new study. Models of the spectrum using organic solid materials produced in realistic simulations in the laboratory strongly indicate that the black matter on half of the surface of Iapetus is indeed organic in nature. The origin and mechanism for emplacement of the black material on the surface of this moon are unknown. The Cassini mission to Saturn will provide data that have a high probability of resolving these issues and further clarifying the apparently unique history of Iapetus.

Other moons of Saturn show similar, though less dramatic, evidence for the presence of macromolecular organic matter mixed with their surface ices, but

the chemistry of the organic material appears to be different. The moons of Uranus, the Neptune moon Triton, and the planet Pluto all have black materials on their surfaces that are presumed to be organic in nature. The origins of this material are likely to be different from that on Iapetus, as well, underscoring the extraordinary variety of compositions and histories that the small bodies of the outer solar system have undergone since their formation. The study in progress at Ames, with colleagues from many other institutions, seeks to explore the nature and origin of organic matter throughout the solar system, and to explicate any astrobiological connections that emerge.

**Point of Contact: D. Cruikshank
(650) 604-4244
dale@ssa1.arc.nasa.gov**

AIRES—The SOFIA Facility Spectrometer

Edwin Erickson, Michael Haas, Sean Colgan

An Ames team was selected by peer review to build AIRES, the airborne infrared echelle spectrometer for SOFIA, the Stratospheric Observatory for Infrared Astronomy. The objective is to develop a facility-class spectrometer for use by the international astronomical community. AIRES will be delivered to the Universities Space Research Association (USRA), NASA's prime contractor for SOFIA, who will operate facility instruments for scientists with approved observing programs.

SOFIA is a unique airborne astronomical observatory currently under development. A Boeing 747 will be equipped to carry a 2.7-meter telescope to be operated at altitudes up to 45,000 feet, allowing infrared astronomical observations that are impossible from Earth. Being developed jointly by NASA and Deutsche Forschungsgemeinschaft für Luft- und Raumfahrt (DLR), the German Aerospace Center, SOFIA will be based at Ames with operations beginning in late 2002.

AIRES will operate at far-infrared wavelengths, approximately 30 to 400 times the wavelengths of visible light. Therefore, it will be ideal for spectral

imaging of gas-phase phenomena in the interstellar medium (ISM), the vast and varied volume of space between the stars. Measurements of far-infrared spectral lines with AIRES will probe the pressure density, luminosity, excitation, mass distribution, chemical composition, heating and cooling rates, and kinematics in the various gaseous components of the ISM. These lines offer invaluable and often unique diagnostics of conditions in such diverse places as star-forming regions, circumstellar shells, the galactic center, starbursts in galaxies, and the nuclei of active galaxies energized by accretion of material on massive black holes. AIRES will provide astronomers with new insights into these and other environments in the ISM. It will also be useful for studies of solar system phenomena such as planetary atmospheres and comets, and a variety of other astronomical problems.

AIRES development began in November 1998. The design incorporates the world's largest monolithic "echelle" grating (see figure 1), an optical

element that will provide good spectral resolution at far-infrared wavelengths. Two-dimensional infrared detector arrays will be used to simultaneously measure spectra in numerous locations on the sky, and to verify the location on the sky where the instrument is acquiring data. During the past year, many significant milestones have been reached, including the following: (a) the optical design has been completed; (b) the echelle grating has been fabricated; (c) the detector data system has been fabricated and tested with the imaging array detector; (d) the baseline project resource requirements have been redefined and the management revised; and (e) an external preliminary design review team, selected by USRA, has approved the project for continued development.

Point of Contact: E. Erickson

(650) 604-5508

erickson@cygnus.arc.nasa.gov



Fig. 1. The ruled echelle grating. Two images of the optical engineer are seen reflected from the facets of the grooves that are at angles of 90 degrees from each other.

Conceptual Study of NGST Science Instruments

Thomas Greene, Kimberly Ennico

The Next-Generation Space Telescope (NGST), the successor of the Hubble Space Telescope, is scheduled for launch in the year 2008. NGST will make unprecedented discoveries in the realms of galaxy formation, cosmology, stellar populations, star formation, and planetary systems. The telescope is currently in the conceptual design phase of development, and Ames has been involved in defining and studying the scientific instrumentation it will need to conduct its observations.

Along with scientists at the University of Arizona (Kimberly Ennico, Jill Bechtold, George Rieke, Marcia Rieke, Jim Burge, Roland Sharlot, and Rodger Thompson), and in partnership with Lockheed Martin (Larry Lesyna and the Advanced Technology Center staff), Ames has led and completed a conceptual study of the entire NGST scientific instrument complement. This team was one of several international teams selected to study NGST science instruments. The Ames-led team conducted trade studies of specific instrument technologies and implementations, and developed a comprehensive integrated science instrument module (ISIM) concept.

The team found that the science drivers of NGST justify observations from visible (0.4 microns) to far-infrared (35 microns, about 50 times longer than visible to the human eye) wavelengths of light. Imaging capability is required throughout this wavelength range, while spectroscopic capability is required at all wavelengths greater than or equal to 1 micron. Several technologies are key to achieving these capabilities within the cost, schedule, and environmental requirements of the NGST mission. Visible and far-infrared detectors could be developed in time for NGST, and several detector cooling options—including pulse tubes and solid H₂ systems—are viable. The team also found that dispersive slit spectrographs are superior to imaging Fourier Transform spectrometers when complete spatial coverage is not required. Dispersive spectroscopy may be best accomplished with conventional slits or micro-shutter arrays instead of micro-mirror arrays because of the large background rejection

(greater than a factor of 1000) required at near-to-far infrared wavelengths.

A complement of seven instrument modules resulted from these scientific and technical considerations by the study team. Two wide-field cameras (each covering about 0.01 square degrees) located directly at the focus of the NGST telescope image visible to near-infrared wavelengths (0.4 to 2.5 microns) in a few broadband filters. A separate visible-light camera covers a smaller field at the maximum resolution of the NGST telescope. The other four modules cover near-to-far infrared wavelengths of light (1 to 34 microns) and are capable of conducting either imaging or dispersive spectroscopic observations with modest fields and good spatial resolution. The capability of providing both imaging and spectroscopy with relatively simple optical designs is enabled by using transmissive dispersion elements (called grisms) for spectroscopy. The conceptual layout of one of these modules is shown in figure 1.

Several technologies must be developed further in order to implement this design concept and to ensure the success of NGST. Increasing the size (number of picture elements) and reducing the noise of infrared detectors will have the greatest scientific

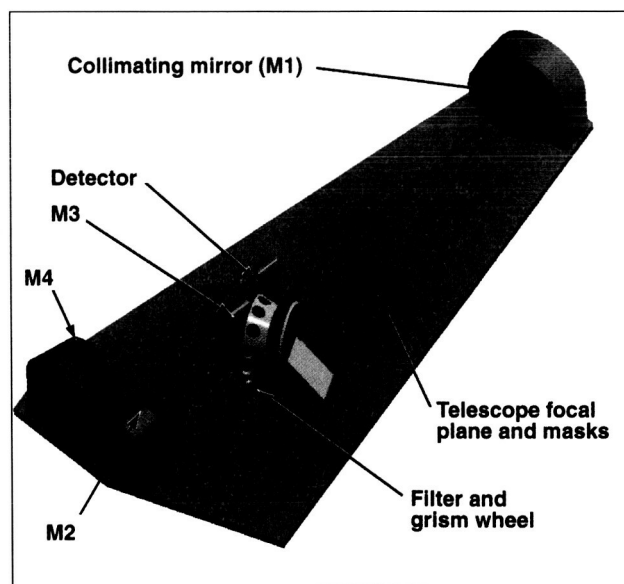


Fig. 1. The optical layout of a single instrument module, which can operate as either a camera or a spectrograph.

impact at relatively modest cost. Ames is already leading this effort for NGST. Reliable closed-cycle cryogenic coolers must also be developed to cool these detectors to temperatures of 4 to 30 kelvin above absolute zero. This task will be eased by the fact that the NGST telescope will always be behind a sun shade and will cool down to approximately 40 kelvin. However, these and all other NGST systems must be very reliable because NGST will be located approximately a million miles from Earth, far beyond the reach of the Space Shuttle, and will not be serviceable by astronauts.

Point of Contact: T. Greene
(650) 604-5520
tgreene@mail.arc.nasa.gov

The SOFIA Telescope Assembly Alignment Simulator

Michael R. Haas, David S. Black, Jeffrey C. Blair, Paul A. Cardinale, Nghia N. Mai, Michael S. Mak, John A. Marmie, Michael J. McIntyre, David D. Squires, Eric Stokely, Ka-cheung Tsui, Bryant C. Yount

The NASA Stratospheric Observatory for Infrared Astronomy (SOFIA) is scheduled to begin routine flight operations from Ames in early 2003. To facilitate installation and integration of science instruments with the observatory, a Telescope Assembly Alignment Simulator (TAAS) is being designed and built. Such a facility is required because of the high flight rate, frequent instrument change-outs, and limited access to the telescope cavity.

The TAAS will be an essential part of the Preflight Integration Facility in the SOFIA Science and Mission Operations Center. Before an instrument flies on SOFIA, it will first be mounted on the TAAS to:

- (a) conform all mechanical and electrical interfaces;
- (b) prepare the instrument for flight and assess its operational readiness;
- (c) optically align the instrument with respect to the telescope; and
- (d) measure the weight and moments of the instrument for use in

balancing the telescope assembly. Because the TAAS has such a fundamental role in the preparation of science instruments for flight, a second unit will be permanently stationed in the Southern Hemisphere for use during deployments.

Figure 1 shows an advanced design for the main mechanical structure of the TAAS. Science instruments mount on the instrument-mounting flange, and their associated electronics are housed in a rack attached to the counterweight plate. In order to provide an accurate mechanical reproduction of the telescope interface, the flange assembly and counterweight plate will be exact duplicates of those on SOFIA. The bearing unit assembly allows the science equipment to be rotated through the full range of elevation angles appropriate for SOFIA. The drive system powers the rotation and maintains a selected elevation angle. Three different infrared light sources have been designed to mount on the rear of the TAAS, for use in instrument alignments. A bore-sight camera assembly will be located in the horizontal tube of the TAAS; it will record focus and bore-sight information and facilitate its transfer to the telescope.

Patch panels that are identical to those on the aircraft will be mounted on the sides of the counterweight rack. Through these panels, the instrument will be connected to all essential services, such as vacuum and gas lines, electrical power, and computer communications, to allow a full operational evaluation of the system. The communications will include connection to the computer simulator of the observatory for protocol evaluation and testing of critical software interfaces.

The TAAS is mounted on load cells so that it can measure the weight and moments of instrument focal-plane packages. These measurements will be used to infer the distribution of counterweights required to balance the SOFIA telescope about all three rotational axes for the given instrument configuration. With this information, the balancing procedure aboard the observatory should take less than an hour.

Preliminary design concepts have been developed for all TAAS subsystems, culminating in a successful preliminary design review in September 1999. Some critical subsystems have been prototyped in the laboratory, including the load cells and a special-purpose controller that modulates the signals from the alignment sources.

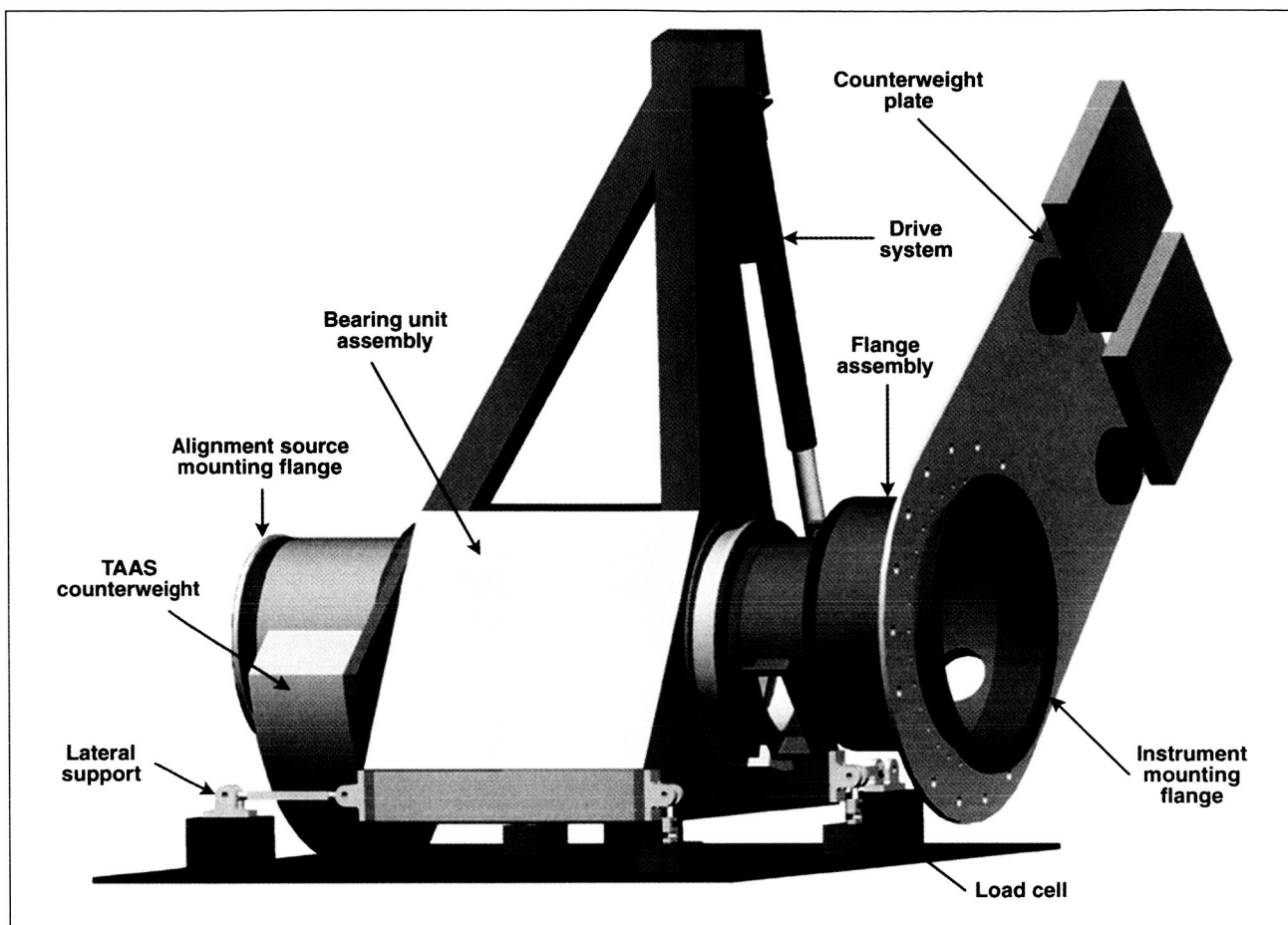


Fig. 1. An advanced design for the Telescope Assembly Alignment Simulator.

Point of Contact: M. Haas
(650) 604-5511
haas@cygnus.arc.nasa.gov

The Center for Star Formation Studies

D. Hollenbach, K. R. Bell, P. Cassen, G. Laughlin

The Center for Star Formation Studies is a consortium of scientists from the Space Science Division at Ames and the Astronomy Departments of the University of California at Berkeley and Santa Cruz. Under the directorship of D. Hollenbach, this consortium conducts a coordinated program of theoretical research on star and planet formation and supports postdoctoral fellows, senior visitors, and students. Consortium members meet regularly at

Ames to exchange ideas and present informal seminars on current research; a week-long workshop on selected aspects of star and planet formation occurs each summer.

In July 1999 the Ames members of the Center together with members of the Stratospheric Observatory for Infrared Astronomy (SOFIA) team held an international workshop entitled "SOFIA and Star Formation." Held on the University of California at Santa Cruz campus, the week-long workshop had approximately 175 attendees. One purpose of this workshop was to bring theoretical and observational astronomers together with the instrumentalists

working on SOFIA instruments in order to stimulate new ideas for SOFIA observational projects related to star formation.

One focus of the 1999 Ames portion of the research work of the Center involved the effect of ultraviolet radiation from young massive stars on the star-forming clouds of gas and dust that typically either surround them or lie close to them. Called "giant molecular clouds" or GMCs, these clouds typically contain 100,000 solar masses of gas and dust and are the dominant sites of star formation in galaxies. The GMCs consist primarily of cold molecular hydrogen gas found in a very clumpy structure bound together by gravity. Thousands of stars are formed in each cloud before it is dispersed in approximately ten million years by the ultraviolet radiation from the most massive stars formed in the GMC. The ultraviolet radiation photoevaporates the clumps in a GMC, destroys the molecules, and heats the gas until the thermal pressure creates a catastrophic expansion of the GMC. These processes disperse the cloud and terminate star formation, and thereby help explain why GMCs do not convert higher fractions of their mass into stars before evaporating into the diffuse interstellar medium. The heating of the gas leads to the emission of characteristic infrared spectra, which can be analyzed to determine the physical and dynamical properties of the evolving clouds.

Another focus of the Ames portion of the Center research in 1999 involved the formation and propagation of spiral density waves in the orbiting disks of gas and dust that circle a newly formed star and ultimately form planets. These spiral density waves affect the evolution of the density and angular momentum in these disks, and, therefore, the planet-forming characteristics of the disks. Analytic analysis and numerical simulations showed that two competing hypotheses explaining the cause of spiral structure in self-gravitating disks had an underlying unity. This finding provided a much better understanding of how mass and angular momentum are transported through protostellar disks. This work could also be generalized to the self-gravitating disks which characterize galaxies, and thereby resolve a long-standing debate in the galactic structure community.

The theoretical models of the Center have been used to interpret observational data from NASA facilities such as the Infrared Telescope Facility

(IRTF), the infrared astronomical satellite (IRAS), the Hubble Space Telescope (HST), and the Infrared Space Observatory (ISO), a European space telescope with NASA collaboration, as well as from numerous ground-based radio and optical telescopes. In addition, they have been used to determine requirements on future missions such as SOFIA and the proposed Space Infrared Telescope Facility (SIRTF).

Point of Contact: D. Hollenbach
(650) 604-4164
hollenbach@ism.arc.nasa.gov

CCD Photometry Tests for Planet Detection

David G. Koch, William J. Borucki, Jon Jenkins, Larry D. Webster, Fred Witteborn

For the first time in history we now know of more planets outside our solar system than in it. All of these extrasolar planets are about the size of Jupiter or larger. The *Kepler Mission* proposes to search for hundreds of Earth-size planets. The concept consists of monitoring 100,000 stars continuously for four years for planetary transits. An Earth-sized transit of a solar-like star produces a relative change in brightness of 8×10^{-3} for a duration of a few to 16 hours, depending on the orbit and inclination of the planet. A technology demonstration showed that a relative precision of better than 2×10^{-5} is achievable when all of the realistic noise sources are incorporated in a full-up end-to-end system. A commercially available back-illuminated charged coupled device (CCD) was used for the tests. The same device can be used in the proposed *Kepler Mission*.

The technology demonstration test facility incorporated the ability to control and measure the following effects on the noise performance of the end-to-end system: varying the CCD operating temperature; changing the focus; varying the photometric aperture; operating over a dynamic range of five stellar magnitudes; working in a crowded star field; reading out the CCD without a shutter; translating the image to several discrete

locations on the CCD; operating with a field star five magnitudes brighter than the brightest target stars; operating with spacecraft jitter up to ten times the anticipated amplitude; and simulating the effects of cosmic rays and stellar variability.

The testbed source incorporates all the characteristics of the real sky that are important to the measurements. It produces the same flux as real 9th to 14th magnitude stars, has the same spectral color as the Sun, has the same star density as the Cygnus region of the Milky Way down to stars as faint as 19th magnitude, has several 4th magnitude stars, and has the ability to produce Earth-size transits for selected stars. The camera simulates all the functions to be performed by the space-borne photometer, namely, fast optics, a flight-type CCD, readout

without a shutter, a high-speed readout of one megapixel per second, and proto-flight data reduction and analysis software. Piezoelectric transducers are used to provide tip-tilt of the camera to reproduce the motion caused by spacecraft pointing jitter.

To fully demonstrate the concept, transits were created during the testing. Representative transits are shown in figure 1 for 9th (left), 12th (middle), and 14th (right) magnitude stars. The transit depth is given in equivalent Earth size, and the error bars are the one-sigma noise for the data.

Point of Contact: D. Koch
(650) 604-6548
dkoch@mail.arc.nasa.gov

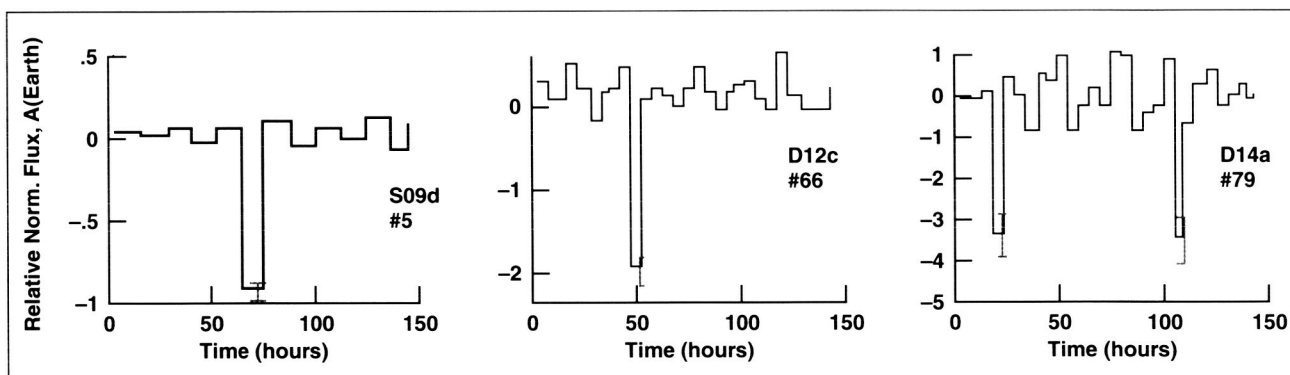


Fig. 1. Simulated transits during the running of the long-duration test with all noise sources.

Minimizing Infrared Stray Light on SOFIA

Allan W. Meyer, Sheldon M. Smith, Chris T. Koerber

The Stratospheric Observatory for Infrared Astronomy (SOFIA) is now being designed and developed, with first light expected in late 2002. Flying at 41,000 feet or higher for 6 hours or more during 120 nights each year, SOFIA will be used for high-resolution observations of celestial objects in the infrared and submillimeter regions, spanning a factor of 1000 in wavelength. In many respects, building SOFIA is a greater challenge than an orbiting observatory would be, but advantages of economy and continuous access make it worthwhile. For work in the infrared, where everything at temperatures above

absolute zero can be a source of background interference, the telescope and associated infrared sensors must be carefully designed and constructed to minimize such background. The far-infrared properties of the telescope surfaces, surrounding cavity walls, and surfaces within focal-plane instruments can be significant contributors to background noise. Infrared radiation from sources well off axis, such as the Earth, moon, or aircraft engines, may be multiply scattered by dust on the optics, the cavity walls, and/or surface facets of a complex telescope structure. This report briefly describes recent efforts at Ames Research Center to evaluate some of the infrared properties of the SOFIA telescope surfaces, and also some of the surface treatments that may be used in focal-plane infrared sensors.

In support of progress in the design and development of the SOFIA telescope, the nonspecular reflectometer (NSR) at Ames was reactivated and upgraded, enabling the NSR to be used to measure infrared reflectance properties for samples of planned SOFIA telescope system structural materials and associated surface treatments. Measurements of specular reflectance and bidirectional reflectance distribution functions (BRDFs) were made at wavelengths from 2.2 to 640 microns, at two angles of incidence, and at scattering angles as far as 85 degrees from normal. Samples of planned telescope system materials included carbon fiber reinforced plastic (CFRP), insulating foams, and Nomex fabric. Samples of candidate surface treatments for focal-plane instruments included two commercial surface treatments and several samples prepared at Ames with black paints and other components. The commercial surface treatments investigated were "Optoblack," a paint-like surface treatment from Labsphere, Inc. (North Sutton, New Hampshire), and "Vel-Black," a carbon fiber applique from Energy Science Laboratories, Inc. (San Diego, California). In general, the samples of telescope structural materials appear to have acceptable far-infrared reflectance and scattering properties, even compared to surface treatments expressly developed to minimize such effects. Figure 1 shows specular reflectance results for the telescope samples, compared to infrared-optimized black paints. The commercial surface treatments appear to have excellent characteristics for use in the far infrared. Samples prepared at Ames performed well when silicon carbide grit was mixed in. These Ames-prepared samples approached but did not equal the performance of more carefully developed infrared black paints such as Ames 24E2 and Ball Infrared Black (BIRB).

These empirical results can now be incorporated into a software model of the SOFIA telescope, which would provide predictions of likely infrared background noise levels. However, it appears already possible to conclude from the results of the work described that the surfaces evaluated will probably not contribute significant infrared stray light.

Point of Contact: A. Meyer
(650) 604-1612
ameyer@mail.arc.nasa.gov

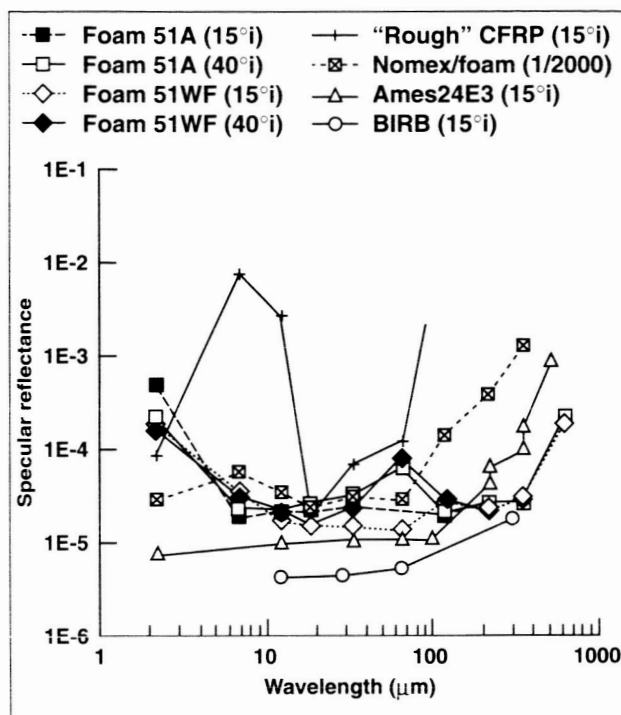


Fig. 1. Surface treatment samples measured by the NASA Ames nonspecular reflectometer, including infrared reflectance spectra for samples of Rohacell white foam, roughened CFRP, Nomex over melamine foam, and, for comparison, previously published data for the black paints Ames 24E2 and BIRB.

Identification of Nitriles in the Interstellar Medium

Yvonne J. Pendleton

The interstellar 4.62-micron band (2165 wavenumber) may be an important contributor to the cyanide (CN) inventory of material available for incorporation into newly forming planetary systems. This band is seen in absorption along lines of sight that pass through icy grains in front of embedded protostars. Therefore, the identification of the interstellar band is important for two reasons: for the astrophysical understanding of organic material in the dense cloud environment, and for the potential relevance to the origin of life, because extraterrestrial

sources of CN groups may have been necessary if the early Earth had a nonreducing environment.

New laboratory results indicate that carbon, nitrogen, oxygen, and hydrogen are active participants in the carrier of the interstellar 4.62-micron band. Results show that ion bombardment of interstellar ice analogs readily produces a band in laboratory residues that is remarkably similar in profile and peak position to that seen in the dense interstellar medium. A shift in band position resulting from deuterium substitution demonstrates that hydrogen is a component of the carrier in the laboratory-produced 4.62-micron band. This finding is in contrast to premature identifications of the isocyanate anion, OCN^- , published recently by other groups. Irradiation of ices through ion bombardment allows testing mixtures that include solid nitrogen, N_2 , a possible source of the available nitrogen in dense cloud ices. If the atmosphere of the early Earth were not overly reducing, as some studies indicate, extraterrestrial sources of CN-bearing molecules may have been necessary for the origin of life, the *in situ* production of prebiotic molecules containing the cyanogen bond would have been difficult. Therefore, the identification of the interstellar 4.62-micron band may include the identification of an extraterrestrial source of CN.

Point of Contact: Y. Pendleton
(650) 604-4391
ypendleton@mail.arc.nasa.gov

Identification of Hydrocarbons in the Diffuse Interstellar Medium

Yvonne J. Pendleton, Louis J. Allamandola

Of relevance to both astrophysics and astrobiology is the nature and evolution of organic material in the interstellar medium (ISM), because the "final" material available for incorporation into planetary systems will determine, in part, the composition of primitive planetesimal bodies, including those capable of delivering organic material to planets

within habitable zones. One interstellar feature of primary relevance, the 3.4-micron hydrocarbon absorption band, has been the focus of a recent investigation into the origin and evolution of the carbonaceous component of the diffuse ISM. The remarkable similarity of the interstellar 3.4-micron band to that seen in the extract of carbonaceous meteorites has further spurred the interest in the origin of the $-\text{CH}_2-$ and $-\text{CH}_3$ groups that result in the interstellar band.

Organic residues created in the laboratory, through the energetic processing of ice mixtures and through electric discharge experiments on hydrocarbon plasmas, have resulted in many claims of spectral matches to the interstellar 3.4-micron band. The laboratory work has been essential in revealing much about the nature of the carrier, and there is consensus that the interstellar band arises from saturated aliphatic hydrocarbons. However, the exact identity of the species responsible for the interstellar band has not yet been revealed. In an effort to further constrain the properties of the true carrier of the interstellar bands, the 3.4-micron laboratory band has been investigated further through the compilation of a database of hydrocarbon candidates from astrophysics laboratories around the world. The laboratory candidates have been compared in detail over the 2- to 9-micron range to the interstellar data from ground-based, airborne, and space observations. Many candidate materials can now be ruled out on the basis of constraints placed upon them from the interstellar data. The interstellar line of sight used in this comparison is toward a star that lies behind the primarily diffuse interstellar medium dust; therefore, contributions from dense molecular cloud ices are insignificant. The Infrared Space Observatory has provided a comprehensive view of this sight line, and it reveals the absence of any strong absorption bands in the 5- to 8-micron portion of the interstellar spectrum. The upper limit of the hydrocarbon bands in the 5- to 8-micron region to those detected at 3.4 microns provides useful constraints upon the laboratory residues. Most of the laboratory residues yield large absorptions in the 5- to 8-micron region, especially those produced through the processing of ices. The most likely candidates remaining are those produced through plasma processing of hydrocarbons. This finding is consistent with recent reports of the 3.4-micron hydrocarbon absorption detected in

the outflow of a carbon star rich in the acetylene (C_2H_2) molecule. Observations of additional interstellar lines of sight through diffuse interstellar medium dust and additional laboratory experiments aimed at the questions posed in this study will be the next steps along the path toward identifying the hydrocarbons in the diffuse ISM. Dust from the diffuse ISM is incorporated into dense molecular clouds, out of which the next generation of stars and planetary systems form. Identification of the diffuse ISM hydrocarbons, which appear so similar to those seen in carbonaceous meteorites, is important to pursue.

Point of Contact: Y. Pendleton
(650) 604-4391
ypendleton@mail.arc.nasa.gov

The SOFIA Water-Vapor Monitor

**Thomas L. Roellig, Robert Cooper, Anna Glukhaya,
Michael Rennick, Brian Shiroyama**

The Stratospheric Observatory for Infrared Astronomy (SOFIA), a 3-meter class telescope mounted in a Boeing 747 aircraft, is being developed for NASA by a consortium consisting of the University Space Research Association, Raytheon E-Systems, and United Airlines. This new facility will be a replacement for the retired Kuiper Airborne Observatory that used to fly out of Moffett Field. As part of this development, NASA Ames Research Center is providing an instrument that will measure the integrated amount of water vapor seen along the telescope line of sight. Since the presence of water vapor strongly affects the astronomical infrared signals detected, such a water-vapor monitor is critical for proper calibration of the observed emission. The design of the water-vapor monitor is now complete, and engineering model units (EMUs) have been constructed for all of the important subassemblies.

The SOFIA water-vapor monitor measures the water-vapor content of the atmosphere integrated along the line of sight at a 40-degree elevation angle by making radiometric measurements of the center and wings of the 183.3-GHz rotational line of water.

These measurements are then converted to the integrated water vapor along the telescope line of sight. The monitor hardware consists of three physically distinct subsystems:

1. The radiometer head assembly contains an antenna that views the sky, a calibrated reference target, a radio-frequency (RF) switch, a mixer, a local oscillator, and an intermediate-frequency (IF) amplifier. All of these components are mounted together and are attached to the inner surface of the aircraft fuselage, so that the antenna can observe the sky through a microwave-transparent window. The radiometer and antenna were ordered from a commercial vendor and modified at Ames to include an internal reference calibrator. Laboratory tests of this subassembly have indicated a signal-to-noise performance over a factor of two better than required.

2. The IF converter box assembly consists of IF filters, IF power splitters, RF amplifiers, RF power meters, analog amplifiers, analog-to-digital (A/D) converters, and an RS-232 serial interface driver. These electronics are mounted in a cabinet just under the radiometer head and are connected to both the radiometer head and the water-vapor monitor CPU. Engineering model units for all the important components in this subassembly, including the entire RF signal chain, the RF detectors, and the low-noise power supplies, have been constructed and tested in the lab. All easily meet their allocated performance requirements.

3. A host CPU converts the radiometer measurements to measured microns of precipitable water and communicates with the rest of the SOFIA mission and communications control system. A nonflight version of this computer has been procured for development and laboratory testing, and the software architecture has been defined. Coding of prototype software has started, and communications between the host CPU and the IF converter box assembly have been demonstrated.

Point of Contact: T. Roellig
(650) 604-6424
troellig@mail.arc.nasa.gov

The Interstellar Production of Biologically Important Organics

Scott A. Sandford, Max P. Bernstein, Jason Dworkin, and Louis J. Allamandola

One of the primary tasks of the Astrochemistry Laboratory at Ames Research Center is to use laboratory simulations to study the chemical processes that occur in dense interstellar clouds. Since new stars are formed in these clouds, their materials may be responsible for the delivery of organics to new habitable planets and may play important roles in the origin of life. These clouds are extremely cold (<50 kelvin), and most of the volatiles in these clouds are condensed onto dust grains as thin ice mantles. These ices are exposed to cosmic rays and ultraviolet (UV) photons that break chemical bonds and result in the production of complex molecules when the ices are warmed (as they would be when incorporated into a star-forming region). Using cryovacuum systems and UV lamps, this study simulates the conditions of these clouds and studies the resulting chemistry. Some of the areas of progress made in 1999 are described below. Figure 1 shows some of the types of molecules that may be formed in the interstellar medium. Laboratory simulations have already confirmed that many of these compounds are made under these conditions.

Polycyclic aromatic hydrocarbons (PAHs) are common in carbonaceous chondrites and interplanetary dust particles (IDPs), are abundant in space, and have been detected in interstellar ices. Results have shown that PAHs that are UV processed in H₂O ices undergo both oxidation and reduction reactions. The resulting species include aromatic ketones, alcohols, ethers, and H_n-PAHs (partially reduced PAHs). In addition, isotopic studies show that this process can enrich PAHs in deuterium, and may explain the D-enrichments seen in aromatics in meteorites. Recent studies on the UV processing of the PAH naphthalene in H₂O ice show that various naphthols and 1,4-naphthaquinone are formed. Since naphthaquinones are common in living systems, and since they perform fundamental roles in biochemistry (they are involved in electron transport), the extraterrestrial delivery of these compounds to the early Earth may be responsible for their presence in biochemistry.

Studies of the complex organics produced when 10 kelvin interstellar ice analogs are UV irradiated have continued. The residues remaining after the ices are warmed have been analyzed by high-performance liquid chromatography (HPLC) and by laser desorption mass spectrometry (in collaboration with Richard Zare and colleagues at Stanford University). This material contains a rich mixture of compounds with mass spectral profiles resembling those found in interplanetary dust particles (IDPs). Surface-tension measurements (made in collaboration with David Deamer of the University of California, Santa Cruz) show that an amphiphilic component is also present. When residues from the present study are dispersed in aqueous media, the organic material self-organizes into 10- to 40-micron-diameter droplets that fluoresce at 300 to 450 nanometers under UV excitation. These droplets have morphologies that are strikingly similar to those produced by extracts of the Murchison meteorite. The amphiphilic nature of these materials is responsible for the molecular self-assembly, and these compounds could have played a role in the formation of early membranous boundary structures required for the first forms of cellular life.

Together, these results suggest a link between organic material photochemically synthesized on the cold grains in dense, interstellar molecular clouds and compounds that may have contributed to the prebiotically important organic inventory of the primitive Earth.

Point of Contact: S. Sandford
(650) 604-6849
ssandford@mail.arc.nasa.gov

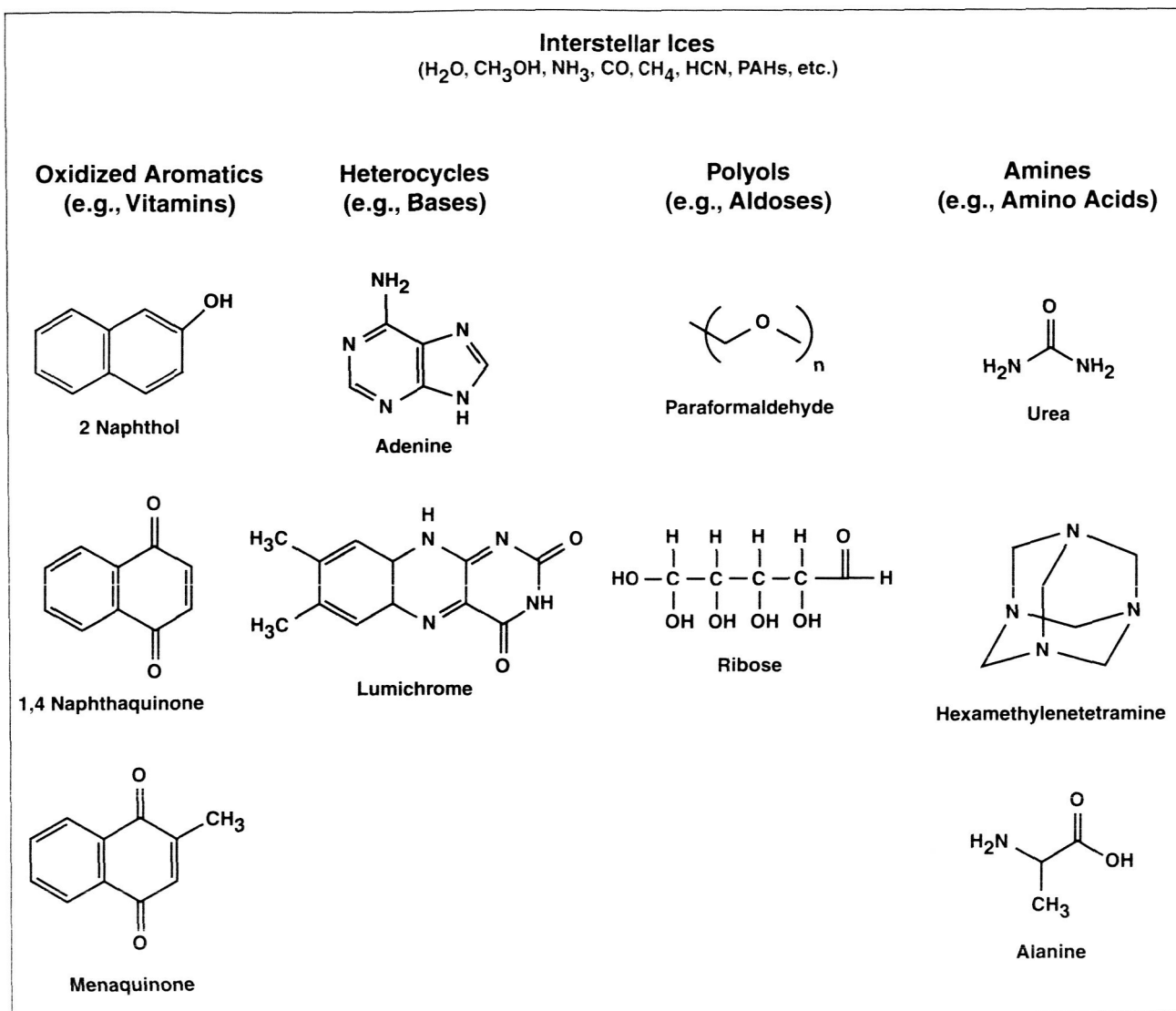


Fig. 1. Some of the classes of compounds that may be produced in low-temperature interstellar ices by UV photolysis. Many of these species have already been identified or tentatively identified in the present interstellar simulations (2-naphthol, 1,4-naphthaquinone, paraformaldehyde, urea, hexamethylenetetramine, and alanine).

Illumination of Young Stellar Disks

K. Robbins Bell

The planets in our solar system formed from a gaseous disk known as the solar nebula. Disk-shaped nebulae thought to be analogous to the solar nebula are now commonly observed around solar mass stars younger than a few million years in nearby regions such as the Taurus-Auriga molecular cloud and the Orion Nebula. Images of these disks are obtained with facilities such as the Hubble Space Telescope; spectra are obtained with the Infrared Astronomical Observatory and various ground-based observatories such as the Keck Telescope on Mauna Kea on the island of Hawaii. Studying these systems provides insight into the development of our own planetary system as well as clues into the likelihood of the evolution of similar life-bearing systems around other stars.

The collapse of a molecular cloud core leads to the formation of a protostellar system composed of a star and a circumstellar disk. Probably 10 to 50% of the final mass of the star is accreted in the initial collapse, which occurs on a dynamical time scale of several tens of thousands of years. Gravitationally induced spiral arms rapidly transport much of the remaining nebular mass inward onto the central protostellar core. At the end of perhaps a hundred thousand years, the system will consist of a central protostar that is slowly contracting and radiating away its excess gravitational energy; it will be surrounded by a disk of remnant material with a mass no greater than one quarter of the mass of the central star. This gaseous disk persists for several million years, during which time it is slowly depleted by accretion onto the central object, dispersal by stellar wind and radiation, and planet formation.

Infrared radiation from these systems can be analyzed to determine the temperature profile of the disk surface. These disks have three major heat sources: heating due to the local release of gravitational energy by material slowly spiraling inward toward the central star; heating due to the capture and reemission of stellar radiation; and heating due

to the capture and reemission of radiation from facing disk surfaces. The latter two components depend sensitively on the shape of the disk. Models that treat each disk annulus as a plane-parallel atmosphere suggest that the distance between midplane and photosphere of the disk at any given radius is largely determined by the opacity of material at the high-density midplane. A schematic profile of a low-mass flux disk is shown in figure 1. The reprocessing of radiation within the system is indicated by arrows.

In the inner regions, the disk is hot enough for dust to be destroyed at the midplane, and the disk thickness increases strongly with radius. In this region, the disk surface is strongly heated by radiation from both the luminous protostar and facing disk surfaces. At larger radii, where the disk is cooler, dust, which provides an additional source of opacity, is condensed throughout the atmosphere of the disk. In this region, the thickness of the disk increases more slowly, and stellar radiation cannot illuminate the surface. The transition between the two regimes occurs at approximately the present-day orbit of the Earth, suggesting that the outer planets formed under cooler conditions than would be expected if the disk were assumed to flare uniformly with radius.

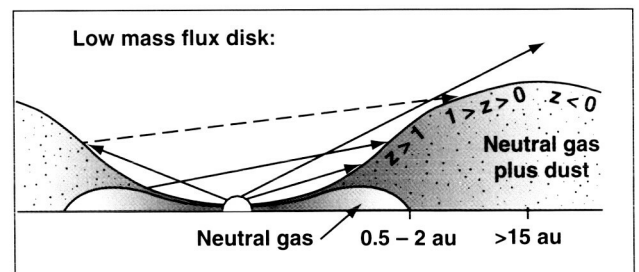


Fig. 1. A schematic profile of a low mass flux disk around a solar mass star. The trend of the disk thickness with radius, $H(r)$, is controlled by the local opacity. Note that $H(r)$ is proportional to r^2 . In the inner regions, the star illuminates the surface of the disk; at larger radii, the disk is in shadow.

Point of Contact: K. Bell
 (650) 604-0788
 bell@cosmic.arc.nasa.gov

Detection of an Extrasolar Planet

William J. Borucki, Douglas Caldwell,
David G. Koch, Larry D. Webster, Jon M. Jenkins,
Zoran Ninkov, Robert Showen

The objective of this research is to determine the occurrence frequency and the properties of extrasolar planets.

Information on the number, size, mass, spacing, and composition of the planets in other planetary systems is needed to refine our models of planetary system formation and the processes that gave rise to their present configurations. The recent discoveries provide tantalizing glimpses of the large variety of planetary systems that exist and make it possible to begin an investigation of the role of the giant planets. To obtain information on the statistical properties of the giant inner planets, and to develop the statistical dependencies of these properties, it is necessary to observe many of these objects for a variety of stellar spectral types and stellar compositions, and for a range of semi-major axes.

A small charged coupled device (CCD) photometer dedicated to the detection of extrasolar planets has been developed at Ames Research Center and put into operation at Mt. Hamilton, California. It simultaneously monitors 6000 stars brighter than 13th magnitude in its 49-square-degree field of view. Observations are conducted all night every clear night of the year. A single field is monitored at a cadence of eight images per hour, for a period of about three months. When the data are folded, in order to discover low-amplitude transits, transit amplitudes of 1% are readily detected. This precision is sufficient to find jovian-size planets orbiting solar-like stars, which have signal amplitudes from 1 to 2%, depending on the inflation of the planet atmosphere and the size of the star.

Recent observations made with the Vulcan photometer produced over 100 variable stars, many not previously known. About 50 of these stars are eclipsing binary stars, several with transit amplitudes of only a few percent. Three stars that showed only primary transits were examined with high-precision spectroscopy. Two were found to be nearly identical stars in binary pairs orbiting at double the photometric period, and the third was found to be a high-mass-ratio single-lined binary star.

The November 22, 1999, transit of a planet orbiting HD209458 was observed and the predicted amplitude and immersion times were confirmed. These observations show that the photometer and the data reduction and analysis algorithms now have the necessary precision to find companions with the expected area ratio for jovian-size planets orbiting solar-like stars.

In early November 1999, two groups announced the discovery of a planet orbiting HD209458 in the Pegasus constellation. The symbols in figure 1 show the extinction-corrected, normalized light curve obtained for HD209458 on November 22, 1999. Because this event was the last opportunity to observe the transit, observations were made, even though the star was setting during the transit. Consequently, only the first portion of the transit is seen. The solid line represents the predictions based on the work of Charbonneau et al. and Castellano et al. (1999). Both the limb-crossing time (25 minutes) and the measured amplitude of the transit (1.6%) are in excellent agreement.

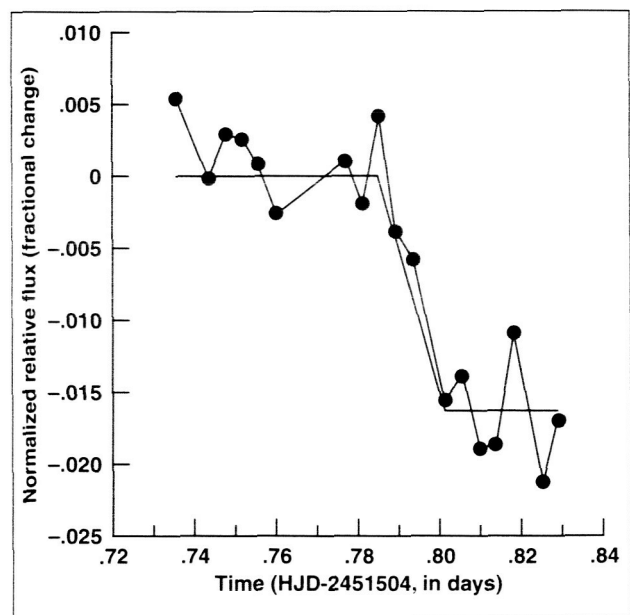


Fig. 1. Comparison of the measured and predicted flux for the November 22, 1999, transit of a planet orbiting HD209458.

Ordinarily, photometry is done as close to the meridian as possible to mitigate the error introduced by scintillation and rapid extinction variations that are associated with high air mass. For this reason, measurements are usually made at an air-mass less than 1.5 and seldom are made at an air mass as large as 2.0. However, to obtain the data on November 22, the measurements were made as the air mass ranged from 1.5 to 4. Figure 2 shows the measured rapid increase in standard deviation (SD) of the fluxes of the seven comparison stars at the time of the measurements. The solid curve shows the expected level of scintillation noise. The agreement between these measurements and the predictions of the scintillation noise demonstrates that the system was operating at a precision limited only by properties of the atmosphere. The observations were terminated at an air mass of 4 because the signal-to-noise ratio had dropped below 2.5 at that point.

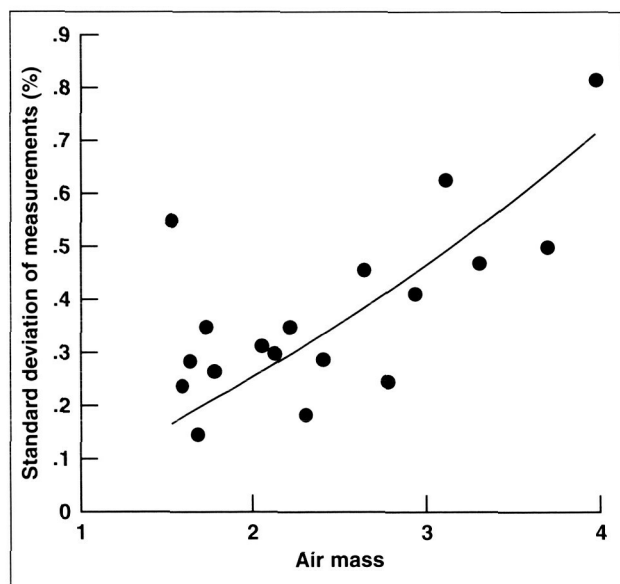


Fig. 2. Comparison of the standard deviation of the fluxes of the comparison stars with the prediction of scintillation noise by Young (1974).

Point of Contact: W. Borucki
 (650) 604-4642
 wborucki@mail.arc.nasa.gov

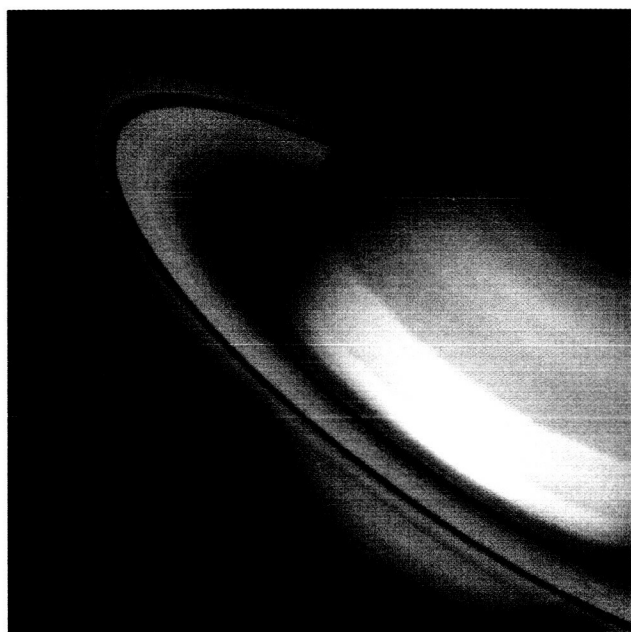
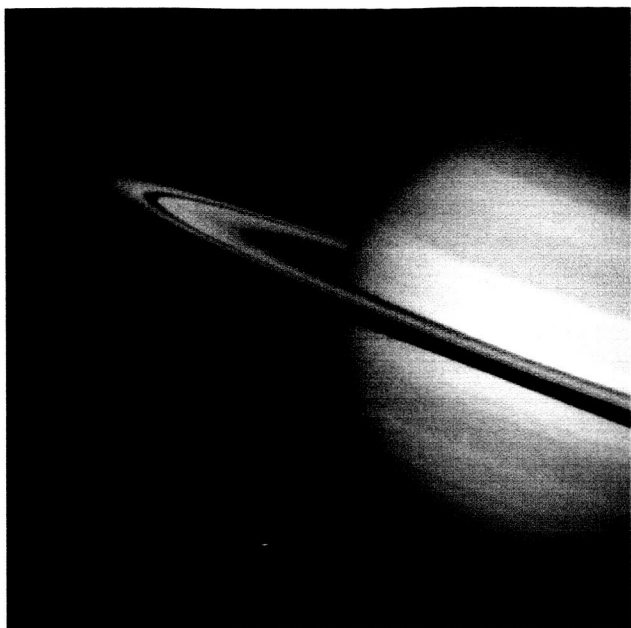
Planetary Rings

J. N. Cuzzi, J. Lissauer, I. Mosqueira, M. Showalter

In addition to the natural curiosity inspired by their unusual appearances, planetary rings present a unique dynamical laboratory for understanding the properties of collisional particle disks that might help us understand the accretion of the planets. Ames maintains the Planetary Data System's Rings Node (<http://ringmaster.arc.nasa.gov/>), which archives and distributes ring data from NASA's spacecraft missions and from Earth-based observatories. The entire archive of images from the Voyager missions to the giant planets is now available on line, with catalogs to help users find the images they need. All the images of Saturn obtained by the Hubble Space Telescope (HST) during 1995, when the rings were seen edge-on to Earth, are available.

An important theoretical advance was taken in the development of a new theory for how narrow, elliptical rings, with nested elliptical orbits, preserve their shape over long periods of time in the face of the tendency of their inner orbits to precess more rapidly than their outer orbits, causing misalignment and collisional disruption. The major previous theory relied exclusively on ring self-gravity to provide the slight counteracting force needed to prevent this precession, but the mass implied was much smaller than that believed to lie in these rings based on other observations. This year, new physics was added to the equations of motion in the form of pressure tensors in dense particle layers that behave like traffic jams. The new physics, in fact, makes it more difficult for self-gravity to maintain the alignment of the nested orbits, and boosts the needed mass density into much better agreement with observations.

New observational results were also obtained from analysis of extensive HST observations of Saturn's rings, taken over the last three years as the ring opening angle increased as seen from the Earth and the Sun (figure 1). Taken in eight different colors (several not observable from Earth), these new observations show for the first time that the ring brightness varies with phase angle but not with ring opening angle. This finding makes it clear that the reflectivity is caused by multiple scattering within a granular regolith on large ring particles, but not between ring particles. This result led to the



realization that the ring particles are less red than previously determined from Voyager observations at a higher phase angle. Furthermore, the HST data provide evidence for increased absorption by water ice in certain parts of the rings relative to others, indicating differences in either the surface coverage or surface grain size on the particles. Also, the optically thinner parts of the rings, where the particles have been known to be darker (its inner or C ring, and the Cassini division lying between the main A and B rings), reveal an unassigned absorption feature in the 850-nanometer spectral range. Tentative evidence for such absorption had been hinted at in earlier observations, but the new observations not only verify its existence, but also clearly show that the absorber is localized to the C ring and the Cassini division. A high-resolution HST image of Saturn's faint G ring that was obtained shows that the radial distribution of large particles is similar to that of tiny dust grains observed by Voyager and Galileo. The HST data are being used now in planning Cassini observations of Saturn that will begin in 2004.

Finally, new analyses of Voyager data show that the bright knots and clumps in the curious F ring of Saturn are transient. A few are seen to appear and then dissipate in a matter of days; these are probably caused by puffs of debris from impacts of meteoroids into the larger ring bodies. However, most clumps persist for a matter of months and are probably caused by the more gentle collisions among the bodies themselves. In addition, smaller ring clumps are periodic, showing the characteristic spacing that would be expected from gravitational interactions with the nearby "shepherding" moon Prometheus. Present dynamical models suggest that this periodic tug between the ring and moons may also give rise to a random component in Prometheus' orbit, as has been observed in recent HST images.

Point of Contact: J. Cuzzi
(650) 604-6343
cuzzi@cosmic.arc.nasa.gov

Fig. 1. Typical HST images of Saturn's rings at two different opening angles. The spatial resolution is adequate to easily resolve color and compositional differences between many different regions of the rings.

Primary Accretion in the Protoplanetary Nebula

J. N. Cuzzi, R. C. Hogan, S. J. Desch, J. M. Paque, A. R. Dobrovolskis

"Primitive" objects in the meteorite record represent the first large bodies to accumulate in the protoplanetary nebula—a vast data set that has had little context for interpretation. The accretion of primitive bodies almost certainly occurred in the presence of gas. Ames' efforts focus on numerical modeling of particle-gas interactions in turbulent flows, and understanding meteorite properties in the light of theoretical models.

A dense layer of particles orbiting in the midplane of a protoplanetary nebula at close to the unperturbed (or Keplerian) orbital rate generates a vertical velocity shear and associated turbulence, which prevents the particles from settling completely to the midplane and becoming gravitationally unstable (that is, from collapsing into planetesimals). However, it was thought possible that damping of the turbulence by the particles themselves might allow the particles to settle into an unstable layer. This year, a study was completed that modeled the evolution of such a layer that incorporated a new model for the damping effects of the particles on their self-generated turbulence. Although turbulence damping does flatten the layer, previously neglected terms were uncovered during the study that disperse the layer even more effectively, with the end result that the layer is even less flattened (more stable) than previously believed.

In prior years, Ames developed a hypothesis to explain the prevalence of millimeter-sized "chondrules" in chondritic meteorites by the mechanism of preferential concentration of aerodynamically selected particles in three-dimensional turbulence. The theory makes specific predictions as to the relative abundance distribution of the concentrated particles. To test the theory, four primitive chondritic meteorites were disaggregated, and the relative

distribution of particles was measured as a function of the product of their radius and density (the important determinants of the aerodynamic stopping time of the particles). Comparisons of the theoretical predictions (open symbols) and meteorite data (filled symbols) are shown in figure 1 for these four meteorites. Relative abundances are plotted as functions of the Stokes number (St), or ratio of particle stopping time to Kolmogorov eddy time. It has been realized for several years that the concentration is maximized for particles with $St = 1$, but not that the distribution function was so narrow.

A multifractal theory was developed to predict the magnitude of turbulent concentration at much higher Reynolds numbers than achievable numerically. The concentration is so large that mass loading (the feedback effect of the particle phase on the gas turbulence itself) must be considered before further modeling efforts can proceed. This theory might be of interest to terrestrial cloud modelers as well.

The prevalence of chondrules in meteorites (up to 80% in some classes) implies that they were pervasive in the nebula. Mineralogical studies imply that the favored melting process occurred on short time scales, over limited spatial scales, and in a relatively cool environment. Lightning, often observed in dry turbulent environments on the Earth, has been studied before and rejected by others. This study combined two new insights: the ability of "triboelectric charging" due to collisions between chemically dissimilar grains (large silicate chondrules and fine metal grains) to produce large positive charges on the silicate chondrules, and the ability of turbulent concentration to concentrate the charged chondrules and build up sufficient voltage to initiate large lightning strokes. Nebula lightning might also have implications for protoplanetary nebula chemistry.

Point of Contact: J. Cuzzi
(650) 604-6343
cuzzi@cosmic.arc.nasa.gov

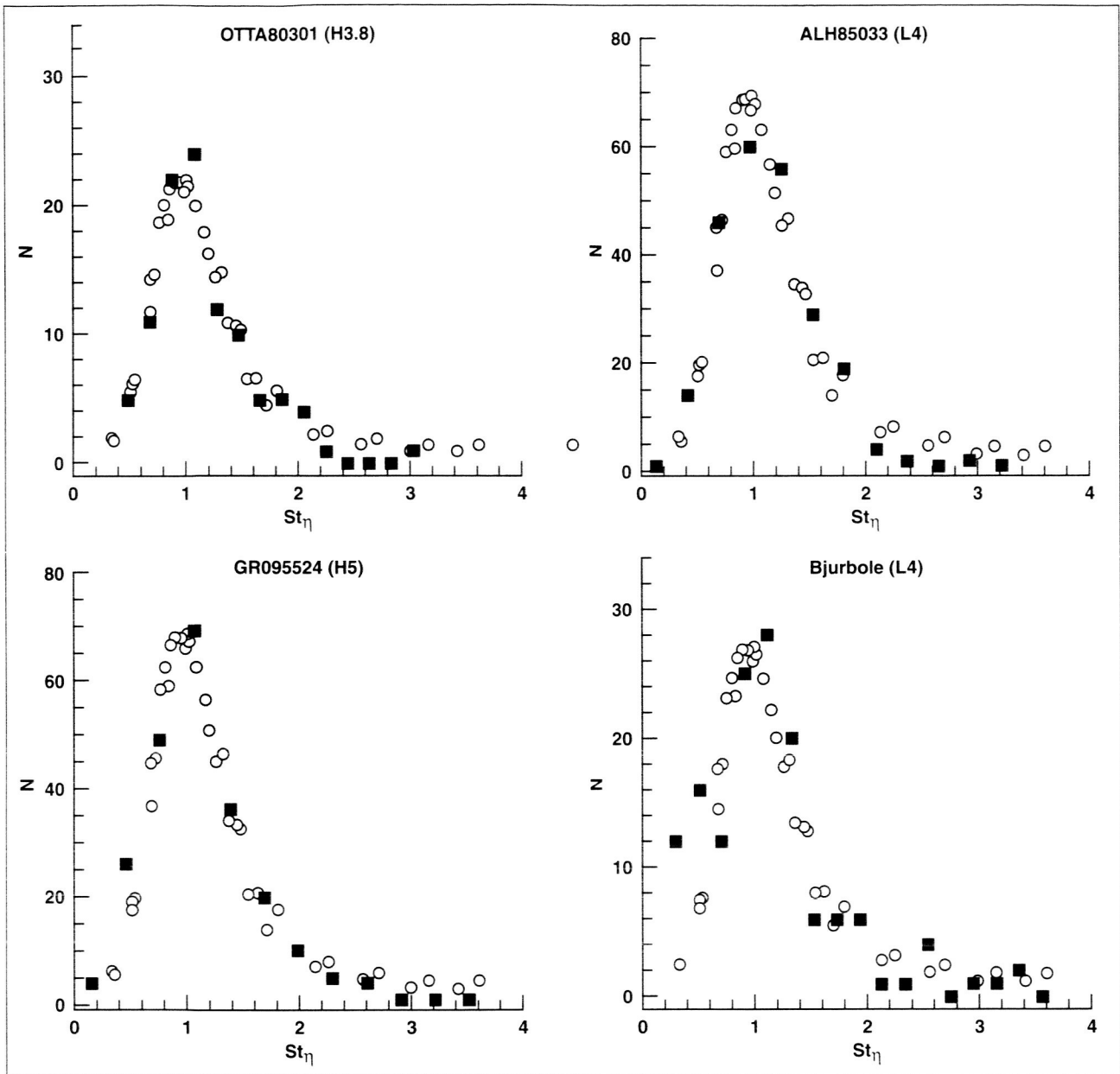


Fig. 1. Predicted (open symbols) and observed (filled symbols) distributions of particle size-density product as functions of their aerodynamic stopping time, as normalized to the Stokes number, St (subscripted here by the Kolmogorov scale), by dividing by the Kolmogorov eddy turnover time. The observed data are from four different primitive meteorite samples. The agreement is quite good. It was also found (not shown here) that using the actual density of each object rather than the average density of all objects noticeably improves the fit, as expected if aerodynamic sorting had operated to determine the chondrule size distribution.

The Calculation of Molecular Opacities

Richard Freedman

The theoretical modeling of the properties and emergent spectra of extra solar giant planets and brown dwarfs requires an accurate and detailed knowledge of the sources of molecular opacity in these objects. In the past few years, many new extra solar planets and brown dwarfs have been discovered using new observational techniques and better, larger telescopes. In order to better understand the physical properties of these new objects and to relate their properties to the properties of other solar systems, astronomers have been using computer-generated models to reproduce their observed properties. This scenario allows a direct comparison between theory and observations and helps to constrain physical properties such as mass, radius, and chemical composition. These objects span the range between the gas giants of our own solar system (Jupiter) and objects almost large enough to burn hydrogen in their interior and thus become stars (brown dwarfs). An accurate theoretical model requires a thorough knowledge of the molecular opacities of a large number of different species, because the temperature in the atmospheres of these objects spans a range from 100 kelvin up to several thousand degrees. Because of the wide range of physical conditions encountered, modelers need molecular opacities up to a range of temperatures that go far beyond the normal range of molecular data from laboratory studies. The purpose of this research is to extend the range of available molecular opacities up to the higher temperatures needed by the modelers.

This extension has been accomplished by using a combination of theoretical techniques combined with available observational data to predict lines of various molecules such as CH₄, VO, and CrH. As an example of what has been accomplished, consider the cases of CH₄, H₂O, and TiO: (methane, water, and titanium oxide). The list of spectral lines was extended for all these species to include lines that will become important at higher temperatures, even though these lines are practically unobservable at room temperatures. Water and methane, in particular, are very important sources of opacity in these objects, and the inclusion of adequate opacity is very

important to properly evaluate their spectra and construct physically realistic models.

In doing this work, the researcher made use of the work of other Ames researchers, especially the work of David Schwenke of the Computational Chemistry Branch. Comparison with observations shows that more work remains to be done to provide opacities that are physically realistic at the highest temperatures, especially for methane and (less so for) water. Even so, the latest models for objects such as the brown dwarf Gl229B (Gliese 229B) show good agreement with the best available observations.

Point of Contact: R. Freedman

(650) 604-0316

freedman@darkstar.arc.nasa.gov

Mars Atmosphere and Climate

**Jeffery L. Hollingsworth, Robert M. Haberle,
James Schaeffer**

Furthering our understanding of the global atmospheric circulation on Mars is the focus of this research at Ames Research Center. As in Earth's atmosphere, Mars' atmospheric circulation exhibits variability over a vast range of spatial and temporal scales. Some of these processes are driven by similar physical processes (for example, Hadley circulation cells; global-scale thermal tidal modes; planetary waves forced via flow over large-scale orographic complexes like Earth's Himalayan plateau; and developing, traveling, and decaying extratropical weather cyclones associated with pole-to-equator thermal contrasts). Other sources of variability arise from distinctly Martian physical mechanisms (for example, condensation (sublimation) during the winter (summer) season of the primary chemical constituent of the atmosphere (predominantly carbon dioxide (CO₂), and regional- and global-scale dust storms). Ultimately, these investigations aspire to improve our knowledge of the dynamics of the planet's present environment and past climates, and from a comparative planetology perspective, to better

understand similar processes that govern the dynamics of the Earth's climate.

In this endeavor, the primary tool used is the Ames Mars General Circulation Model (MGCM). The MGCM is a time-dependent, three-dimensional, numerical model of the hydrodynamic state of the atmosphere as determined by self-consistent algorithms for radiative (for example, solar and infrared absorption, emission and scattering in the planet's tenuous and frequently dust-laden atmosphere) and near-surface processes (for example, a boundary-layer dissipation associated with atmospheric turbulence). In parallel efforts, spacecraft data from the recent Mars Pathfinder mission and the ongoing Mars Global Surveyor (MGS) mission are utilized to validate the climate-simulation results, while at the same time both mechanistic and full-up MGCM simulations can offer a global context for the remotely sensed data.

Investigation of the middle- and high-latitude meteorological environment using a very-high-resolution version of the MGCM has recently been conducted. This research is motivated by Hubble Space Telescope (HST) observations of "comma"-shaped cloud formations and large-scale dust activity in the polar region during early northern spring and summer, and by MGS Mars Observer Camera (MOC) imaging of condensate cloud structures in the polar environment during this season. Modeling at high spatial resolution is necessary in order to illuminate processes important to local and regional dust activity, as well as condensate cloud formation, structure, and evolution within the edge of Mars' seasonal polar caps. It has been found that near-surface and upper-level fronts (that is, narrow zones with enhanced mass density, momentum, and thermal contrasts within individual extratropical cyclones) can form in Mars' intense high-latitude baroclinic zone, and the associated frontal circulations are sufficient to raise dust in high latitudes.

Shown in figure 1 in a spherical projection view are examples of these results for simulations that include recent MGS Mars Observer Laser Altimeter (MOLA) topography in the climate model. Solid contours correspond to potential temperature and arrows correspond to the instantaneous horizontal wind. Near the prime meridian (center longitude of each panel), a clear rarefaction, stretching and deformation of the temperature field, can be seen. This rarefaction is caused by intense local circulations associated with traveling weather systems in middle latitudes (that is, transient baroclinic eddies). These systems are Mars analogs of traveling high- and low-pressure systems that occur in Earth's extratropics associated with instability of the tropospheric jet stream. Note the profound sharpness of the frontal systems, as well as their vast north-south (that is, meridional) scale. The weather fronts appear to be favorably triggered near the high-relief regions of the western hemisphere and subsequently intensify rapidly in the low-relief areas to the east. Based on low-horizontal-resolution modeling of Mars' transient baroclinic waves, the latter geographic region corresponds to a preferred region for cyclone development (that is, a "storm zone").

Both the data analysis and modeling efforts can significantly enhance the assessment of Mars' present climate, and thereby provide a more comprehensive climate database for future missions scheduled during the Mars Surveyor program.

Point of Contact: J. Hollingsworth
(650) 604-6275
jeffh@humbabe.arc.nasa.gov

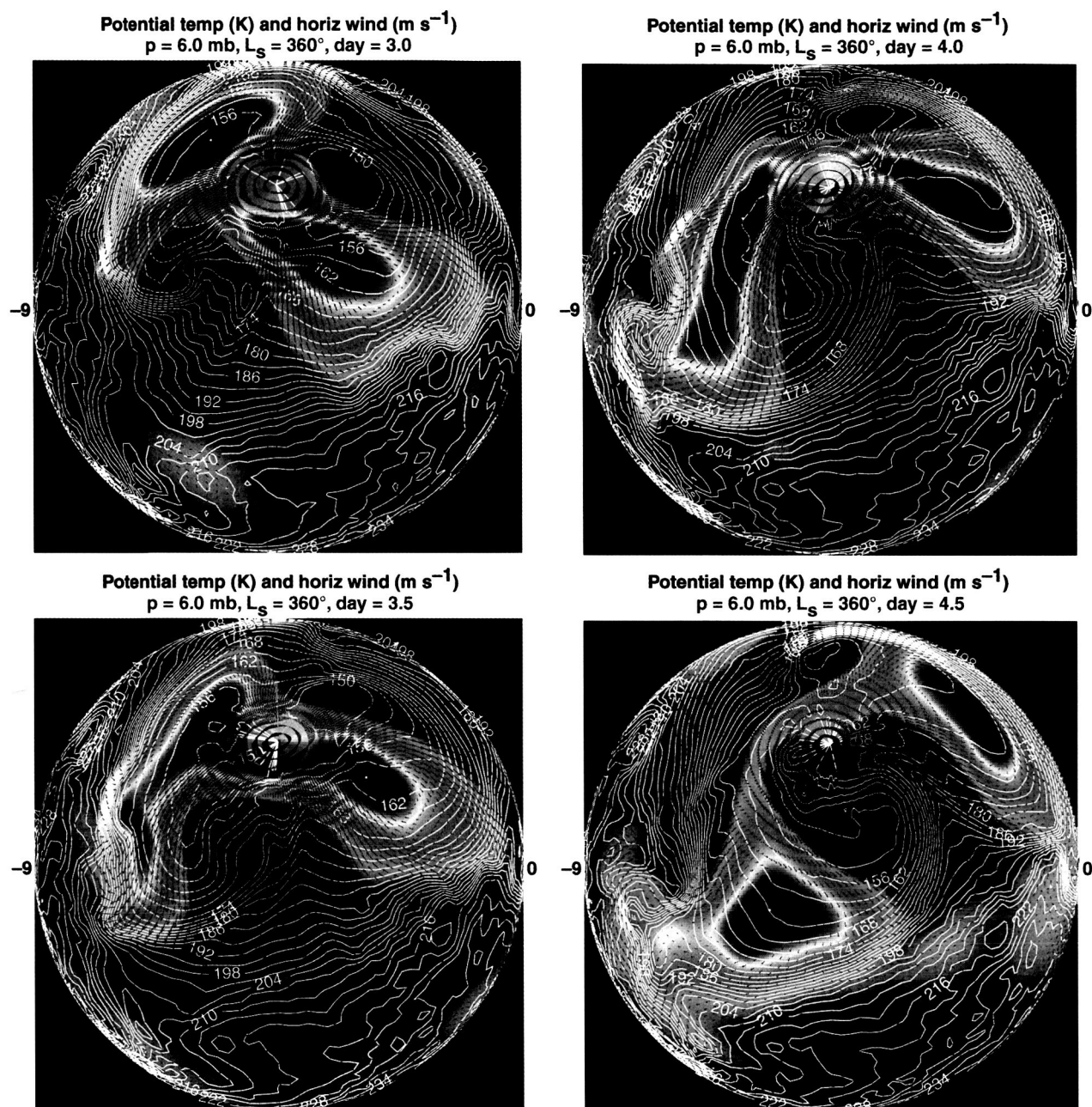


Fig. 1. Potential temperature (kelvin) and horizontal wind (meters per second) at the 6-millibar surface, and instantaneous surface pressure anomaly (color) on (a) day 3.0, (b) day 3.5, (c) day 4.0, and (d) day 4.5, in a MGCM numerical experiment using MGS/MOLA topography. High (anticyclonic) pressure anomaly is red and low (cyclonic) pressure anomaly is black/purple. The temperature contour interval is 3 kelvin.

Stability and Chaos in Planetary Systems

Gregory Laughlin

One of the major news stories of the year was the detection of multiple planets around a Sun-like star (Upsilon Andromedae). Aside from being a "first" detection, this discovery was very interesting because the arrangement of the three planets in the Upsilon Andromedae system is drastically different from the arrangement of our own system. The two outer Upsilon Andromedae planets are considerably more massive than Jupiter, and they have orbits that are much more eccentric than those of the major planets in our system. However, the radial velocity observations used to make the discovery can determine only a lower limit for the planetary masses. Furthermore, there were several different data sets compiled by competing teams of observers. Two important questions thus remained, both of which were addressed by Ames-based theoretical research: (a) What is the true mass of the planets? and (b) Which set of published orbital parameters best represents the true configuration of the system?

Work in FY99 focused extensively on these questions, and examined other aspects of the general

problem of planetary orbital stability. By performing over ten billion years worth of numerical integrations covering many different configurations that are compatible with the observed data from the Upsilon Andromedae system, the Ames research effort significantly narrowed the possible orbital parameters of the system. It was proved that in order for the system to survive over the 2–3-billion-year age of the parent star, the orbital planes of the planets are being viewed close to edge-on. This finding indicates that the companion masses are close to their minimal, nominal values, and are hence true planets. It was also shown that the observations of the team from the University of California at Berkeley were likely to be the most accurate. The Ames effort has now been confirmed by several other teams of researchers.

In a related line of research, large-scale numerical experiments have shown how the effects of the close passage of a binary pair of stars can disrupt an otherwise orderly system of planets (see figure 1). This effect is now understood to be important in the dense open clusters that are the birthplace of many stars. In the FY99 research, the simulations were extended to study the ramifications of this process for the history and future of our own solar system. The research showed that the solar system has existed more or less in isolation since its birth. The nearly perfect circular orbit of Neptune indicates that the Sun has never suffered a significant encounter with

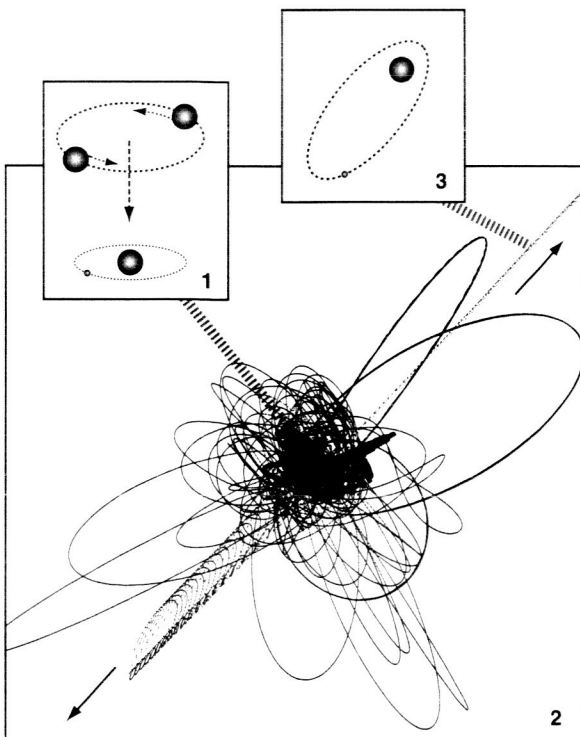


Fig. 1. The computer simulation of figure 1 shows the outcome of a close encounter between a red dwarf binary pair and the Sun-Earth system. The red dwarf pair approaches the Sun from a direction perpendicular to the figure plane. Earth is almost immediately handed off to the smaller star and stays with that star for three long, looping excursions. After slightly more than 1000 years, Earth is recaptured by the Sun, and remains in a solar orbit for the next 6500 years, as the Sun suffers many complicated close encounters with the other stars. After 7500 years, Earth is captured into orbit around the larger red dwarf star, and soon thereafter this star escapes with the Earth in tow. This particular simulation is one of several million performed in order to understand how planetary systems are affected by encounters with the other stars.

another star, suggesting that low-density regions of star formation such as the Taurus Molecular Cloud are the most promising nurseries for planets that eventually develop Earth-like environments. One interesting auxiliary result was the calculation of the odds of Earth being ejected or captured from the solar system by another star prior to the Sun's red giant phase: a scant one part in one hundred thousand!

Point of Contact: G. Laughlin
(650) 604-0125
gpl@acetylene.arc.nasa.gov

Stability of the Upsilon Andromedae Planetary System

Jack J. Lissauer, Eugenio Rivera

This project studies the dynamical properties of planetary systems that are consistent with the observational data on the three-planet system orbiting the nearby main sequence star Upsilon Andromedae. Some configurations consistent with the data originally announced by the discovery team are found to be stable for at least one billion years, whereas in other configurations planets can be ejected into interstellar space in less than 100,000 years. The typical path to instability involves the outer planet exciting the eccentricity of the orbit of the middle planet to such high values that it ventures close to the inner planet. In some stable systems a secular resonance between the outer two planets prevents close approaches between them by aligning their longitudes of periastron (that is, the orientations of their elliptical orbits). In relatively stable systems, test particles (which can be thought of as representing asteroids or Earth-like planets that are too small to have been detected to date) can survive for long periods of time between the inner and middle planets, as well as exterior to the outer planet. No stable orbits between the middle and outer planets were found.

Point of Contact: J. Lissauer
(650) 604-2293
lissauer@ringside.arc.nasa.gov

Hydrodynamic Simulations of Asteroid Impacts on Venus

Kevin Zahnle, Donald G. Korycansky

Impact cratering is strongly affected by the presence of an atmosphere. Our solar system offers four relevant targets: Venus, Titan, Earth, and Mars. Our greatest concern is with the Earth, but Venus is the best subject to study, because its atmosphere is about 100 times thicker than the Earth's, and the surface of Venus is randomly peppered with a thousand craters, most of which are apparently little altered since their creation. Thus Venus provides the ideal testbed for theories of atmospheric permeability to stray cosmic bodies—there is both strong atmospheric interaction and enough craters to provide ground truth to calibrate results.

In this study, numerous two-dimensional (2-D) high-resolution hydrodynamical simulations of asteroids striking the atmosphere of Venus were performed. The computations used ZEUS, a grid-based Eulerian hydro-code designed to model the behavior of gases in astrophysical situations. The numerical experiments address a wide range of impact parameters (velocity, size, and incidence angle), but the focus is on 1-, 2-, and 3-kilometer-diameter asteroids, because asteroids of these sizes are responsible for most of the impact craters on Venus. Asteroids in this size range disintegrate, ablate, and decelerate in the atmosphere, yet retain enough impetus to make large craters when they strike the ground. Smaller impactors usually explode in the atmosphere without cratering the surface.

In the simulations, the impactor is broken up by aerodynamic forces generated by the rapid deceleration of the bolide and the shearing flow that develops around it. This results in a complicated and turbulent flow at high Mach number, featuring a broad range of exponentially growing unstable waves. The simulations are sensitive to small differences (both physical and computational) in the initial conditions of the computation. It is found that the shape, resolution, velocity, or other details of the impact can strongly influence which wavelengths grow first, and how quickly. The evolution of each impact is unique, highly chaotic, and sensitively dependent on details of the initial conditions. Atmospheric permeability

thus becomes somewhat probabilistic. One lumpy object might fail to reach the surface, while another object identical except for different lumps might leave a 10-kilometer crater. The impact process is chaotic at some level; this study concentrated on extracting robust and useful results from the welter of detail that emerges from the numerical hydro-code simulations. The sensitivity of the computational results to seemingly innocuous and inconsequential differences in the model appears to be a real, physically based characteristic of the impact process, generated by the nonlinear development of the hydrodynamical instabilities. The chaotic character of the impact process adds extra scatter, as it were, to the distribution of results that would already exist because of variations in the parameters of incoming impactors, such as shape, impact velocity, etc.

Because most of the larger impactors disintegrate by shedding fragments generated from hydrodynamic instabilities, a simple heuristic model of the mechanical ablation of fragments was developed, based on the growth rates of Rayleigh-Taylor instabilities. In practice, the range of model behavior can be described with one free parameter. This "ablation" model supplements the more traditional "pancake" model that treats the impactor as a single hydrodynamically deforming body. The two models have different and somewhat overlapping realms of validity. The key distinction between large and small impactors is that compression waves can cross the smaller impactor before the hydrodynamic instabilities mature, thus involving the whole object in the hydrodynamics. By contrast, the larger impactor can have its front face stripped off before the trailing hemisphere is noticeably distorted. For Venus, the pancake model generally works better for impactors smaller than 1–2-kilometer diameter, and the ablation model generally works better for impactors larger than 2–3 kilometers.

Point of Contact: K. Zahnle
(650) 604-0840
kzahnle@mail.arc.nasa.gov

SPACE TECHNOLOGY

Onboard Autonomy and Contingent Planning for Rovers

J. L. Bresina, R. Washington, D. E. Smith, K. Golden

The Pathfinder mission demonstrated the potential for robotic Mars exploration, but at the same time indicated the need for increased rover autonomy. The highly ground-intensive control with infrequent communication and high latency limited the effectiveness of the Sojourner rover. This project set out to increase the flexibility and robustness of Mars rovers by developing a contingent sequence language, a contingent planner/scheduler to support generation of such sequences, and an onboard executive system that can execute contingent sequences, manage resources, and perform fault diagnosis.

The first step was the design of a new commanding language, called the Contingent Rover Language (CRL). A key feature of CRL is that it enables the encoding of contingent plans specifying what to do if a failure occurs, as well as what to do if a serendipitous science opportunity arises. For example, a CRL plan could specify the following contingent rover behavior: when a failure occurs, execute a contingency plan to recover from the failure; if none is available, then execute a contingency plan to acquire additional data to support failure diagnosis and recovery by the ground operations team.

The current autonomy architecture (see figure 1) consists of a contingency planner/scheduler, a conditional executive, a resource manager, and a

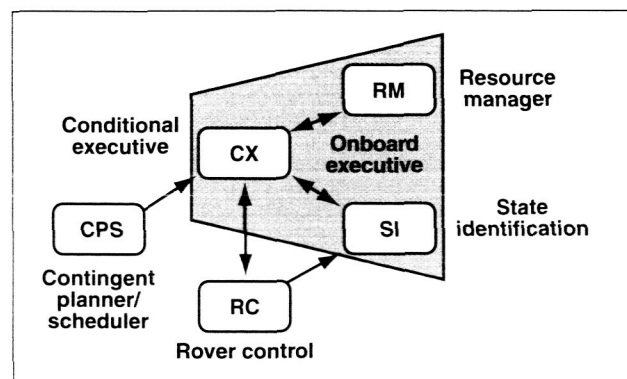


Fig. 1. The rover autonomy architecture.

state-identification component. The contingency planner/scheduler, CPS, is given high-level science goals; it generates a temporally flexible schedule along with contingency plans for possible execution failures and serendipitous science opportunities. The contingent schedule is refined with help from a rover operator and then sent to the onboard conditional executive, CX. These commands are sent to the real-time control system, with results coming back via state monitors into the state identification system, SI, which infers the system state from the monitored information and updates the state for CX. If commands fail or schedule constraints are violated, CX tries to recover using contingency plans.

Resources on rovers are severely limited and at the same time critical for mission success. An onboard, run-time resource manager, RM, receives estimated resource profile information from tasks, monitors current and planned resource usage, and reacts to changes in resource availability. Accounting for the complete state of the rover, diagnosis enables earlier fault detection and produces fewer false

alarms than fault diagnostic systems, like those on Sojourner, which simply trigger on particular anomalies. The State Identification component (SI) eavesdrops on commands sent by CX to the rover. Based on inputs from low-level monitors, the commands executed on the rover, and a declarative model of the rover, SI infers the most likely current state of the rover. SI also provides a layer of abstraction to the executive, allowing plans to be specified in terms of component modes, rather than in terms of low-level sensor values.

The particular characteristics of Mars rover operations require a significant level of rover autonomy and an ability to handle resource constraints and unpredictable events. Ames researchers have designed an architecture for rover autonomy that includes contingency planning on ground and flexible, robust execution of conditional sequences on board. The onboard executive draws on model-based fault diagnosis and dynamic resource management to maximize its science return. In February 1999, some of these rover autonomy technologies were demonstrated as part of a field test in the Mojave Desert with the Marsokhod rover, which appears in the right image of figure 2. During this exercise, both advanced rover technologies and science investigation strategies for planetary surface operations were demonstrated.

Point of Contact: J. Bresina
(650) 604-3365
jbresina@mail.arc.nasa.gov

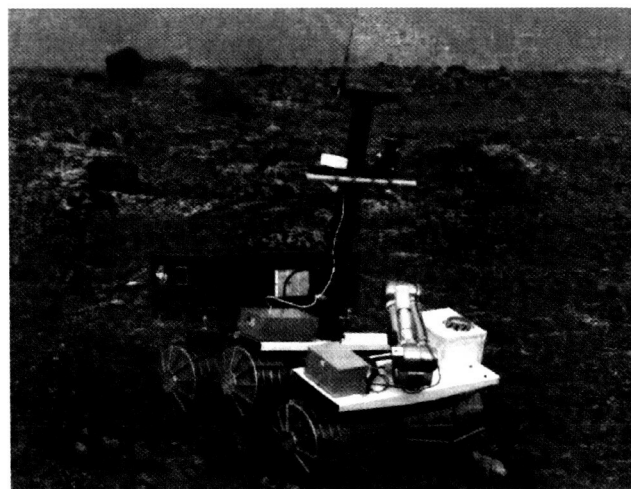
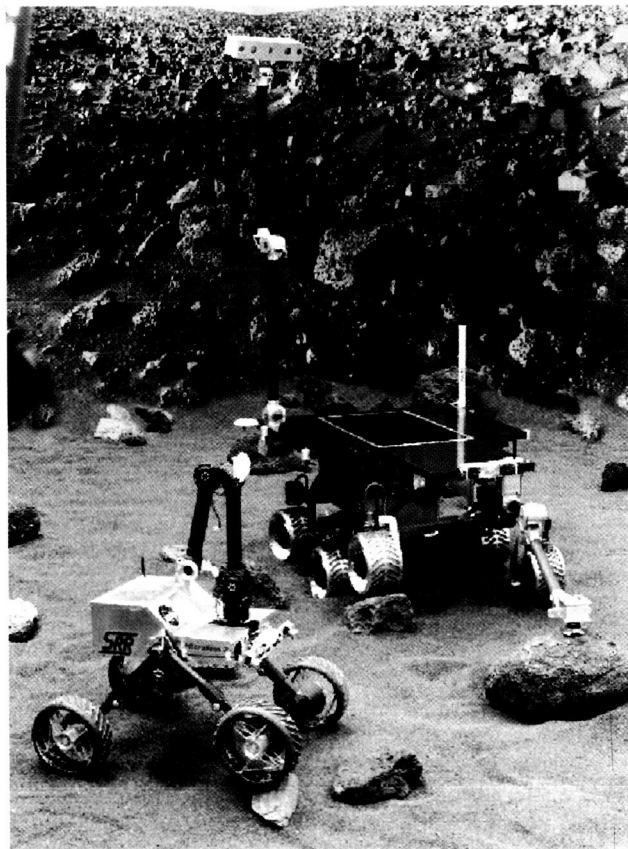


Fig. 2. Example target application platforms.

Automated Hardware Design via Evolutionary Search

Jason D. Lohn, Silvano P. Colombano

The goal of this research is to investigate the application of evolutionary search to the process of automated engineering design. Evolutionary search techniques involve the simulation of Darwinian mechanisms by computer algorithms. In recent years, such techniques have attracted much attention because they are able to tackle a wide variety of difficult problems and frequently produce acceptable solutions. The results obtained are usually functional, often surprising, and typically "messy" because the algorithms are told to concentrate on the overriding objective and not elegance or simplicity.

Automation of engineering design has numerous advantages. First, faster design cycles translate into time and, hence, cost savings. Second, automated design techniques can be made to scale well and hence better deal with increasing amounts of design complexity. Third, design quality can increase because design properties can be specified *a priori*. For example, size and weight specifications of a device, smaller and lighter than the best known design, might be optimized by the automated design technique. The domain of electronic circuit design is an advantageous platform in which to study automated design techniques because it is a rich design space that is well understood, permitting human-created designs to be compared to machine-generated designs.

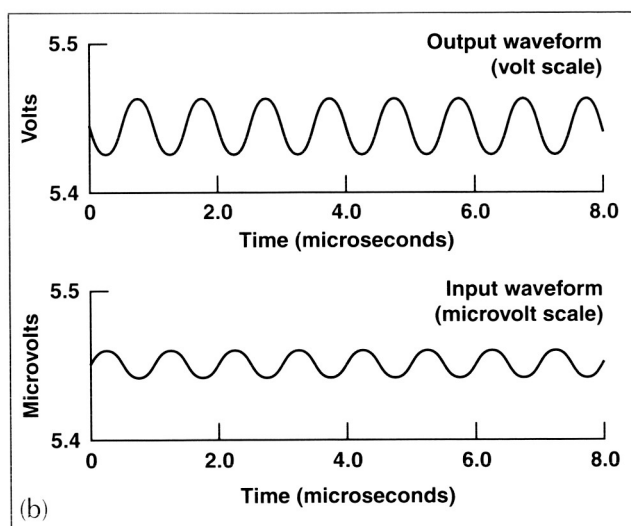
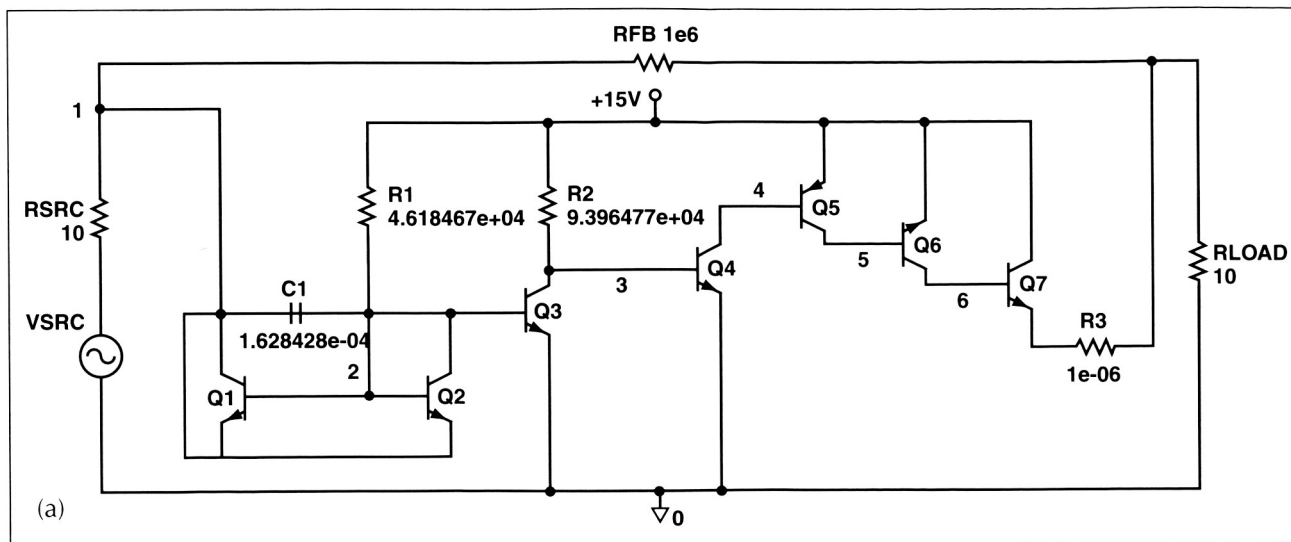
The overall goal of the evolutionary algorithms developed for circuit design was to automatically produce high-level integrated electronic circuit designs whose properties permit physical implementation in silicon. This process entailed designing an effective evolutionary algorithm and solving a difficult multiobjective optimization problem. FY99 saw many accomplishments in this effort.

First, the linear representation of circuits—a circuit-constructing programming language—was shown to be effective when used in an evolutionary algorithm. Transistor-placing language constructs were added since transistors are ubiquitous in analog integrated circuit design. Second, a technique for using coevolutionary search was shown to be better than manually encoded fitness schedules and as effective as using a single fitness function. Third, a 32-node parallel supercomputer, tailored for evolutionary algorithms, was obtained and deployed for automated circuit design. In addition, the parallel algorithm software was significantly enhanced to improve performance.

Coevolutionary search works by pitting two populations against each other, much like two teams of chess players, where all players on team A play all players on team B in a sequence of matches. The coevolution can be set up as a competition, as in the chess game metaphor, as a cooperation, or as a hybrid of the two. For circuit design, a competitive coevolution was used: a population of circuits was pitted against a population of circuit performance requirements. As soon as circuits were able to solve the most difficult performance requirements, those requirements were adjusted so that they would be more difficult to meet.

The system developed has successfully generated circuit designs for analog filters and amplifiers. Figure 1 shows an evolved 85-decibel (dB) amplifier (a circuit that outputs a voltage that is approximately 18,000 times the input voltage), its performance characteristics, and its genetic representation. This design is electrically well behaved, but is not yet implementable because of specifications that were not included in the fitness function.

Point of Contact: J. Lohn/S. Colombano
(650) 604-5138/4380
jlohn@ptolemy.arc.nasa.gov
scolombano@mail.arc.nasa.gov



```

transistor(N, ACTIVE_NODE, NEW_NODE, INPUT_NODE);
transistor(N, BASE, ACTIVE_NODE, PREVIOUS_NODE);
resistor_cast_to_ps(4.618467+04);
capacitor_cast_to_input(1.628423E-04);
transistor(N, NEW_NODE, ACTIVE_NODE, GROUND_NODE);
resistor_cast_to_ps(9.396477E+04);
transistor(N, NEW_NODE, ACTIVE_NODE, GROUND_NODE);
transistor(P, NEW_NODE, ACTIVE_NODE, PS_NODE);
transistor(N, NEW_NODE, ACTIVE_NODE, PS_NODE);

```

(c)

Fig. 1. (a) Circuit schematic of evolved 85-dB amplifier. The design of this circuit—topology, component types, component values—was produced automatically by the parallel evolutionary design algorithm. (b) Small-signal behavior of the evolved amplifier. Traces show the output is inverted and amplified. (c) Genetic representation of the evolved amplifier. The evolved amplifier is designed using a special circuit design programming language devised by the authors.

AutoBayes—Automatic Synthesis of Statistical Data Analysis Programs from Bayesian Networks

Bernd Fischer, Tom Pressburger, Johann Schumann

The goal of the AutoBayes project is to make statistical data analysis easier and more accessible to scientists by automatically synthesizing efficient data-analysis programs from statistical models that are used for the definition of valid information. Data analysis can be defined as any process that extracts more abstract information from mere data. It includes such diverse tasks as general parameter estimation and curve fitting, clustering and classification, data compression, fusion of heterogeneous data sources, change and anomaly detection in time-series or image data, or image segmentation. Although there are many approaches to data analysis, statistical data analysis is the only mathematically rigorous approach. In statistical data analysis, a statistical model is used to define how much information the data originally contains, and thus, how much statistically valid information can ultimately be extracted from the data. This approach is standard in medical sciences such as epidemiology, where the cost of wrong conclusions can be high, and statistical data analysis is now becoming more widespread within the fields relevant to NASA. Unfortunately, the development of statistical data-analysis programs is expensive and time-consuming, and it requires expertise at the intersection of computer science, statistics, and the application.

AutoBayes uses a notation based on Bayesian networks to specify the statistical model. A Bayesian network is essentially a directed, acyclic graph where the nodes represent random variables, that is, the known (that is, data) or unknown (that is, model parameters) objects of interest, and the edges represent conditional dependency or influence. The network thus encodes the full joint probability distribution over the model. This study has extended the standard notation to handle identically distributed random variables (for example, sensor arrays or image pixels) more efficiently.

Figure 1 illustrates a simple but typical data-analysis problem, a so-called "mixture problem": given the data points, which are specified to have been generated from several Gaussian distributions

with unknown mean and variance, summarize each cluster by its most likely mean and variance.

AutoBayes generates programs that apply known statistical techniques, for example, "Expectation Maximization," to solve the given statistical problems. For each technique, the AutoBayes program knows the conditions under which the technique is applicable, the class of data-analysis problems the technique solves, and how the technique is applied to a specific problem. The generation process takes place in the framework of automated theorem proving, guided by the applicability conditions of the statistical techniques. The theorem-proving framework lends some assurance that the generated program is correct.

FY99 saw the completion of the first prototype of the AutoBayes synthesis system. AutoBayes extracts the network from a textual specification language (see figure 2 for a possible model of the mixture problem) and currently generates code in Matlab or C++; other target languages can be added easily. It has been tested on several textbook examples. Researchers expect to apply it to an image-processing problem arising from a project searching for planets around other stars by looking for the dip in brightness as the planet transits in front of the star.

Point of Contact: B. Fischer
(650) 604-2977
fisch@ptolemy.arc.nasa.gov

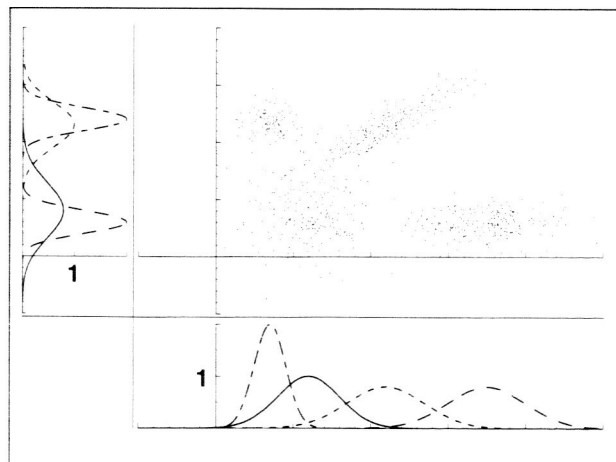


Fig. 1. Example problem—mixture of Gaussians.

```

constant n_points;
constant n_classes;

probability rho[n_classes];

random mu_x[n_classes];
random mu_y[n_classes];
random sigma_x[n_classes];
random sigma_y[n_classes];

random c[n_points];

data x[n_points]
data y[n_points]

c ~ discrete(rho)

x[i] ~ gaussian(mu_x[c[i]], sigma_x[c[i]];
y[i] ~ gaussian(mu_y[c[i]], sigma_y[c[i]];

optimize P(x, y | rho, mu_x, mu_y, sigma_x, sigma_y)
for rho, mu_x, mu_y, sigma_x, sigma_y;

```

Fig. 2. Example specifications.

Propellant Preservation for Mars Missions

Peter Kittel

The last few years have seen extensive technology planning for human missions to Mars. These missions will make extensive use of cryogenic propellants, some of which will be transported to Mars. Additional propellants will be manufactured, liquefied, and stored on Mars. The missions that use these propellants could start early this century. Although many of the plans are still evolving, it has been possible to derive a set of cooler requirements. Recent estimates of these requirements are given here along with a discussion of whether the requirements can be met with existing coolers and coolers currently being developed.

In recent years, a variety of transportation scenarios have been considered. The analysis reported here relates to one of the more promising nonnuclear options. It makes use of solar electric propulsion (SEP). The SEP baseline concept follows:

1. A SEP tug boosts the TMI (trans-Mars injection) stage to a highly elliptical orbit. This phase requires

400 days of propellant storage for the TMI piloted stage and 250 days for the TMI cargo stages.

2. The ascent and descent stages require about 580 days of propellant storage for the piloted mission and 550 days for the cargo case. These stages use oxygen (O₂) and methane (CH₄) for propellants.

3. The TEI (trans-Earth injection) stage requires a storage duration of 1200 days. This stage uses hydrogen (H₂) as the propellant.

4. All tanks are cooled by cryocoolers to eliminate boil off.

5. The tank design is standardized to 3.29-meter-diameter spheres.

Fixing the volume results in the stages having multiple tanks, with many of the tanks full at launch.

A thermal model was used to estimate the cooler requirements. This model could estimate the tank size and mass for MLI (multilayer insulation) insulated tanks with and without coolers. The cooling power and the mass of the power source and radiators were included for ZBO (zero boil-off) storage. In the first case, the volume of the tank was variable. The volume was adjusted until it was large enough to accommodate the boil-off during the mission and still preserve the required propellant until it was needed. In the latter case, the volume was fixed. An optional cooled shield has been included in the model for hydrogen tanks.

The results of the model are presented in Table 1. Pulse tube coolers that can meet these requirements are being developed.

Point of Contact: P. Kittel
(650) 604-4297
pkittel@mail.arc.nasa.gov

Table 1. Minimum set of coolers assuming 250 kelvin heat rejection temperature

Cooler	Cooler Power (Watts)	Temperature (kelvin)
Single stage	11.8	97.2
Two-stage		
First stage	18.6	85
Second-stage	1.2	22.8

Verification and Validation of Autonomous Systems

Charles Pecheur

Ames researchers, in collaboration with Carnegie Mellon University (CMU), are developing technologies for rigorously verifying requirements for software models used in autonomous controllers for space devices. These models describe the different components and failure modes of a complex device such as a spacecraft. They are used by the Livingstone fault recovery system to detect, diagnose, and recover from failures by comparing the observed condition of the spacecraft with the one predicted by the model.

Ames and CMU software scientists have developed a translation program that converts Livingstone models to the input language of SMV (Symbolic Model Verifier), a powerful verification tool based on symbolic model checking. The Livingstone-to-SMV translator is currently being used at Kennedy Space Center by engineers developing a Livingstone controller for the In-Situ Propellant Production (ISPP) system, a chemical processing device that will produce spacecraft fuel using the carbon dioxide found in the atmosphere of Mars. They annotate the Livingstone model with formally expressed requirements, using general logic notation or predefined templates. A requirement can state, for example, that the system can reconfigure itself when a valve is stuck. As shown in figure 1, the model and

requirements are translated and fed into SMV, which searches all possible situations allowed by the model for violations of the requirement. When a violation is found, SMV provides a counter-example scenario that is crucial for diagnosing the source of the problem. These counter-examples are translated back in terms of the original Livingstone model.

The Livingstone-to-SMV translator has also been used for other Livingstone applications, such as the Remote Agent autonomous spacecraft controller, and different robot controllers at CMU. The use of formal verification allows developers of Livingstone applications at Kennedy Space Center and elsewhere to better understand and improve the quality of their Livingstone models. As the number of components grows, the number of possible fault scenarios increases exponentially; for example, the current model of ISPP has about 10^{50} possible states. Although a case-by-case test suite can cover only a tiny fraction of these states, the symbolic technique used in SMV has the power to exhaustively consider the whole space, thus giving very reliable answers. The translator completely shields the Livingstone users from the technicalities of SMV, giving them the benefits of formal verification within their familiar Livingstone environment.

Point of Contact: C. Pecheur
(650) 604-3588
pecheur@ptolemy.arc.nasa.gov

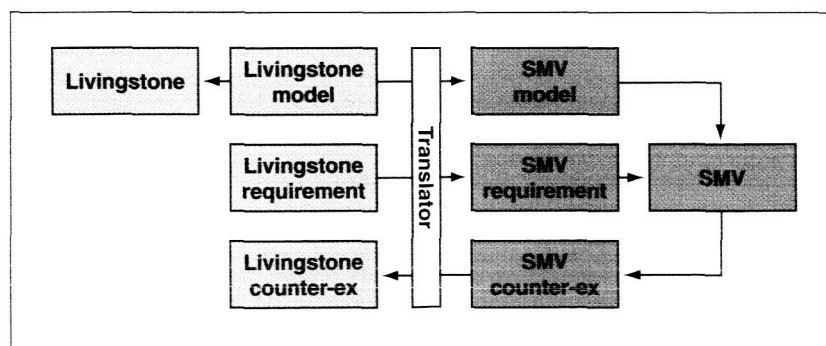


Fig. 1. Sitting in between the Livingstone fault recovery system and the SMV symbolic model checker, the translator developed at Ames and CMU provides Livingstone application developers with the powerful verification capabilities of SMV, while shielding them from the technicalities of the SMV tool.

Knowledge Management for Distributed Scientific Project Teams

Richard Keller

Managing the information generated during the course of a scientific investigation is both a challenging and an essential task for NASA scientists. During an investigation, experimental records must be kept up-to-date and made accessible to all members of a scientific team. After an investigation, a thorough set of records is essential for historical documentation, reproducibility, and overall scientific credibility. These information-management requirements are particularly challenging when scientific work is carried out by large, geographically distributed teams, but even for small, colocated teams or individual scientists, knowledge management has become a time-consuming, frustrating exercise. Ames researchers are developing a suite of sophisticated information-sharing tools to address these complex knowledge-management issues.

The *ScienceOrganizer* tool provides a centralized project information resource that is accessible to an entire scientific team over the World Wide Web. In the field or in the laboratory, *ScienceOrganizer* serves as a collection point for data, notes, records, and images generated by project participants and the scientific instruments they operate. Users can upload project information from local computers directly into the *ScienceOrganizer* repository using Internet protocols. By using a shared Web repository, the distributed team has immediate access to the most recent project information without the coordination overhead of exchanging information via File Transfer Protocol (FTP), e-mail, fax, or other more conventional means. After project completion, the repository serves as a durable archive and preserves the scientific record for future investigators. *ScienceOrganizer* features a "threaded" information repository that maintains explicit links capturing semantic relationships among stored information resources. Threading enables users to locate, track, and organize interrelated pieces of scientific data.

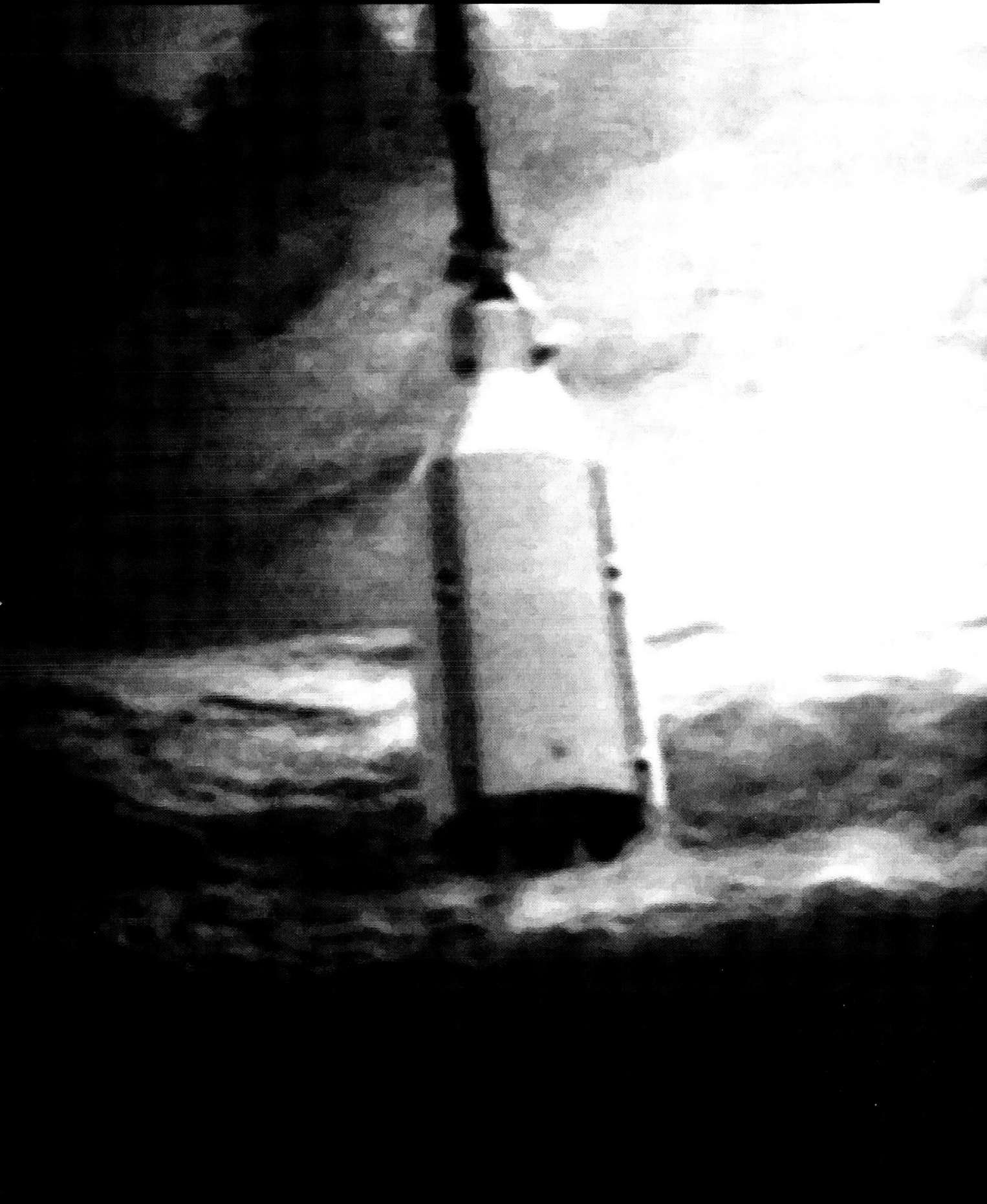
Today, a variety of different media and instruments are used to record scientific data, which may be collected and stored at remote locations. Organizing and accessing this information can be a logistical nightmare involving the coordination and integration of handwritten notes, e-mail, text documents, and a jumble of multiformatted data files and images generated by scientific software and instruments.

ScienceOrganizer enables users to work with this variety of source data by combining key elements present in numerous different types of knowledge-management systems. These elements include *document-sharing systems*, which provide Web interfaces to upload or download documents stored on a central file server; *electronic notebooks*, which attempt to replace paper scientific and engineering recordbooks with semistructured digital notebooks containing bitmap or digital versions of notes, sketches, images, etc.; *laboratory information-management systems* (LIMS), which are database systems that store information about laboratory samples, including the results of analytical chemistry tests performed by hand or by automated means; and *personal information-management systems* (PIMS), which organize and store personal contacts, appointments, notes, e-mail, and records for PC or personal digital assistant (PDA) users.

As an adjunct to *ScienceOrganizer*, initial standalone versions of two auxiliary tools have been developed: the *Shared Image Annotator* and the *Remote Instrument Controller*. The *Shared Image Annotator* allows multiple distributed users to simultaneously annotate and view image files stored in the repository. This tool can be used to facilitate real-time scientific consultations over the Web. The *Remote Instrument Controller* permits users to remotely control and monitor a scientific instrument, and acquire sensor data for direct storage into the *ScienceOrganizer* repository.

Point of Contact: R. Keller
(650) 604-3388
keller@ptolemy.arc.nasa.gov

Human Exploration and Development of Space Enterprise



Overview

The Human Exploration and Development of Space (HEDS) enterprise has as its mission "...to open the space frontier by exploring, using, and enabling the development of space and to expand the human experience into the far reaches of space." Ames supports this mission by conducting important research in space, supporting ground facilities, managing spaceflight projects, and developing advanced technologies to help pave the way for an established human presence in space. Critical research is carried out at varying gravity levels on complex and unique biological, chemical, and physical systems that influence human adaptation. Understanding the role gravity plays on living systems is fundamental to achieving many of the goals of NASA's Astrobiology program.

Procedures and technologies to prevent or mitigate the debilitating effects of reduced gravity and the psychological stresses of long-term confinement along with regular and emergency medical care are fundamental prerequisites for future planetary exploration. Providing opportunities for research that promise to benefit life on Earth, whether through knowledge, new technologies, or the excitement that discovery brings, is also vital to Ames' HEDS activities. NASA's overall vision to "boldly expand

A remote underwater camera photographed a NASA-Ames designed probe entering a hot spring at Yellowstone National Park. The probe was the first of its kind to explore the super-heated geothermal springs in Yellowstone Park and was designed to search for multicellular organisms not seen by traditional environmental researchers (MONSTERS). The so-called MONSTER camera was used to explore many hot springs in Yellowstone Park to depths as great as 20 meters and temperatures as high as 120 °C. The search for MONSTERS will continue with more elaborate robotic systems that can cope with extreme environments.

frontiers in air and space, to inspire and serve America, and to benefit the quality of life on Earth" is achieved at Ames in its support of the following HEDS goals:

- Expand the space frontier
- Expand scientific knowledge
- Enable and establish a permanent and productive human presence in Earth orbit
- Share the experience and discovery of human spaceflight

The articles in this section are presented under five subsections, reflecting each of the HEDS goals presented above and also including the goals of the Astrobiology program. They are astronaut health, fundamental science, improving space travel, technology transfer, and astrobiology support. Several directorates within Ames support the HEDS enterprise and the Astrobiology program. In a similar cross-over manner, many of the efforts described herein address more than one of the stated topics.

One of the earliest alerts to the adverse effects of spaceflight on animals was bone weakening. Since then, numerous studies have been carried out to determine the source, magnitude, time course, and particular regions most affected by unloading. In FY99, researchers at Ames conducted a ground study using a standard animal model to determine if the metatarsal bone of the foot—subject to stress fractures in runners—is as vulnerable to demineralization as the calcaneus bone of the heel. Because previous space research has indicated that bone loss differs throughout the skeleton, and even regionally within a bone, this work continues to aid in the development of countermeasures designed to maintain bone mass in targeted areas.

Research at Ames continues to work toward the improvement of space travel, particularly in developing equipment to operate safely and effectively within the confined, yet unrestrained, environment of microgravity. The design, development, and testing of advanced technologies remains a high priority. Biotelemetry, the capability needed to remotely monitor health and behavior in small mammals and humans in space without impacting either parameter, has been a focal point for technology development for the past few years. In FY98, an implantable pill-shaped biotelemetry that could measure pressure and temperature was developed and tested. This year marked the addition of a pH monitoring capability

to the system, which will greatly enhance its utility for spaceflight research and Earth-based health care.

The assurance of a safe, habitable, environment—one that protects from extreme physical parameters while ensuring a constant source of food, air, and water—is mandatory as we extend human exploration beyond Earth orbit. Because safety of the crew is foremost, technology dedicated to ensuring optimum performance in hazardous or stressful conditions is a priority. Collaborating with Johnson Space Center (JSC), Ames has adapted a Physiological Signal Conditioner that processes biopotential signals such as EEG and ECG to meet the need for human response measurement capabilities.

Safety goes hand-in-hand with habitability. Ames continued its ongoing efforts to develop life-support capabilities for long-duration travel and habitation on other planets. An activated carbon regeneration system to produce nitrogen and carbon dioxide from inedible biomass and a prototype vapor phase ammonia removal process have been demonstrated. These systems take us one step closer to realizing an efficient regenerating life-support environment in space.

It is essential that Ames develop both the engineering technologies that enable such missions and the biomedical technologies to ensure human health, safety, and productivity in an extremely harsh environment. *Habitation*—the need for a safe and efficient environment for the crew; *biomedical countermeasures*—technologies and procedures that maintain the crews' health and performance during and following spaceflight; and *medical health care delivery*—routine and emergency treatment of the crew throughout their mission are the chief drivers behind each HEDS activity supported at Ames.

ASTRONAUT HEALTH

The Effect of Unloading on the Metatarsal Bone of the Rat

Sara B. Arnaud, R. E. Grindeland

The bones of the feet are likely to lose mineral during spaceflight because they are not functioning to support body weight in space. Although loss of bone from the heel bone (calcaneus) during spaceflight is well documented, loss of mineral from other bones in the feet of astronauts has not been quantified. A possibly vulnerable candidate is the metatarsal, which, as a weight-bearing bone in runners, is vulnerable to stress fractures.

To explore the potential for bones of the feet to lose mineral, a model of a metatarsal in mature rats exposed to a spaceflight was used. The experiment was designed to analyze the third metatarsal, depicted in the first figure, at the start and after one, four, and eight weeks of unloading of the hindlimbs by tail suspension. In this model, the hindpaws are raised about one centimeter off the floor of the cage. At the end of the experiment, the animals were weighed. The third metatarsal from the right foot of each group of rats was removed, dried, and ashed at 600 degrees Centigrade (°C) to determine the mineral content. The soleus muscle, which regularly atrophies in this model, was also removed and weighed.

Body weights decreased about 10% during the first week of the experiment and remained stable thereafter. The body weights in the suspended animals remained lower than in the controls. The soleus muscle, illustrated in the first figure, gradually decreased after one week of unloading to 72% of control, and after 8 weeks of unloading to 38% of control, as shown in the second figure (panel A). The third metatarsal weights showed no differences in any group, as illustrated in panel B of the second figure.

The finding of normal mineralization in the third metatarsal in spite of 8 weeks of unweighting, sufficient to cause atrophy in the soleus muscle, was unexpected. Chemical analysis of the collagen from the diaphysis of the tibiae from this study by others shows changes consistent with a mineralization defect in that bone. Previous researchers have

measured the amount of load imposed on the hindlimbs during normal walking in the rat and found it to be 60% of the body weight. How the metatarsal functions in supporting this weight is not precisely known. It is known that bone turnover in mature rats is exceedingly slow, especially when compared to human bone. Eight weeks of unloading may not be sufficient time to show the mineral loss in this species. Additionally, a small decrease in the bone mineral content of a small bone may not be detectable by these methods, which have a limit of detection in the order of 50 milligrams of mineral. Whatever the explanation, the observation illustrates both bone and species specificity of detectable osteopenia following skeletal unloading.

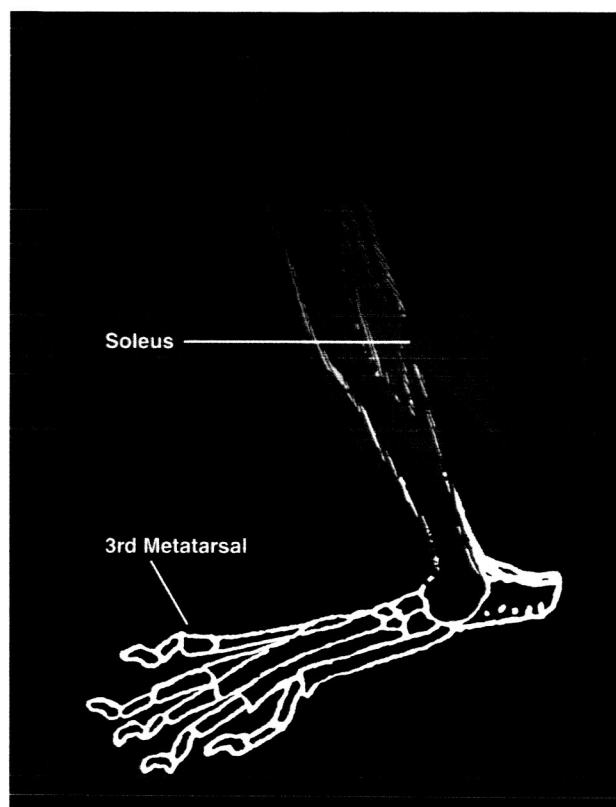


Fig. 1. The leg of the rat showing the central third metatarsal bone and the soleus muscle.

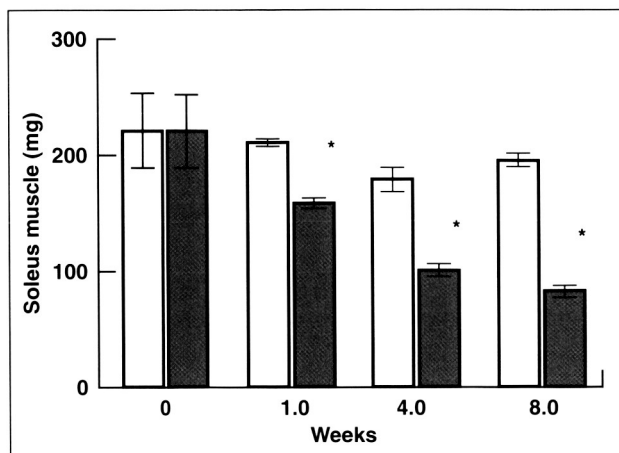


Fig. 2(a). Soleus muscle weights in 400-gram male rats exposed to 8 weeks of hindlimb unloading (shaded) compared to ambulatory controls. Asterisks indicate differences, significance at $p < 0.05$.

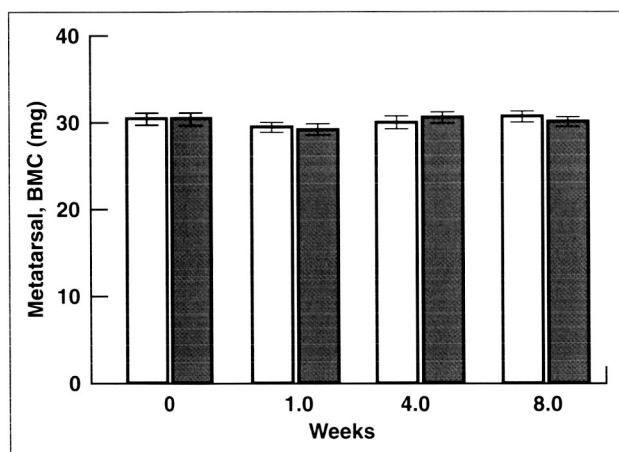


Fig. 2(b). Bone mineral content in the third metatarsal of 400-gram male rats exposed to 8 weeks of hindlimb unloading (shaded) compared to ambulatory controls. None of the apparent differences are significant at $p < 0.05$.

Point of Contact: S. Arnaud
(650) 604-6561
sarnaud@mail.arc.nasa.gov

Inducing Presyncope in Men: A Comparison of Two Stimuli

Patricia S. Cowings, William B. Toscano,
Bruce Taylor

NASA has identified cardiovascular deconditioning as a serious biomedical problem associated with long-duration exposure to microgravity in space. High priority has been given to the development of countermeasures for this disorder and the resulting orthostatic intolerance (sudden drop in blood pressure while standing) experienced by crewmembers upon their return to the norm of Earth. This in turn leads to presyncopal symptoms, that is, feeling lightheaded or dizzy just prior to fainting.

The primary purpose of the present study was to directly compare two tests of orthostatic tolerance in normal adult men. The first was a supine lower-body negative pressure (LBNP) test and the second was a combined test of head-up tilt (HUT) and LBNP. In order to test countermeasures for postflight orthostatic intolerance, investigators needed to understand the nature of physiological responses to a gravitational stress. This study would determine which of these types of tolerance tests is best suited for evaluating treatments or countermeasures that will be used to help future astronauts adapt more readily to microgravity as well as to facilitate readaptation to Earth.

Eight men, average age 37.5, were tested. Several physiological responses were measured using the Autogenic-Feedback System-2 (AFS-2), which is designed for monitoring crewmembers in space. Each subject received one supine LBNP test and one HUT + LBNP test, administered at one-week intervals.

The LBNP device is a clear plastic tube (mounted on a tilt-table), which covered the subject's feet and legs while he was lying flat on his back (supine), and was sealed at the waist with a soft rubber strip. Ten minutes of resting baseline data were collected, then the air was removed from the LBNP tube with a vacuum system. Removing the air from the tube had the effect of pulling blood from the subject's upper body down to the legs, resulting in lowered blood pressure as gradually more air was removed at increments of 10 mm Hg (millimeters of mercury) every three minutes. The maximum negative pressure was -100 mm Hg. The HUT + LBNP was essentially

the same as the one described above with one important difference; after the 10-minute resting baseline, the table was tilted upward at the head to 60 degrees for an additional 10 minutes before air was removed from the lower chamber.

Results showed that subjects could tolerate the supine LBNP significantly longer than the combined HUT + LBNP ($p < 0.0004$) (figure 1). There were significant differences between the tests for heart rate ($p < 0.003$), stroke volume ($p < 0.04$), peripheral blood volume ($p < 0.02$), and thoracic fluid volume ($p < 0.016$). In all cases the magnitude of physiological changes from baseline were much greater for the HUT + LBNP than for supine LBNP, that is, higher stress levels than the supine LBNP. The HUT + LBNP can be used to reliably induce presyncope in men; however, data suggest that this device, as used in the present study, produces too strong a stimulus for testing countermeasures when used with normotensive subjects.

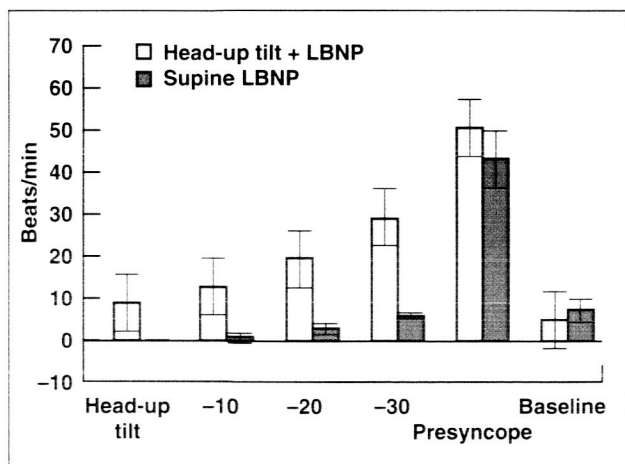


Fig. 1. Heart rate expressed as mean changes from pretest baseline during supine LBNP alone and 60-degree HUT combined with LBNP ($N = 8$). The x-axis depicts HUT, -10 mm Hg, -20 mm Hg, -30 mm Hg, presyncope (just prior to fainting), and the return to supine during posttest baseline.

Point of Contact: P. Cowings
(650) 604-5724
pcowings@mail.arc.nasa.gov

FUNDAMENTAL SCIENCE

Synaptogenesis in Microgravity (NIH.B1)

Deborah Reiss-Bubenheim, Paul Savage

The flight experiment National Institutes of Health.Biology 1 (NIH.B1) was flown on the space transport system (STS-93) in late July, 1999. NASA Ames Research Center collaborated with BioServe Space Technologies, a NASA-sponsored Commercial Space Center (CSC), to develop an enhancement to the Group Activation Package (GAP) and the Isothermal Containment Module (ICM), shown in the first figure, flown within the Commercial Generic BioProcessing Apparatus (CGBA) payload. The collaboration evolved from the needs of both organizations to fly middeck experiments on the STS-93 mission. The NIH.B1 experiment was entitled "Effects of Spaceflight on *Drosophila* Neural Development," and was led by Principal Investigator, Haig Keshishian, Harvard. This experiment was designed to investigate the effects of microgravity on a transgenic fruit fly line that expresses green fluorescent protein (GFP) to visualize singly identified motoneurons and their muscle targets, as shown in the second figure.

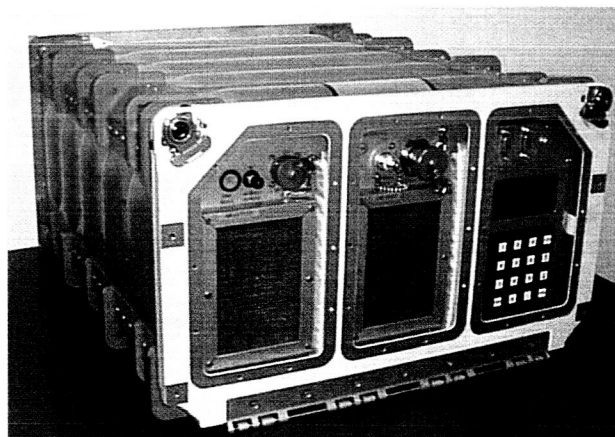


Fig. 1. The Isothermal Containment Module (ICM) used in STS-93.

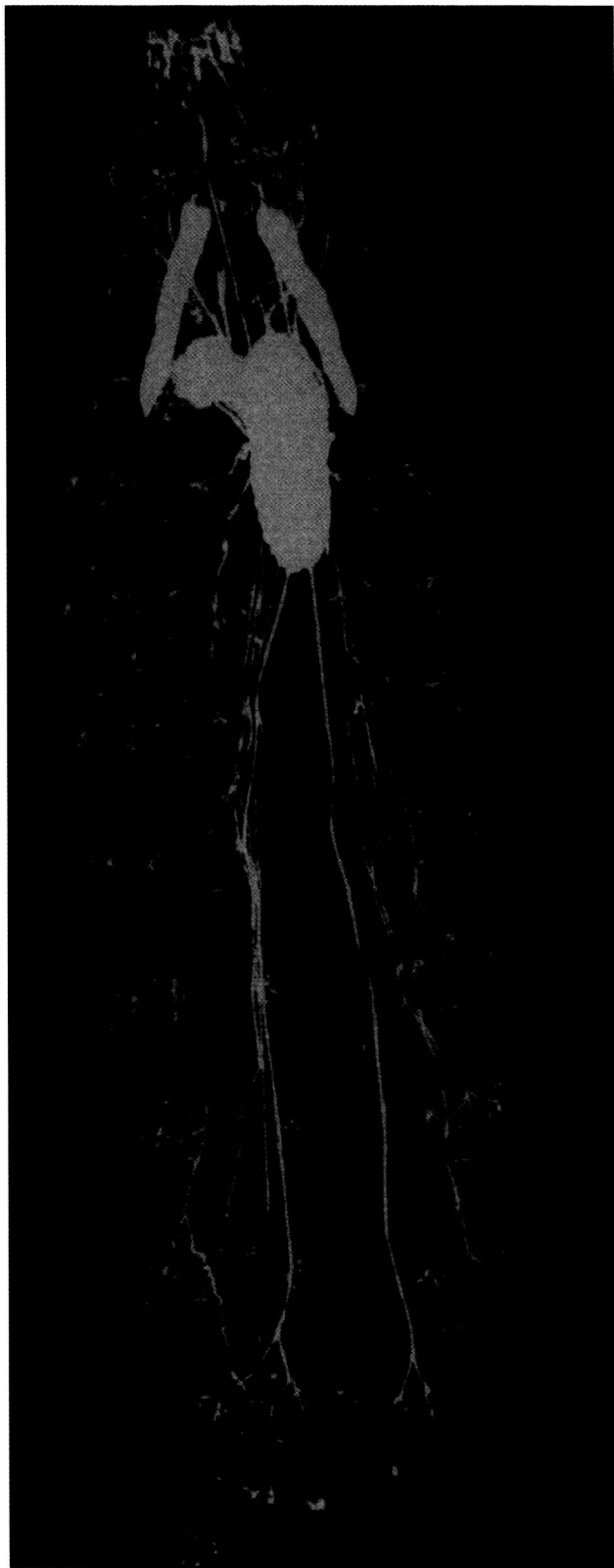


Fig. 2. Drosophila fruit fly with fluorescent marker.

Drosophila embryo development can be suspended and resumed by temperature shifts. The flight experiment design made it possible to accurately control and examine discrete developmental exposures covering critical times in the differentiation of the motor neurons. A mix of embryos and larvae at specific developmental stages were prepared by the investigator before the flight. Specimens were launched at 11 degrees Centigrade (°C). During flight, the temperature was elevated to 25 °C for a specific duration, which allowed development, and then returned to 11 °C after a preselected time period and prior to landing. This scenario stopped developmental activities or "froze" development in time. In this manner, the experiment could definitely correlate happenings at microgravity versus happenings at unit gravity. Unfortunately, there were electrical problems encountered with the startup of the BioServe ICM unit in the shuttle, and the experiment was unsuccessful because it could not proceed through the designated temperature regimens. This experiment is scheduled for a reflight with a newly upgraded ICM unit in late summer 2000.

Point of Contact: P. Savage
(650) 604-5940
psavage@mail.arc.nasa.gov

Visual Motion Integration and Segmentation

**Lee Stone, Brent Beutter, Jean Lorenceau,
Guillaume Masson, Daniel Mestre**

Much has been learned about the human ability to detect and discriminate information within local patches of image motion, and a model consisting of motion-energy detectors is a good descriptor of human low-level motion detection. This simple quasilinear view, however, does not adequately describe human performance in motion tasks that require either global integration across the image or segmentation of multiple overlapping independent motions presented simultaneously, yet these two abilities are essential components of many aerospace tasks. The overall goal of this project is to understand human performance in visual motion integration and segmentation tasks. The specific aim is to examine the abilities and limitations of humans to perform the global integration used to estimate object direction, and to use motion cues to segment images into discrete objects.

Current models of human motion processing use a first stage of local motion-energy sensors and a second-stage integration rule that combines local edge-motion signals to derive a global object-direction signal. Research has shown that simple vector averaging of the local motion signals cannot account for human direction judgments. Furthermore, by showing that the static spatial configuration influences motion integration, it has been demonstrated that no algorithm that merely combines local motion information can account for human performance.

Another difficult problem facing the human visual system is deciding when to combine local motion signals (that is, to assume they come from the same object) and when to segregate them (that is, to assume they come from different objects) as a first step in using motion to determine depth relationships. A clear understanding of this ability and its limitations is critical for the design of head-up, augmented-reality, or any other display that uses superimposed imagery. The limitations in human visual segmentation performance related to three factors were measured: mean speed, eccentricity, and spatial scale. The major findings are summarized in the figure. They are: (1) that segmentation from speed cues breaks down at mean speeds above approximately 8 degrees per second; and, (2) that the spatial resolution of the segmentation process is quite fine even in the visual periphery. Both of these findings are consistent with the view that the primary visual cortex (V1) plays a critical role.

Point of Contact: L. Stone
(650) 604-3240
lstone@mail.arc.nasa.gov

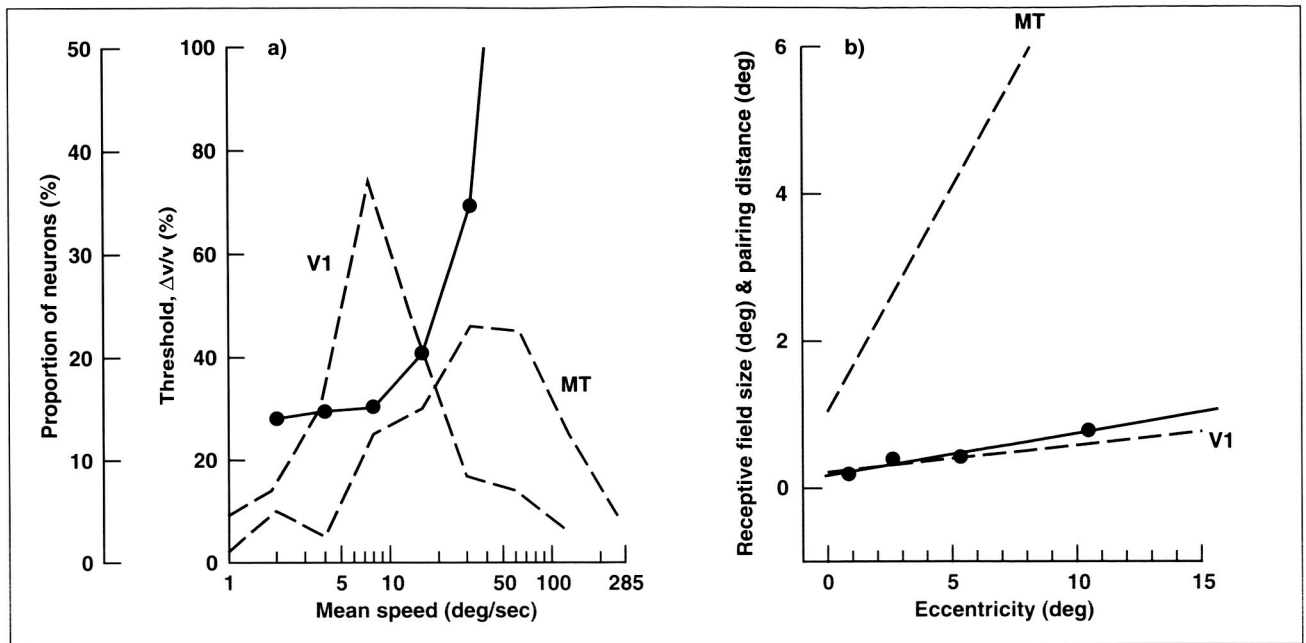


Fig. 1. Human speed-based segmentation performance. a. Human speed-segmentation thresholds are plotted as a function of mean display speed (solid circles and trace). Note the sharp decrement in performance for speeds above approximately 8 degrees per second, consistent with the range of speed tunings found in the primary visual cortex (V1) and inconsistent with the higher speed range of extrastriate visual cortical areas beyond V1, such as the middle temporal area (MT). The distributions of preferred speeds for neurons in areas V1 and MT (from earlier studies by others) are shown for comparison as dashed traces. b. The minimum spatial scale for segmentation (pairing distance) is plotted as a function of eccentricity in the visual field (solid circles and trace). Note that the smallest effective spatial scale for segmentation remains small (approximately 1 degree) even out to approximately 15 degrees of eccentricity. Again, such performance is consistent with a mechanism with a receptive field size similar to that of V1 neurons and much smaller than those of MT neurons (plotted for comparison as dashed traces from earlier studies by others).

Computational Models of Human Eye-Movement Behavior

Lee Stone, Brent Beutter, Miguel Eckstein, Jean Lorenceau

Humans interact with visual displays not by passively absorbing the information like a fixed camera, but by actively searching for areas with relevant information, and by following the motion of features of interest. The specific aim of this project is to develop and test computational models of human eye-movement control with particular emphasis on

two types of eye-movement behaviors: search saccades and smooth pursuit. The overall goal is to incorporate the knowledge of eye-movement behavior acquired in our laboratory into computational models that can serve as design tools in the development of safer, more effective visual displays, interfaces, and training methods, matched to human abilities and limitations.

Most current models of human vision have focused on the passive ability to detect, discriminate, or identify targets in noise in carefully controlled laboratory conditions in which eye movements are suppressed. However, when humans interact with a

display during aerospace tasks (for example, air traffic controllers monitoring aircraft), their eyes jump from one location to another using rapid eye movements (saccades) to point central gaze, the region of highest resolution, at the current object of interest. This active search process greatly enhances visual performance. Two major categories of models have been proposed to explain search performance: guided-search and signal-detection-theory models. Unfortunately, the former category predicts reaction time, while the latter predicts localization accuracy. To enable a direct comparison of these two models, an extension to the guided-search model that allows it to predict localization performance was developed. Both models are being tested to determine which is the better predictor of human performance.

When display targets move, humans generate smooth tracking eye movements (pursuit) to follow the motion of the current object of interest. This ability is crucial when using a display to perform tasks involving motion estimation (for example, landing the shuttle by aligning a moving target with a reference within a heads-up display). Current pursuit models assume that pursuit merely minimizes the physical image motion on the back of the eye (the retina). This study has demonstrated that this simple view cannot explain the full range of human pursuit behaviors, especially the ability to track targets accurately even when one's view is partially blocked. The new control framework for pursuit, shown schematically in the figure, is consistent with new behavioral data from this study, as well as what is known of the neurophysiology and anatomy of the primate brain. This research suggests that pursuit is driven by an estimate of target motion constructed at the highest level of the brain (the cortex) and shared with perception, rather than by the simple quasi-reflexive integration of lower-level retinal-error signals.

Point of Contact: L. Stone
 (650) 604-3240
 lstone@mail.arc.nasa.gov

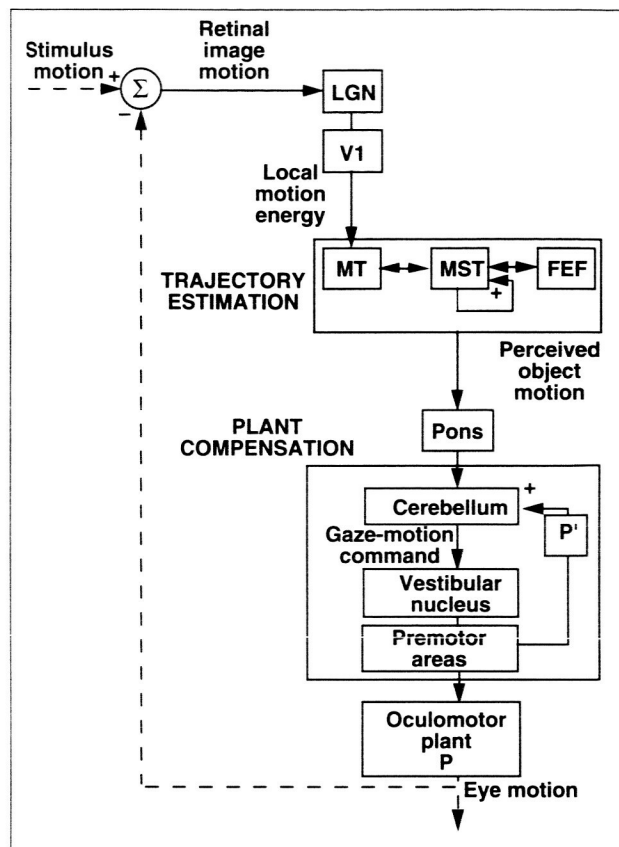


Fig. 1. A two-stage control strategy for pursuit. Rather than raw image motion, the main driving input is perceived object motion, which is computed in the visual cortex. Once object motion is computed, the remaining transformation needed to optimize performance is compensation for the dynamics of the visco-elastic properties of the eye (the oculomotor "plant" with transfer function P). This compensation can be achieved by positive feedback through the cerebellum (with $P' \sim P$ to eliminate the lag associated with P) consistent with the observed neural responses in the cerebellum. LGN, lateral geniculate nucleus; V1, primary visual cortex; MT, middle temporal area; MST, medial superior temporal area; FEF, frontal eye fields.

pH Biotelemetry Transmitter

John W. Hines, Michael G. Skidmore

Ames continued its development of pill-shaped biotelemetry for measuring physiological parameters during space life sciences experiments with the addition of a pH biotelemetry. These devices could eventually be used to monitor animal health parameters and the performance of self-contained biological systems aboard the International Space Station (ISS) Gravitational Biology Facility, and can be readily adapted to monitor the health of astronauts in the Human Research Facility. The equipment has enormous potential outside NASA as well.

A first prototype of an implantable pH biotelemetry has recently been developed (figure 1). This device can accurately measure pH in the range of 2 to 12, and the battery-powered transmitter has a range of approximately 6 feet and an expected lifetime of 6 months. The pH is measured by small, catheter-based ion-selective electrodes that are connected to an integrated pH-meter and radio frequency (RF) transmitter that sends the measurement information to an external receiver and is

displayed in real time by a LabVIEW program. The next development effort will be the miniaturization of the pH biotelemetry into a pill-sized device.

As an initial test, the device is currently being prepared for measurements of rumen pH in cattle at the University of California at Davis (UCD). Besides allowing NASA to test the performance of the biotelemetry in a large animal, this experiment gives doctors at UCD valuable information for nutritional management of dairy cattle.

NASA is interested in this technology for long-duration monitoring of research subjects in space-flight. Astronauts and the life sciences experiments they oversee are in a remote and inaccessible environment. Their health and performance must be monitored as unobtrusively as possible so as not to interfere with ISS operations or with onboard experimental results. The pill-sized biotelemetry have direct application to plant and animal experiments where the device can be inserted, implanted, or ingested to obtain optimum information in situ. The same biotelemetry electronics, configured in a Band-Aid® arrangement with lightweight, flat polymer batteries, could be applied externally for noninvasive monitoring of astronaut health.

There are numerous possible future commercial applications of these new pill transmitters. Patients with digestive disorders could swallow a pH pill

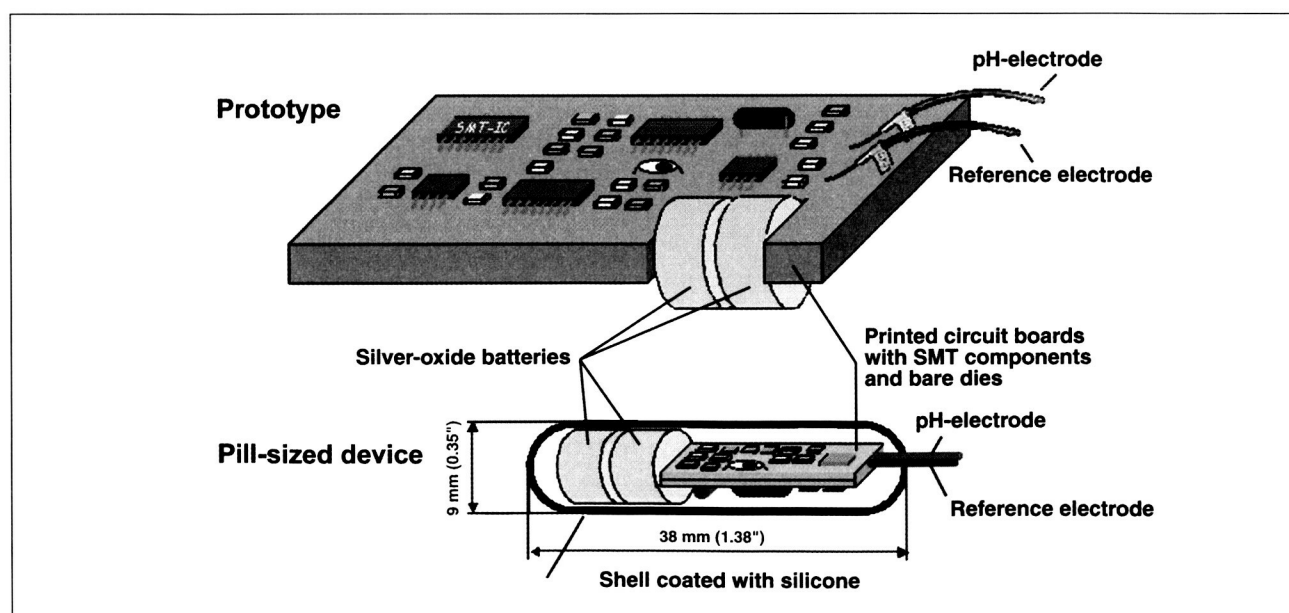


Fig. 1. The pH biotelemetry.

transmitter that monitors gastrointestinal acidity, or a pressure pill transmitter that gives data about contractions of intestinal smooth muscle, allowing doctors to better diagnose gastrointestinal problems. There is also great potential in sports medicine. Pill transmitters can monitor the performance and stress levels of athletes as they train. In addition, the military has expressed interest in similar devices to monitor the health and performance of soldiers in hostile environments.

Point of Contact: M. Skidmore
(650) 604-6069
mskidmore@mail.arc.nasa.gov

Physiologic Signal Conditioner for Crew Hazards and Error Management

John W. Hines, Charlie Friedericks, Robert Ricks

The Ames Research Center (ARC) Physiological Signal Conditioner (PSC) has been adapted to meet the requirements of the Crew Hazards and Error Management (CHEM) project of the Flight Dynamics and Controls Division at Langley Research Center. This new unit is an eight-channel physiologic signal processor designed to meet the need for human response measurement technologies. The purpose of these technologies is to assess an aircraft crew's ability to perform flight management tasks effectively in real or simulated stressful situations.

The PSC-CHEM, shown in the figure, processes biopotential signals, such as EEG, ECG, EMG, and others, as well as body temperature, respiration, and motion activity. The eight channels can be configured to measure any combination of these four signal types. The biopotential signals are sensed with self-sticking snap electrode patches. Cables snap onto the electrodes and have quick push-on/pull-off connectors for the PSC. Temperature sensors, motion sensors, and respiration bands have integral cables with push-on connectors for the PSC. All sensors can be attached to the crewmember independent of the PSC, and the PSC can be attached to the crew chair or to the crewmember if mobility is required while taking measurements.

The PSC is powered with internal rechargeable batteries. Processed physiologic signals are digitized for serial output, and the serial connection to a computer permits the user to view real-time signals. Custom software on the computer allows the user to interact with the PSC to adjust signal gain and filtering and allows the user to store the signals for later processing and review. For completely untethered operation, the serial cable is replaced with a telemetry interface. The telemetry system employs frequency hopping spread spectrum (FHSS) compatible with systems proposed for the International Space Station.

Future CHEM project requirements for additional physiologic or environmental parameters can be accommodated by the PSC-CHEM. Sensors and analog signal-processing circuitry would be developed to fit directly into the PSC and to conform to the user data-processing system. Also, as an operational system, the PSC-CHEM serves as a test platform to determine a baseline for some of the human factors requirements for a smaller, modular, wearable PSC for aviation and spaceflight applications.

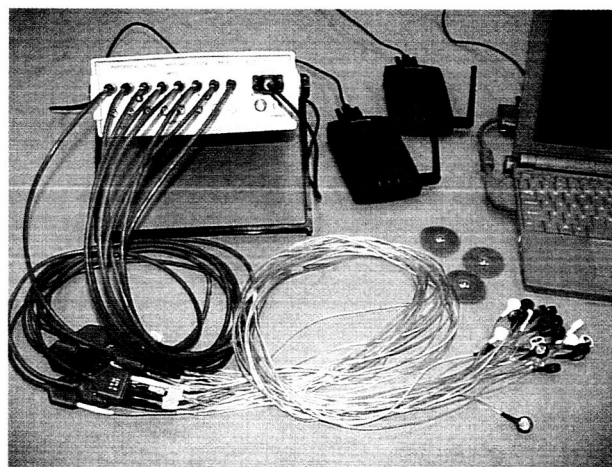


Fig. 1: *Physiological Signal Conditioner for the Crew Hazards and Error Management Project (PSC-CHEM).*

Point of Contact: M. Skidmore
(650) 604-6069
mskidmore@mail.arc.nasa.gov

BIONA-C Inflight Technology Demonstration

John W. Hines

The Biological Ion Analysis in the Cell Culture Module (BIONA-C) flew onboard the space transport system (STS-93) (July 23–27, 1999) as a technology demonstration of the capability to monitor and control pH measurements during spaceflight. Working with the U. S. Army Medical Research and Material Command (USAMRMC) and in close collaboration with the Cell Culture Module (CCM) team from the Walter Reed Army Institute of Research (WRAIR), Ames Research Center (ARC) developed BIONA-C as an autonomous monitoring and control system for a spaceborne hollow-fiber bioreactor experiment. BIONA-C monitored the pH and temperature of circulating media and controlled the collection of samples and addition of nutrients for the cells growing in the ARC Rail, shown in the figure.

The BIONA-C Rail contains four independent fluid paths that circulate media to support cell growth. In each path, media flows through a separate bioreactor where fluids can transfer across a permeable membrane to the cell culture, but cells cannot enter the fluid path. In two of the fluid paths the sensors are located directly in the circulating media ("online"), taking continuous pH measurements. Calibration of the online sensors occurs on Earth before and after the experiment. In the other two paths a precision pump periodically transfers media samples from the circulating media path to the sensors. This "offline" configuration allows the sensors to be calibrated inflight between each sample reading.

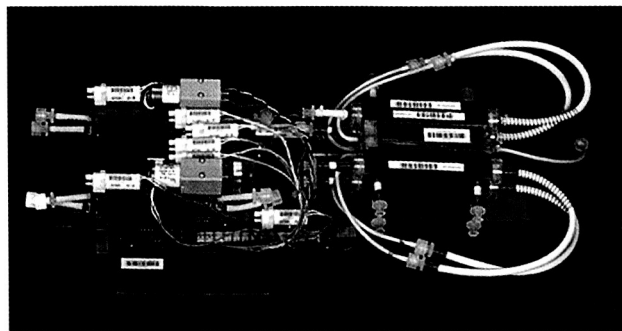


Fig. 1. BIONA-C Rail.

The sensor arrays are sealed and electron beam sterilized. Sterile practices are used during all experimental preparation, rail priming, and sensor calibration. When operating, the rail maintains the temperature of the bioreactor and oxygenator assembly at 37 degrees Celsius.

The capability to monitor and control bioprocess experiments gives BIONA-C enormous potential in the areas of space genomics, evolutionary biology, and astrobiology. The system has applications in cell growth and plant growth facilities in space. It can also be utilized in developing long-term, closed human habitats for future Mars exploration. The BIONA-C technology can be adapted to perform in measurement stations that search for life in extreme environments such as ocean floor hydrothermal vents.

Point of Contact: M. Skidmore

(650) 604-6069

mskidmore@mail.arc.nasa.gov

Solid-State Compressors for Mars ISRU

John Finn, Lila Mulloth, Bruce Borchers

One important way to extend the science and exploration capabilities of Mars surface missions is to use the readily available Mars atmosphere as a resource to provide critical supplies that would otherwise limit the mission or make it too expensive. Compressed and purified gases, oxygen, important chemicals, and even rover and rocket fuel can be manufactured largely from Martian atmospheric gases, saving the costs of their transport from Earth and ensuring that a mission doesn't end when it "runs out of gas." These techniques are examples of a popular mission strategy that is generally termed "in situ resource utilization," or ISRU.

The Mars atmosphere consists mostly of carbon dioxide, with relatively small amounts of nitrogen and other gases. At about 0.7 kiloPascals (0.1 pounds per square inch) total pressure, the mixed gases are too thin to be useful directly, so the atmospheric constituents must be separated from each other and

compressed. Ames Research Center (ARC) is developing solid-state adsorption compression and separation technology to acquire the Mars atmospheric constituents and make them available for downstream processing or direct use.

The ARC adsorption compression technology uses a zeolite adsorbent bed that can adsorb large quantities of carbon dioxide at the ambient temperature and pressure of the Mars surface. Its capacity for the other Mars gases is much lower; these gases are drawn through the adsorbent and stored in a second bed for later processing. When the adsorbent is saturated with carbon dioxide, the compressor is isolated and warmed. Carbon dioxide then evolves from the sorbent, resulting in a rapid pressure increase inside the compressor. When the pressure reaches a desired level, the carbon dioxide can be drawn off. The supplied pressure is easily regulated by controlling the power level of the compressor heater. When the supply of carbon dioxide is exhausted, the bed is allowed to cool and to adsorb another load of carbon dioxide. The cycle can be repeated indefinitely.

The first uses for this adsorption compression technology will be on robotic exploration missions. A prototype for adsorption compression at this mission scale is shown in the figure. The one-kilogram device shown has been tested successfully under simulated Mars surface conditions, under which it produces approximately 15 grams of carbon dioxide per day at a pressure of 120 kiloPascals (17.4 pounds per square inch), and requires an average of 7 watts of power during 5 hours of production. Larger-scale productions will be more economical as the fraction of structural mass decreases, with an anticipated daily production level of about 250 grams carbon dioxide per kilogram of compressor mass.

Point of Contact: J. Finn
(650) 604-1028
jfinn@mail.arc.nasa.gov

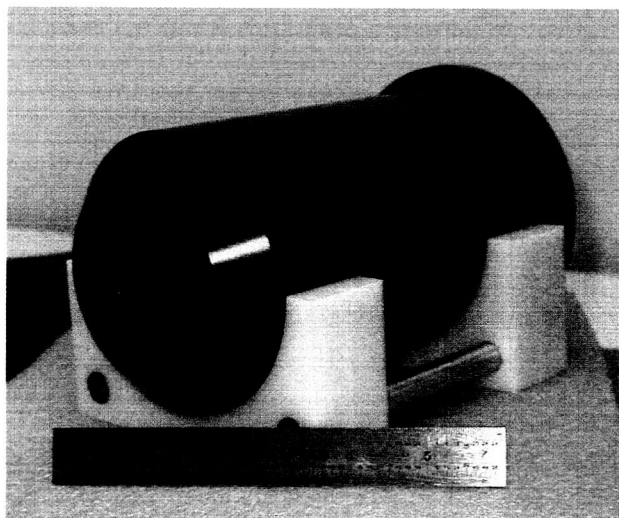


Fig. 1. Prototype solid-state adsorption compressor for Mars carbon dioxide, 15 grams/day scale. A nitrogen/argon mixture is produced as a byproduct.

Dynamic Modeling of Life Support Systems

Cory Finn and Harry Jones

Dynamic system models have been developed that track the flow of material through a regenerative life support system over time periods of months to years. These models are being used to help evaluate system design and operation issues for the Advanced Life Support Systems Integrated Test Bed (ALSSITB). The model captures the main flow stream characteristics associated with atmosphere regeneration, water recovery, crop growth, food processing, and waste processing. The system simulation quantifies the variations in stream flow rates and subsystem processing rates so that estimates can be made on buffer requirements for various system configurations and design options. It is also being used to investigate scheduling, operations, and control issues.

Dynamic modeling is an important tool for developing robust system designs. Static or steady-state models are often used to obtain estimates on nominal processor flow rates and resupply requirements. However, more detailed system design

requires information on processor operation ranges and system buffer requirements that are a function of the system dynamics and control strategy. In general, the level of model complexity needed increases throughout the system design cycle. In the early design phase, simple dynamic models provide useful information for estimating the processing rates and storage sizes needed to meet all the system performance specifications. More complex models are needed for the design of control systems, the development of failure recovery approaches, and the plan for adding redundancy to the system in order to improve system safety and reliability.

A top-level dynamic system model of the ALSSITB has been developed at Ames Research Center (ARC) to investigate system design issues. The ALSSITB is currently being developed by Johnson Space Center (JSC) to support long-duration human testing of integrated life support systems. It comprises a set of interconnected test chambers with a sealed internal environment capable of supporting a four-person test crew for periods exceeding one year. The life support systems to be tested will consist of both biological and physical/chemical technologies that perform air revitalization, water recovery, biomass production, food processing, and solid waste processing. A variety of system designs for the ALSSITB have been studied to date.

Each system design is described in terms of the set of technologies used, the configuration of the technologies in the system, and the manner in which the system is operated. The overall technology set available for consideration includes technologies that provide various levels of regeneration. For example, life support consumables can be either supplied or produced, and waste products can be either processed, dumped, or stored. An optimal system generally consists of some combination of resupply, in situ resource utilization, venting, dumping, and material recycling using physical/chemical or biological processors. System configuration refers to the manner in which the processors are connected for a given set of technologies. For example, multiple flow paths are possible, as well as various options for the placement and sizing of buffers. System operation strategies need to be investigated because some system components can be operated in numerous ways. Some technologies can be operated in either batch

mode or continuous mode. For batch operation, the batch sizes and operation schedule can vary. For continuous operation, processing rates can be either constant or variable, and the operational parameters, control objectives, and constraints can vary.

Among the ALSSITB designs simulated thus far are systems with different air revitalization systems using various circulation patterns, technology sets, and operational strategies. For each system design that was simulated, the results were compared with those of a baseline to see how well each system met performance criteria by maintaining controlled atmospheres, adequate reserves, etc., and to determine the required capacity for the various processors and storages.

Point of Contact: C. Finn
(650) 604-5518
cfinn@mail.arc.nasa.gov

Activated Carbon from Inedible Biomass

John Fisher, Suresh Pisharody

As manned missions become longer, resupply of life support materials becomes increasingly more difficult and expensive. The expense of resupply can be avoided by regenerating life support materials. Bioregeneration involves the use of plants to grow food, but plants generate a large amount of inedible biomass, which must be recycled. Incineration is one of the most promising technologies for recycling wastes such as inedible biomass. Unfortunately, inherent to the process of incineration is the formation of undesirable byproducts such as nitrogen oxides (NO_x) and sulfur oxides (SO_x). Conventional incineration technologies treat offgases, such as NO_x and SO_x , by using selective catalytic reduction processes, but these technologies require the injection of expendables such as ammonia to treat the NO_x . Activated carbon can also be used to remove NO_x and SO_x via the process of adsorption.

The Solid Waste Resource Recovery project group is investigating unique ways to use crop wastes to make activated carbon. This process would

eliminate the need for expendables in the flue gas cleanup during long-duration, manned space missions. It may be possible to make this activated carbon from the inedible biomass available from growing plants in space. Over 40 crops are being considered for food production. One or more of these plants, which will provide the nutritional needs of crews on long missions, may be a good raw material for making activated carbon.

The flow diagram in figure 1 shows the planned role of the activated carbon as part of the incineration process for resource recovery. The contaminants in the flue gas are adsorbed on activated carbon at room temperature. In a regeneration process at high temperatures, the adsorbed NO_x is reduced by the carbon-forming nitrogen gas (N_2) and carbon dioxide. The offgases formed during the activation process are directed back into the incinerator. After several regenerations, the spent carbon is mixed with

the incinerator feed and is converted to carbon dioxide and water in the incinerator. Thus contaminants are removed without the need for resupply.

The challenge is to make quality activated carbon, a highly porous, carbonaceous material. The porous structure is controlled by the nature of the starting material and the process used for carbonization and activation. Conversion of inedible biomass to activated carbon and the use of activated carbon to convert adsorbed NO_x to N_2 gas has been successfully demonstrated at Ames Research Center. There is an excellent chance that this research will result in a process that will one day be used to manufacture activated carbon in space for use in the life support system.

Point of Contact: J. Fisher
(650) 604-1859
jfisher@mail.arc.nasa.gov

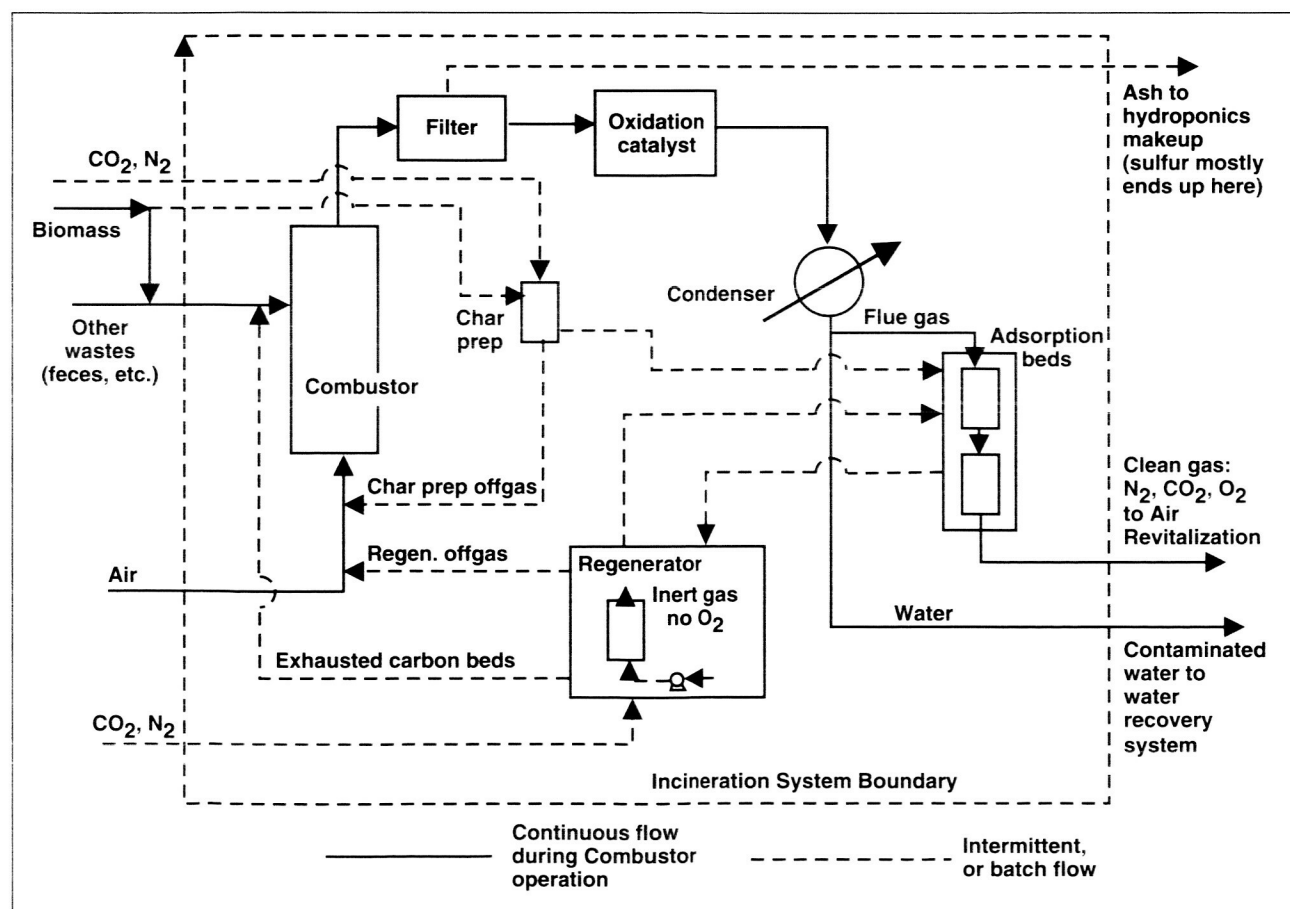


Fig. 1. Flow diagram of reactive carbon for flue gas cleanup.

Mobile Exploration System

Richard Alena

The Mobile Exploration System (MEX) research project is a distributed information system designed to assist planetary exploration operations that consist of three primary nodes with unique computational capabilities appropriate for its operational function, linked together via high-speed radio communication systems. The three nodes include a science center node, a base camp node, and a mobile node, which are packaged to endure the rigors of wilderness traverses. Each operational node allows humans at that location to participate in the exploration activity. Figure 1 shows the three nodes schematically.

The science center computational node, supported by several Web and video teleconferencing servers, represents the Earth-based mission control and planetary science data systems. Consultation with remote institutions and scientists is supported via Internet-based collaboration tools.

Housed in the base camp work tent, the second node represents the planetary habitat that will act as the primary point of contact for explorers engaged in extravehicular activities. This node consists of a series of workstations and data servers supported by a wired local-area network. It is linked with the science

center using two geosynchronous satellite links, one using a commercial C-band service, and the other using the Advanced Communications Test Satellite. Tests of satellite link quality at high latitudes (75°) were performed as part of the FY99 Houghton Mars Project field tests at Houghton Crater.

The third node is the mobile exploration computation and communication system. This mobile node is connected to base camp using two medium-range radio links, dubbed the Crater Area Network (CAN), which consists of a medium-rate omnidirectional radio system for vital communication and control, and a high-rate network packet radio supporting video teleconferencing with real-time monitoring of high-resolution cameras and instruments. This dual-link communication model is similar to that used for planetary spacecraft; it incorporates the best features of both types of radio systems. The CAN was field tested by setting up repeaters on a high hilltop two miles from base camp and using an all-terrain vehicle (ATV) to test link quality and reliability in different locations.

A human-centered system design approach is being used for the development of the MEX, focusing on the explorers who conduct field geology and biology surveys, and incorporating the results of work practice studies being conducted at Ames. The mobile node has a server computer, mounted on the

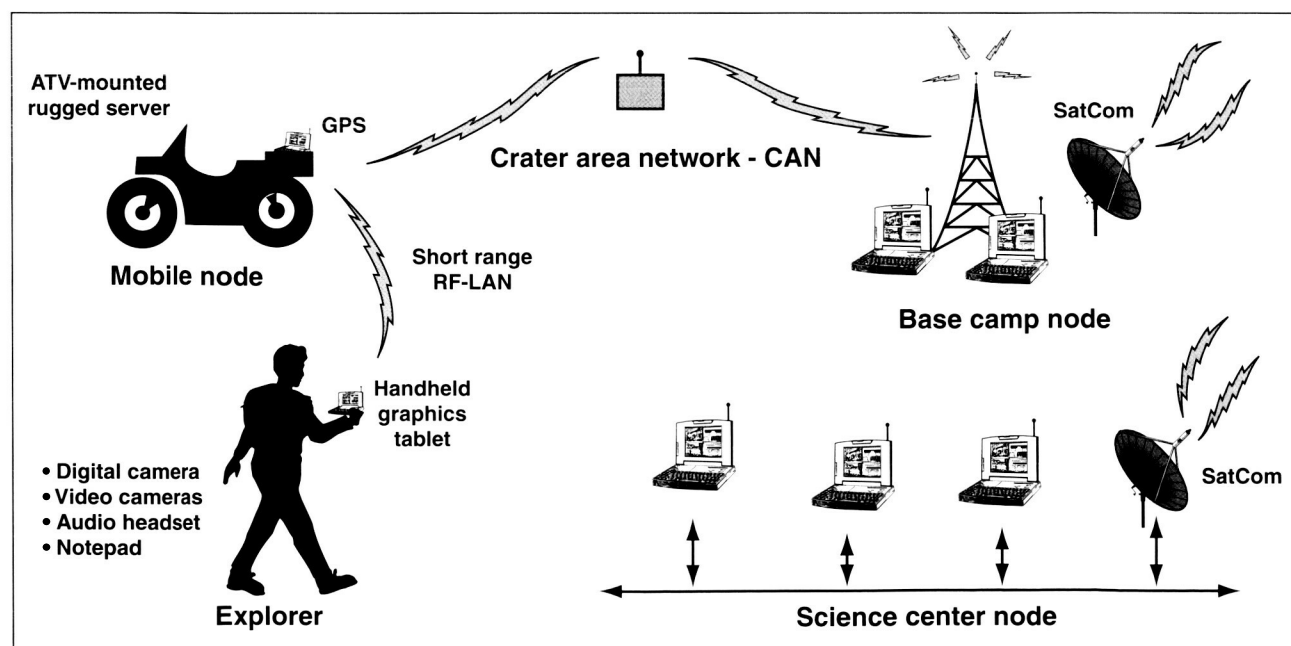


Fig. 1. The Mobile Exploration System.

ATV, which is continuously operated during traverses mapping the route in real time using a Global Positioning System (GPS). This system gives the explorers their location and a topographic map of the local area at all times. Additionally, video cameras allow people at base camp to view the terrain seen by the exploration party. Text or audio communications between the mobile node and base camp are also supported. Pen-based graphical tablets can be used to control the applications resident on the server, providing a human/computer interface usable in both rain and bright sun. Experiments in voice recognition and other user interface modalities are ongoing.

The primary goals for the FY99 field season were to test satellite communications, base-camp computational infrastructure, and the performance and deployment of the CAN radio systems. These goals were fully met, and resulted in certain design improvements.

Point of Contact: Richard Alena
(650) 604-0262
ralena@mail.arc.nasa.gov

Development of the Vapor Phase Catalytic Ammonia Removal Process

Michael Flynn, Bruce Borchers

Ames Research Center (ARC) has recently completed the development and testing of a prototype Vapor Phase Catalytic Ammonia Removal (VPCAR) system that represents the next generation in spaceflight water recovery systems. Water is the single largest resupply requirement associated with human spaceflight, accounting for 87% by mass of an astronaut's daily metabolic requirement. The VPCAR system achieves a mass metric almost an order of magnitude better than the current state-of-the-art water processors. (Mass metric is a technique used to reduce all performance parameters into launch mass.) Incorporating the VPCAR technology into human spaceflight missions could potentially save hundreds of millions of dollars in resupply costs, depending on the specific mission scenario. As a

result, a human-rated version of the VPCAR technology has been authorized for development, and when completed it will be used for human testing in a closed chamber.

The VPCAR process is a two-step distillation-based water processor. The current configuration of the technology is shown in figure 1. The VPCAR process is characterized by the use of a wiped-film rotating-disk vacuum evaporator to volatilize water, small molecular weight organics, and ammonia. This vapor stream is then oxidized in a vapor phase catalytic reactor to destroy any contaminants. The VPCAR process uses two catalytic beds to oxidize contaminants and decompose any nitrous oxide (N_2O) produced in the first bed. The first catalytic bed oxidizes organics to carbon dioxide (CO_2) and water, and ammonia to N_2O and water. This oxidation reactor contains 1% platinum on alumina pellets and operates at about 523 kelvin (K). The second catalytic bed reduces the N_2O to nitrogen and oxygen. This reduction catalyst contains 0.5% ruthenium on alumina pellets and operates at about 723 K. The reactor and distillation functions occur in a single modular process step, no scheduled maintenance is required, and the system has no resupply requirements. The process achieves between 97 and 98% water recovery.



Fig. 1. Vapor Phase Catalytic Ammonia Removal (VPCAR) water recycling system.

The VPCAR activity is significant because it represents the development of the next generation of life support water recovery technology. It also shows how the research and development capabilities of one NASA center can be integrated into the operational requirements of another NASA center to reduce the cost of human spaceflight programs. Ames has been involved from the first principle definition to the model development, bench-scale and lab-scale prototype development, and contract management of the development of a human-rated version of the technology for transfer to a NASA spaceflight center. Johnson Space Center will develop the final spaceflight version.

Point of Contact: M. Flynn
(650) 604-3205
mflynn@mail.arc.nasa.gov

Human-Centered Computing Studies on the NASA Haughton-Mars Project

William J. Clancey, Maarten Sierhuis, Pascal Lee

During the past two field seasons, July 1998 and 1999, Ames researchers investigated the field practices of scientists and engineers at Haughton Crater on Devon Island in the Canadian Arctic, 500 miles north of the Arctic Circle, under the auspices of the NASA Haughton-Mars Project (HMP). On the HMP, human-centered computing (HCC) studies (part of Exploration Research) are aimed at determining how human explorers might live and work on other planetary objects, in particular on Mars.

This broad HCC investigation of field life and work practice spans social and cognitive anthropology, psychology, and computer science. The investigation involved systematic observation and description of work activities, locations, and learning in the field, constituting an ethnography of field science at Haughton. The focus was on human behaviors—what people do, where, when, with whom, and why. By locating behavior in time and place—in contrast to a purely functional or “task-oriented” description of work—the group identified

patterns constituting the choreography of interaction between people, their habitat, and their tools.

To develop requirements for new kinds of tools for living and working on Mars, the group focused on the existing representational tools (such as documents and measuring devices), learning and improvisation (such as use of the Internet or informal assistance), and prototype computational systems brought to the field.

In addition to observing by participating in the expedition, human-centered computing scientists took extensive photographs and videos, which were analyzed for patterns. For example, to understand the relation between how technologies were used in different work and living spaces, a video camera was placed between the shared work tent, the natural sciences tent, and the large dome tent, with a view of the all-terrain vehicles (ATV) parked on the terrace in front (figure 1). During a three-hour period, quarter-size video frames (320 x 240 pixels) were directly captured to computer disk every 3 seconds (a compromise between storage and visible information). This video therefore logged occupation and motion between four key areas of the base camp, as well as capturing use of some personal tents. The layout was of special interest because motion between the work and dome tents might correspond to the upper and lower decks in a Mars habitat.

The resulting video was coded on a spreadsheet. Durations of visits and number of people occupying each area were calculated in Excel. Averages and



Fig. 1. Example frame, showing an exit event from work tent and (at least) two people at the ATV staging area.

totals were graphed to show correlations (see figure 2). One unexpected result is that the data allows measuring the effect of a schedule change (delay in departure of a traverse by 1.5 hours) on both individual and group occupation of the different areas. For example, movement between the dome and work tents (the two "floors") peaked each time occupation at the ATV area peaked, and reached a minimum during the delay period. Further analysis showed a great variation that was later explained by considering the actual activities of individuals and their roles in the camp, as revealed by observation, interviews, and surveys.

Topics especially relevant to computer system design were highlighted by a written survey completed by the participants in the month following the expedition. Important findings are summarized in table 1. The greatest surprise was the number of people who downloaded and/or learned to use new software. Aside from laptop computers, the most prevalent use of computing was with the digital camera. The average number of digital photographs was 137, yet only two people used a photo database

Table 1. Computer and digital device usage during HMP-99 expedition (N = 25)

Computer Usage	Percentage
Used a computer	92%
Browsed web	68%
Downloaded software	32%
Learned to use new software	52%
Sent e-mail	88%
Used e-mail daily	60%
Sent digital photographs	52%
Informed colleagues or sought advice	64%
Watched a full DVD movie	76%
Used a digital camera	64%
Used a computer outside or in personal tent	16%

(on average 204 conventional photographs were taken per person).

These investigations suggested several hypotheses that are shaping operations planning and technology design:

- Exploration is not just about covering the most area in the most time; continuously revisiting places is essential.
- During an expedition like the Houghton-Mars Project, conceptual change includes organizational roles, not just scientific theories.
- Living on Mars might change scientific practice, physically constraining how the work is done, and how analysis and publication are coordinated.
- An important use of computers will be for life support automation and mediating communication with Earth, not just for assisting scientists in direct field exploration.
- Protocols for Mars/Earth communications should be designed to help Mission Control learn about human activities on Mars, and adjust its support role as surface practices develop.

Point of Contact: W. Clancey
 (650) 604-2526
bclancey@mail.arc.nasa.gov

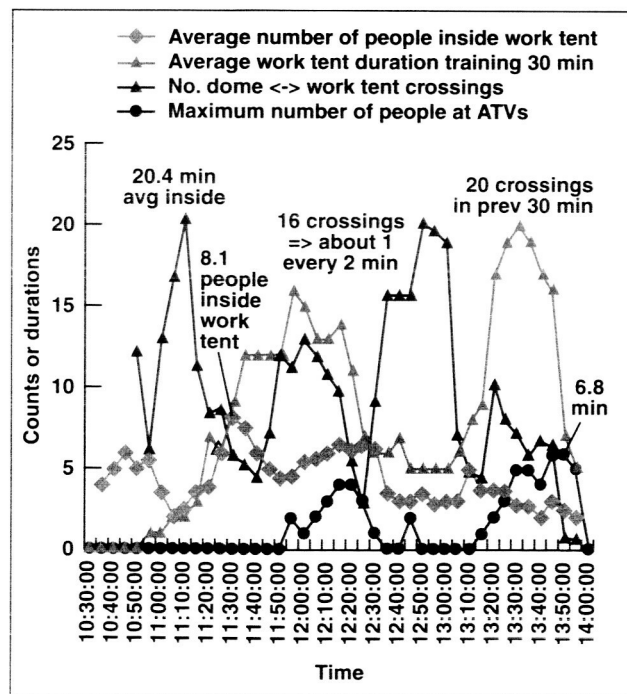


Fig. 2. Average number of people inside work and dome tents and at ATVs, showing correlation at noon and 1:40 p.m. expected EVA departure times. During intervening wait, work tent duration increased dramatically and crossings between tents dropped.

Brahms: Human-Centered Modeling and Simulation

Maarten Sierhuis, William J. Clancey, Ron van Hoof

Ames researchers are combining computational simulation with ethnographical field-observation methods and techniques from the social sciences and knowledge engineering in order to better understand and design the necessary collaboration between man and machine. Researchers are developing a multiagent modeling and simulation environment called Brahms, originally an acronym for "Business Redesign Agent-Based Holistic Modeling System," but now used as an internal product name for the modeling language, as well as the set of tools that comprises the product. Brahms facilitates an engineering paradigm shift from current system-centered engineering to a more human-centered engineering approach, in which an understanding of users of technology is at the center.

The Brahms environment consists of numerous software tools including a multiagent programming language for modeling people's behaviors, geographical environment, movements, communication, systems and tools used in activities, as well as system behaviors. Brahms agents can represent people as well as (intelligent) systems. It also includes a

simulation engine for executing Brahms models, a modeling environment for developing and debugging models, and a graphical tool for displaying the result of a multiagent simulation (see figure 1).

The research focuses on investigating the work activities and collaboration between participants in the deployment of complex systems on planetary extravehicular activities (EVAs). During the FY99 Haughton-Mars Project field season at Devon Island, in Nunavut, Canada, researchers observed and videotaped scientists in the field deploying a multitude of systems (for example, the Haughton Crater Network, ultraviolet (UV) boxes, ground temperature sensors, ozone measurement equipment). To understand the complex work activities of astronauts and Mission Control, researchers are studying the work practices of deploying the Apollo Lunar Surface Experiments Package (ALSEP) during the Apollo missions. The Brahms tool is being used to model and simulate the work activities of the Apollo astronauts on the Moon, as well as the communication between the astronauts and mission control on Earth.

A simulation model of the Apollo 12 ALSEP offload activity was created to test the Brahms language capabilities for modeling the work practices of a complex deployment activity during a planetary EVA. To develop the Apollo 12 ALSEP offload model, researchers used historical Apollo archives of

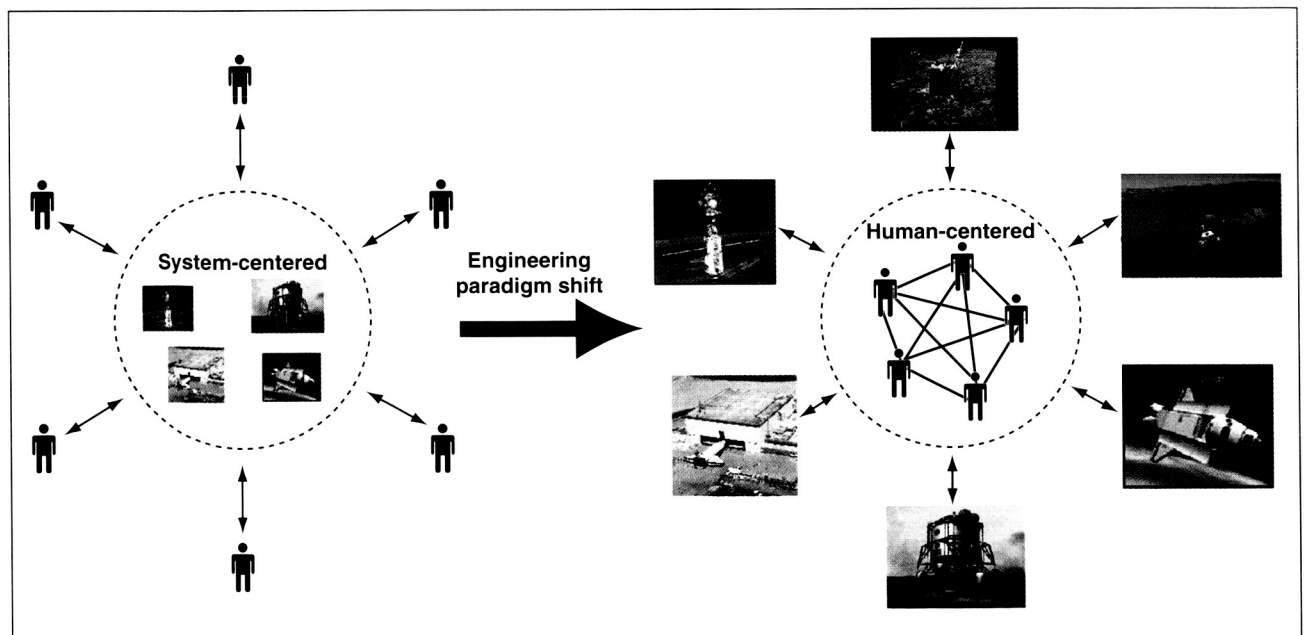


Fig. 1. Brahms environment.

astronaut communications, lunar surface procedures, videos, and photographs. From this historical data the multiagent and object behavior models and the geographical model were designed. To understand the impact of time delays between Mission Control and the astronauts on the Moon, a reusable voice-loop library model was developed to simulate the 1.25 second one-way delay. Using this voice-loop model, the Brahms simulation includes a simulation of communication between Apollo lunar surface astronauts and capsule communicator (CAPCOM). Figure 2 is the Brahms graphical display tool showing the agents' hierarchical subsumed activities over time.

The Apollo 12 Brahms simulation allowed for detailed qualitative and quantitative work system analysis of the collaborative activities, communication, use of space, tools, and systems during the ALSEP offload. The result of the experiment proves that the Brahms multiagent programming language is powerful enough to represent the activities, collaboration, and communication of people and systems, as well as the influence of the geographical context on their behavior.

Point of Contact: M. Sierhuis
 (650) 604-4917
 msierhuis@mail.arc.nasa.gov

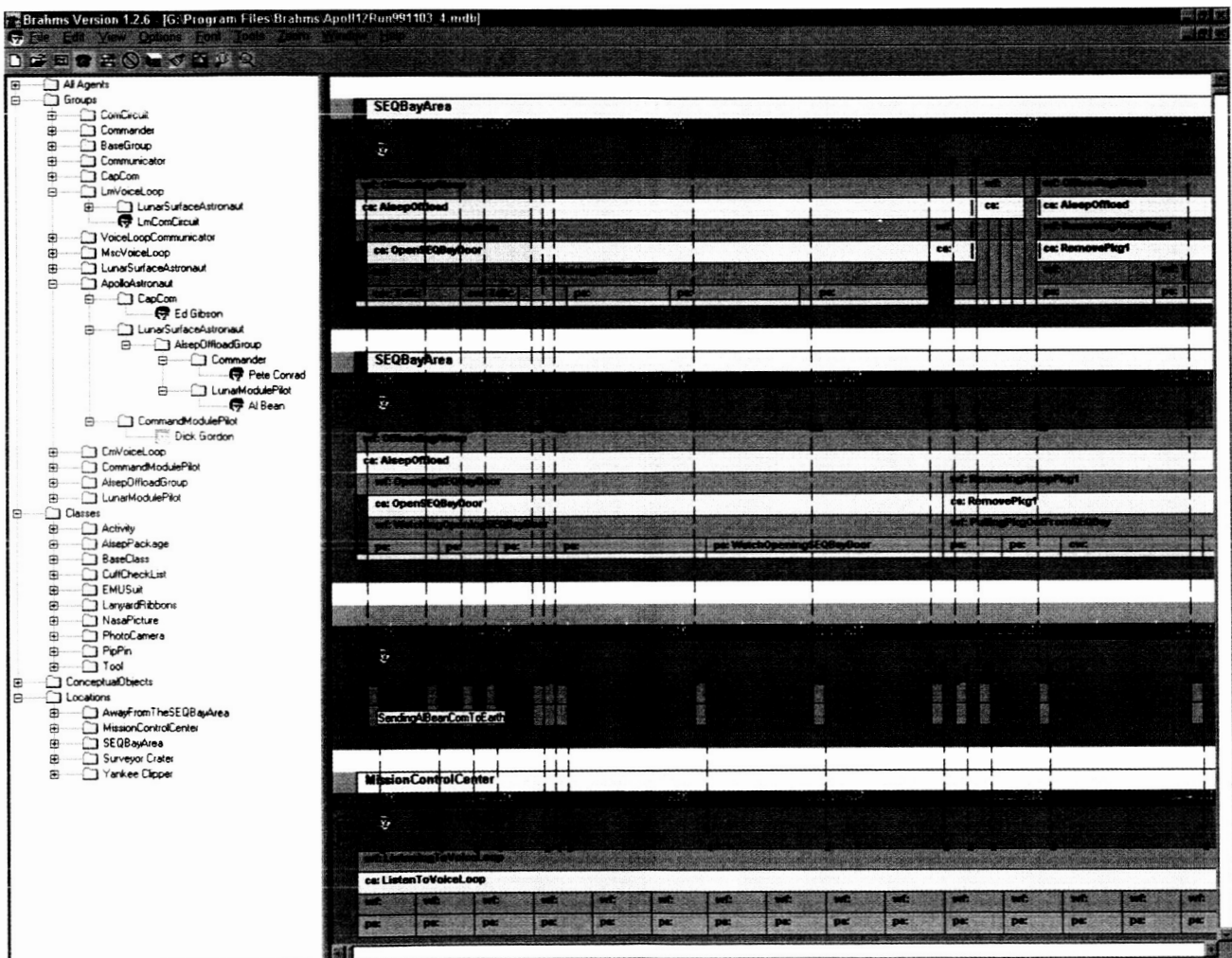


Fig. 2. Brahms graphical display tool.

Human-Centered Computing at Mission Control

John O'Neill, Roxana Wales

Ames researchers are studying how mission operations (ops) are conducted at Johnson Space Center Mission Control with the goal of improving the information technology support, practices, and facilities in which mission operations are conducted. This work has led to the development of "ops assistants," tools specifically designed to support the work of flight controllers in Mission Control (figure 1).

The first ops assistant that has been developed is a tool to support the logging and handover practices of flight controllers. During a shift, flight controllers "log," or record, all events of interest. At the end of the shift, the flight controller "hands over" to a new flight controller. The handover process involves the new flight controller getting up-to-date on any configuration changes, any open problems or issues, and any significant activities that occurred since he or she was last on the shift.

The logging/handover tool supports the logging and handover process by providing an interface for logging events of interest; it stores these events in a database, tracks open issues, and enables users to

construct narratives about the status of issues. One of the key benefits of storing logs and handover records in a database is enabling the search for similar problems across shifts, missions, and generations of flight controllers.

The first two applications for the logging/handover tool are supporting the work of the capsule communicator (CAPCOM) (the astronaut in Mission Control who is responsible for all conversations with the astronauts in the spacecraft) in both the Shuttle Mission Control Center and the International Space Station (ISS) Mission Control Center, and the Station Duty Officer in the ISS Mission Control Center.

In FY99, Ames researchers conducted ethnographical observations of CAPCOM and Station Duty Officer work practices in Mission Control, and conducted participatory design sessions. The next phase will be in situ evaluations of the logging/handover tool in use by CAPCOMs and Station Duty Officers in Mission Control.

In addition, this project is investigating how Mission Control's operations will need to change for Mars operations because it takes 20 minutes for communication signals to travel between Earth and Mars. Mission Control's operation has traditionally been set up for interactive real-time communications. In FY99, the first step in analyzing how Mission Control could operate for a Mars operation was taken by setting up a "Mission Control" operation for the Houghton Expedition. The Houghton Expedition is an annual Mars analog study conducted on Devon Island in the Arctic Circle. Fieldwork conducted both at Devon Island and Mission Control is helping to define the requirements for information and information technology support for future Mission Control operations.

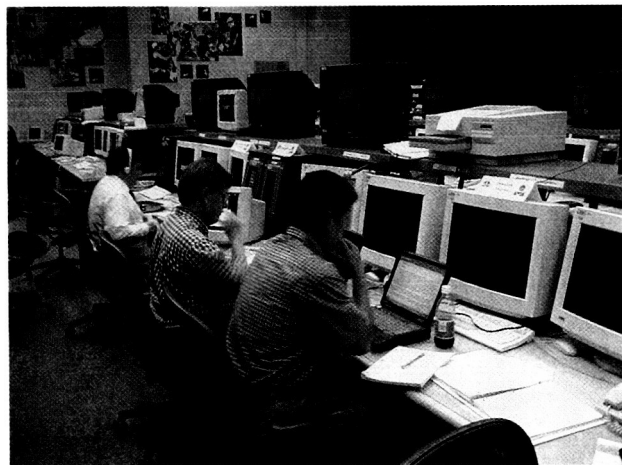


Fig. 1. Mission Control.

Point of Contact: J. O'Neill
 (650) 604-2975
joneill@mail.arc.nasa.gov

TECHNOLOGY TRANSFER

NASA Technology Helps Patients on Earth and Addresses Fundamental Questions on Human Autonomic Function

Patricia S. Cowings, William B. Toscano,
Hani Rashed

Dysautonomia is a term used to describe a wide variety of disorders in the human autonomic nervous system (ANS). An example of one such condition is Chronic Intestinal Pseudo-Obstruction Syndrome (CIPS), a rare disease of gastric dysmotility—the cause of which is unclear and for which pharmaceutical treatments are often ineffective. Symptoms of CIPS including nausea, vomiting, bloating, gaseousness and abdominal pain, and hypotension (low blood pressure) leave many patients with a very low quality of life. The primary purpose of this research is to determine if Autogenic-Feedback Training Exercise (AFTE) will provide relief from the symptoms of nausea and/or hypotension.

AFTE is a physiological conditioning procedure developed at Ames Research Center as a treatment for motion and space motion sickness. This method has been shown to reduce or eliminate the symptoms of motion sickness, and can be used to train control of blood pressure as a potential

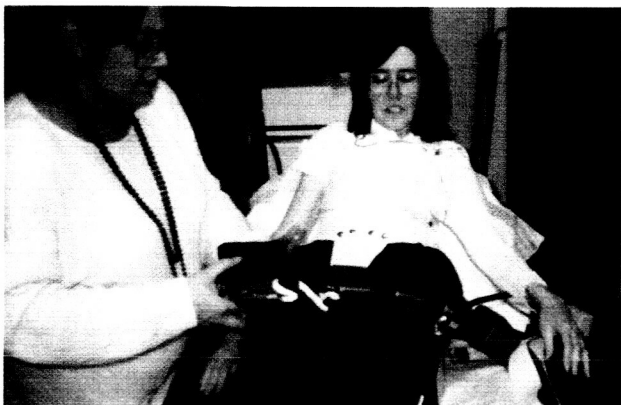


Fig. 1. An Autogenic Feedback Training Exercise (AFTE) test with a patient whose autonomic nervous system no longer functions properly. AFTE reduced her symptoms of nausea and improved (restored) gastric function.

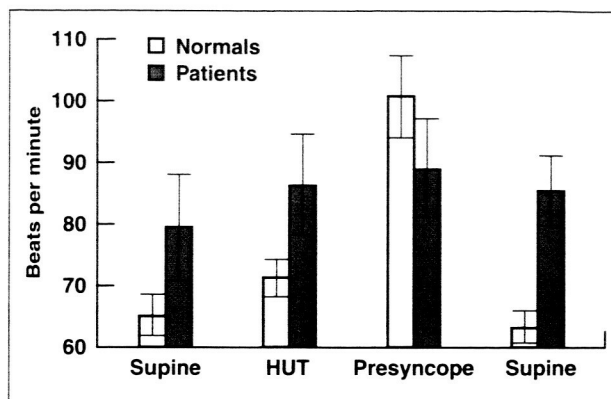


Fig. 2. A comparison of the average heart rate responses of normal subjects and patients during 60-degree head-up tilt (HUT) tests designed to induce presyncope (that is, just prior to fainting). $N = 8$ per group.

treatment for hypotension. The end result is a normalization of autonomic balance (see figure 1).

One of the first steps in this project was to determine differences in autonomic function between normal subjects and patients. Changes in physiological responses were measured during tests designed to induce the early symptoms of presyncope, for example, dizziness, and lightheadedness experienced just prior to fainting. The stimulus used for patients was a 60-degree head-up tilt (HUT) table test (figure 2). A much stronger stimulus of HUT combined with lower-body negative pressure (HUT + LBNP) was required to produce presyncope in normal healthy subjects who rarely reach presyncopal symptoms in response to 10-minute exposure to 60-degree HUT alone. The higher resting level of heart rate in CIPS patients during pretest baseline (supine), and their smaller heart rate increases in response to stimulation when compared to normal subjects, illustrates one aspect of autonomic dysfunction presented by patients with this diagnosis.

Physicians at the University of Tennessee have initiated AFTE trials with 23 patients. Following training, 78% of patients reported a reduction in gastric discomfort, with an associated "normalizing" of their gastric motility observed in electrogastrogram measures in 52% of the cases. However, only 26% showed an improvement in blood flow adjustment to posture. One possible explanation is that the patients received more training for control of gastrointestinal than cardiovascular responses, or that the

training effects were specific to gastrointestinal function in these patients. A second explanation concerns the training schedule and tools employed by University of Tennessee physicians, where too long an interval between lessons may have led to "forgetting" of learned responses and indicated the necessity for relearning.

Point of Contact: P. Cowings
 (650) 604-5724
 pcowings@mail.arc.nasa.gov

Perceptual Impact of Predictive Compensation for Time Delays in Virtual Environments

Bernard D. Adelstein, Stephen R. Ellis, Jae Y. Jung

In visually presented virtual environments (VE), measured displacement of the observer's head is used to position and orient the viewed simulation content in head-mounted or other types of video displays. Because of latencies within and between individual VE system hardware and software components, time delay in rendering the visual consequences of input

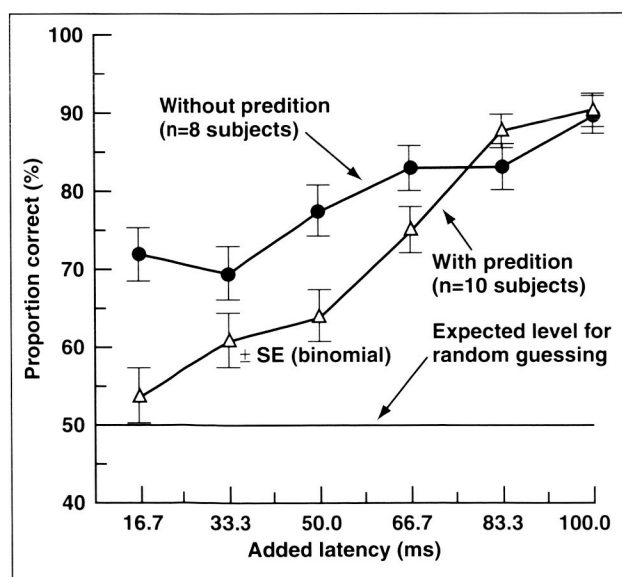


Fig. 1. Generic predictor and uncompensated VE discriminability.

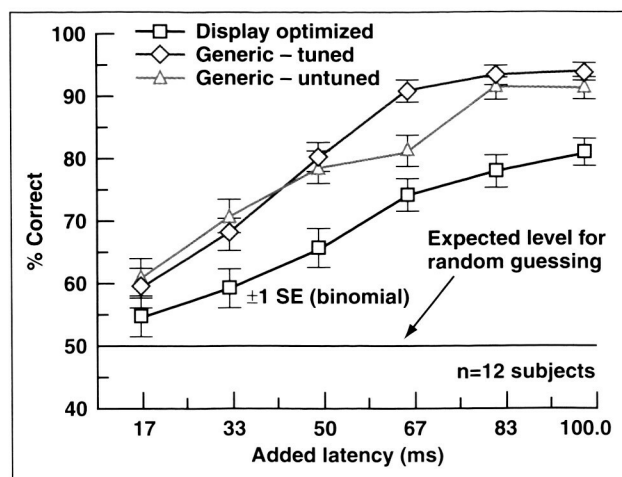


Fig. 2. Discriminability of different predictor designs.

motion is unavoidable. These delays disrupt image stability and, therefore, can disturb the observer's sense of presence and ability to perform useful work in a VE. Predictive compensation software, by extrapolating ahead in time, offers means to mitigate the consequences of VE delays. However, prediction introduces noise and overshoot artifacts into measured human motion that can be as perceptually disruptive as the original uncompensated VE time delay. The immediate objective of this work is to ascertain the perceptual impact of artifacts arising from predictive compensation of VE time delay, and ultimately to use this understanding to guide the design of novel compensation schemes.

A psychophysical method was developed that has allowed the first experimental assessments of the direct perceptual impact of VE motion artifacts induced by different predictive compensation schemes. In the experiments, subjects move their heads in a stereotyped periodic motion while viewing a VE that contains a single, simple, stationary object. Under one condition, the VE operates at its baseline latency. Under the second condition, an artificially added time delay is predictively compensated back to the baseline. In principle then, overshoot, noise, and any other artifacts of imperfect prediction should be the only source of discernible differences between the two. Subjects

are asked to judge in a signal-detection paradigm whether the sequentially paired stimuli differ. If the predictive compensation were perfect, subject judgments would be correct at the 50% rate expected for random guessing. The procedure is repeated for different levels of added time delay and different predictor compensator designs.

The protocol was employed in two experiments. In the first experiment, one group of subjects compared the baseline VE latency against the output of a generic predictor that compensated for added delays between 16.7 and 100 milliseconds. For the second group of control subjects, these added delays were not compensated in any way. Results (figure 1) show that the generic predictor, even though not tuned to the specific characteristics of the VE system hardware or software, offers benefit at the smaller latencies because its artifacts are less discriminable than the comparable uncompensated control condition delays.

This observation motivated a second study in which three competing predictor designs were evaluated, this time by a single group of subjects. One compensator was the untuned generic predictor from the first study. The second predictor had the same generic design but was tuned for the specific VE system and subject motion task. The third was optimized to minimize jitter artifacts specifically as rendered in a VE head-mounted display. Results (figure 2) indicate that, although tuning the generic filter had little effect, the display-based optimization made the prediction artifacts less discriminable to the subjects. Offline analysis indicates that the improved perceptual characteristics of the display-based optimization are due to its ability to predict slower volitional motion, while at the same time, unlike the other predictor designs, not magnifying high-frequency jitter.

It is important to note that though predictive compensation can diminish the perceptibility of VE latency, the designs tested have not yet attained the 50% discrimination level of "perceptually perfect" prediction. Moreover, predictor discriminability increased with the addition of time delay, indicative of the challenges in compensating the longer VE delays that will be associated with Internet and

satellite communication. The experimental assessment procedure described here, however, will serve to guide the development of new VE predictive compensation schemes and ultimately to validate whether these new designs can predict with the desired level of perceptual transparency.

Points of Contact: B. D. Adelstein/S. R. Ellis
(650) 604-3922/6147
dadelstein@mail.arc.nasa.gov
sellis@mail.arc.nasa.gov

Center for Health Applications of Aerospace Related Technologies (CHAART)

**Byron Wood, Louisa Beck, Brad Lobitz, Matt Bobo,
Cindy Schmidt, Jian Zheng**

The goal of the Center for Health Applications of Aerospace Related Technologies (CHAART) is to promote the application of remote sensing (RS), geographic information systems (GIS), and related technologies to issues of human health through education, training, and technology transfer. The primary focus of CHAART in FY99 was to support existing, and develop new, collaborations in the application of RS/GIS to studies of human health and surveillance of infectious diseases.

In FY99, CHAART completed another round in the training program for human health investigators. The goals of the training program have been to support human health investigators who integrate RS/GIS into their existing studies, and to facilitate the transfer of RS/GIS technologies to develop sustainable within-country capabilities. With these goals in mind, CHAART participated in several studies of remote sensing of various parasitic and infectious diseases around the world. At the end of FY99, CHAART had received new requests for RS/GIS training from investigators in India, Japan, Korea, Ghana, Ethiopia, Mali, Brazil, and the United Kingdom.

Members of the CHAART staff continued to collaborate with other investigators on the applica-

tion of RS/GIS to specific disease issues through Interagency Agreements with the National Institutes of Health (NIH), Centers for Disease Control and Prevention (CDC), National Oceanic and Atmospheric Administration (NOAA), U.S. Geological Survey (USGS), and university investigators. The collaborative applications of CHAART technologies include development of a national risk map for Lyme disease in the Northeastern U.S.; effects of climate change on both Lyme and Hantavirus in the U.S.; ecology of malaria vectors in Kenya; and cholera in Bangladesh and Latin America.

In addition, a new RS/GIS training collaboration in health applications is being developed with the World Health Organization's (WHO's) Special Programme for Research and Training in Tropical Diseases (TDR). This is an outgrowth of the 1995 joint TDR/CDC/NASA training workshop in Guatemala, the 1998 workshop in China, and the 1999 UNISPACE III conference in Austria. CHAART investigators continue to collaborate with the United Nations (UN)/WHO interagency Roll Back Malaria and HealthMap programs. A series of meetings were also held between representatives of the World Bank's AFTH-2, CHAART, and NASA Headquarters, Life Sciences Division to define the goals and objectives of the NASA/World Bank collaboration. This collaboration will also include participation by WHO's HealthMap group. An agreement between NASA's Ames Research Center and the World Bank's AFTH-2 program is currently under development and is expected to be signed in early 2000. New opportunities in training are also being discussed with NOAA (climate variability and health) and the USGS (database development and integration in health planning and surveillance).

NASA CHAART also participated in the development of a National Science Foundation (NSF)/NIH interagency Request for Proposals on the Ecology of Disease. The role of CHAART will be to provide RS/GIS training in support of funded research proposals. Discussions continue between CHAART and the staff of the U.S. Embassy to develop a U.S./Japan collaboration in RS/GIS and health.

Point of Contact: B. Wood
(650) 604-4187
blwood@mail.arc.nasa.gov

ASTROBIOLOGY IMPLEMENTATION

Geothermal Springs Camera and Sensor Probe

Jonathan Trent, John W. Hines, Charlie Friedericks, Richard Daily

The Geothermal Springs Camera and Sensor Probe (aka Mini Monster Cam) is a research instrument developed to support the search for life in extreme temperatures. The purpose of the probe is to find and observe eukarya (multicell organisms) in the depths of geothermal hot springs. Although we know that single-cell organisms proliferate in hot springs, the probe will help prove or disprove the existence of eukarya (Mini Monsters) that might feed on the single-cell organisms. This work is part of a larger effort to define the limits of life on Earth to help narrow the search for life on other planets. During a deployment to Yellowstone National Park (see figure 1), the probe was lowered 60 feet into geothermal springs with temperatures up to 120 degrees Celsius.

The 5-inch-diameter probe holds two underwater cameras, a dissolved oxygen sensor, a pH and temperature sensor, and a pressure (depth) sensor. Each camera and sensor has a 100-foot cable; this setup and a steel pull cable are covered with a plastic sheath for ease of handling. The sensors and cameras are connected to an instrument case that contains the system batteries, two digital video monitor/recorders,

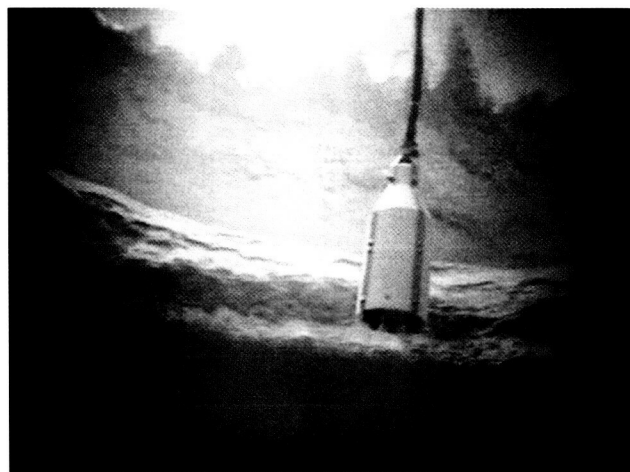


Fig. 1. The probe enters a hot spring at Yellowstone.

electronic instrumentation for the sensors, and a laptop computer for data viewing and storage (figure 2). The instrument case is specially fitted on a backpack for use at field sites inaccessible to vehicles. To precisely position the probe over the springs, a rigging system of tripods, ropes, and pulleys is set up. The rigging allows for safe operation around the deadly hot pools while making minimal environmental impact.

The two cameras in the probe are commercially made cameras designed for inspecting hot plumbing. One camera focuses to infinity and the other has a macro lens to look closely at life forms directly in front of it. The probe can be fitted with removable bait baskets in front of the camera to enhance the prospects of observing life in extreme temperatures. Exploring the biology of hydrothermal vent systems on Earth has piqued NASA's interest because it is currently thought that hydrothermal vent systems are the most likely habitats for life on Mars and Europa, a moon of Jupiter.

Point of Contact: M. Skidmore
(650) 604-6069
mskidmore@mail.arc.nasa.gov

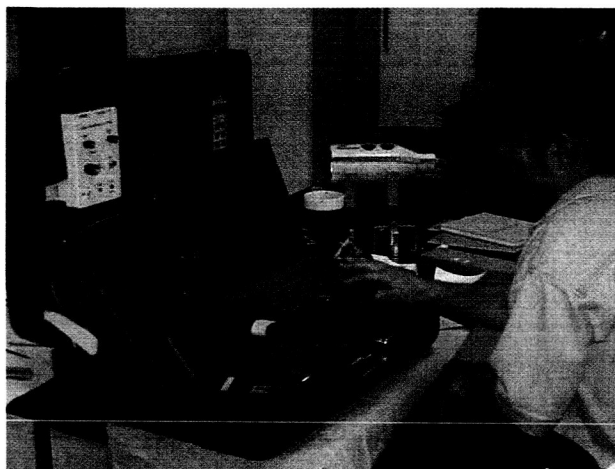
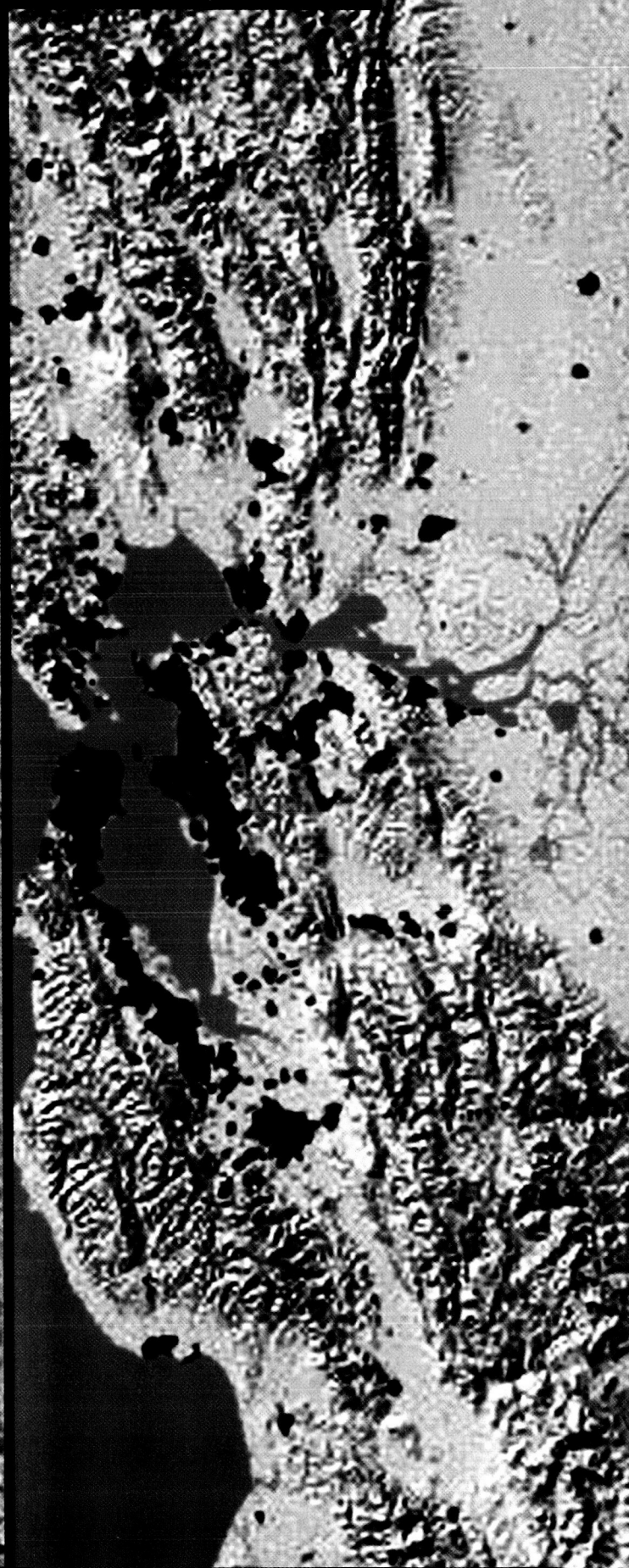
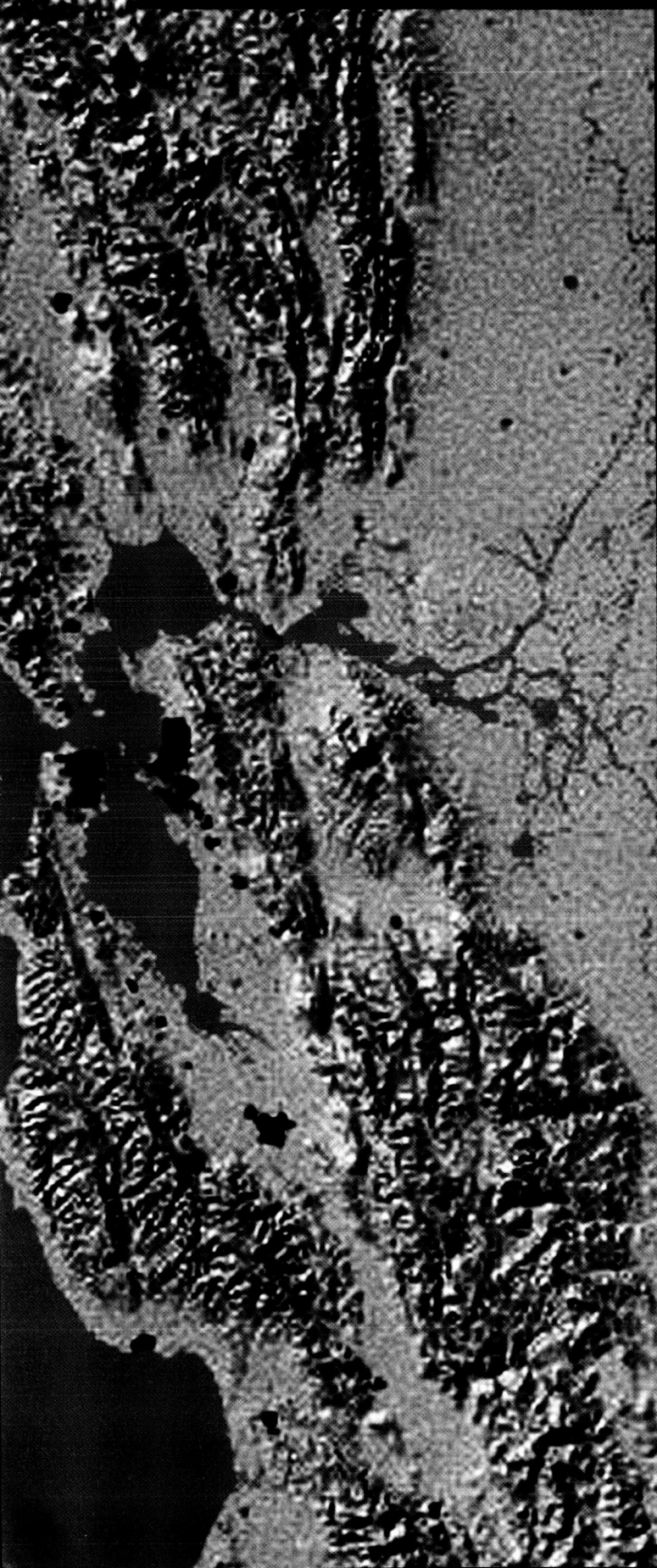


Fig. 2. Testing at ARC.

Earth Science Enterprise





Overview

NASA's Office of Earth Science (OES) studies the total Earth environment: atmosphere, ice, oceans, land, and biota, and their interactions in order to understand the effects of natural and human-induced, near-term changes of the global environment, and to lay the foundation for long-term environment and climate monitoring and prediction. During FY99, numerous research and technology objectives were achieved that directly address the principal goals of the OES Enterprise, that is, to

- Expand scientific knowledge of Earth's environmental system
- Enable the productive use of OES science and technology
- Disseminate information about Earth's system

Ames Research Center supports the OES by conducting research and by developing technology with the objective of expanding our knowledge of Earth's atmosphere and terrestrial ecosystems. These are also goals of the Agency's astrobiology research and technology efforts, for which Ames is the lead Center. A complementary objective is to apply the knowledge thus gained to solving practical, everyday problems and to transfer the technology and knowledge to users outside NASA.

Key components of the Earth Science Enterprise research programs at Ames include the study of the physical and chemical processes of biogeochemical cycling; the dynamics of terrestrial ecosystems; the chemical and transport processes that determine atmospheric composition, dynamics, and climate; and the physical processes that determine the behavior of Earth's atmosphere and those of other solar system bodies.

Time series of urban growth (shown in black) for the San Francisco Bay Region of California. Data were derived from historical sources and satellite imagery.

At Ames, scientists and technical personnel design methods and means for making remote sensing and in situ measurements, develop them, and use them in making experimental measurements. In addition, they use airborne and satellite sensor data to perform computer simulations of atmospheric and ecosystems processes in efforts to understand the exchanges that occur between the biosphere and the atmosphere.

Ames scientists conceive and develop advanced instrumentation to meet the measurement requirements of all supported enterprises, emphasizing both airborne and selected spacecraft sensors. Project managers and project scientists provide science-mission management and science leadership for major NASA science programs as well as for other agency science programs. Staff scientists create and develop applications programs that utilize both proven and developing technology. Additionally they transfer developed scientific knowledge and technology to commercial and private interests, to national and international governmental agencies and ministries, to other disciplines, and to educational institutions.

Principal research concerns include environmental issues related to stratospheric ozone depletion, perturbations in the chemical composition of the atmosphere, and climatic changes resulting from clouds, aerosols, and greenhouse gases. The development and application of new technologies that are required to provide insight into these matters are of special interest. Numerous state-of-the-art instruments are flown successfully, and significant data are collected for stratospheric and tropospheric research.

The Airborne Sensor Facility (ASF) provides remote sensing support for Office of Earth Science investigations, and for calibration and validation studies for the Earth Observing System (EOS). ASF is responsible for maintaining and operating a suite of OES facility sensors that are made available to the science community at large through the NASA flight request process. The systems are flown on various NASA, U.S. Department of Energy, and other aircraft, as required.

The ASF has component laboratories for data processing, flight operations, sensor calibration,

systems development, and data telemetry. Current activities are centered on the moderate resolution imaging spectrometer (MODIS) and the advanced spaceborne thermal emission and reflection radiometer (ASTER) airborne simulators (the MODIS Airborne Simulator, MAS, and the MODIS ASTER instrument, MASTER), which are being used to characterize calibration sites and to develop algorithms for the new EOS AM-1 satellite systems. These data are processed into a calibrated Level-1B product at the ASF, and delivered to the instrument science teams via the EOS Distributed Active Archive Centers (DAACs).

Research results and technology developments are published in the scientific literature. Additionally, many of these results are disseminated to the commercial and educational communities, thereby contributing to a better public understanding of the Earth Science Enterprise within NASA.

A Design Model for the Digital Array Scanned Interferometer

Stephen E. Dunagan, Philip D. Hammer

An instrument model has been developed for the digital array scanned interferometer (DASI) sensor. This model predicts instrument performance in the context of specific measurement applications, and may be used to evaluate the instrument for a range of potential missions. The model may also be used to tune a design to meet specific measurement requirements, and it provides the foundation for onboard adaptation of the sensor for mission-specific measurements in a "smart-sensor" environment.

The DASI instrument is capable of acquiring remotely sensed imagery with (dimensionless) resolving power in the range of 10 to 1000. A DASI is remarkable for its compact optical design and robust mechanical configuration. In contrast with more conventional grating and prism imaging spectrometers, the most important distinguishing characteristic is that spectral resolving power is not directly dependent on the input slit aperture width, permitting very high optical throughput for carefully designed systems. The type of DASI discussed here operates in "pushbroom" mode, relying on spacecraft or aircraft motion to sweep out the along-track spatial dimension of a remotely sensed image. The sensor comprises an objective, input slit aperture, collimated interferometer section, imaging optic, and focal plane arrays (FPA). The interferometer section relies on polarization optics, a bi-refrigrant Wollaston prism, and an anamorphic optical component to create an interferogram across the along-track dimension of the FPA, which is a real-time analog to the scanned output of a Michelson interferometer.

The instrument model incorporates ideal optics relations for predicting imaging and magnification for the objective, collimating, cylindrical, and focusing lenses. The equations that comprise the model permit calculation of the along-track instantaneous field of view as a function of input slit aperture width, and also the straightforward cross-track angular resolution and swath angular width. The along-track spatial

resolution is degraded by motion of the spacecraft (aircraft) during the frame integration time of the array detector, resulting in an elongated effective along-track angular resolution.

Detailed modeling of interferometric phenomena within the sensor and translating this information to spectral resolution and bandwidth specifications is more complex. Spectral resolution is a function of the maximum path difference. (This statement is also true for a grating spectrometer, because it is the number of grooves that gives the theoretical resolving power. The product of the number of grooves and grating groove spacing is the grating width, or path difference over which beams interfere to yield the spectrum). The limiting effective aperture for a well-designed DASI system is the width of the detector array, which may be related to an effective aperture in the Wollaston by means of the magnifications associated with the imaging lens and (anamorphic) cylinder lens. These dimensions permit the calculation of a maximum wave number resolution and corresponding wavelength resolution.

Other important modeling considerations include the evaluation of clear aperture requirements within the instrument, and the effect of real optics on the interference and imaging functions of the sensor. Vignetting of the interferogram (in one or both dimensions of the array) is minimized by proper optical design choices. The amplitude effects of vignetting can be accounted for during calibration. However, the signal-to-noise ratio (SNR) suffers as detected flux decreases because of vignetting and/or cosine effects related to the large field of view the DASI achieves in the spatial dimension. The projection of the array width to the plane of fringe localization within the Wollaston is a good indicator of the along-track clear aperture requirement for the collimated section.

The cross-track (y) dimension is subject to other constraints. The effective slit length requirement based on utilization of the entire array detector may be calculated from the projection of the array length to the slit. Nearly parallel skew rays entering the system from the periphery of object space (located near infinity) are focused by the objective lens to the

edge of the slit. Rays from the aperture edges of the objective lens must traverse the entire interferometer without clipping in order to avoid vignetting effects that precipitate undesirable loss of intensity (and SNR) at the edges of the FPA. The refraction of rays in the zero-power polarizer, Wollaston prism, and cylindrical lens elements in the collimated section of the interferometer may be estimated by evoking a $\sin(u) \cong \tan(u)$ approximation. This analysis draws attention to the need for very fast collimating and imaging lenses. Alternatively, the instrument field of view (limited by the combination of objective focal length and slit length) and light gathering capability (limited by the f-ratio of the objective) may be reduced to meet the practical aperture limitations placed on the imaging lens.

This model has been formalized in concise mathematical form and prepared for publication. Ongoing work is directed at the development of model elements for two additional instrument characteristics that are very important for matching an instrument design to a particular application. These include the modeling of instrument throughput, including SNR as a function of spectral reflectance and atmospheric conditions, and the instrument lineshape. Work is also under way on a ray-tracing model for generalized two-beam interferometric instruments that will enable the formulation of more advanced designs and the realization of the full potential of DASI-type instruments. William H. Smith (Department of Earth and Planetary Sciences, Washington University) collaborated in this work.

Point of Contact: S. Dunagan
(650) 604-4560
sdunagan@mail.arc.nasa.gov

Fires, Floods, and Deforestation— Disaster Management Using Remote Sensing Technology

James A. Brass, Vincent Ambrosia, Robert Higgins

Worldwide, 70 major disasters requiring international assistance occur each year. These disasters result in 133,000 deaths, 140 million homeless, and \$440 billion in property damage. In the last decade, U.S. property loss has averaged \$54 billion per year. Obviously, disasters are expensive to manage and they result in destruction to homes and businesses, and loss of commerce and lives.

Through NASA's Office of Earth Science Natural Hazards Program, technology is being developed and tested to support the management mitigation of natural and man-made disasters. In cooperation with the U.S. Forest Service Riverside Fire Laboratory, an aircraft system has been developed to collect visible, infrared, and thermal data for disaster characterization and monitoring. The digital data are compressed onboard the aircraft and sent to the Internet for data distribution and information extraction.

Two major efforts were completed in FY99. The U.S./Brazil Global Change and Environmental Monitoring Program was continued to characterize fire effects and deforestation on the rainforest and savanna ecosystem of northern Brazil. This effort resulted in describing the variation in fire types throughout both ecosystems; differing fire intensities and duration will result in variation in nutrient movement, greenhouse gas generation, and plant succession. In addition, the relationship between deforestation and fire occurrence was examined to determine the role of fire in deforestation activities.

Gigabytes of image data were collected over the northern part of Brazil. Preliminary results indicate a large variability between fires and within fires (often flame temperatures range between 600 degrees Centigrade (°C) and 1000°C). In addition, fire characteristics such as the duration of smoldering and flaming activity within fires were extremely variable, resulting in different trace-gas species and amounts being produced by the fires.

The second major effort in FY99 was the demonstration and operational use of remote sensing for fire management. The Airborne Infrared Disaster

Assessment System (AIRDAS) onboard the U.S. Forest Service (USFS) twin-engine Navajo was used to detect and characterize wildland fires and prescribed burns for various government agencies. The AIRDAS is a unique, four-channel line scanner that is well calibrated for measuring fire intensities and fire-line dimension. The data collected during these missions supported agency operations as well as NASA's fire research objectives. Multiple flights were made over wildfires in California to support firefighting activities and mitigation efforts. Additional flights were made for the government of Mexico, Bureau of Indian Affairs (Colorado), National Center for Atmospheric Research (Alaska), and Association of Bay Area Governments (Diablo Mountains). In all cases, the AIRDAS characterized fire-front movement, smoke production, and fire intensity for near-real-time management objectives and research applications. The results of these flights demonstrated the utility of AIRDAS for disaster management and provided fire information valuable to ecosystem and atmospheric research.

Collaborators in this research include Philip Riggan and Robert Lockwood (U.S. Forest Service), João Antonio Peréira (IBAMA, Brazil), Eric Stoner (U.S. Aid for International Development—Brazil), Heliosa Miranda and Antonio Miranda (University of Brasilia, Brazil), and Thelma Krug (Brazilian Space Institute, Brazil).

Point of Contact: J. Brass
(650) 604-5235
jbrass@mail.arc.nasa.gov

Modeling Leaf and Canopy Reflectance

Lee Johnson, Christine Hlavka

Leaf/canopy model simulations and measured data were used to derive information on the form and strength of the nitrogen (N) "signal" in near-infrared (1100–2500 nanometer (nm)) spectra of fresh leaves. Simulations across multiple species indicated that in total, protein absorption decreased near-infrared reflectance and transmittance by up to 1.8% and 3.7% respectively, and all other inputs held constant. Associated changes in spectral slope were generally in the range of $\pm 0.02\%$ per nanometer. Spectral effects were about an order of magnitude more subtle for a smaller, though potentially ecologically significant, change in N concentration of 0.5% over measured. Nitrogen influence on spectral slope was fairly consistent across four empirical data sets as judged by wavelength dependence of N correlation. The observed and simulated data showed similar trends in sensitivity to N variation. Further, these trends were in reasonable agreement with locations of absorption by protein-related organic molecules. Improved understanding of the form and strength of the N signal under differing conditions may allow development of reasonably robust spectral measurement and analysis techniques for "direct" (based strictly upon N-related absorption features) N estimation in fresh leaves. A pragmatic approach for remote sensing might additionally consider surrogate measures such as chlorophyll concentration or canopy biophysical properties.

Collaborators in this research include Barry Ganapol (Departments of Aerospace/Mechanical Engineering and Hydrology/Water Resources, University of Arizona) and Barbara Bond (Department of Forest Science, Oregon State University).

Point of Contact: L. Johnson
(650) 604-3331
ljohnson@mail.arc.nasa.gov

New Approaches to Using Remotely Sensed Data for Mapping Biophysical Variables

Jennifer Dungan, Joseph Coughlan

Maps of biophysical variables are needed at many scales, from the field scale (for example, maps of fire risk) to the global scale (for example, maps of terrestrial biomass). In particular, biophysical variables concerning the quantity and distribution of vegetation amount are critical to many Earth Science studies. Current methods of predicting vegetation amount use remotely sensed images to provide a spatially exhaustive data source, and regression models and maximum-likelihood methods are typically used for producing maps from these images. Geostatistical approaches, which assume spatial dependence, have an untapped potential to map vegetation amount using information gained from images.

Two geostatistical methods, cokriging and conditional simulation, were contrasted with regression in terms of their accuracy and uncertainty description. For a synthetic data set constructed from imaging spectrometer data, regression was most accurate when ground and spectral variables were very closely related. Cokriging was more accurate in all other situations. Conditional simulation, though not as accurate, was superior to the other two methods in reproducing the univariate and spatial characteristics of vegetation amount. For a real data set from western Montana (USA), over 300 ground measurements of conifer canopy cover made in each of two years by the U.S. Forest Service and collocated spectral index (normalized difference vegetation index (NDVI)) values from Landsat TM were used to predict canopy cover in a 97-square-kilometer subarea. The nonlinear regression model between canopy cover and NDVI had statistically identical parameters in both years, but prediction intervals were very wide, and accuracy was low at test points. Cokriged maps had much higher accuracy, but were affected by the small sampling fraction and clumped distribution of ground measurements. Conditionally simulated realizations using collocated cokriging displayed the desirable aspects of cokriging and at the same time presented plausible global and spatial

distributions of canopy cover and were, therefore, considered preferable to the cokriged maps.

Related work was accomplished on a case study to test the implications of using inaccurate estimates of vegetation type derived from remote sensing for the results of deterministic ecosystem models. A conditional simulation method was used to model inaccuracy, and the results were fed into the Carnegie/Ames/Stanford Approach (CASA) terrestrial biomass model. The range of results faithfully straddled the true answer, while a result that did not incorporate inaccuracy of the image-derived maps was too low.

Phaedon Kyriakidis of Stanford University collaborated in this research.

Point of Contact: J. Dungan
(650) 604-3618
jdungan@mail.arc.nasa.gov

Satellite Estimates of Terrestrial Biomass and the Effects of Deforestation on the Global Carbon Cycle

**Christopher Potter, Steven Klooster,
 Vanessa Brooks Genovese, Alicia Torregrosa,
 Matthew Bobo**

Investigators of the Ecosystem Science and Technology Branch are generating new global model estimates for terrestrial biomass sources of atmospheric carbon dioxide (CO₂). This ecosystem simulation modeling uses a combination of global satellite observations, predictions of above-ground biomass based on climate and satellite vegetation indexes, and the most current data on country-by-country changes in global forest cover (1990 to 1995), which are compiled regularly by the Food and Agricultural Organization (FAO) of the United Nations. The model estimates for carbon fluxes, which include forest area regrowth and expansion of carbon sinks in temperate and boreal forest zones, are based on the most recent global maps for observed climate, elevation, soils, plant cover, and changes in forest areas from natural and human forces.

Results of this global modeling analysis suggest that net terrestrial losses of CO_2 from changes in the world's forest ecosystems were between 1.2 and 1.3 petagrams (Pg) of carbon per year for the early 1990s (see figure 1). Forest regrowth can add about 0.09 Pg of carbon annually to the North American terrestrial carbon

sink. Hence, this ecosystem modeling indicates that total annual accumulation of atmospheric carbon in terrestrial ecosystems of North America could offset about one-fifth of the continental carbon source from fossil fuel burning in the late 1980s.

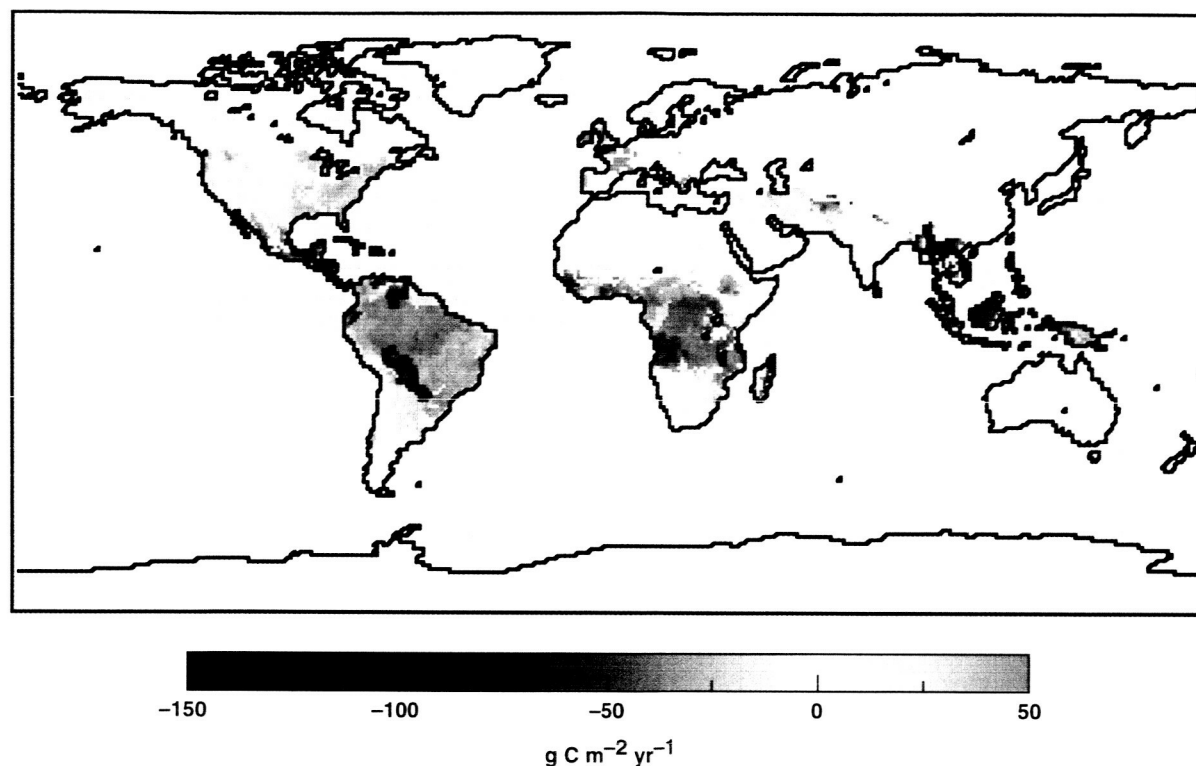


Fig. 1. Global carbon flux resulting from annual changes in forest area. Predictions are based on the satellite-derived NASA-CASA model predictions of standing plant biomass, combined with FAO (1997) forest conversion rates for 1990–1995. Negative flux values (–) indicate loss of carbon (C) to the atmosphere from deforestation, whereas positive flux values (+) indicate gains of C from the atmosphere resulting from forest regrowth or expansion.

Point of Contact: C. Potter
(650) 604-6164
cpotter@mail.arc.nasa.gov

Urban Dynamics—Analyzing Land Use Change in Urban Environments

**William Acevedo, Lora R. Richards,
Janis T. Buchanan, Whitney R. Wegener**

In FY99, the Earth Resource Observation System (EROS) staff at Ames continued managing the U.S. Geological Survey's (USGS) Urban Dynamics Research program, which has mapping and analysis activities at five USGS mapping centers. Historic land use reconstruction work continued while activities in geographic analysis and modeling were expanded.

Retrospective geographic information system (GIS) development—the spatial reconstruction of a region's urban land-use history—focused on the Detroit River Corridor, California's Central Valley (see figure 1), and the city of Sioux Falls, South Dakota. The Detroit River study is in collaboration with staff at the USGS Great Lakes Science Center in Ann Arbor, Michigan. The spatial history of land-use change and shoreline development was constructed in order to assess the human pressures that have affected the Detroit River ecosystem. Land-use change will be correlated with losses of fish and wildlife habitat along the river. The growing concern over the effects of sprawl and unchecked urbanization in California's Central Valley initiated a preliminary assessment of urban growth over time. The data were used to help decision-makers in educating the public regarding future growth and environmentally sustainable economic growth in the valley. The Sioux Falls, South Dakota, study was undertaken to examine the development patterns of a typical Midwestern city unrestrained by hydrologic or physiographic features. The transportation network and the extent of developed land were reconstructed for eight time periods. Regional planners and local educators will use the data to increase public awareness.

Geographic analysis work focused on the comparative analysis of urban land-use change for six selected cities. Population totals, area summaries, rates of change, historical events, and spatial patterns were compiled and are undergoing statistical analysis.

Modeling activities involved the continued collaboration with researchers at the University of California, Santa Barbara (UCSB), and the Environmental Protection Agency in modeling urban growth and land-use change in the Mid-Atlantic region. Additional funding from the National Science Foundation (NSF) initiated work between UCSB, USGS, and the Los Alamos National Laboratory in the development of an integrated environment for modeling urban growth.

EROS/Ames staff initiated a new project working together with local county planners and conservation groups in California's Central Valley to develop an integrated environment of data, scientific information, analyses, predictive models, advanced visualization techniques and decision support tools for improving the way scientific information is used in local decision making.

Collaborators in this research include Keith Clarke (University of California at Santa Barbara), Dave Hester (U.S. Geological Survey), Steen Rasmussen (Los Alamos National Laboratory), Bruce Manny (U.S. Geological Survey), and Carol Whiteside (Great Valley Center).

**Point of Contact: W. Acevedo
(650) 604-5299
wacevedo@usgs.org**

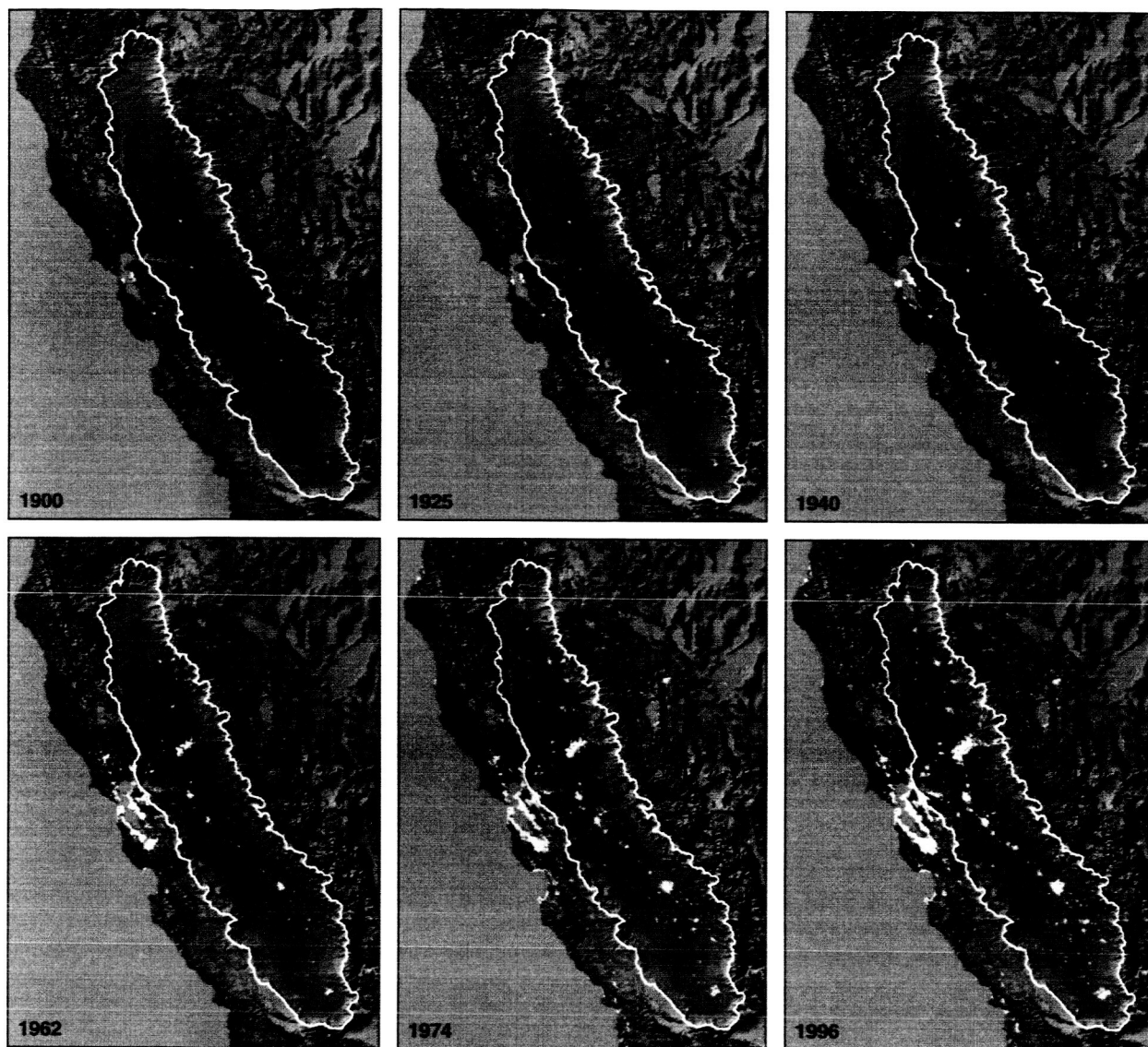


Fig. 1. Historical maps, remotely sensed imagery, and related farmland mapping surveys were used to reconstruct this temporal view of urban growth in California's Central Valley and the adjacent San Francisco Bay area. The Central Valley has a population of more than 5 million, a number that is projected to triple by 2040. The American Farmland Trust, a national organization that works to preserve agricultural lands, estimates that more than a million acres of Central Valley farmland will be lost to urbanization by 2040 if current growth patterns continue. Research on land-use change in the Central Valley will enhance the understanding of urban growth and its effects on people, the landscape, and the economy.

Calculation of Global Warming Potentials

Timothy J. Lee

The objectives of this project are to (1) calculate the global warming potential (GWP) of various halons that are either currently used or may be used in the semiconductor industry, and to (2) compare and contrast the GWP for these various halons in order to evaluate their relative merits with respect to their potential effect on the global environment. In order to accomplish these objectives, there was a need to calculate two quantities reliably: (1) the rovibrational transition energies, and (2) the integrated infrared (IR) band intensities.

Earth's average global temperature has been rising over the last decade, and several analyses have pointed out the global consequences of even a 2–3°C increase. Much has been said about the amount of carbon dioxide vented into the atmosphere by human activities, but the release into the atmosphere of other trace compounds such as hydrofluorocarbons (HFCs), hydrochlorofluorocarbons (HCFCs), chlorofluorocarbons (CFCs), perfluorocarbons, or other halons is likely to be more important. Some of these compounds are more than 100,000 times more effective as greenhouse gases than carbon dioxide, and because of their long atmospheric lifetimes, the effects of their presence will be felt for decades. In this study, investigation of the GWP of molecules employed in the semiconductor industry, either in the manufacturing process or in the cleaning process, is undertaken. Figure 1 shows that these compounds have the potential to close the "atmospheric window" in Earth's atmosphere, leading to significant global warming.

State-of-the-art methods now can calculate rovibrational transition frequencies to within a few wave numbers, more than adequate for this study, but less information is available regarding the calculation of accurate IR band intensities. Thus, the first study was devoted to the investigation of the levels of theory necessary to calculate reliable IR band intensities. This study was accomplished by first

searching the literature to determine a set of benchmark CFCs and HCFCs for which reliable experimental data exist for the IR intensities of their bands that appear in the "atmospheric window." Several levels of theory have been tested. Results indicate that modest levels of theory are adequate for calculating reliable GWPs, especially considering the fact that what is most important is the relative GWPs between various molecules. Agreement between experiment and theory for the benchmark molecules was excellent.

All these compounds possess vibrational frequencies in the "window" region that have large IR intensities because of the very polar nature of the bonds involving the halogen atom (leading to large intensities) and the [force constants/atomic masses] ratio, which causes several stretching and bending frequencies to appear between 700 and 1500 per centimeter (cm^{-1}). Estimates based on the IR intensities present in the window region indicate that these compounds are among those that are 100,000 times more effective greenhouse gases than carbon dioxide.

All of these compounds, however, are not equal when it comes to GWPs. Their relative GWPs depend upon two factors: (1) the total amount of IR absorption that occurs in the window region, and (2) the relative atmospheric (tropospheric) lifetimes. Other considerations can be used in deciding which compound to use in an industrial process, such as the fact that hydroxy radical (OH) will abstract a

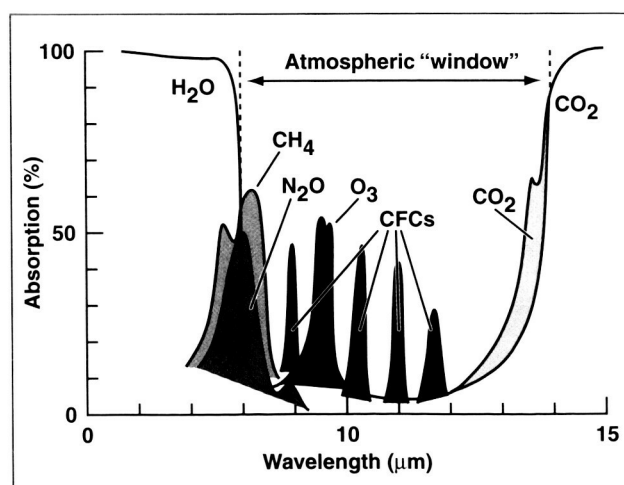


Fig. 1. Atmospheric window in the Earth's atmosphere and the absorption of IR radiation by CFCs in the window region.

hydrogen (H) atom much more readily than a halogen atom (because the second O-H bond in water is very strong relative to C-H bond energy). Consequently, HFCs and HCFCs have significantly lower tropospheric lifetimes (and GWPs) relative to similar CFCs or perfluorocarbons.

Although it will be possible to determine relative GWPs for different source gases relatively easily, all these compounds have significant GWPs (because of their large IR intensities in the window region). Hence, it is probably best for industries to adopt abatement procedures when using these types of compounds.

Point of Contact: T. Lee
(650) 604-5208
tlee@pegasus.arc.nasa.gov

Environmental Research Aircraft and Sensor Technology—New Technologies for Earth Science

Stephen S. Wegener, James Brass

The Environmental Research Aircraft and Sensor Technology (ERAST) project is an Aerospace Technology Enterprise (NASA Headquarters Code R) program designed to provide focus for critical technology development and flight demonstration that reduces the technical and economic risk of using remotely piloted aircraft (RPA) as a means to collect scientific data in a timely and cost-effective manner. A government industry alliance (ERAST) is flying RPA in science missions with 400-pound (lb) (182 kilogram (kg)) payloads to altitudes of 55,000 feet (ft) (16.7 kilometers (km)).

Ames has the leadership role in developing sensors and science missions for ERAST. In FY99, ERAST passed a major milestone by supporting the Uninhabited Aerial Vehicle/Atmospheric Radiation Measurement (UAV/ARM) Tropical Cirrus Mission from Barking Sands, HI. Ames provided the coordination to match science needs and ERAST flight opportunities to meet this milestone. ERAST sensor support also developed one of the key instruments flown by an Ames investigator. Seven science flights were

conducted during the four-week series. The total flight time above 16.7 km was 16.5 hours. Flights to 16.7 km were the highest the UAV/ARM payload has ever flown.

The ERAST Science and Sensor Element also promoted new RPA payloads and missions for atmospheric science, remote sensing, and others, including:

- Disaster management with Global Disaster Information Network (GDIN)
- Over-the-horizon (OTH) and real-time technologies for missions and vehicles
- Support of the development of the Earth Sciences Enterprise NASA Research Announcement for science and applications
- Promotion of the partnership between California Resources Agency—ARC and ERAST to systematically map California in a high-resolution sharable digital database
- Promotion of the Commercial Remote Sensing Program partnership with ERAST

The ERAST Science and Sensor Element also promoted educational and commercial outreach to support existing and planned RPA science activities at various conferences and exhibitions. One highlight included producing the Hawaii State Fair CD, which provided an overview of the ERAST, the Pathfinder, the Remote Sensing imagery from Hawaii, including flight maps, a mini-tutorial on remote sensing, and an explanation of how the imagery was acquired and manipulated. Examples of many images were provided along with simple procedures to access some 1400 images archived in Hawaii. Collaborators in this research include Susan Schoenung (Longitude 122° W), and Don Sullivan and Vince Ambrosia (Johnson Controls World Services).

Point of Contact: S. Wegener
(650) 604-6278
swegener@mail.arc.nasa.gov

Estimation of Aerosol Direct Radiative Effects from Satellite and In Situ Measurements

Robert W. Bergstrom, Philip B. Russell, Beat Schmid, Jens Redemann, Dawn McIntosh

Ames researchers have combined measurements from satellite, aircraft, and the surface to estimate the effect of airborne particles (aerosols) on the solar radiation over the North Atlantic region. These aerosols (which come from both natural and pollution sources) can reflect solar radiation, causing a cooling effect that opposes the warming caused by carbon dioxide. Recently, increased attention has been paid to aerosol effects to better understand the Earth climate system.

The researchers started with aerosol amounts estimated using the advanced very-high-resolution radiometer (AVHRR) instrument aboard the National Oceanic and Atmospheric Administration-11 (NOAA-11) satellite. Expressed in terms of light attenuation, or "optical depth," these aerosol amounts had been derived by other researchers for cloud-free days during the four seasons. The Ames team combined the satellite-derived aerosol optical depths with other aerosol properties (size distribution, light absorbing fraction, dependence of optical depth on light color) determined by aircraft measurements in two coordinated field campaigns. The first campaign was the Tropospheric Aerosol Radiative Forcing Observation Experiment (TARFOX) that was carried out off the eastern coast of the United States over the North Atlantic in the summer of 1996. The other campaign was the Second Aerosol Characterization Experiment (ACE-2) that was carried out over the North Atlantic off the coasts of Europe and North Africa in the summer of 1997. Ames researchers played significant roles in both of these experiments.

Figure 1 illustrates the calculated aerosol-induced effect on the net solar radiative flux at the tropopause during winter, spring, summer, and fall. As shown, the average flux changes are -1.7 , -4.8 , -5.1 , and -2.3 watts per square meter (W/m^2) for the winter, spring, summer, and fall respectively, -3.5 W/m^2 being the annual average. For aerosols with no absorption, the annual average is -4.8 W/m^2 .

The researchers used the International Satellite Cloud Climatology Project (ISCCP) cloud frequency data to estimate the impact of clouds on the aerosol effects. In general, clouds reduce the aerosol effects by attenuating the sunlight so that less can be reflected by the aerosol. Figure 1 shows that the clouds reduce the aerosol effect such that the regional averages fall to -0.8 and -1.1 W/m^2 for the absorbing and nonabsorbing aerosol, respectively.

These aerosol effects can be compared to a positive flux change of about 2.5 W/m^2 caused by the increases of carbon dioxide and other greenhouse gases over the past century. Thus, the aerosol effects (which come from both natural and pollution sources) are comparable, but opposite in sign, to the greenhouse gas effects. As shown by figure 1(c), within the aerosol plume coming off the eastern United States, the cloud-free, summer aerosol effect exceeds the greenhouse gas effect. Note that all the flux changes described above are at the top of the troposphere (~ 10 kilometer (km) altitude). Other work by the Ames team shows that aerosol-induced flux changes at the Earth surface can be larger still.

Finally, the study compared the satellite-derived results to those of previous studies that used chemical transport models. Although the methodologies have significant differences, the results of the study appear to agree with recent estimates from the chemical transport models.

Point of Contact: P. Russell
(650) 604-5404
prussell@mail.arc.nasa.gov

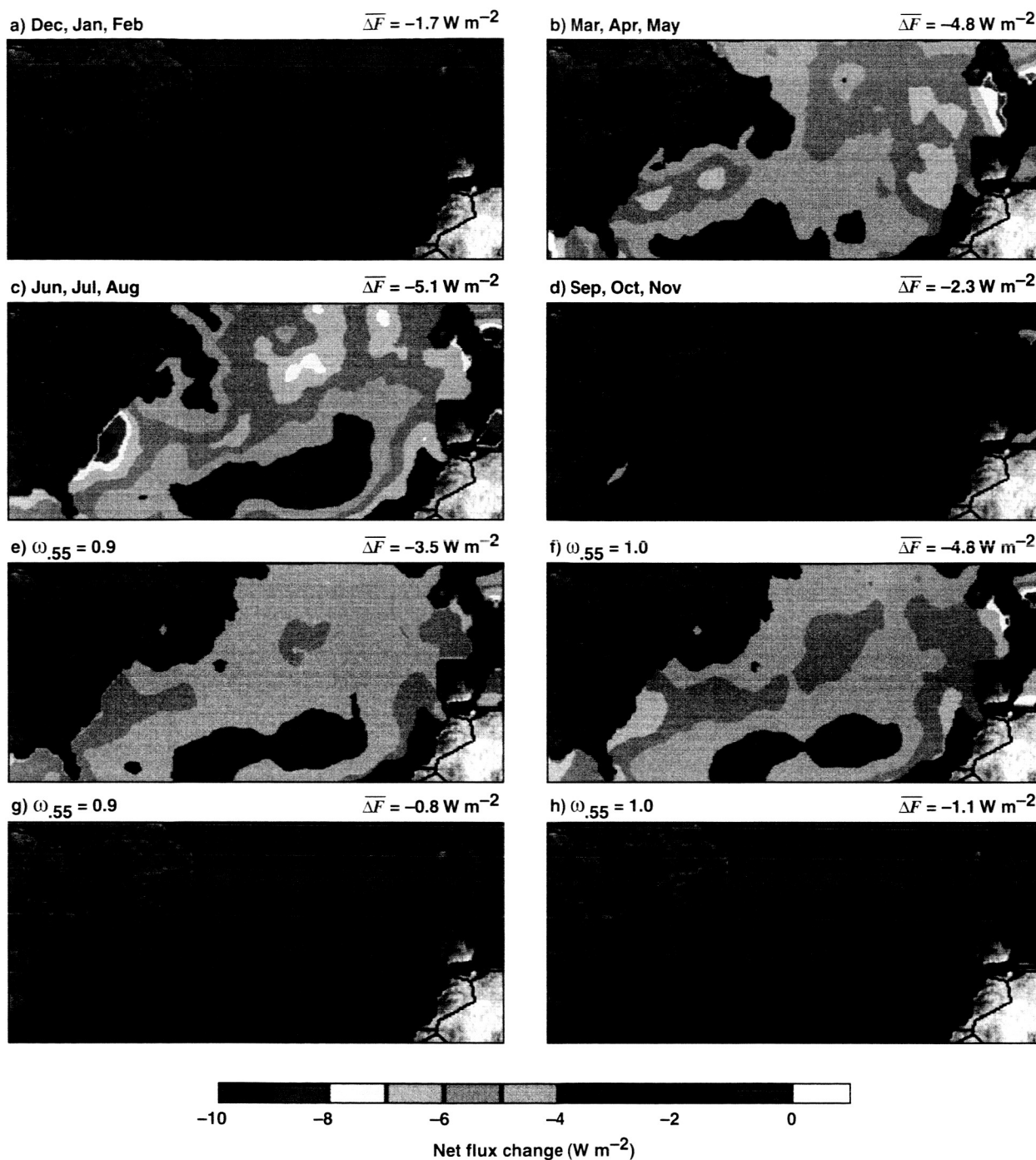


Fig. 1. Aerosol-induced change in net shortwave flux at tropopause ($\lambda < 4 \mu\text{m}$). Results are based on AVHRR/NOAA aerosol optical depths (AODs) reported by Husar et al. [1997] for the period July 1989–June 1991. The aerosol model uses a typical column size distribution from TARFOX. Values above each frame are averages for the 25° to 60° N region, excluding African dust. (a–d) seasonal average with single scattering albedo $\omega(550) = 0.9$; (e–f) annual average (no clouds) for $\omega(550) = 0.9$ and $\omega(550) = 1.0$; (g–h) annual average (ISCCP clouds).

Quantifying the Intercontinental and Global Reach and Effects of Pollution

Robert B. Chatfield, Zitan Guo

The Atmospheric Chemistry Modeling Group is participating in an international effort to explore the projected interactions of the atmosphere with biota, human activity, and the natural environment over the next three decades. The group uses computer simulations and statistical analyses to compare theory and observations of the composition of the lower atmosphere. This study of global habitability change is part of a more ambitious activity to understand global habitability. This broad planetary understanding is central to planetary habitability, biomarker detection, and similar aspects of Astrobiology.

The group has made highly detailed studies of immense intercontinental plumes that affect the chemistry of the global atmosphere, especially the region below the ozone (O_3) layer whose chemical composition defines the conditions for healthy humans and the biosphere. For some decades there has been concern about the pollution from cities and industrial burning and its possible effect in increasing smog ozone, not only in continental regions, but also in plumes that spread downwind. Recently, there has been new concern about another kind of pollution plume. Projections for a greatly expanded aircraft fleet imply that there will be plumes of nitrogen oxides (NO_x) from jet exhaust in the Northern Hemisphere downwind of major air traffic routes. Both of these are tied to large-scale O_3 in the troposphere, where it is toxic to humans and plant tissues.

Modeling at Ames, confirmed at the Royal Dutch Meteorological Institute, suggests that the NO_x pollution emitted from aircraft engines plays a surprisingly large role in producing pollutant ozone between 5 and 12 kilometers (km) in the atmosphere, that is, below the main O_3 layer shield. This could be determined only by close analysis of observed data and computer simulations. A large airborne observational project, the SASS Ozone and Nitrogen Oxides Experiment (SONEX), was mounted over the North Atlantic in October and November, 1997. The modeling group provided detailed pollution weather forecasts to the aircraft scientists in the field for planning and immediate analysis of the measurements. The group simulated chemical

species with separately defined sources and simple transformation rules. Separate tracers were used to follow NO_x from industry and cities, from the newly suspect aircraft, and from lightning. Because there is no directly measurable indicator of aircraft-origin NO_x , simulations like those done at Ames are the only clear indicator of origins. Figure 1 shows the first-principles calculation of the effect of aircraft on the atmosphere at aircraft flight level, and also the amount that best matches observations. Careful statistical techniques were used to match the "fingerprints" (similar patterns of ups and downs) of observed NO_x peaks with the simulated tracers. They were "robust" against intermittent failures of simulation, such as missed weather forecasts. The second scale in figure 1 shows the amount required by such matching. In summary, the group has shown that the effects of aircraft emissions are widespread, they contribute much to the upper tropospheric chemistry, and they may be underestimated by perhaps a factor of two or more.

More theoretical studies have also aided Ames research. Work with Dalhousie University, Nova Scotia, has helped unravel the processes of ozone "superproduction." Not only NO_x , but also a supply of active photochemical species—radicals such as hydroxyl radical (OH) and hydroperoxy radical (HO_2)—are required to describe the O_3 and oxidation chemistry of the upper troposphere. One proffered counter-explanation of O_3 superproduction is that there might be an unmeasured, unnamed source of these radicals that could explain the O_3 production results, such as acetone. Analyses have shown that such sources should decrease the available NO_x to much lower quantities. Although this work has not pinpointed a solution to the "superproduction" dilemma, it has helped make connections between the situational modeling and global analysis simulations.

The Atmospheric Modeling Group has continued its highly detailed studies of global lower-atmospheric chemistry to describe the spread of smog-like pollution around the world. Studies have documented the exact African sources of pollutant compounds such as carbon monoxide (CO) and O_3 , which the NASA DC-8 aircraft discovered in the middle and upper troposphere over Tahiti and even more remote regions of the Pacific Ocean. Previous ideas held that this region was a permanently pristine

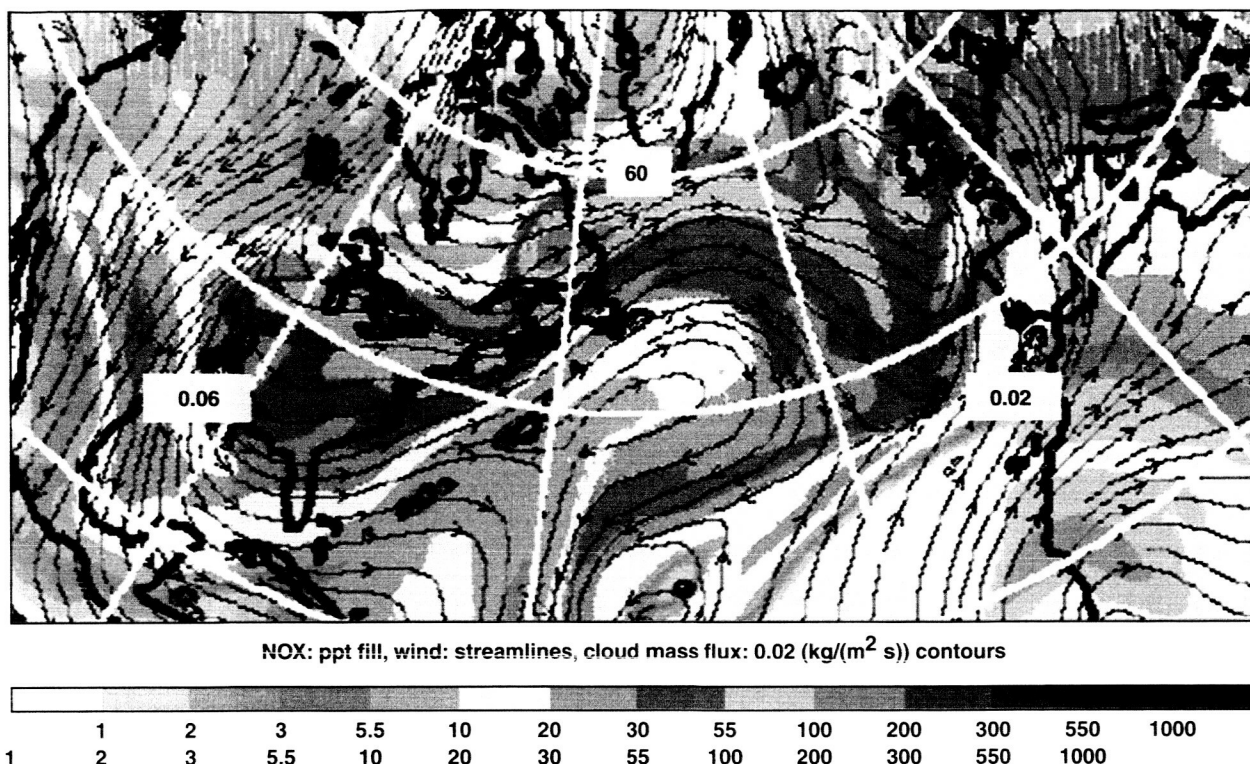


Fig 1. Spread of chemically active NO_x from main aircraft corridors throughout the North Atlantic Ocean. The first scale, molecules per 10¹² molecules (ppt), comes from direct calculation. The lower scale, however, which is almost two times higher, compares more directly to the data.

region. However, work recently published by the group has illustrated the role of thunderstorm clouds over the continents of Africa and South America in producing large plumes of pollution. Additionally, that work made important quantitative checks on the simulation of cloud venting.

The group has also shown how long, coherent strands of pollution were found to pulse along the subtropical jet region. Regions of the South Pacific once thought to be months removed from pollution effects were sporadically affected within 5 to 15 days. Individual storms over Africa were pinpointed as major pollution sources in several cases, but the large-scale buildup over the burning continents also contributed. This work continued the group's study of important CO features observed from the NASA Measurement of Air Pollution from Space (MAPS) satellite sensor, and on board the NASA DC-8, during the Pacific Exploratory Mission, Phase A (PEM-T A). These studies prepare for the instrument named

MOPITT, which measures CO from the Earth Observing System (EOS) Terra satellite. Collaborators in this research include Ian Folkins (Dalhousie University, Halifax, Nova Scotia), and Glenn Sachse (NASA Langley Research Center).

Point of Contact: R. Chatfield
 (650) 604-5490
chatfield@clio.arc.nasa.gov

SAGE III Ozone Loss and Validation Experiment

Michael Craig, Stephen Hipskind, Wendy Dolci

The SAGE III Ozone Loss and Validation Experiment (SOLVE) campaign is cosponsored by the NASA Upper Atmosphere Research Program, the Atmospheric Effects of Aviation Project, the Atmospheric Chemistry Modeling and Analysis Program, the Earth Observing System Validation Program, and the European Science Commission. It is the largest field experiment ever conducted to examine stratospheric ozone levels over the Arctic region. The mission will be conducted during the 1999–2000 winter from Kiruna, Sweden, and will employ multiple aircraft, balloons, ground-based instruments, satellites, and an extensive theory team to examine the processes that control polar to midlatitude stratospheric ozone levels. The experiment will acquire correlative measurements needed to validate the Stratospheric Aerosol and Gas Experiment (SAGE) III satellite to help quantitatively assess high-latitude ozone loss. The results of the SOLVE campaign will both expand the understanding of polar ozone processes and provide greater confidence in current ozone monitoring capabilities.

Managed by the Earth Science Project Office at Ames Research Center, the SOLVE campaign includes over 350 scientists, engineers, and technicians from many NASA centers, other Government agencies, and universities across the world. More information, including the experiment overview, goals, schedule, instrument payloads, mission details, and science team members, can be found at the SOLVE Web page (<http://cloud1.arc.nasa.gov/solve>).

The first part of the SOLVE campaign began in November, 1999, with launches of in situ and remote stratospheric balloon payloads. These launches, just prior to the appearance of cold stratospheric temperatures below 195 K, enabled the experiment to obtain samples of the polar vortex in its initial condition prior to the appearance of polar stratospheric clouds (PSCs). These observations were important for interpreting the subsequent cold temperature chemistry and ozone loss later in the experiment.

The NASA DC-8 began its first deployment on December 1, 1999. The objective was to obtain

remote measurements of the initial states for ozone (O_3), reactive nitrogen (NO_y), reactive chlorine (Cl_y) compounds, aerosols, and the nitric acid (HNO_3) and water (H_2O) vapors that will eventually condense to form PSCs. The DC-8, however, observed colder than normal temperatures in the early vortex lifetime, and observed Type-1a PSCs on several flights. Including the transits, the DC-8 had a total of eight successful flights and made the first coordinated science flight over Russia.

Jim Anderson (Harvard University), Paul Newman and Mark Schoeberl (NASA Goddard Space Flight Center), and Owen B. Toon (University of Colorado) collaborated in this research.

Point of Contact: M. Craig
(650) 604-6586
mcraig@mail.arc.nasa.gov

Stratospheric Tracer-Field Measurements with a New Lightweight Instrument: The Argus Spectrometer

Max Loewenstein, Hansjürg Jost,
B. Jeffries Greenblatt

Argus is a new, lightweight spectrometer designed for measuring the stratospheric nitrous oxide (N_2O) and methane (CH_4) tracer fields in situ from balloons and aircraft. It is a second-generation instrument drawing on the experience gained with the very successful Atmospheric Laboratory for Applications and Science (ATLAS) instrument measuring N_2O and flying on the NASA ER-2 since 1986.

During the past several years Argus was part of the Observations from the Middle Stratosphere (OMS) balloon payload probing the tropical and mid-latitude stratosphere in studies of transport issues related to dispersion of aircraft exhaust. A major concern motivating these studies was the potential for nitrogen oxides (NO_x) generated in the exhaust plume of a supersonic high flyer to reach the tropical ozone production region by rapid transport from a

midlatitude flight corridor. NO_x is effective in destroying ozone (O_3) in a well-known catalytic cycle that can proceed rapidly under stratospheric photochemical conditions.

Several results from research carried out with the Argus instrument are described below.

Tracer Laminae in the Tropics – Transport of air from the midlatitudes into the tropics in the stratosphere is known to be inhibited by a “transport barrier.” The existence of such a barrier was already well known from satellite studies of dispersion of the Mt. Pinatubo aerosol cloud, following Pinatubo’s eruption in June, 1991. On the other hand, some transport of stratospheric air into the tropics is known to occur from the detailed study of tracer mean vertical profiles in the tropics. Interest in this issue centers on the fate of aircraft exhaust products injected into the midlatitude stratosphere, and their potential impact on the tropical ozone production region.

During an OMS balloon launch from 7° S in Brazil in November, 1997, thin laminar regions of low N_2O on the normal tropical profile of this tracer were observed. (N_2O is lower in the midlatitude stratosphere than in the tropics at the same altitude.) The data indicated clearly midlatitude values of N_2O in the tropics. This appears to be a direct observation of the process of rapid transport into the tropics of midlatitude stratospheric air masses. The observations suggest that this transport is episodic, possibly the result of breaking of midlatitude stratospheric waves (Rossby waves).

Long-Lived Arctic Winter Vortex Remnant – During an OMS balloon launch (in conjunction with ER-2 flights) from Fairbanks, Alaska, in late June, 1997, several layers of unusually low values in the N_2O and CH_4 tracer fields were encountered. These were clearly “remains” of the winter polar vortex with the observed filaments preserving very low tracer values characteristic of the interior of the vortex which had subsided from higher altitudes during the previous winter. The unusual, possibly unique, quality of the discovery was that these layers had maintained their integrity for about two months, from the time of vortex breakup sometime in late April until their observation in late June.

Intercomparison Flights with ATLAS and Other Tracer Instruments – Plans to design a new ER-2 instrument or to fly Argus on the ER-2, in both cases

for the purpose of replacing the older and heavier ATLAS instrument, has motivated two separate flight intercomparison campaigns. In the fall of 1998, Argus and ATLAS flew together on the ER-2 in an otherwise unrelated atmospheric radiation campaign called CiRex (Cirrus Radiation Experiment). In the fall of 1999, a comparison of several N_2O instruments was carried out in preparation for the SOLVE (SAGE II Ozone Loss and Validation Experiment) Arctic Ozone mission to take place in January through March of 2000.

Both of these intercomparison campaigns provided an opportunity to pass the pedigree of N_2O tracer field measurements made by ATLAS, and widely accepted as a standard in the ER-2 airborne measurement community, on to the new Argus instrument. The importance of this transfer is the significant weight reduction realized by the dual channel Argus instrument, thus allowing space for additional payload in the wide-ranging ER-2 atmospheric chemistry payload suite.

Point of Contact: M. Loewenstein
(650) 604-5504
mloewenstein@mail.arc.nasa.gov

TRMM/ Large-Scale Biosphere Atmosphere Experiment in Amazonia (LBA)

Steve Hipskind, Michael Craig, Tom Kalaskey

The TRMM/LBA mission was conducted in January and February, 1999, from several sites in the lower Amazonian region of Brazil. TRMM is the Tropical Rainfall Measuring Mission satellite. The experiment was conducted as part of the larger umbrella mission, Large-Scale Biosphere/Atmosphere Experiment in Amazonia (LBA). TRMM/LBA was one in a series of global field experiments that were planned to obtain ground validation measurements in support of the TRMM satellite mission. The objective of the field campaign was to obtain measurements for a tropical continental site, which would provide for the validation of the physical assumptions required

for the retrieval of precipitation data from the satellite. To obtain these measurements, TRMM/LBA employed a large and complex suite of measurement platforms deployed to Brazil. The instrumentation consisted of two ground-based Doppler radars, two research aircraft, special radiosonde sites, a vertical profiler, tethersonde, meteorological flux tower, and an array of radiometers, rain gauges, and disdrometers for measuring rainfall drop size distributions.

The TRMM satellite carries two primary instruments for obtaining precipitation measurements from space: a passive microwave instrument, the TRMM Microwave Imager (TMI), and the Precipitation Radar (PR). These are the primary instruments for which validation data are required.

The focus of the field measurements was the dual Doppler coverage of the two ground-based radars. One radar was the S-band, polarizing radar from the National Center for Atmospheric Research in Boulder, Colorado. The other was the C-band radar from NASA Wallops Flight Facility in Virginia. The two radars were installed just outside of the city of Ji-Parana in the western state of Rondonia, Brazil. The objective was to make the aircraft measurements within the overlapping, dual Doppler coverage of the two radars. The aircraft used were the NASA ER-2 and the University of North Dakota Citation. The ER-2 carried remote sensing instruments to act as a surrogate satellite, and in situ cloud physics instruments to obtain direct measurements of the cloud drop size distributions. The ER-2 was based in Brasilia, which is approximately 1500 kilometers (km) east of the ground site at Ji-Parana. The Citation was based at an airfield in Porto Velho, which is approximately 100 km west of Ji-Parana. The Citation carried in situ instrumentation for obtaining detailed microphysical data in clouds and precipitation. With the aircraft and ground-based instrumentation, it was possible to obtain a complete three-dimensional picture of the structure and dynamics of the precipitating cloud systems. The microphysical data provided detailed information on the state (liquid or ice) and size distribution of the precipitation.

TRMM/LBA was a collaborative mission between NASA and the Brazilian Space Institute (INPE), with significant participation from the University of Sao Paulo. In addition to the NASA mission, a large European effort was conducted concurrently in close

coordination with TRMM/LBA and the Brazilian scientists. TRMM/LBA participants came from NASA, the National Oceanic and Atmospheric Administration (NOAA), the National Center for Atmospheric Research (NCAR), and several universities and private research companies. The Earth Science Project Office at Ames Research Center managed the field campaign; NASA participants came from Goddard Space Flight Center, Marshall Space Flight Center, and Jet Propulsion Laboratory. The overall scientific direction of the project was provided by S. Rutledge, Colorado State University.

The primary focus of the mission was on the ground instrumentation sites in and around Ji-Parana. Both aircraft left their respective airfield bases and flew over the radar coverage area around Ji-Parana. In addition to the large radars, the NOAA's Aeronomy Laboratory set up wind profilers at the airport in Ji-Parana. These were vertically pointing radars that obtain wind profiles from the surface to about 10 km. NASA Goddard and the University of Iowa provided video disdrometers that use high-speed digital cameras to obtain rainfall-drop-sized distributions. Many surface rain gauges were distributed in concentrated networks to obtain the spatial distribution of rainfall. The University of Virginia (UVA) supplied a tethered balloon system that made continuous vertical profiles of the basic state variables and wind components from the surface to 1500 meters. UVA also set up and operated a meteorological tower and an acoustic sounder, which were set up in a large pasture down the hill from the C-band radar.

The mission was successful. Precipitation was plentiful, the instrumentation worked well, and the radars were operated 24 hours per day, seven days per week. The experiment used 100 ER-2 flight hours and approximately 60 Citation flight hours.

Collaborators in this research include Ramesh Kakar (NASA Headquarters), Steven Rutledge (Colorado State University), Quincy Allison (SIMCO Electronics), Steve Gaines and Joe Goosby (Raytheon Corp.), Betty Symonds (Science Applications International Corporation), and Sue Tolley (SIMCO Electronics).

Point of Contact: R. Stephen Hipskind
(650) 604-5076
shipskind@mail.arc.nasa.gov

ATMOSPHERIC PHYSICS

Corrections and Additions for the HITRAN Water Vapor Spectroscopic Database

Lawrence P. Giver, Charles Chackerian, Jr.,
David W. Schwenke

Systematic errors have been found and corrected in the HITRAN (High-Resolution Transmission Molecular Absorption Database) water vapor line absorption intensities in the visible and near-infrared spectral regions. The HITRAN database has been used extensively in the calculation of atmospheric absorption of solar radiation. The most important corrections found were a 14.4% increase of the intensity of the 940-nanometer (nm) band and an 8.7% increase of the intensity of the 820-nm band. These systematic errors in the HITRAN tabulations were due to errors in the unit conversion from the measurements published in centimeter/(centimeter atmosphere) ($\text{cm}^{-1}/(\text{cm-atm})$) to the HITRAN common units $\text{cm}^{-1}/(\text{molecule}/\text{cm}^2)$. Because the absorption of water vapor in these important regions is greater than has been used in model calculations for the Earth's atmospheric absorption, there is a diminished necessity for an hypothesized "continuum absorption" in the atmosphere.

These corrections have been applied to the HITRAN water vapor line list above 8000 cm^{-1} and have been submitted to HITRAN for posting on its website update page. In addition, measurements and assignments of some weak water vapor lines in this region (not included in the HITRAN list) have been reported.

Prasad Varanasi (State University of New York at Stony Brook) and Richard S. Freedman (SPRI) collaborated in this research.

Point of Contact: L. Giver
(650) 604-5231
lgiver@mail.arc.nasa.gov

How Effectively Can Freeze-Drying by Optically Thin, Laminar Cirrus Dehydrate Air Rising Slowly Across the Tropical Tropopause

Eric Jensen, Andrew Ackerman, Leonhard Pfister

Over the past 20 years, many theories have been proposed to explain the extreme dryness of air in the tropical lower stratosphere. Recent observations suggest that the flux of air into the stratosphere may be dominated by slow ascent across the tropopause throughout much of the tropics. In this study, cloud model simulations were used to show that laminar, optically thin cirrus clouds (frequently observed near the tropopause) can effectively freeze-dry air entering the tropical stratosphere. A detailed ice cloud microphysical model coupled to a large-eddy simulation dynamical model was used for these simulations. As shown in the top panel of the figure, if no cloud forms, the slow ascent across the tropopause will eventually increase the water vapor mixing ratio above 5 parts per million by volume (ppmv). These values are much higher than observed water vapor mixing ratios. However, if we include cloud formation, then the slow ascent drives adiabatic cooling and nucleation of a small number of ice crystals ($<10/\text{liter}$). These crystals grow rapidly and precipitate out within a few hours. The ice crystal nucleation and growth prevents the relative humidity (with respect to ice) from rising above the threshold of ice nucleation (130–160%) and limits the water vapor mixing ratio above the tropopause to 3–4 ppmv (bottom panel of figure). The nucleation threshold depends upon the aerosol composition in the tropopause region, which is not well known. Simulations including gravity waves propagating through the model were also done. Temperature oscillations driven by the waves drive nucleation of larger ice number densities and more complete dehydration of the rising air. These conditions promote the effectiveness of upper tropospheric aerosols as ice nuclei and the climatology of waves in the tropopause region. In situ tropical humidity observations from several field experiments have been gathered. These measurements included accurate water vapor sensors mounted on the NASA ER-2 as well as balloon-borne instruments. The humidity observations provide a few

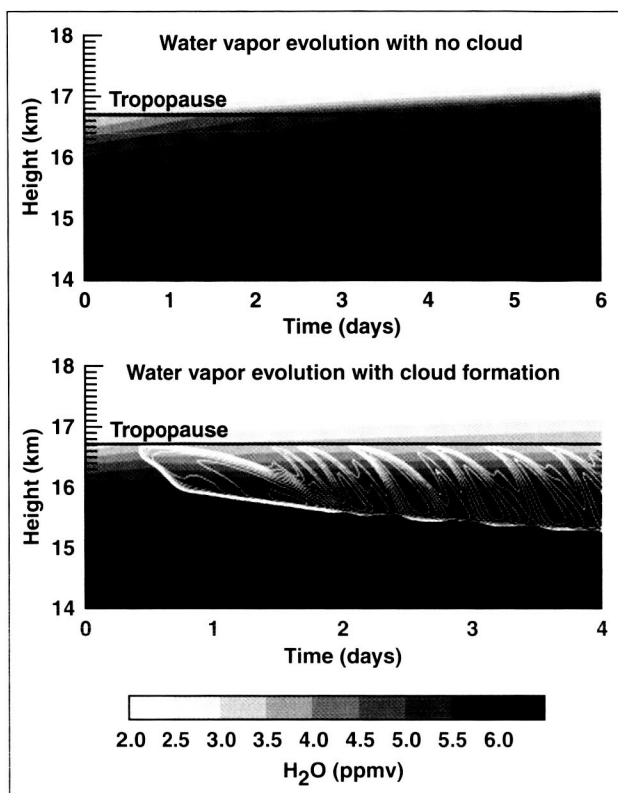


Fig. 1. Contours of water vapor mixing ratio (shading) are plotted versus time and height. The top panel shows that if no cloud forms, ascending air transports excessive amounts of water across the tropopause into the stratosphere. The bottom panel shows the dehydration of rising air if cloud formation is included in the model. The white contours show the cloud ice water content.

examples of supersaturated air near the tropopause (as predicted by the model); however, further observations of water vapor and wave motions near the tropical tropopause are required to clarify the cloud formation and dehydration process.

Point of Contact: E. Jensen
(650) 604-4392
ejensen@sky.arc.nasa.gov

Lofting of Soot Particles into the Middle Atmosphere by Gravito-Photophoresis

Rudolf F. Pueschel, Guy V. Ferry,
Anthony W. Strawa

The observed existence of soot aerosol at 20-kilometer (km) altitude (which arguably is generated by aircraft flying in corridors at 10–12 km) requires a transport mechanism in a thermally stable stratosphere that is different from isentropic or dynamic mixing. Such a mechanism could be provided by gravito-photophoresis, induced by the incidence of sunlight on strongly absorbing fractal soot particles. This particle absorptivity, in conjunction with uneven surface-coating of sulfuric acid and their fractal nature, makes soot particles (with maximum dimensions approaching 1 micrometer) particularly conducive to gravito-photophoresis. It is the requirement of a restoring torque that orients the particle with respect to gravity. This required force is provided by the fractal characteristics of soot, and a body-fixed photophoretic force is given by asymmetric thermal accommodation coefficients across the uneven surface of the particle.

During the Subsonic Assessment (SASS) Ozone and Nitrogen Oxides Experiment (SONEX) field campaign in 1997, soot aerosol was sampled in commercial airline flight corridors over the northeastern Atlantic, and the gravitational and gravito-photophoretic forces acting on those soot particles were computed. The result is that 16% by number, corresponding to 51% by mass, of a soot particle size distribution could be lofted against gravity by gravito-photophoresis. The calculated vertical velocities, exceeding settling velocities by up to a factor of 30, suggest that it takes about 30 years to transport soot from 10 to 20 km and 20 years to transport soot from 20 to 80 km. On the basis of current stratospheric soot loading, the resulting soot mass flux at 20-km altitude is 5×10^{-18} grams per square centimeter per second ($\text{g cm}^{-2} \text{sec}^{-1}$), which is within one order of magnitude of the influx of meteoritic dust into the mesosphere from outer space.

The effect of gravito-photophoresis is strongly altitude dependent. With increasing pressure near the Earth's surface, the lofting force falls off quickly. Above the mesopause, the lofting force becomes smaller because of a dominating energy loss by

radiation rather than by molecular heat transfer. Thus, gravito-photophoretic lofting forces are most effective within the altitude range between 10 and 85 km, making aircraft soot emitted in commercial flight corridors subject to lofting up to the mesosphere.

The current mass loading of soot in the middle atmosphere is too small to cause a direct absorption effect that would be comparable to the extinction of light by scattering on mesospheric cloud particles. However, it is conceivable that soot in the mesosphere has indirect effects by providing freezing nuclei for mesospheric ice particles to form. In addition, soot might contribute to the ionization of the mesosphere to affect the appearance of polar mesospheric summer radar echoes.

Collaborators in this research include H. Rohatschek (University of Linz, Austria), Sunita Verma (Science Systems & Application, Inc.), Nina Boiadjieva (San Jose State University), and Steve Howard (Symtech Corporation).

Point of Contact: R. Pueschel
(650) 604-5254
rpueschel@mail.arc.nasa.gov

Physical and Chemical Properties of Aerosols and Cloud Particles

Anthony W. Strawa, Rudolf F. Pueschel, Katja Drdla, Guy V. Ferry, Max Loewenstein, Paul Bui

Recent modeling studies have suggested a link between black carbon aerosol (BCA) and ozone chemistry via the reduction of nitric acid, nitrogen dioxide, and ozone on BCA particles. The ozone reaction converts ozone to oxygen molecules, while nitric acid can react to form nitrogen oxide (NO_x). Also, a buildup of BCA could reduce the single-scatter albedo of aerosol below a value of 0.98, a critical value that has been postulated to change the radiative effect of stratospheric aerosol from cooling to warming. Correlations between measured BCA amounts and aircraft usage have been reported.

Attempts to link BCA to ozone chemistry and other stratospheric processes have been hindered by questions concerning the amount of BCA that exists in the stratosphere, the magnitude of reaction probabilities, and the scarcity of BCA measurements. The primary objectives of the Ames team (as part of the Photochemistry of Ozone Loss in the Arctic Region in Summer (POLARIS) mission) were (1) to determine the distribution of sulfate and soot aerosols, and (2) to determine the role of these aerosols in stratospheric photochemistry.

To facilitate measurements, a system that automates the operation of the Ames Wire Impactors (AWI) was designed, fabricated, and flown successfully on POLARIS. This system alleviates the pilot workload and allows the experimenter the flexibility to sample at predetermined altitudes, locations, or temperatures.

Because of the fractal nature of BCA, modification of the AWI data-analysis procedures was required in which the collection of BCA is modeled as a fractal aggregate. The new method results in an increase in the measured BCA surface area of about 15 times and an increase in soot loading of about 6 times over the previously used approach. Despite this increase, BCA surface area is only about 10% of the measured sulfuric acid aerosol surface area.

Including heterogeneous reactions on BCA in a photochemical model can affect photochemistry, leading to renoxification and increased ozone depletion. However, these predicted effects are not supported by the POLARIS observations, in particular the nitrogen oxide/reactive nitrogen (NO_x/NO_y) ratios. Including BCA reactions does not statistically improve the agreement between model and measurement in any of several scenarios considered. Furthermore, if the reactions cause even partial carbon oxidation, the BCA would be consumed at a rate inconsistent with POLARIS observations. These inconsistencies lead to the conclusion that the presence of BCA in the stratosphere did not affect stratospheric photochemistry during POLARIS.

Measurements of aircraft plumes indicate that aircraft emit substantial numbers of volatile and nonvolatile particles during flight. These observations have caused concern that commercial aviation sources may significantly influence heterogeneous processes, cloud formation, and microphysics in the

upper troposphere and lower stratosphere. As part of the Subsonic Assessment (SASS) Ozone and Nitrogen Oxides Experiment (SONEX), the objectives of the Ames team were (1) to measure the distribution of aerosol and cloud during the mission in order to determine the fraction of total aerosol that can be attributed to aircraft-generated sulfur, and (2) to determine the relevance of this aerosol as a marker of aircraft-influenced air and its effects on the regional climate.

An instrument based on the thermal volatilization of aerosols was fabricated and flown on the SONEX mission to discriminate sulfuric acid, ammonium sulfate/bisulfate, and nonvolatile aerosols during the mission. Using this instrument, a significant increase in the sulfuric acid aerosol was observed under conditions where other indicators suggested that the air parcels were influenced by aircraft exhaust. Most of these occurrences were above 9 kilometer (km) altitude. The sulfuric acid aerosols do not appear to measurably affect surface area and volume of the background aerosol because of their small diameter, and, therefore, do not appear to affect radiative transfer directly. Only a very small fraction of the nonvolatile aerosols could be identified as BCA.

Collaborators in this research include R. Salawitch (Jet Propulsion Laboratory), R. S. Gao and J. Elkins (National Oceanic and Atmospheric Administration), M. Yasuda (San Jose State University), K. K. Perkins (Harvard University), R. Cohen (University of California at Berkeley), S. Howard (Symtech Corporation), and S. Verma (Science Systems & Application, Inc.).

Point of Contact: A. Strawa
(650) 604-3437
astrawa@mail.arc.nasa.gov

Quantifying Denitrification and Its Effect on Ozone Recovery

Azadeh Tabazadeh

Upper Atmospheric Research Satellite (UARS) observations indicate that denitrification occurs in the Antarctic, without significant dehydration, during mid to late June (see figure 1). In contrast, UARS data show no indication for the presence of large-scale denitrification in the Arctic, even during the coldest winters of the last decade (see figure 1). The fact that denitrification occurs in the Antarctic in a relatively warm month raises concern about the possibility for the occurrence of this event in a future colder, and possibly more humid, lower stratosphere, as a result of climate change and/or natural variability, and its subsequent effect on ozone recovery. Polar stratospheric cloud (PSC) lifetimes required for Arctic denitrification to occur in the future were contrasted against the current Antarctic cloud lifetimes during early and mid to late June. Ozone sensitivity calculations show that widespread denitrification can enhance future Arctic ozone loss by about 40% during the coldest winters of the next century.

It is well known that PSCs play an important role in the formation of the springtime Antarctic "ozone hole" by activating chlorine and denitrifying the stratosphere. Because similar levels of active chlorine concentrations have been measured in both polar vortices, the lack of extensive denitrification observed in the Arctic has been speculated to be one of the main factors currently preventing the formation of an Arctic "ozone hole." At Ames, and for the first time, a quantitative study was done on the denitrification process that explains why this event currently occurs extensively in the Antarctic and not the Arctic, using data obtained from numerous different instruments onboard the UARS.

Until now, a few studies have implied that Arctic denitrification, during the coldest winters of the last decade, has already contributed significantly to the depletion of ozone inside the Arctic vortex. On the other hand, a wealth of available information suggests that the apparent and simultaneous loss of both ozone and reactive nitrogen in the Arctic is often purely a result of dynamical mixing of different air masses with high and low values of both species that is unrelated to denitrification. Also, most in situ and

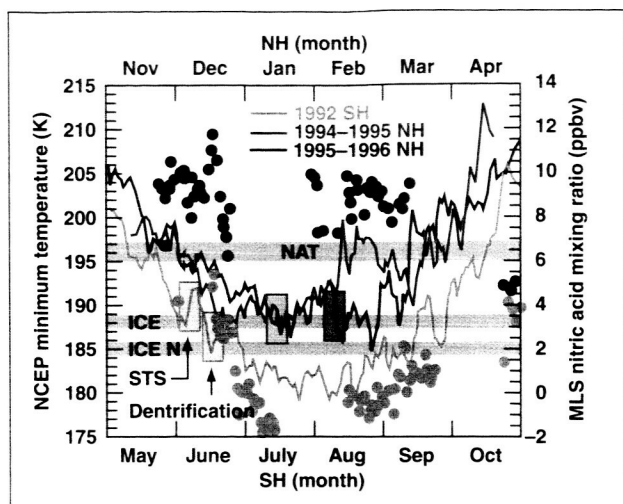


Fig. 1. Minimum temperatures are shown for a selected number of polar winters at the 50-millibars (mb) pressure level, which is near the 450 K potential temperature surface. The periods for ternary PSC formation and denitrification during the Antarctic winter of 1992 are marked in the figure as blue boxes. The NAT (nitric acid trihydrate) and ice envelopes (shaded gray) show temperatures at which nitric acid and water saturate to form nitric acid trihydrate and water ice particles, respectively. The ice nucleation envelope marks the temperature at which ice clouds can nucleate in the stratosphere. The critical temperature envelopes are calculated for nitric acid and water vapor mixing ratios of 9 to 12 parts per billion by volume and 4 to 5 parts per million by volume, respectively, based on in situ observations. Two Arctic study periods are also marked in the plot as magenta and gray boxes for the 1994–1995 and 1995–1996 winters, respectively. Symbols shown are the time series of microwave limb sounder gas-phase nitric acid averaged and binned between the 75°S and 75°N for the Antarctic and the two Arctic winters, respectively.

balloon data sets showing denitrification in the Arctic are collected either directly over or downwind of mountainous terrain (mainly over Greenland and Norwegian mountains), where lee waves could strongly affect the local reactive nitrogen (and/or water vapor) profile through small-scale cloud processing. However, the fact that satellite data show no indication of widespread denitrification in the

Arctic at present suggests that the local perturbations caused by lee waves are not of global or even regional significance.

To resolve the controversy between space, in situ, and balloon observations regarding denitrification in the Arctic, a new concept was introduced at Ames that compared and contrasted “PSC lifetimes” between the two hemispheres to investigate whether PSC lifetimes could have been long enough in the past Arctic winters to have led to widespread denitrification. The concept of PSC lifetime provides new insights into how long a PSC must persist in the winter for the denitrification process to occur, and why the event currently occurs only in the Antarctic. Further, it is planned to show that future forecasted perturbations in temperature and water vapor can increase Arctic PSC lifetimes to the point where denitrification can occur during the coldest winters of the next century with important implications for Arctic ozone recovery.

Collaborators in this research include Michelle Santee (Jet Propulsion Laboratory) and Patrick Hamill (San Jose State University).

Point of Contact: A. Tabazadeh
(650) 604-1096
atabazadeh@mail.arc.nasa.gov

Reduction of Trade-Cumulus Cloud Cover Due to Solar Heating by Dark Haze

Andrew Ackerman

The radiative forcings of aerosols represent a leading source of uncertainty in recent assessments of radiative forcings due to industrial activity. Although aerosol residence times are short (approximately one week or less, compared to ~50 years for carbon dioxide molecules), and they influence the radiation budget only during the day, it is estimated that by increasing reflection of sunlight, the cooling effects of aerosols may offset the radiative forcing (globally averaged). The traditional radiative forcings due to aerosols are (1) direct, by which aerosols directly scatter and absorb sunlight (cooling and heating effects, respectively), and (2) indirect, by which

aerosols increase cloud albedo, thereby reflecting more sunlight back to space (a cooling effect). Globally integrated, these forcings are estimated to range between 1 and 2 watts per square meter (W/m^2).

A primary objective of the Indian Ocean Experiment (INDOEX) was to quantify the indirect forcing of aerosols. Although a murky haze covered the Arabian Sea (during the northeast monsoon, with predominant flow off the Indian subcontinent), few clouds were found. Perhaps the presence of dark haze and the lack of clouds are not merely coincidental, but are connected. Under current evaluation is the possibility that absorption of solar energy by the dark haze dries the air sufficiently to dissipate the clouds.

The predominant cloud type expected at those latitudes is trade-cumulus, in which cloud coverage is largely determined by the coverage of stratiform "anvils" that remain after cumulus convection. The lifetime of these anvils (and therefore, their time-averaged coverage) decreases as the relative humidity of the air in which they are embedded decreases. To evaluate this hypothesis, Ames researchers ran a three-dimensional (3-D) model of cloud simulations (based on observations of trade-cumulus observed under clean conditions in the Atlantic) under clean and polluted conditions. For the indirect effect, cloud droplet concentrations were doubled from 250 to 500 per cubic centimeter ($/\text{cm}^3$), resulting in a diurnally averaged indirect radiative forcing of -12 watts per square meter (W/m^2) at the top of the atmosphere (a cooling effect), half of which is due to simply distributing cloud water over a greater surface area, and half of which is due to decreased precipitation. However, if a dark haze is also included, as observed during INDOEX in 1999 (with aerosol-induced heating rates of 2 kelvin per day (K/d) at noon), the boundary layer dries significantly during the daytime, resulting in a noticeable reduction in cloud coverage during the afternoon (see figure). The reduction in cloud coverage overwhelms the indirect cooling effect and leads to a net radiative forcing of 9 W/m^2 (a strong heating effect) for the conditions simulated. Because light-absorbing aerosols are found downwind of industrial continents, these results suggest the possibility that the global cooling effect of aerosols may be drastically overestimated.

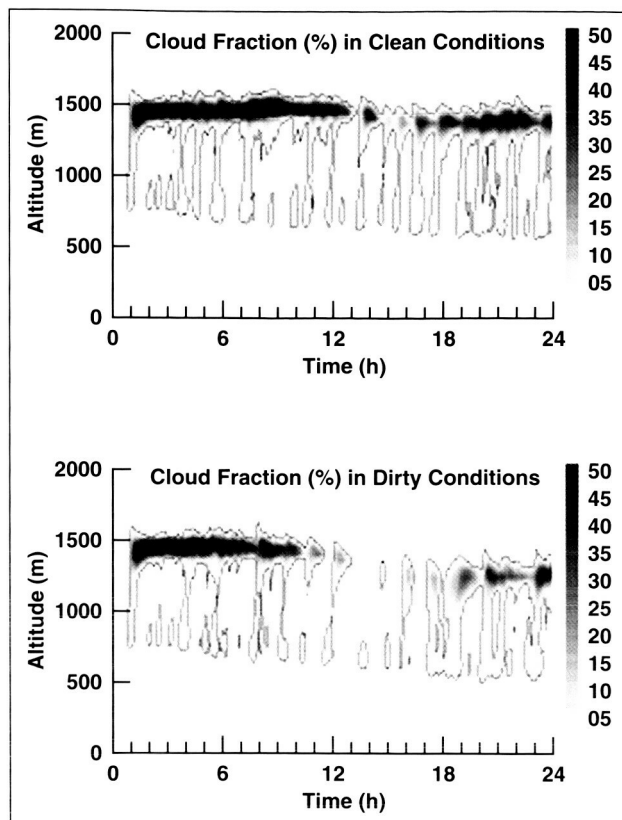


Fig. 1. This figure shows time-height contours of cloud fractional coverage (%) in 3-D model simulations of trade-cumulus in clean air (top) and in dirty air (bottom). Changes in droplet concentrations and the aerosol-induced heating in the dirty simulation are described in the text.

Collaborators in this research include Owen B. Toon (University of Colorado) and David E. Stevens (Lawrence Livermore National Laboratory).

Point of Contact: A. Ackerman
(650) 604-3522
ack@sky.arc.nasa.gov

Uncertainty and Validity of Aerosol Radiative Forcing Determinations

Peter Pilewskie, Warren Gore, Larry Pezzolo

In February and March 1999, Ames participated in the Electro Optical Propagation around Coastal Environments (EOPACE) experiment in Duck, North Carolina, to characterize the radiative effects of boundary layer marine aerosol near the Outer Banks region of the coast of North Carolina. The NASA Ames solar spectral flux radiometer (SSFR), as shown in figure 1, was integrated on the Center for Interdisciplinary Remotely Piloted Aircraft Studies (CIRPAS) Twin Otter to measure zenith irradiance and nadir radiance (see figure 2). Data have been used to characterize the sea surface reflectance in a coastal region and to compare with open ocean reflectance for purposes of improving aerosol optical depth retrievals from the advanced very-high-resolution radiometer (AVHRR) satellite instrument. The Twin Otter was also equipped with microphysical sensors

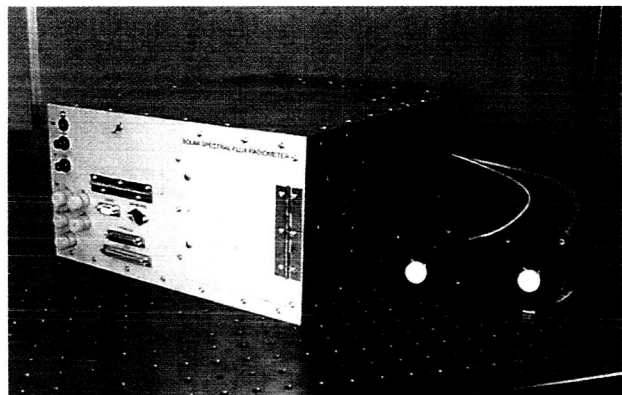


Fig. 1. Solar Spectral Flux Radiometer.



Fig. 2. DOE Twin Otter.

to measure the extinction of the aerosol. The study determined the net solar radiative forcing of the aerosol and examined dependencies of radiative parameters on wind speed and surface roughness. This research represents an important test of the previous discovery of a bias between measured and modeled spectral irradiance that is highly correlated with water vapor, and increases at a rate of 8 watts per square meter per centimeter ($\text{W/m}^2/\text{cm}$) of water vapor (see figure 3).

Another aspect of this research is to modify the radiative transfer model used in a model developed at Ames to incorporate new spectral bandpasses that match that of the SSFR. The newly generated k-distributions will be compiled using the line-by-line code LBLTRM developed by Atmospheric and Environmental Research (AER). Testing began in summer 1999, and it is anticipated that the completed radiative transfer model will be operational by the first half of FY00. Analysis will be applied to the previous aerosol/water vapor study described above and to the EOPACE Duck data set. Estimates of solar spectral radiative forcing will be generated from both studies.

Collaborators in this research include Robert Bergstrom (Bay Area Environmental Research Institute), Maura Rabbette (National Research Council Associate) and John Pommier (Symtech Corporation).

Point of Contact: P. Pilewskie
(650) 604-0746
ppilewskie@mail.arc.nasa.gov

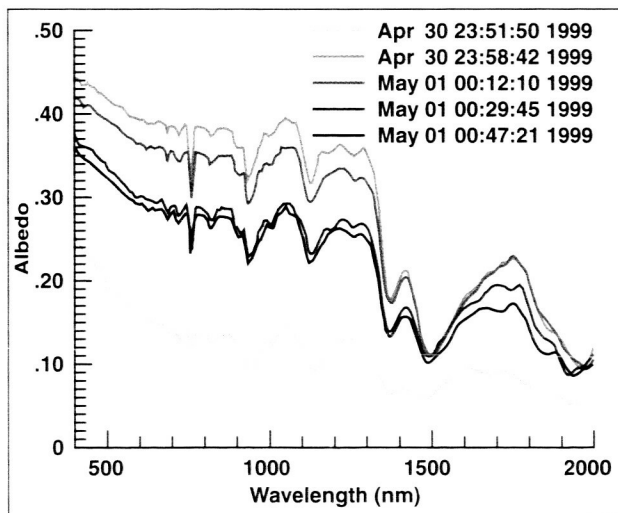


Fig. 3. Altus SSFR Spectral Albedo.

REPORT DOCUMENTATION PAGEForm Approved
OMB No. 0704-0188

Public reporting burden for this collection of information is estimated to average 1 hour per response, including the time for reviewing instructions, searching existing data sources, gathering and maintaining the data needed, and completing and reviewing the collection of information. Send comments regarding this burden estimate or any other aspect of this collection of information, including suggestions for reducing this burden, to Washington Headquarters Services, Directorate for Information Operations and Reports, 1215 Jefferson Davis Highway, Suite 1204, Arlington, VA 22202-4302, and to the Office of Management and Budget, Paperwork Reduction Project (0704-0188), Washington, DC 20503.

1. AGENCY USE ONLY (Leave blank)		2. REPORT DATE December 2000	3. REPORT TYPE AND DATES COVERED Technical Memorandum	
4. TITLE AND SUBTITLE Ames Research Center Research and Technology Report 1999			5. FUNDING NUMBERS 992-23-10	
6. AUTHOR(S) Ames Investigators				
7. PERFORMING ORGANIZATION NAME(S) AND ADDRESS(ES) Ames Research Center Moffett Field, CA 94035-1000			8. PERFORMING ORGANIZATION REPORT NUMBER A-0003831	
9. SPONSORING/MONITORING AGENCY NAME(S) AND ADDRESS(ES) National Aeronautics and Space Administration Washington, DC 20546-0001			10. SPONSORING/MONITORING AGENCY REPORT NUMBER NASA/TM-1999-209618	
11. SUPPLEMENTARY NOTES Point of Contact: Dr. Stephanie Langhoff, Chief Scientist, Ames Research Center, MS 230-3, Moffett Field, CA 94035-1000 (650) 604-6213 or contact the person(s) designated as the point of contact at the end of each article.				
12a. DISTRIBUTION/AVAILABILITY STATEMENT Unclassified — Unlimited Subject Category 99 Distribution: Standard Availability: NASA CASI (301) 621-0390			12b. DISTRIBUTION CODE	
13. ABSTRACT (Maximum 200 words) <p>This report highlights the challenging work accomplished during fiscal year 1999 by Ames research scientists, engineers, and technologists. It discusses research and technologies that enable the Information Age, that expand the frontiers of knowledge for aeronautics and space, and that help to maintain U.S. leadership in aeronautics and space research and technology development. The accomplishments are grouped into four categories based on NASA's four Strategic Enterprises: Aero-Space Technology, Space, Human Exploration and Development of Space, and Earth Science.</p> <p>The primary purpose of this report is to communicate knowledge—to inform our stakeholders, customers, and partners, and the people of the United States about the scope and diversity of Ames' mission, the nature of Ames' research and technology activities, and the stimulating challenges ahead. The accomplishments cited illustrate the contributions that Ames is making to improve the quality of life for our citizens and the economic position of the United States in the world marketplace.</p>				
14. SUBJECT TERMS Aeronautics, Space transportation, Space sciences, Earth sciences, Life sciences, Information technology, Research and technology			15. NUMBER OF PAGES 207	
			16. PRICE CODE A10	
17. SECURITY CLASSIFICATION OF REPORT Unclassified	18. SECURITY CLASSIFICATION OF THIS PAGE Unclassified	19. SECURITY CLASSIFICATION OF ABSTRACT	20. LIMITATION OF ABSTRACT	